ANALYSIS
OF
BINDING HETEROGENEITY

Maarten Nederlof

Promotor: dr. W.H. Van Riemsdijk,   hoogleraar Bodemscheikunde
Co-promotor: dr. ir. L.K. Koopal,   universitair hoofddocent bij de
                                                       vakgroep Fysische en Kolloïdchemie

Maarten Nederlof

Analysis of Binding Heterogeneity

Stellingen

1) De afleiding van de Differential Equilibrium Function, zoals gegeven door Gamble et al., is inconsistent, omdat in deze afleiding tegelijkertijd de Langmuir isotherm en de Condensatiebenadering daarvan gebruikt wordt.
Dit proefschrift.
D.S. Gamble, A.W. Underdown, C.H. Langford (1980). Copper(II) titration of fulvic acid ligand sites with theoretical, potentiometric, and spectrophotometric analysis.
Anal. Chem. 52, 1901-1908.

2) Het rekening houden met de experimentele fout in meetdata is minstens zo belangrijk als een goede benaderingsmethode voor het berekenen van distributies.
Dit proefschrift.
W. Fish, D.A. Dzombak and F.M.M. Morel (1986). Metal-humate interactions.
2. Application and comparison of models. Environ. Sci. Technol. 20, 676-683.
D.R. Turner, M.S. Varney, M. Whitfeld, R.F.C. Mantoura and J.P. Riley (1986). Electrochemical studies of copper and lead complexation by fulvic acid. I. Potentiometric measurements and a critical comparison of metal binding models.
Geochim. Cosmochim. Acta 50, 289-297.

3) De conclusie van Bartschat et al. dat koper-ionen voornamelijk op relatief grote deeltjes adsorberen en protonen op kleine, omdat de invloed van zoutsterkte op de binding sterk verschilt, kan alleen hard gemaakt worden als een zuur-base titratie wordt uitgevoerd met hetzelfde materiaal als waaraan de koperadsorptie bepaald is.
B.M. Bartschat, S.E. Cabaniss and F.M.M. Morel (1992). Oligoelectrolyte model for cation binding by humic substances. Environ. Sci. Technol. 26, 284-294.

4) Het Equilibrium Partitioning (EP) model zoals dat gebruikt wordt voor organische verontreinigingen bij het beoordelen van de kwaliteit van bodems is niet geschikt in het geval van zware metalen door het niet-lineaire karakter van de binding van zware metalen aan bodembestanddelen.
D.M. Di Toro et al. (1991). Technical basis for establishing sediment quality criteria for nonionic chemicals using equilibrium partitioning. Environ. Tox. Chem. 10, 1541-1583.

5) Bij het normaliseren van toxicologische gegevens voor zware metalen naar een standaardbodem moeten niet alleen organische stof en lutumgehalte worden beschouwd, maar in ieder geval ook de pH, gezien de grote invloed van de pH op het bindingsgedrag.
N.M. Van Straalen and C.A.J. Denneman (1989). Ecotoxicological evaluation of soil quality criteria. Ecotox. Environ. Saf. 18, 241-251.

6) De door Verweij berekende vrije koperconcentratie in bio-assays met algen op basis van EDTA complexering is waarschijnlijk te hoog, omdat Cu sterk bindt aan het oppervlak van de algen.

W. Verweij (1991). Speciation and bioavailability of copper in Lake Tjeukemeer. Proefschrift, Landbouwuniversiteit Wageningen.

M.L.S. Simões Gonçalves and A.C. Lopes da Conceição (1991). Interactions of heavy metals with organisms and proteins. Sci. Total Environ. 103, 185-198.

7) Het begrip 'biologische beschikbaarheid', dat door velen te pas en te onpas wordt gebruikt, behoeft een nadere definiëring om het eenduidig bespreekbaar te maken en het te kunnen kwantificeren.

W.H. Van Riemsdijk (1990). Capita selecta bodemchemische aspekten van biologische beschikbaarheid.

8) In verband met het inschatten van risico's voor het milieu is het relevanter om gereinigde grond te beoordelen op basis van restconcentraties dan op basis van reinigingsrendement.

G.A. Brown and H.A. Elliott (1992). Influence of electrolytes on EDTA extraction of Pb from polluted soil. Water Air and Soil Pollution 62, 157-165.

9) Wanneer wiskundige bewerkingen met computerprogramma's als Mathematica en Derive uitgevoerd kunnen worden, dan kan in het wiskunde onderwijs beter aandacht besteed worden aan het begrip van die bewerkingen dan aan het kunnen uitvoeren van 'trucjes'.

10) Wanneer 'fuzzy mathematics' in de bodemverontreiniging toegepast wordt, zoals Burrough beschrijft voor landevaluatie en bodemkartering, vervaagt het verschil tussen wel en niet verontreinigde gronden.

P.A. Burrough (1989). Fuzzy mathematical methods for soil survey and land evaluation. J. Soil Sci. 40, 477-492.

11) De wervingstekst '*Landbouwuniversiteit Wageningen, het natuurlijk milieu voor wetenschap*' had in het geval van de studierichting Bodem, Water Atmosfeer beter kunnen luiden '*Landbouwuniversiteit Wageningen, wetenschap voor het natuurlijk milieu*'.

Wervingsadvertentie studierichting Bodem, Water, Atmosfeer.

12) '*Quod gratis affirmatur, gratis negatur*'; igitur exploratori propositum est argumenta adferre.

13) Volgens Van Dale is bier een alcoholhoudende drank en dus is alcoholvrij bier een contradictio in terminis.

Van Dale, Woordenboek der Nederlandse taal.

14) Scouting, da's pas leven !

Stellingen, behorende bij het proefschrift "Analysis of binding heterogeneity".
Maarten Nederlof, Wageningen, 24 juni 1992.

Abstract

Nederlof, M.M., 1992. Analysis of Binding Heterogeneity.
Ph.D. thesis, Wageningen Agricultural University,
Wageningen, The Netherlands.
ISBN 90-5485-014-0; 256 pages

Binding heterogeneity, due to different functional groups on a reactive surface, plays an important role in the binding of small molecules or ions to many adsorbents, both in industrial processes and in natural environments. The binding heterogeneity is described by a distribution of affinity constants since the different functional groups have different affinities for the adsorbing species.

Three appraoches are discussed to obtain distribution functions on the basis of adsorption isotherms: the Local Isotherm Approximation (LIA), the Affinity Spectrum (AS) and the Differential Equilibrium Function (DEF). The methods are compared both on the basis of their derivation and on their ability to reproduce (known) distribution functions. All methods discussed need derivatives of the binding function, which are hard to obtain from experimental data. In order to apply the methods to experimental data a smoothing spline routine was adapted for the present problem. The methodology is applied to proton and copper binding to fulvic acids.

Analogous to the heterogeneity analysis for binding under equilibrium conditions, a procedure was derived to determine first order rate constant distributions. The newly developed method is called LOcal Decay function Approximation (LODA). Also here an adapted smoothing spline routine is used to apply the method to experimental data. The method is illustrated by copper dissociation data from estuarine humic material.

Finally it is shown how on the basis of the obtained distribution function a suitable model can be chosen for the description and prediction of binding or dissociation data.

Additional index words: Condensation Approximation, LOGA, LODA, affinity distribution, dissociation rate, rate constant distribution, metal ion binding, fulvic acid, experimental error, smoothing spline

Ter nagedachtenis aan mijn vriend en scout

Wouter Heino van de Kamp

(overleden 20 januari 1990)

Er is een tijd waarop een leermeester
zijn leerlingen niet meer voorgaat maar volgt.
Hij wijst hen niet meer de weg
want zij hebben zelf een kompas in zich.
Hij heeft geen goede raad meer voor hen
want ze luisteren nu naar hun eigen hart.
Hij weet dat al zijn lessen en richtlijnen
nergens anders hebben heengewezen
dan naar ieders eigen vermogen
om de stand der sterren te zien
en de tekenen te lezen langs de weg.
Hij weet dat hij een mijlpaal is langs de weg:
als de reizigers er langs gekomen zijn,
keren ze zich niet meer om naar hem.
Hij staat stil bij zichzelf
en denkt na of hij zijn eigen spoor weervindt
in het opgejaagde stof van de weg.

Uit: F. Cuvelier, De stad van axen.

Voorwoord

Ja, daar ligt dan, na vier jaar zwoegen, het proefschrift !

Een woord van dank aan een ieder die op de een of andere manier een bijdrage heeft geleverd aan dit proefschrift, inhoudelijk dan wel mentaal, is dan ook op zijn plaats.

Allereerst wil mijn beide begeleiders bedanken. Willem van Riemsdijk, mijn promotor, was altijd bereid om manuscripten te lezen en om nieuwe ideeën aan de hand te doen, die in een 'achternamiddag' uitgewerkt konden worden. Willem, na zeer vele achternamiddagen kwam dit proefschrift tot stand. Luuk Koopal, mijn copromotor, wil ik bedanken voor zijn niet aflatende inzet voor het corrigeren van manuscripten. Luuk, vrijwel alle pagina's van dit proefschrift zijn wel eens 'grijs' geweest van het commentaar, waardoor de tekst (nog) beter werd.

Vervolgens wil ik mijn kamer- en lotgenoot Han de Wit bedanken voor zijn steun en begrip als ik weer even niet zag zitten. Han, het was prettig om samen met jou gedurende die vier jaar een kamer te delen en vele kopjes koffie te nuttigen.

Ik mag natuurlijk de studenten niet vergeten die ik heb mogen begeleiden en die steeds een stimulans vormden om de zaak weer eens op een rijtje te zetten alvorens weer verder te gaan. In willekeurige volgorde: Esther Schoen, Mari Marinussen, Stephan Gruijters, Christel Verhulst, Peter Venema, Koos Verloop, Patrice Theunissen, en Karin Ordelmans. Tot slot een speciaal woord van dank aan een tijdelijk medewerker waarvan de kans dat ik zijn naam verkeerd spel bijzonder groot is: Iraj Manuchehri.

De vakgroep Bodemkunde en Plantevoeding wil ik bedanken voor de gastvrijheid en de ondersteuning, en het Speerpuntprogramma Bodemonderzoek voor het scheppen van de finaciële mogelijkheden voor het projekt.

Ten slotte, maar zeker niet in het minst, wil ik Karin bedanken voor het ontwerp van de omslag van dit proefschrift en de verdere 'produktiebegeleiding'. Karin, jouw eindeloze morele steun heeft me ook door de laatste loodjes heen geholpen.

Maarten Nederlof
Wageningen, mei, 1992.

Contents

Quis leget haec ?

CHAPTER 1

Introduction

General Introduction

Soil pollution has become a major topic of concern in the Netherlands. Very many locations are considered to be so polluted that treatment is necessary. It is estimated that $5 \cdot 10^4$ million guilders are needed to clean all these sites. Soil quality standards play an important role in the assessment of contaminated sites. The absolute values of these standards are subject of discussion (1-3). They are based on total contents of a contaminant in soil samples and are the same for all soil types. It is clear that when a contaminant is strongly adsorbed to the soil material, as may occur in clay soils and soil with a high organic matter content, the risk of leaching to the groundwater and of toxic effects on biota will be limited. When a contaminant is not or only weakly adsorbed, as may occur in sandy soils with a low organic matter content, the opposite applies and the contaminant will leach easily to the groundwater and will be readily available for biota. In addition, environmental conditions as pH and ionic strength strongly influence the binding behaviour. Therefore, the soil quality standards should be differentiated to different soil types and different conditions and may result in a different priority list for cleaning of contaminated sites (3).

Moreover, when the soil is to be cleaned, differences in binding behaviour are also important, they strongly influence the possibility and the efficiency with which soils can be cleaned. The Netherlands Integrated Soil Research Programme was set up to bring together information and to perform additional research in order to develop methods for a better risk assessment of pollutants and to find new techniques for cleaning soils. Also internationally the soil quality problem is becoming more and more important resulting also in support of the EC for research in this area.

In soil research often empirical models are used to describe the binding behaviour of pollutants, or chemical species in general, to the soil material. Application of the Freundlich isotherm is a typical example of this approach (4). Coefficients of such a relation are correlated with soil parameters such as clay content, pH, organic matter content etc (5). These relationships may be very useful to describe the variations in binding behaviour for a given group of soil samples. However, the coefficients have limited general validity and reveal little insight in the binding mechanisms.

3

Ideally one wants to predict the binding behaviour for a given set of soil parameters and conditions. In order to be able to make such predictions, processes underlying the observed binding behaviour should be studied thoroughly. Binding models based on physical chemical considerations (6-9) play in this prediction a major role. Since the binding strongly varies with soil composition (10-13) and since the dependency on conditions is different for different reactive surfaces (6,7), the binding behaviour of soil components, such as metal (hydr)oxides (14-21), clay minerals (22-26) and organic matter (27-35), is often studied separately. Final goal is to estimate the binding of a pollutant to a whole soil sample on the basis of submodels for the binding of the pollutant to the individual components.

Of the soil components studied, organic matter is the least understood. This is probably due to the fact that organic matter consists of a mixture of macromolecules that can not be defined rigourously. Thus, studying the behaviour of organic matter in terms of separate components as can be done for oxides (36-39) and clay minerals (40-43), is not useful. Moreover, extraction of organic matter from soils is rather difficult in the sense that the material may change its characteristics due to the extraction procedure (44). The study of separate (simple) organic molecules as representatives of the organic matter in soils may give some information (45), but gives a too simple picture of the organic matter as a whole. Organic matter fractions such as the fulvic and humic acids are defined operationally on the basis of an extraction procedure (46).

Natural organic matter is characterised by a wide range of functional groups that differ in their affinity for binding of cations. This leads to chemical heterogeneity. This is a heterogeneity on the molecular level, which is of a completely different order than the heterogeneity observed within soil parameters on a field scale. Apart from field scale heterogeneity also the chemical heterogeneity on the molecular scale may be very important in the risk assessment of contaminated sites. A mean value of the different affinity constants may not give a reasonable characterisation of a situation. Sometimes a conditional average affinity constant is used (47,48). However, this description gives a poor indication of the binding behaviour when environmental conditions change. Pollutants adsorbed on sites with a lower affinity than the mean value are easily released when the concentration in solution is lowered. On the other hand pollutants adsorbed on sites with a higher affinity than

the mean value will be strongly bound and will not become available. When the soil material is to be cleaned, high affinity sites may cause severe problems, because it will be difficult to desorb pollutants from these sites.

Chemical heterogeneity not only influences the distribution of a chemical over various types of binding sites under equilibrium conditions, but it also strongly affects the rate of dissociation. These kinetic aspects may also have large consequences with respect to the mobility and bioavailability of chemicals in soils.

In order to predict the behaviour of chemicals in the environment, models that describe the binding behaviour are essential. Because of a lack of knowledge, in practice often a certain binding model is chosen in a rather arbitrary way. Model constants are obtained by fitting available data to the model. This is a rather unsatisfactory situation. This situation can be improved by performing a heterogeneity analysis on binding data of the material as an aid to select a physically realistic binding model. Heterogeneity analysis may also give more insight in the fundamental aspects of binding or in the kinetics of the release of chemicals.

In this thesis methods are presented that are capable of retrieving a distribution of binding constants or a distribution of rate constants from experimental data. The methodology is applied to binding of protons and heavy metal ions to natural organic matter. Natural organic matter was chosen because it is known to be chemically heterogeneous and because it plays an important role with respect to the behaviour of metal ions in the environment, both in terrestrial and aqueous systems.

In addition to the chemical heterogeneity, the compounds show variable charge characteristics. This implies that metal ion binding depends on pH and ionic strength. Metal ion binding to humic materials is thus always a multi-component adsorption process. The study of ion binding to these materials is rather complicated both with respect to performing adsorption experiments and with respect to modelling the underlying processes.

In literature no satisfactory binding model is at present available for the description of metal ion binding to natural organic matter. A realistic binding model should at least be capable to take into account effects of variable charge, chemical heterogeneity and competition on the binding behaviour of metal ions. One of the aims of this thesis, in combination with the thesis of De Wit (49) is to develop a satisfactory ion binding model that is applicable to natural organic matter. De Wit (50, 51) has

5

developed a procedure that can assess the effect of variable charge independently from effects of chemical heterogeneity. This procedure was called the master curve procedure.

The affinity distribution may be derived from either a master curve or directly from a measured binding function. Application of the heterogeneity analysis to a binding function that is not corrected for environmental conditions leads to a so called "apparent" distribution function. When the electrostatic effects are taken into account explicitly an "intrinsic" distribution can be obtained that does not depend on environmental conditions, but only on the chemical properties of the material itself. Both types of distributions have been determined and are used to aid the selection of a binding model.

Heterogeneity Analysis Methods

Basic idea of the heterogeneity analysis is that the binding behaviour of a hetero-geneous system can be described by the summation of the binding to individual site types, weighted by their fractions (52,53). The binding behaviour for each site type separately is described by the local isotherm, for which often the Langmuir isotherm is used (52-54). When a continuous range of affinity constants is assumed, the heterogeneity is described by a continuous distribution function and the overall binding equation becomes an integral equation with the local isotherm as kernel. This integral equation is a so called Fredholm integral equation of the first kind. With a known overall binding function and an assumed local isotherm the Fredholm equation is difficult to solve for the distribution function, both numerically and analytically (55,56).

Although in the early literature the problems related with the Fredholm integral equation have not always been recognized, the study of the chemical heterogeneity is not new. Simms (57) reports already in 1926 that stability constants may vary with concentration for organic ligands. Scatchard (58) developed in 1949 a graphical method to determine a limited number of stability constants together with the relative occurrence of the corresponding site types. In the field of viscoelastic materials Nolle (59) found in 1950 that the first derivative of their intensity function was a measure of the heterogeneity. Schwarzl and Staverman (60,61) elaborated this idea further and generalized the methodology to different types of processes.

Ninomiya and Ferry (62) developed a different calculation scheme to obtain the distribution function. Much later in 1975 this idea was picked up by Hunston (63), who introduced the name Affinity Spectrum (AS) for the distribution function. Since then the method has been used frequently in literature (64,65). In the field of binding of ions to natural ligands the Differential Equilibrium Function (DEF) method (66-69) was developed to characterise the chemical heterogeneity.

In the field of physical chemistry the chemical heterogeneity of, for instance, catalyst surfaces has been studied. Roginsky (70) developed in 1948 the Condensation Approximation (CA), which approximates the local isotherm by a step function in order to solve the integral equation analytically. Harris (71) further analysed this concept. A first improvement of the CA method was the asymptotically correct approximation (ACA) proposed by Cerofolini (72,73). Later, a semi-analytical method based on a Taylor series expansion of the true distribution was developed by Hsu, Jagiello and Rudzinski (74,75).

Also numerical procedures were developed (76-79). In recent work the ill-posedness of the Fredholm integral equation is taken into account explicitly by using regularisation (80-83) or singular value decomposition (84,85). The numerical methods are successful when applied to data that cover a wide range of relative occupation. With natural samples, however, only a window of coverages is obtained and results are relatively less accurate.

It was already mentioned that also the kinetic heterogeneity may be an important aspect in the risk assessment of pollutants in environmental systems (63,86-89). For the determination of first order rate constants similar techniques can be applied as developed for the equilibrium affinity distribution functions. The basic concept is very similar. In this case the overall decay function is assumed to be the summation of the decay functions for the individual site types, weighted by their fraction (90). The dissociation reaction for one site type is described by the local decay function, for which a first order expression is used. Each site type is thus characterised by a dissociation rate constant and a fraction. For a continuous range of dissociation constants the summation becomes an integration which again results in a Fredholm integral equation. The distribution of rate constants can be found by inverting the integral equation. Again this is a difficult task and approximations are needed to find an analytical expression for the first order rate constant distribution function.

7

In the treatment of Schwarzl and Staverman (60,61) mentioned above a first order decay function was already used as kernel. The method was, however, never applied to the dissociation kinetics of metal ligand complexes. Olson has developed a second order method using the inverse Laplace Transform (LT) technique (91,92) and applied the method to Cu-humate dissociation data for estuarine humic material (93).

Outline of this thesis

In the first part of the thesis the determination of affinity distributions on the basis of equilibrium binding data is dealt with. In Chapter 2 the existing semi-analytical methods CA, ACCA, RJ and AS, are discussed and compared on the basis of synthetic (accurate) data to study their abilities under ideal situations. In addition a new local isotherm approximation method is introduced named LOGA. It is shown that all these semi-analytical methods can be derived mathematically using the same concept, namely an approximation of the local isotherm. This family of methods is denoted by LIA (Local Isotherm Approximation).

In Chapter 3 the derivation of the DEF method is analysed and a corresponding local isotherm approximation is derived. Also the derivation of the AS method is analysed in more detail than is done in chapter 1. The DEF method is compared to the LIA methods on the basis of accurate synthetic binding data.

It appears from chapter 2 and 3 that for all methods under consideration one or more derivatives of the binding function are required, which are hard to obtain from experimental data which are prone to experimental errors (94,95). A proper data processing is necessary to prevent spurious peaks in the distribution. In Chapter 4 .n adapted smoothing spline procedure (96-99) is presented to deal with this problem. It also allows for the determination of confidence intervals to indicate the uncertainty in the obtained distribution which results from experimental error. The method is applied to a set of Copper binding data on humic material measured by Hansen et al. (100).

In Chapter 5 it is shown how heterogeneity analysis can be used in combination with the master curve procedure of De Wit et al. (50,51). The master curve method

8

is applied to charge pH curves obtained for a fulvic acid measured by Dempsey and O'Melia (101). It is also shown how on the basis of the performed analysis a model can be developed that describes and predicts the charging behaviour.

In Chapter 6 the approach of Olson (90) to obtain first order rate constant distributions with the second order inverse laplace transform technique (LT2) is evaluated and the first and third order LT technique are presented. Subsequently the approach of Schwarzl and Staverman (SS) is elaborated. In analogy with the LIA methods the local decay function approximation (LODA) method is developed. In order to apply the method to experimental data the smoothing spline procedure developed for the determination of derivatives of the equilibrium binding function is used.

In Chapter 7 the newly developed LODA method is applied to the kinetics of dissociation of copper that is bound to dissolved organic matter. The original data were obtained by Olson. Results are compared with those obtained by Olson using the second order LT method.

Finally in Chapter 8 some challenges for future research are presented.

References

(1)   Van Straalen, N.M.; Denneman, C.A.J. *Ecotox. Environ. Saf.* 1989, *18*, 241-251.

(2)   Van de Meent, D.; Aldenberg, T.; Canton, J.H.; Van Gestel, C.A.M.; Slooff, W. *Streven naar waarden, achtergrondstudie ten behoeve van de nota "Milieukwalliteitsnormering water en bodem"*, RIVM rapport nr. 670101001, 1990 (in Dutch).

(3)   Berg, R. van den; *Bodem*, 1991, *1*, 113-119 (in Dutch).

(4)   Sposito, G. *Soil Sci. Soc. Am. J.* 1980, *44*, 652-654.

(5)   Gerritse, R.G.; Van Driel, W. *J. Environ. Qual.* 1984, *13*, 197-204.

(6)   Bolt, G.H.; Van Riemsdijk, W.H. in *Soil Chemistry. B. Physico Chemical Models*, Bolt, G.H., Ed., Elsevier, Amsterdam, 1982, pp. 459-504.

(7)   Van Riemsdijk, W.H.; Bolt, G.H.; Koopal, L.K. In *Interactions at the Soil Colloid - Soil Solution Interface*; Bolt, G.H.; De Boodt, M.F.; Hayes, M.H.B.; McBride, M.B., Eds.; Kluwer Academic Publishers: Dordrecht, 1991; pp 81-114.

(8)   Schindler, P.W. in *Heavy Metals in the Environment*, Vernet, J.-P., Ed., Trace Metals in the Environment 1, Elsevier, Amsterdam, 1991, 95-124.

(9)   Gupta, S.K. in *Heavy Metals in the Environment*, Vernet, J.-P., Ed., Trace Metals in the Environment 1, Elsevier, Amsterdam, 1991, 55-66.

(10)   Garcia Miragaya, J.; Page, A.L. *Water, Air, Soil Pollution* 1978, *9*, 289-299.

(11)   Chardon, W.J. *Mobiliteit van cadmium in de bodem*, Bodembescherming no 37, Staatsuitgverij, Den Haag, 1984, pp 197.

(12)   Christensen, T.H. *Water, Air, Soil Pollution* **1984**, *21*, 105-114.

(13)   Christensen, T.H. *Water, Air, Soil Pollution* **1987**, *34*, 305-314.

(14)   Bowden, J.W.; Posner, A.M.; Quirk, J.P. *Aust. J. Soil Res.* **1977**, *15*, 121-136.

(15)   Davis, J.A.; James, R.O.; Leckie, J.O. *J. Colloid Interface Sci.* **1978**, *63*, 481-499.

(16)   Kinniburgh, D.G.; Barker, J.A.; Whitfield, M. *J. Colloid Interface Sci.* **1983**, *95*, 370-384.

(17)   Koopal, L.K.; Van Riemsdijk, W.H.; Roffey, M.G. *J. Colloid Interface Sci.* **1987**, *118*, 117-136.

(18)   Hiemstra, T.; Van Riemsdijk, De Wit, J.C.M. *J. Colloid Interface Sci.* **1989**, *133*, 105-117.

(19)   Hiemstra, T.; Van Riemsdijk, W.H.; Bolt, G. *J. Colloid Interface Sci.* **1989**, *133*, 91-104.

(20)   Dzombak, D.A.; Morel, F.M.M. *Surface Complexation Modeling. Hydrous Ferric Oxide*, Wiley, New York, 1990, pp 393.

(21)   Schindler, P.W.; Sposito, G. in *Interactions at the Soil Colloid - Soil Solution Interface*, Bolt, G.H.; De Boodt, M.F.; Hayes, M.H.B.; McBride, M.B., Kluwer Academic Publishers, Dordrecht, 1991, Chapter 4, 115-145.

(22)   Gaines, G.L.; Thomas, H.C. *J. Chem. Physics.* **1952**, *21*, 714-718.

(23)   Bolt, G.H. *Neth. J. Agric. Sci.* **1967**, *15*, 81-103.

(24)   Tiller, K.G.; Gerth, J.; Brummer, G. *Geoderma* **1984**, *34*, 1-16.

(25)   Ziper, C.; Komarneni, S.; Baker, D.E. *Soil Sci. Soc. Am. J.* **1988**, *52*, 49-53.

(26)   Gaston, L.A.; Selim, H.M. *Soil Sci. Soc. Am. J.* **1990**, *54*, 1525-1530

(27)   McBride, M.B. in *Interactions at the Soil Colloid - Soil Solution Interface*, Bolt, G.H.; De Boodt, M.F.; Hayes, M.H.B.; McBride, M.B., Kluwer Academic Publishers, Dordrecht, 1991, Chapter 5, 149-176

(28)   Saar, R.A.; Weber, J.H. *Can. J. Chem.* **1979**, *57*, 1263-1268.

(29)   Perdue, E.M.; Lytle, C.R. In *Aquatic and Terrestrial Humic Materials*; Christman, R.F; Gjessing, E.T., Eds.; Ann Arbor Science: Ann Arbor, 1983; Chapter XIV.

(30)   Cabaniss, S.E.; Shuman, M.S.; Collins, B.J. In *Complexation of Trace Metals in Natural Waters*; Kramer, C.J.M.; Duinker, J.C., Eds.; Martinus Nijhoff/ Dr.W. Junk Publishers: The Hague, 1984, pp 165-179.

(31)   Perdue, E.M. *In Humic substances in soil, sediment and water: chemistry, isolation and characterization*; Aiken, G.R.; Mcknight, D.M.; Wershaw, R.L.; Maccarthy, P., Eds.; Wiley Interscience: New York, 1985, pp 493-526.

(32)   Sposito, G. *CRC Crit. Rev. Environ. Control* **1986**, *16*, 193-229.

(33)   Ephraim, J.; Alegret, S.; Mathuthu, A.; Bicking, M.; Malcolm, R.L.; Marinsky, J.A. *Environ. Sci. Technol.* **1986**, *20*, 354-366.

(34)   Buffle, J. *Complexation Reactions in Aquatic Systems: An Analytical Approach*. Ellis Horwood: Chichester, 1988.

10

(35)   Hering, J.G.; Morel, F.M.M. *Environ. Sci. Technol.* **1988**, *22*, 1237-1243.

(36)   Westall, J.; Hohl, H. *Adv. Colloid Interface Sci.* **1980**, *12*, 265-294.

(37)   Benjamin, M.M.; Leckie, J.O. *J. Colloid Interface Sci.* **1981**, *83*, 410-419.

(38)   Schenck, C.V.; Dillard, J.G. *J. Colloid Interface Sci.* **1983**, *95*, 389-409.

(39)   Huang, C.P.; Hsiesh, Y.S.; Park, S.W.; Ozden Corapcioglu, M.; Bowers, A.R.; Elliot, H.A. in *Metals, Speciation, Separation and Recovery*, Patterson, J.W; Passino, R., Eds. Lewis Publishers, Michigan, 1987.

(40)   Egozy, Y. *Clays and Clay Minerals.* **1980**, *28*, 311-318.

(41)   Inskeep, W.P.; Baham, J. *Soil Sci. Soc. Am. J.* **1983**, *47*, 660-665.

(42)   Puls, R.W.; Bohn, H.L. *Soil Sci. Soc. Am. J.* **1988**, *52*, 1289-1292.

(43)   Hirsch, D.; Nir, S.; Banin, A. *Soil Sci. Soc. Am. J.* **1989**, *53*, 716-721.

(44)   Tanford, C. *Physical Chemistry of Macromolecules*, Wiley, New York, 1961.

(45)   Sillén, L.G.; Martell, A.E. *Stability Constants of Metal Ion Complexes*, The Chem. Soc., London, 1964.

(46)   Stevenson, F.J. *Humus Chemistry. Genesis, Composition, Reactions* Wiley-Interscience, New York, 1982.

(47)   Gamble, D.S. *Canadian J. Chem.* **1970**, *48*, 2662-2669.

(48)   Gamble, D.S.; Underdown, A.W.; Langford, C.H. *Anal. Chem.* **1980**, *52*, 1901-1908.

(49)   De Wit, J.C.M., Ph.D. thesis, Agricultural University Wageningen, 1992, in prep.

(50)   De Wit, J.C.M.; Van Riemsdijk, W.H.; Nederlof, M.M.; Kinniburgh, D.G.; Koopal, L.K. *Anal. Chim. Acta* **1990**, *232*, 189-207.

(51)   De Wit, J.C.M.; Nederlof, M.M.; Van Riemsdijk, W.H.; Koopal, L.K. *Water Air and Soil Pollution*, **1991**, *57-58*, 339-349.

(52)   Jaroniec, M. *Adv. Colloid Interface Sci.* **1983**, *18*, 149-225.

(53)   Jaroniec, M.; Bräuer, P. *Surf. Sci. Rep.* **1986**, *6*, 65-117.

(54)   Dzombak, D.A.; Fish, W.; Morel, F.M.M. *Environ. Sci. Technol.* **1986**, *20*, 669-675.

(55)   Noble, B. In "The State of the Art in Numerical Analysis" (D. Jacobs, Ed.) . Academic Press, p. 915 (1979).

(56)   Baker, The numerical treatment of differential equations. Oxford University Press, Oxford (1977).

(57)   Simms, H.S. *J. Am. Chem. Soc.* **1926**, *48*, 1239-1250.

(58)   Scatchard, G. *Ann. N.Y. Acad. Sci.* **1949**, *51*, 660-672.

(59)   Nolle, A.W. *J. Polym. Sci.* **1950**, *5*, 1-54.

(60)   Schwarzl, F.; Staverman, A.J. *Physica* **1952**, *18*, 791-798.

(61)   Schwarzl, F.; Staverman, A.J. *Appl. Sci. Res.* **1953**, *4*, 127-141.

(62)   Ninomiya, K.; Ferry, J.D. *J. Colloid Interface Sci.* **1959**, *14*, 36-48.

(63)   Hunston D.L. *Anal. Biochem.* **1975**, *63*, 99-109.

(64) Thakur, A.K.; Munson, P.J.; Hunston, D.L.; Rodbard, D. *Anal. Biochem.* **1980**, *103*, 240-254.

(65) Shuman, M.S.; Collins, B.J.; Fitzgerald, P.J.; Olson, D.L. In *Aquatic and Terrestrial Humic Materials*; Christman, R.F.; Gjessing, E.T., Eds.; Ann Arbor Science: Ann Arbor, 1983; Chapter XVII.

(66) Langford, C.H.; Gamble, D.S.; Underdown, A.W.; LEE, S. In *Aquatic and Terrestrial Humic Materials*; Christman, R.F.; Gjessing, E.T., Eds.; Ann Arbor Science: Ann Arbor, 1983; Chapter XI.

(67) Gamble, D.S.; Langford, C.H. *Environ. Sci. Technol.* **1988**, *22*, 1325-1336.

(68) Altmann, R.S.; Buffle, J. *Geochim. Cosmochim. Acta* **1988**, *52*, 1505-1519.

(69) Buffle, J.; Altmann, R.S.; Filella, M.; Tessier, A. *Geochim. Cosmochim. Acta* **1990**, *54*, 1535-1553.

(70) Roginsky, S.S. *Adsorption catalysis on heterogeneous surfaces.* Academy of Sciences U.S.S.R.: Moscow, 1948; (in Russian).

(71) Harris, L.B. *Surface Sci.* **1968**, *10*, 129-145.

(72) Cerofolini, G.F. *Surf. Sci.* **1971**, *24*, 391-403.

(73) Cerofolini, G.F. *Thin Solid Films* **1974**, *23*, 129-152.

(74) Hsu, C.C.; Wojciechowski, B.W.; Rudzinski, W.; Narkiewicz, J. *J. Colloid Interface Sci.* **1978**, *67*, 292-303.

(75) Rudzinski, W.; Jagiello, J.; Grillet, Y. *J. Colloid Interface Sci.* **1982**, *87*, 478-491.

(76) Ross, S. and Morrison, I.D., Surface Sci. **1975**, *52*, 103.

(77) Sacher, R.S. and Morrison, I.D., J. Colloid Interface Sci. **1979**, *70*, 153.

(78) Papenhuijzen, J. and Koopal, L.K., In *Adsorption from solution* (Ottewill, R.H., Rochester, C.H. and Smith, A.L. Eds.), Academic Press London, 1983, p. 211.

(79) House, W.A. In *Colloid Science,* Specialist Periodical Report 4; Everett, D.H., Ed.; Royal Soc. Chem., London, 1983, pp 1-58.

(80) Philips, D.L., J. Assoc. Comp. Mach. **1962**, *9*, 84-97.

(81) Tikhonov, A.N., Sov. Math. **1963**, *4*, 1035, 1624.

(82) Twomey, S., J. Assoc. Comp. Mach. **1963**, *10*, 97.

(83) House, W.A. *J. Colloid Interface Sci.* **1978**, *67*, 166-180.

(84) Koopal, L.K.; Vos, C.H. *Colloids Surf.* **1985**, *14*, 87-95.

(85) Vos, C.H.; Koopal, L.K. *J. Colloid Interface Sci.* **1985**, *105*, 183-196.

(86) Hoffman, M.R. *Environ. Sci. Technol.* **1981**, *15*, 345-353.

(87) Anderson, M.A.; Morel, F.M.M. *Limnol. Oceanogr.* **1983**, *27*, 789-813.

(88) Lavigne, J.A.; Langford, C.H.; Mak, M.K.S. *Anal. Chem.* **1987**, *59*, 2616-2620.

(89) Hering, J.G.; Morel, M.M. *Environ. Sci. Technol.*, **1990**, *24*, 242-252.

(90) Olson, D.L.; Shuman, M.S. *Anal. Chem.* **1983**, *55*, 1103-1107.

(91) Doetsch, G. *Theorie und Anwendung der Laplace Transformation*; Springer: Berlin, 1937.

(92) Widder, D.V. *The Laplace Transform;* Princeton University Press: Princeton, 1946, p 406.

12

(93)   Olson, D.L.; Shuman, M.S. *Geochim. Cosmochim. Acta*, **1985**, *49*, 1371.

(94)   Turner, D.R.; Varney, M.S.; Whitfield, M.; Mantoura, R.F.C.; Riley, J.P. *Geochim. Cosmochim. Acta* **1986**, *50*, 289-297.

(95)   Fish, W.; Dzombak, D.A.; Morel, F.M.M. *Environ. Sci. Tech.* **1986**, *20*, 676-683.

(96)   Reinsch, C.H. *Numer. Math.* **1967**, *10*, 177-183.

(97)   Craven, P.; Wahba, G. *Numer. Math.* **1979**, *31*, 377-403.

(98)   Silverman, B.W. *J.R. Statist. Soc. B.* **1985**, *47*, 1-52.

(99)   Woltring, H.J. *Adv. Eng. Software* **1986**, *8*, 104-107.

(100)   Hansen, A.M.; Leckie, J.O.; Mandelli, E.F.; Altmann, R.S. *Environ. Sci. Technol.* **1990**, *24*, 683-688.

(101)   Dempsey, B.A.; O'Melia, C.R. In *Aquatic and Terrestrial Humic Materials*; Christman, R.F., Gjessing, E.T., Eds.; Ann Arbor Science: Ann Arbor, MI, 1983; Chapter XII, pp 239-273.

CHAPTER 2

Determination of Adsorption Affinity Distributions: A General Framework for Methods Related to Local Isotherm Approximations

Abstract

A family of methods is presented for the determination of the adsorption affinity distribution function for a heterogeneous surface from single component adsorption data. It is possible to deal with different types of local isotherms and with random and patchwise heterogeneity. The general concept is that an approximation of the local isotherm is used to solve the integral equation analytically for the distribution function without making a priori assumptions about the distribution. The method is worked out for FFG type equations as local isotherm with an interaction parameter incorporated. Examples are given for the Langmuir local isotherm. The simplest form of this family of local isotherm approximations (LIA) is the step function (STEP), known as the condensation approximation (CA). The first order Affinity Spectrum (AS_1) strongly resembles the CA distribution. Both methods result in general in a too wide affinity distribution. An alternative is the use of a linear approximation (LINA) of the local isotherm. These LINA methods cause a widening and an asymmetric deformation of the true distribution. The asymptotically correct condensation approximation (ACCA) is a member of this group. A substantially better approximation is achieved by considering the local isotherm and its approximations on a logarithmic concentration (or mole fraction) scale (LOGA). The distributions obtained with the Rudzinski Jagiello (RJ) method and the second order affinity spectrum (AS_2) method can be interpreted as members of the LOGA group. Parameter optimization in the LOGA case has resulted in two other solutions which are better approximations than the RJ and AS_2 method.

Introduction

Adsorbents both in natural systems and in many industrial processes are chemically heterogeneous. To describe the overall adsorption on such surfaces the distribution of affinity constants is needed in combination with a model for a homogeneous 'sub-surface' (1-3). In practice, analytical expressions for the overall isotherm are often used, which are based on a priori assumptions about the type of local isotherm and the type of distribution (4-8). When the distribution is known and roughly fits the presumed function, there is no objection against fitting the parameters of such an analytical isotherm to experimental data. However when no information on the distribution is present the procedure is entirely empirical and the coefficients cannot be interpreted physically.

In that case the distribution function should be determined first. In addition, for complicated distributions (e.g., multi peak distributions), analytical expressions of the overall isotherm are not available. So methods are needed to obtain the distribution function without making a priori assumptions about its shape. It is the purpose of this paper to discuss some of these methods.

Adsorption on a heterogeneous surface can be considered as adsorption on a collection of homogeneous subsurfaces. The homogeneous subsurface being an ensemble of sites for which the standard Gibbs energy of adsorption, or the intrinsic affinity, is a constant. In the presence of lateral interactions the standard Gibbs energy of adsorption, representing the surface-adsorbate interactions, is not the only contribution to the adsorption Gibbs energy, the lateral interactions also contribute and have to be accounted for separately. The way this is done depends on the type of heterogeneity. General practice is to consider two limiting situations, random and patchwise heterogeneity (1). For a random heterogeneous surface the lateral interactions are taken into account over the entire surface. For a patchwise heterogeneous surface the lateral interactions are taken into account per patch. In the latter case boundary effects are neglected.

By incorporating the adsorbate-adsorbate interactions separately from the adsorbate-surface interactions it is possible to retain the standard Gibbs energy of adsorption, or the intrinsic affinity for each homogeneous sub-surface, as a separate parameter. When lateral interactions are not considered explicitly only an 'apparent' affinity distribution can be found.

17

In principle, for a continuous distribution of intrinsic affinities, the summation over all homogeneous subsurfaces can be done by integrating over all possible values of the intrinsic affinity, K, leading to (1-3):

$$\Theta(x) = \int_\Delta \theta(K,x,C)f(\log K)\,d\log K \tag{1}$$

In eq 1 $\Theta(x)$ is the overall adsorption, $\theta(K,x,C)$ is the local isotherm describing the adsorption on an ensemble of 'equal intrinsic affinity' sites, $f(\log K)$ the distribution of the intrinsic affinities and Δ is the range of the $\log K$ values.

To obtain $f(\log K)$ from adsorption data it should be realized that equation 1 is a Fredholm integral equation of the first kind. Solution of such an equation with respect to $f(\log K)$ when both $\Theta(x)$ and $\theta(K,x,C)$ are known is a difficult problem (9,10). In view of this, two main routes have been followed in literature to solve eq 1 for $f(\log K)$. The first group of methods is concerned with complicated special numerical methods, which consider the instability of the Fredholm equation explicitly. Examples of these methods are Singular Value Decomposition (SVD) (11,12), regularization (13-17) and to a lesser extent CAEDMON (18-20). The second group of methods uses specific approximations of the local isotherm equation so that relatively simple analytical expressions can be obtained for the distribution functions at the expense of deviations with respect to the local isotherm. In view of the uncertainties involved in the choice of an exact local isotherm this disadvantage may not be too serious. The advantage is that a stable analytical solution for $f(\log K)$ is obtained without much effort.

A second advantage of these Local Isotherm Approximation or LIA methods is that one point of the isotherm and its direct neighbourhood corresponds with one point in the distribution function. In other words, not the whole isotherm is involved in the computation of one point of the distribution function. Consequently, when only a part of the overall isotherm is available the distribution function can still be obtained in this range. This is an important aspect in the case of the study of natural adsorbents where often only a relatively small 'window of data' is available. Application of the numerical methods to a limited window of data is not straight-forward.

18

A third advantage of the LIA approach is that, by adjusting the parameters, different local isotherms can be used without changing the analytical expressions of the distribution function.

In the present paper we restrict ourselves to methods which use a local isotherm approximation. Examples of LIA are the Condensation Approximation (CA) (21,22) and the Asymptotically Correct Condensation Approximation (ACCA) given by Cerofolini (23,24). Alternative methods which lead to similar expressions for the distribution function are the Rudzinski Jagiello (RJ) method (25-27) and the Affinity Spectrum method (AS) (28-30). A brief overview of these methods is given by Nederlof et al. (31). It will be shown that the results of the RJ and AS method correspond with those obtained with specific local isotherm approximations.

Local Isotherm Equation

In order to solve $f(\log K)$ from eq 1 a local isotherm function is required. The present treatment is based on the following general equation for adsorption in a monolayer:

$$\theta(K,x,C) = \frac{KCx}{1+KCx} \tag{2}$$

where x is the mole fraction in the case of adsorption from solution or the relative pressure in the case of gas adsorption, K is the intrinsic affinity , which can be written as $\log K = -0.4343\Delta g_a^\circ/RT$, and C a factor accounting for the lateral interactions or more in general the nonideality. With respect to Δg_a° it should be noted that Δg_a° does not contain the ideal configurational entropy for localized adsorption, which is retained in the form of the local isotherm. However Δg_a° contains other entropy contributions such as the 'thermal' entropy. In the case of gas adsorption on surfaces without micropores these contributions are in general small and then Δg_a° is dominated by the enthalpic interactions. For adsorption from solution often the nonconfigurational entropy can not be neglected and Δg_a° is a true Gibbs energy (20).

19

Expressions for the function C can, for instance, be derived on the basis of a 'mean field' or 'Bragg Williams' approximation taking into account nearest neighbour interactions only. In that case the well-known Frumkin-Fowler-Guggenheim (FFG) equation (32-34) results and for C we may write:

$$C = \exp(-\omega\theta') \qquad (3)$$

where ω represents a net standard Gibbs energy of lateral interaction. For random heterogeneous surfaces $\theta' = \Theta$, for patchwise surfaces $\theta' = \theta$. In general ω should be seen as an adjustable constant for a certain adsorbate system containing both enthalpic and entropic contributions. For $\omega = 0$ (or $C = 1$) eq 2 reduces to the Langmuir equation. In that case the type of heterogeneity is immaterial.

For charged surfaces C also includes the effects of the electric field (7,35). In the case of mobile adsorption C should also include a factor accounting for the extra configuration entropy so that the Hill De Boer equation results (36,37). In conclusion eq 2 is rather 'flexible' and well suited as a simple equation for either gas adsorption in the monolayer region or for adsorption from solution.

Based on the measured adsorption data and the expression for C eq 1 can in principle be solved with respect to $f(\log K)$. With eq 2 as local isotherm in general only a numerical solution is possible, even if $C = 1$ (1). For analytical solutions eq 2 has to be replaced by a suitable approximation. The various ways to approximate the local isotherm will be discussed in the next sections.

Local Isotherm Approximation (LIA) : General Concept

The basic principle of the LIA method is the subdivision of the local isotherm in two parts so that eq 1 is no longer a Fredholm equation of the first kind, but a combination of two Volterra integrals. Subjects of study are the type of function used to approximate the true local isotherm and the value of Kx where the local isotherm is to be subdivided. When the local isotherm is subdivided in two parts eq 1 for the overall isotherm can be written for each value of the mole fraction $x = x^*$ as:

20

$$\Theta(x^{*}) = \int_{0}^{\log K^{*}} \xi_1(K,C,x^{*}) f(\log K) \, d(\log K) +$$

$$\int_{\log K^{*}}^{+\infty} \xi_2(K,C,x^{*}) f(\log K) \, d(\log K) \tag{4}$$

The functions $\xi_1(K,C,x)$ and $\xi_2(K,C,x)$ are the approximations of the two parts of the local isotherm and $K^{*}x^{*}$ is the value of Kx at which the local isotherm is subdivided (the breakpoint value). For each chosen x^{*} the local coverage is a function of KC according to eq 2. Running through the whole range of $x = x^{*}$ from $\Theta = 0$ to $\Theta = 1$ automatically implies that the whole range of KC values is covered. Equation 4 can be solved for $f(\log K^{*})$. By using the relation between x^{*} and K^{*} derived from the breakpoint value, the distribution can be expressed as function of $\Theta(\log x)$, the overall isotherm.

General and convenient choices for ξ_1 and ξ_2 are respectively:

$$\xi_1 = \alpha_1(Kx)^{\beta_1} \tag{5a}$$

$$\xi_2 = 1 - \alpha_2(Kx)^{-\beta_2} \tag{5b}$$

The absence of C in these equations will be explained below. Introduction of these functions in equation 4 leads to :

$$\Theta(x^{*}) = \int_{0}^{\log K^{*}} \alpha_1(Kx^{*})^{\beta_1} f(\log K) \, d(\log K) + \int_{\log K^{*}}^{\infty} 1 \cdot f(\log K) \, d(\log K) +$$

$$- \int_{\log K^{*}}^{\infty} \alpha_2(Kx^{*})^{-\beta_2} f(\log K) \, d(\log K) \tag{6}$$

The terms $\alpha_i(x^{*})^{\beta_i}$ can be placed in front of the integral sign, since the mole fraction and the lateral interaction itself are independent from $\log K$. The expression for $f(\log K^{*})$ can now be solved analytically for appropriate values of α_i and β_i. Solutions

21

are given below for three types of local isotherm approximations. The first is a step function ($\alpha_1 = \alpha_2 = 0$), the second is a linear function until $\theta = 1$ is reached ($\alpha_1 = \alpha$ and $\alpha_2 = 0$), and the third is symmetrical in $\theta = 0.5$ on a logarithmic scale ($\alpha_1 = \alpha_2 = \alpha$ and $\beta_1 = \beta_2 = \beta$). In all cases the distribution function can be presented as a combination of derivatives of the overall isotherm with respect to $\log x$.

The values of the parameters α_i and β_i and $K^* x^*$ depend on the functional form of C and the type of heterogeneity. For random surfaces $C = C(\Theta)$, so that C and x can be combined in one parameter $x' = xC$. Substitution in eq 2 gives:

$$\theta_r = \frac{Kx'}{1 + Kx'} \tag{7}$$

In mathematical sense eq 7 is equivalent to eq 2 with $C = 1$. For this situation a series of solutions is presented in the next sections. The relation between $\log x$ and $\log K$ is in this case determined by $\log K = -\log x' = -\log x - \log C(\Theta)$. Hence, for a random surface, the effect of the lateral interactions, as represented by C, appears in the transformation of the $\log x$ axis into the $\log K$ axis only.

For patchwise surfaces $C = C(\theta)$ and the values of α_i, β_i and $K^* x^*$ will depend on C. To select the best parameter values it is useful to write the local isotherm as:

$$Kx = \frac{\theta_p}{(1 - \theta_p)} \frac{1}{C(\theta_p)} \tag{8}$$

and to compare this with the LIA in the form:

$$Kx = \left(\frac{\xi_1}{\alpha_1} \right)^{1/\beta_1} \tag{9a}$$

$$Kx = \left(\frac{1 - \xi_2}{\alpha_2} \right)^{-1/\beta_2} \tag{9b}$$

22

Once the values of α_i, β_i and K^*x^* are selected, the distribution as function of $\log x^*$ can be derived. The thus formulated LIA approach is quite general. The local isotherm can be approximated by adjusting the parameters α_i, β_i and the breakpoint value K^*x^*.

For each chosen local isotherm the fit with the LIA is optimized by adjusting the breakpoint value K^*x^* and the parameters α_i and β_i if not chosen a priori. As criteria for the optimization of these parameters the Lagrangian Distance method (LD) and the method of Least Sum of Squares (LSS) will be used (23). The LD method minimizes the largest distance between the true local isotherm and its approximation, whereas the LSS method minimizes the square of the difference between the two isotherms, integrated over the whole x or $\log(x)$ range.

The application of the LIA method will, in principle, never lead to the correct distribution even with exact data. Harris (22) has formulated an equation which describes the relation between the true distribution and the approximating distribution:

$$f'(\log K') = \int_\Delta f(\log K)\Phi(\log K, \log K')\,\mathrm{d}(\log K) \qquad (10)$$

In eq 10 $f(\log K)$ is the true distribution function, $f'(\log K')$ is the approximation of the true distribution and $\Phi(\log K, \log K')$ is a weighting function depending on the chosen LIA. Hence, with eq 10 the effect of the approximation of a local isotherm can be shown. The better $\Phi(\log K, \log K')$ corresponds to the Dirac Delta function the better is the approximation. For a wide weighting function details of the true distribution function are smeared out.

Examples to Illustrate the Methods

In this paper various LIA methods are worked out on the basis of eq 2 with $C = 1$. The methods are illustrated by the analysis of four sets of synthetic data, because the true distribution should be known in order to be able to evaluate the results obtained with the different methods. We use exact data to show the result that can

23

be obtained under ideal conditions. A preliminary discussion of the treatment of experimental errors is given elsewhere (38). The first two data sets are generated using the Langmuir-Freundlich equation :

$$\Theta(x) = \frac{(\bar{K}x)^m}{1 + (\bar{K}x)^m} \tag{11}$$

In eq 11 $\bar{K}$ is a weighted average K -value corresponding with the maximum in the affinity distribution and m determines the width of the affinity distribution. Equation 11 is applied with $m = 0.9$ and $m = 0.4$ (Figure 1 a , curve A and B, respectively). The corresponding distributions (4,5) are shown in Figure 1b, curves A and B, respectively. The third data set is based on the Generalized Freundlich equation :

$$\Theta(x) = \left(\frac{\bar{K}x}{1 + \bar{K}x} \right)^m \tag{12}$$
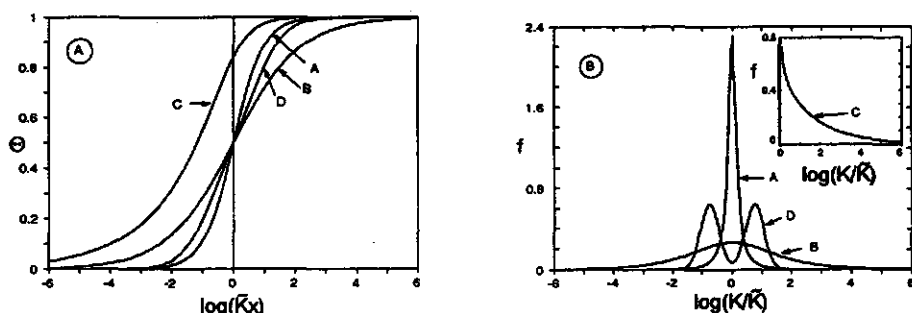

Figure 1a: Overall isotherms for four cases. A: Langmuir Freundlich isotherm (eq 11) with m=0.9. B: Langmuir Freundlich isotherm (eq 11) with m=0.4. C: Generalized Freundlich isotherm (eq 12) with m=0.25. D: The overall isotherm based on a bi-gaussian distribution (eq 13) with $\alpha_1 = \alpha_2 = 1.$, $\beta_1 = \beta_2 = 1.$ and $\Delta \log K = 1.5$.

Figure 1b: The affinity distributions corresponding to the overall isotherms of Fig. 1a.

24

using $m = 0.25$ (see Figure 1a, curve C). $\breve{K}$ and m have the same meaning as in eq 11. Equation 12 is based on a very asymmetric distribution, which has an asymptote at $\log(K/\breve{K}) = 0$ (4,5) (see Figure 1b, curve C). The fourth data set is obtained by inserting a bi-gaussian distribution in combination with eq 2 ($C = 1$) in the overall adsorption equation (1). The equation for such a bi-gaussian distribution is:

$$f(\log K) = \frac{1}{\sqrt{\pi}}\left(\frac{\gamma_1}{\sqrt{\nu_1}} + \frac{\gamma_2}{\sqrt{\nu_2}}\right)^{-1}\left[\gamma_1 \exp\left\{-\nu_1\left(\log\frac{K}{K_1}\right)^2\right\} + \gamma_2 \exp\left\{-\nu_2\left(\log\frac{K}{K_2}\right)^2\right\}\right] \quad (13)$$

In eq 13 the values of γ_i are the relative weights of the peaks, ν_i determine the widths and K_i represent the positions of the peaks. The distribution is shown in Figure 1b (D) with $\gamma_1 = \gamma_2, \nu_1 = \nu_2 = 1$. and $\Delta K = 1.5$. The resulting adsorption isotherm is presented in Figure 1a (D), where $\log\breve{K} = 0.5(\log K_1 + \log K_2)$.

LIA Using a Step Function (STEP)

Condensation Approximation

Roginsky (21) and later Harris (22) introduced the Condensation Approximation (CA) in which the local isotherm is replaced by a step function. For the Langmuir local isotherm this approximation is rather poor, but for more steep local isotherms this approximation becomes much better. In terms of our general approximate local isotherm (eq 5) a step function results for $\alpha_1 = 0$ and $\alpha_2 = 0$ and the local isotherm approximation can be written as (Figure 2):

$$\xi(K,x) = 0 \qquad \text{for} \qquad Kx \leq K^*x^* \qquad (14)$$

$$\xi(K,x) = 1 \qquad \text{for} \qquad Kx > K^*x^*$$

In equation 14 K^*x^* is the point at which the isotherm is subdivided. The value of $\theta^*(K^*x^*)$ can be found by both the LD method and the LSS method (24). Both result in $\theta^* = 0.5$ and thus in $K^*x^* = 1$. This determines at the same time the relation
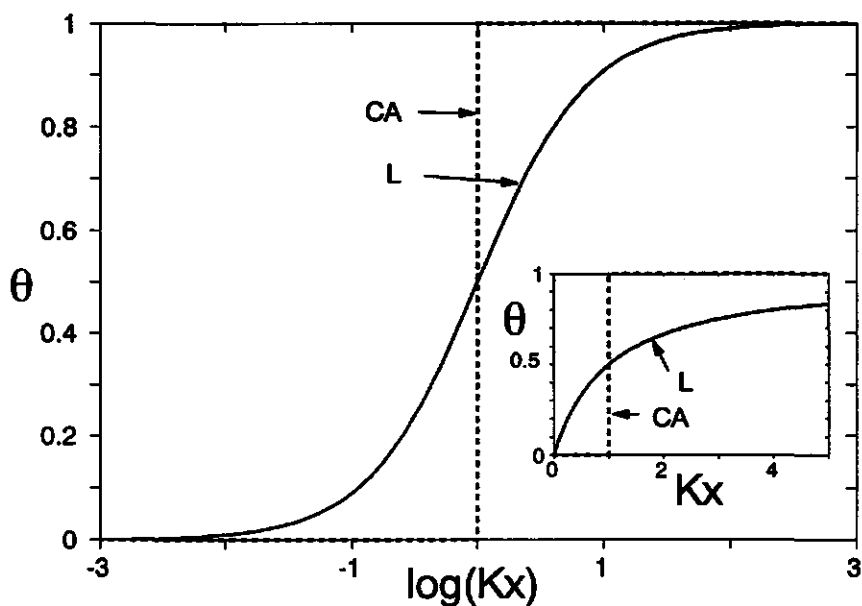
25

Figure 2: The CA isotherm approximation and the Langmuir local isotherm (L) as a function of log(Kx) and of Kx (inset).

between K^* and x^*: $K^* = 1/x^*$. Taking $\alpha_i = 0$ in equation 6 leads to:

$$\Theta(x^*) = \int_{\log K^*}^{\infty} 1 . f(\log K) \, d(\log K) \tag{15}$$

Taking the first derivative of eq 15 to $\log K^*$ gives:

$$\frac{\partial \Theta(x^*)}{\partial \log K^*} = -f(\log K^*) \tag{16}$$

Transforming the $\log K^*$ to $\log x^*$ with $K^* = 1/x^*$ and leaving out the asterisks we obtain the final result:

26

$$f_{CA}(\log K) = \frac{\partial \Theta(x)}{\partial \log x} \qquad (17a)$$

$$\log K = -\log x \qquad (17b)$$

So the CA distribution is obtained by taking the first derivative of the adsorption isotherm with respect to $\log x$. Harris (22) has shown that in this case the weighting function in eq 10 is the first derivative of the true local isotherm to $\log K$. This is a bell-shaped function. The CA distribution can thus be seen as a weighted average of the real distribution, at each point the average involves a rather wide weighting function centred around $K = K^*$.

First Order Affinity Spectrum

The first order Affinity Spectrum method developed by Ninomiya and Ferry (28) was introduced for the calculation of the relaxation time spectrum of viscoelastic data. Though based on another principle in the derivation, it has a strong resemblance to the CA method:

$$f_{ASI}(\log K) = \frac{\Theta(ax) - \Theta(x/a)}{2 \log a} \qquad (18a)$$

$$\log K = -\log x \qquad (18b)$$

where a is a constant. Plotted as a function of $\log x$, $\Theta(ax)$ and $\Theta(x/a)$ are the same as $\Theta(x)$ but shifted over a distance of $\log a$ to the right and to the left, respectively. When the parameter $\log a$ tends to zero eq 18 gives exactly the same result as the CA method. According to the authors an advantage of the method is that eq 18 doesn't use derivatives but directly measured data, equally spaced with a distance $\log a$. However, discretization of eq 17 leads to the same equation, if the stepsize $\Delta \log x$ is denoted by $\log a$. When $\log a$ is larger than the interval between the measured data a smoothing effect is obtained.

The derivation of eq 18 is based on the principle that the closer the kernel (the local isotherm) of the Fredholm integral equation resembles the Dirac-Delta function, the more the distribution function corresponds to the (transformed) overall adsorption isotherm. The method uses a linear combination of overall isotherms in

27

such a way that the kernel, which is the linear combination of local isotherms, of the new Fredholm integral equation becomes a bell shaped function resembling the Dirac-Delta function. This bell-shaped function is mathematically equivalent to the weighting function in eq 10.

The first order affinity spectrum (AS_1) is thus simply a subtraction of two shifted overall isotherms, divided by the distance between them, which is equivalent to a numerical approximation of the first derivative of the overall isotherm with respect to $\log x$. Here $\log a$ is the stepsize in the numerical differentiation which need not to be the interval between measured data.
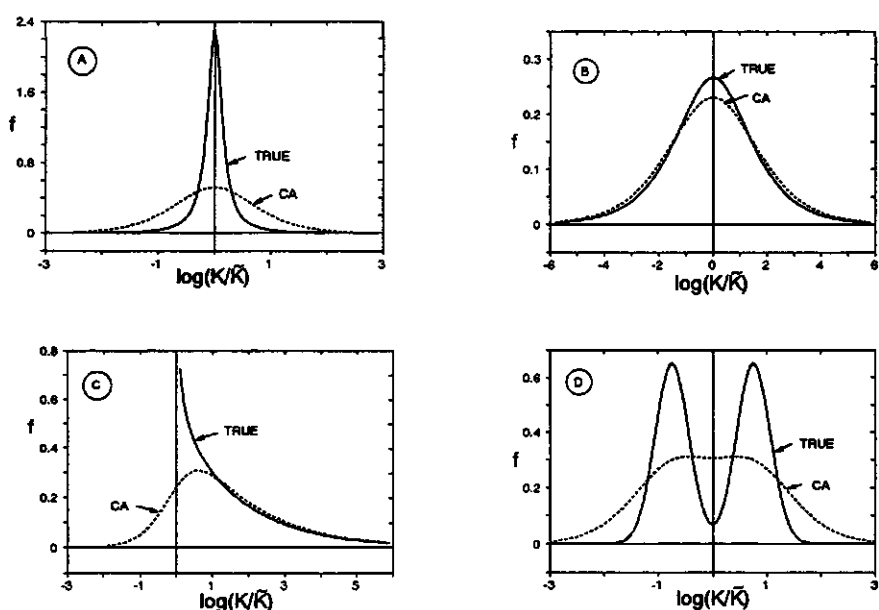

Figure 3: The CA approximations and the true affinity distributions of examples A, B, C and D (see Fig. 1a).

28

Comparison of $f_{CA}(logK)$ with $f(logK)$

To compare the CA result with the true distribution the four (example) isotherms have been analyzed. The result is shown in Figure 3.

For a nearly homogeneous situation the CA distribution is far too wide, see Fig. 3a. The bell-shaped weighting function as derived by Harris (22) has the effect that the distribution is flattened and details are lost. When the true distribution is rather wide this effect is much less pronounced and the CA method suffices (Figure 3b). Figure 3c, which shows the asymmetric distribution, also illustrates this. The steep part of the distribution is very badly recovered by the CA distribution, but the tail of the distribution is well described. In Figure 3d it is shown that two peaks which are closely adjacent to each other cannot be discriminated by the CA method. In general it can be concluded that sharp details in the distribution function are lost. The results of the first order affinity spectrum will be the same, except when $\log a$ is far larger than the stepsize used in the numerical differentiation at the CA-method. In that case the distribution is even more flattened than $f_{CA}(logK)$.

Linear Local Isotherm Approximation (LINA)

General form of the LINA distribution function

In a linear local isotherm Approximation (LINA) the first part of the local isotherm is replaced by a linear function with slope α from $\theta = 0$ to $\theta = 1$ and the second part by the horizontal function $\theta = 1$. In principle the isotherm could include a step from a certain value to $\theta = 1$, so that the first linear part doesn't have to reach $\theta = 1$, then the local isotherm becomes discontinuous. The problem with such approximations is that the distribution function can't be given explicitly. A differential equation in $f(logK)$ is then the result. We will not consider such cases here. This LINA local isotherm can be written as (Figure 4):

$$\xi(K,x) = \alpha Kx \qquad \text{for} \qquad Kx \le K^*x^* \qquad (19)$$

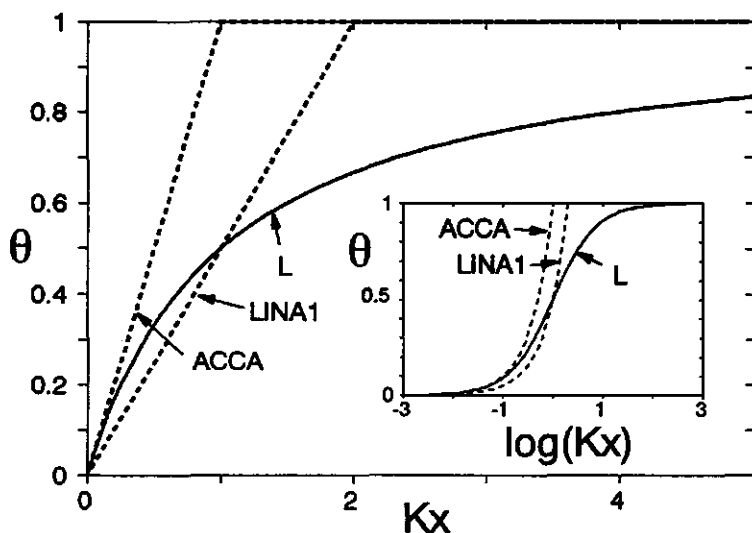$$\xi(K,x) = 1 \qquad \text{for} \qquad Kx > K^*x^*$$

Figure 4: The ACCA and LINA₁ isotherm approximations and the Langmuir local isotherm (L) as a function of Kx and of log(Kx) (inset).

Since we want the linear part of the approximate isotherm to reach $\theta = 1$, the point where the isotherm is subdivided is at $K^*x^* = 1/\alpha$. In terms of the general approximate local isotherm equation (eq 5) LINA corresponds with $\alpha_1 = \alpha$, $\beta_1 = 1$ and $\alpha_2 = 0$. Using these parameters eq 6 becomes:

$$\Theta(x^*) = \int_0^{\log K^*} \alpha K x^* f(\log K)\, d(\log K) + \int_{\log K^*}^{\infty} f(\log K)\, d(\log K) \qquad (20)$$

In eq 20 x^* can be replaced by $1/\alpha K^*$ and put in front of the integral sign. To find an expression for the distribution function we proceed by differentiating equation 20 with respect to $\log K^*$:

30

$$\frac{\partial \Theta(x^*)}{\partial \log K^*} = -\frac{1}{0.4343K^*} \int_0^{\log K^*} Kf(\log K)\,d(\log K) \tag{21}$$

Multiplication of both sides of eq 21 by -0.4343 followed by a second differentiation with respect to $\log K^*$, and using eq 21 again, results in:

$$-0.4343\frac{\partial^2 \Theta(x^*)}{\partial \log K^{*2}} = f(\log K^*) + \frac{\partial \Theta(x^*)}{\partial \log K^*} \tag{22}$$

Replacing $\log K^*$ by $-\log(\alpha x^*)$ and leaving out the asterisks the distribution function is found as:

$$f_{LINA}(\log K) = \frac{\partial \Theta(x)}{\partial \log x} - 0.4343\frac{\partial^2 \Theta(x)}{\partial \log x^2} \tag{23a}$$

$$\log K = -\log(\alpha x) \tag{23b}$$

On the $\log(Kx)$ scale the factor α means a shift of the local isotherm approximation over a distance of $\log \alpha$.

The selection of a value for α depends on the actual local isotherm. A well-known solution is the so called Asymptotically Correct Approximation (ACCA) treated below. A general advantage of LINA over CA is that all sites are gradually covered.

Asymptotically Correct Condensation Approximation (ACCA)

The Asymptotically Correct Condensation Approximation (23), is a special case of the LINA method with $\alpha = 1$:

$$f_{ACCA}(\log K) = \frac{\partial \Theta(x)}{\partial \log x} - 0.4343\frac{\partial^2 \Theta(x)}{\partial \log x^2} \tag{24a}$$

$$\log K = -\log x \tag{24b}$$

31

The advantage of the ACCA is that in the Henry region, i.e., for very low mole fractions or surface coverages, the isotherm approximation corresponds with the Langmuir local isotherm. In other words the approximation is asymptotically correct. A disadvantage is that for higher concentrations a relatively poor approximation of the local isotherm results.

Cerofolini (24) remarks already that the ACCA distribution is sharper than the CA distribution but that the ACCA distribution is not centred on the correct value of the adsorption energy (see Figure 5). As stated above, varying the slope of the linear part can shift the distribution to a better position, the shape of the distribution however remains unchanged. Optimization of this slope will be treated below.

Optimization of the slope of the linear isotherm

Equation 23 provides the general solution for the LINA distribution, the choice of α should be such that the linear isotherm corresponds as close as possible with the true local isotherm. However, several criteria, leading to different values of α, can be used to find the optimal slope of the linear isotherm . So the actual choice of α is somewhat arbitrary. Both the LSS method and the LD method to obtain α will be discussed in somewhat more detail. For a linear Kx scale the LSS method leads to the root of the following function :

$$-2\ln\left(1 + \frac{1}{\alpha}\right) + \frac{6\alpha - 1}{3\alpha^2} = 0 \tag{25}$$

Solving equation 25 gives $\alpha \approx 0.3$. The LSS method used on a $\log(Kx)$ scale, which pays more attention to the low mole fraction range, results in :

$$2\ln\left(1 + \frac{1}{\alpha}\right) - \frac{1}{\alpha} = 0 \tag{26}$$

from which $\alpha \approx 0.4$ is found.

Alternatively the LD method can be used. The LD is the largest distance on the θ -scale between the Langmuir and the linear isotherm. Because the approximating isotherm has two parts, minimizing one distance is not sufficient. A satisfactory

result is obtained by minimizing the sum of two LD's, one before the intersection point of both local isotherms and one at $Kx = 1/\alpha$. The resulting distances are, respectively:

$$\Delta_1 = -2\sqrt{\alpha} + (\alpha + 1) \qquad (27a)$$

$$\Delta_2 = \frac{\alpha}{\alpha + 1} \qquad (27b)$$

The value of α ($0 < \alpha < 1$) which minimizes the sum of these two distances is obtained by solving eq 28:

$$\sqrt{\alpha^5} - \sqrt{\alpha^4} + 2\sqrt{\alpha^3} - 2\sqrt{\alpha^2} + 2\sqrt{\alpha} - 1 = 0 \qquad (28)$$

This results in $\alpha \approx 0.5$. For $\alpha = 0.5$ the linear isotherm intersects the Langmuir isotherm at $\theta = 0.5$. This result is used for the examples. LINA using this value of α will be denoted by LINA$_1$.

Comparison of $f_{LINA_1}(logK)$ with $f(logK)$

In Figures 5a-5d the ACCA distributions and the LINA$_1$ distributions are presented for the four example isotherms. For all examples the LINA approximation leads to an asymmetric deformation of the true distribution. For the nearly homogeneous situation the obtained distribution is much too wide (Figure 5a), but somewhat sharper than the CA distribution. The ACCA distribution is centred around a lower affinity than the true distribution. The high affinity range is recovered reasonably well, because the ACCA isotherm is in the low mole fraction region asymptotically correct. The LINA$_1$ method shifts the distribution to higher affinities, so that the positions of the LINA$_1$ peak and that of the true distribution coincide approximately. However for high affinities the approximation is not as good as $f_{ACCA}(logK)$. Also for the symmetrical and wide distribution (Figure 5b) the LINA peaks are somewhat higher than the CA peaks. The LINA$_1$ method results in a distribution at a much better position than the ACCA does. Because of the asymmetric deformation of the distribution the LINA$_1$ result is hardly better than the CA distribution.
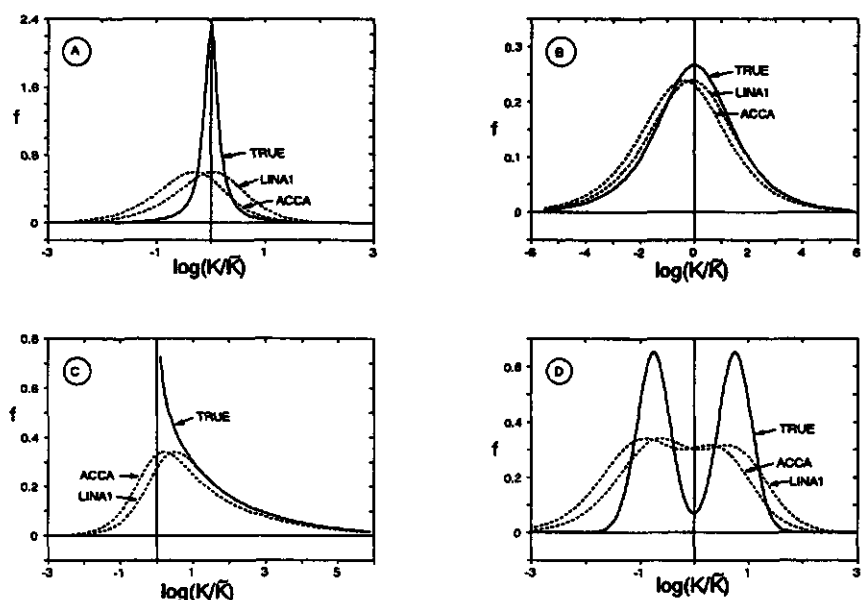
33

Figure 5: The ACCA and LINA₁ approximations and the true affinity distributions of examples A, B, C and D (see fig. 1a).

For the asymmetric example (Figure 5c) the overall result is hardly better than the CA approximation except that the peak of the ACCA distribution is somewhat sharper. LINA₁ gives a much better result. For the double Gaussian case (Figure 5d) the LINA₁ method introduces a shoulder in the distribution. Although the resemblance with the true distribution is still very poor, a hint is given that the large peak is built up from two smaller peaks.

Logarithmic Symmetrical Local Isotherm Approximation (LOGA)

General form of the distribution function for a continuous LOGA

Instead of using a linear Kx scale a logarithmic Kx scale also can be used. An important feature is that on the $\log(Kx)$ scale the Langmuir local isotherm is symmetrical in $\theta = 0.5$, while the LINA isotherm, for instance, is not. This provides the suggestion to consider a group of isotherm approximations that are also

symmetrical in $\theta = 0.5$. According to eq 10 a symmetrical LIA will lead to a symmetrical weighting function and thus also to a symmetrical deformation of the true distribution function. The general form of the isotherm approximation is obtained from equation 5 when $\alpha_1 = \alpha_2 = \alpha$ and $\beta_1 = \beta_2 = \beta$. The local isotherm can be written as :

$$\xi = \alpha(Kx)^\beta \qquad \text{for} \qquad Kx \leq K^*x^* \qquad (29)$$

$$\xi = 1 - \frac{\alpha}{(Kx)^\beta} \qquad \text{for} \qquad Kx > K^*x^*$$

The second part of the isotherm is the image of the first when mirrored in $\theta = 0.5$. For $\alpha \neq 0.5$ eq 29 leads to a distribution function which can be given only implicitly, because for $\alpha \neq 0.5$ the isotherm is discontinuous at $\theta = 0.5$. Restricting ourselves first to continuous local isotherms, an explicit analytical expression can be derived for $f_{LOGA}(\log K)$. For $\alpha = 0.5$ all isotherm approximations of eq 29 intersect the true local isotherm at $\theta = 0.5$ and are continuous at this point.

For the derivation of $f_{LOGA}(\log K)$ we will consider first the simple case that $\alpha = 0.5$ and $\beta = 1$. Using these parameters in the overall isotherm equation (eq 6) gives:

$$\Theta(x^*) = \int_0^{\log K^*} 0.5Kx^* f(\log K)\,d(\log K) +$$

$$\int_{\log K^*}^\infty f(\log K)\,d(\log K) - \int_{\log K^*}^\infty \frac{1}{2Kx^*} f(\log K)\,d(\log K) \qquad (30)$$

Since on the $\log(Kx)$ scale the true and the approximate local isotherm are symmetrical in $\theta = 0.5$ the isotherm is subdivided at $\theta^*(K^*x^*) = 0.5$, thus $K^*x^* = 1$. Using this, x^* can be replaced by $1/K^*$ and put in front of the integral signs. Equation 30 becomes:

$$\Theta(x^*) = \frac{1}{2K^*} \int_0^{\log K^*} Kf(\log K) \, d(\log K) +$$

$$\int_{\log K^*}^{\infty} f(\log K) \, d(\log K) - \frac{K^*}{2} \int_{\log K^*}^{\infty} \frac{1}{K} f(\log K) \, d(\log K) \qquad (31)$$

As our aim is to write the distribution function $f(\log K)$ explicitly, we have to get rid of the integrals in which the $f(\log K)$ is given implicitly. Taking successive derivatives of eq 31 with respect to $\log K^*$ it follows that the integrals, in which the distribution function is given implicitly, return in the same form with other constants in front of it. So it is possible to combine the derivatives to obtain an explicit equation in $f(\log K^*)$. The first derivative of equation 31 with respect to $\log K^*$ is:

$$\frac{\partial \Theta(x^*)}{\partial \log K^*} = -\frac{1}{2(0.4343)K^*} \int_0^{\log K^*} Kf(\log K) \, d(\log K) -$$

$$\frac{K^*}{2(0.4343)} \int_{\log K^*}^{\infty} \frac{1}{K} f(\log K) \, d(\log K) \qquad (32)$$

The second derivative of eq 31 with respect to $\log K^*$ is :

$$\frac{\partial^2 \Theta(x^*)}{\partial \log K^{*2}} = \frac{1}{2(0.4343)^2 K^*} \int_0^{\log K^*} Kf(\log K) \, d(\log K) +$$

$$-\frac{K^*}{2(0.4343)^2} \int_{\log K^*}^{\infty} \frac{1}{K} f(\log K) \, d(\log K) \qquad (33)$$

Finally the third derivative becomes:

$$\frac{\partial^3 \Theta(x^*)}{\partial \log K^{*3}} = -\frac{1}{2(0.4343)^3 K^*} \int_0^{\log K^*} Kf(\log K) \, d(\log K) +$$

$$-\frac{K^*}{2.(0.4343)^3} \int_{\log K^*}^{\infty} \frac{1}{K} f(\log K) \, d(\log K) +$$

$$\frac{1}{(0.4343)^2} f(\log K^*) \tag{34}$$

The combination of eqs 32 and 34 results in:

$$f(\log K^*) = -\frac{\partial \Theta(x^*)}{\partial \log K^*} + (0.4343)^2 \frac{\partial^3 \Theta(x^*)}{\partial \log K^{*3}} \tag{35}$$

Using the transformation $\partial \log(K^*) = -\partial \log(x^*)$ we can express equation 35 in terms of derivatives with respect to the mole fraction x :

$$f_{LOGA}(\log K) = \frac{\partial \Theta(x)}{\partial \log x} - 0.189 \frac{\partial^3 \Theta(x)}{\partial \log x^3} \tag{36a}$$

$$\log K = -\log x \tag{36b}$$

The derivation of the approximation with $\alpha = 0.5$ and a variable β in the local isotherm formula is completely analogous and leads to:

$$f_{LOGA}(\log K) = \frac{\partial \Theta(x)}{\partial \log x} - \frac{0.189}{\beta^2} \frac{\partial^3 \Theta(x)}{\partial \log x^3} \tag{37a}$$

$$\log K = -\log x \tag{37b}$$

To obtain close agreement between the approximate and the true local isotherm the value of β can be optimized. However for $\beta \neq 1$ negative parts in the distribution may occur. For the Langmuir isotherm the result is $\beta = 0.7$ for both the LSS and the LD methods. This approximation will be denoted as LOGA1. For $\beta = 1$ the dis-

tribution has no negative parts, provided that exact data are available. This can be demonstrated by assuming an overall isotherm equal to the local (Langmuir) isotherm.

Second Order Affinity Spectrum

For $\beta = 1$, $f_{LOGA}(\log K)$ approximates the distribution function found with the second order affinity spectrum method (AS$_2$) (29,30), when $\log a \rightarrow 0$. The AS$_2$ method is given by:

$$f_{AS2}(\log K) = \frac{\Theta(ax) - \Theta(x/a)}{2\log(a)} -$$

$$\frac{a}{(a-1)^2}\left\{\frac{\Theta(a^2x) - \Theta(x/a^2)) - 2(\Theta(ax) - \Theta(x/a))}{2\log(a)}\right\} \quad (38a)$$

$$\log K = -\log x \quad (38b)$$

When the stepsize $\log a$ approaches zero the affinity spectrum equation reduces to eq 36. The second order affinity spectrum method is thus for exact data equivalent to the LOGA method with $\beta = 1$ (Figure 6), when the derivatives are taken numerically. In principle higher order affinity spectra methods can also be derived, but the accuracy of the data is usually not sufficient. As in the AS$_1$ method $\log a$ is used in practice as a primitive smoothing factor and should be in the range 0.2-0.3 (29). However with exact data this aspect can be neglected.

The Rudzinski Jagiello method (RJ)

Hsu et al. (25) and later Rudzinski et Jagiello (26,27) also obtain a specific form of eq 37. In this case $\beta = \sqrt{6}/\pi \approx 0.79$ (Figure 6). This means that for nearly homogeneous systems the computed distribution may have negative parts. For the Langmuir local isotherm the result is:

$$f_{RJ}(\log K) = \frac{\partial\Theta(x)}{\partial\log x} - 0.310\frac{\partial^3\Theta(x)}{\partial\log x^3} \quad (39a)$$
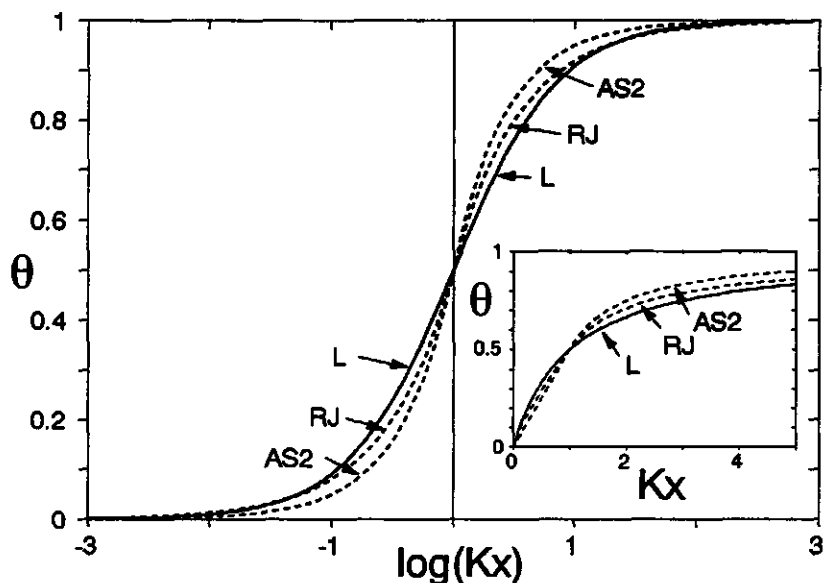
$$\log K = -\log x \quad (39b)$$

38

Figure 6: The AS$_2$ and RJ isotherm approximations and the Langmuir local isotherm (L) as a function of log(Kx) and of Kx (inset).

In the derivation of the RJ method no local isotherm approximation is assumed. The derivation starts with the formulation of Harris (22) for the relation between the CA approximation and the true distribution function given by eq 10. In this case the weighting function is a function of the first derivative of the Langmuir local isotherm with respect to $\log x$, which is a bell-shaped function. Then the true distribution under the integral sign is developed in a Taylor series, around $Kx = 1$. The terms of the series expansion include only the even derivatives of the true distribution function with respect to $\log K$, which terms can be placed in front of the integral signs. The remaining integrals can be solved analytically.

In this way the CA approximation is related to a series development in successive even derivatives of the true distribution function. When only the first term of the series is retained the resulting distribution equals the CA approximation. When also the second term of the series is considered the RJ method results. The second term in the series is a function of the second derivative of the true distribution

function which is approximated by the third derivative of the overall isotherm with respect to $-\log x$. In this way the RJ distribution is expressed as a combination of the first and the third derivative of the overall adsorption isotherm.

Comparison of $f_{AS2}(logK)$ and $f_{RJ}(logK)$ with $f(logK)$

In Figures 7a-7d the RJ and the AS_2 distributions can be compared.
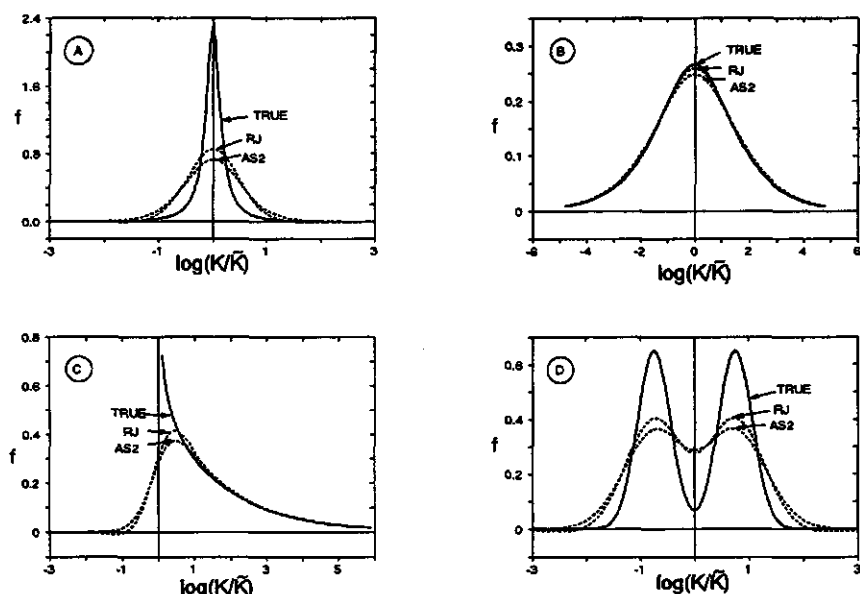

Figure 7: The AS_2 and RJ approximations and the true affinity distributions of examples A, B, C, D (see Fig. 1a).

Figure 7a shows that the RJ method results in a peak somewhat sharper than that of the AS_2, but renders also negative parts in the distribution, which are not realistic. However, the differences are small. The results are far better than the CA and LINA distributions. For a rather wide distribution the RJ method gives nearly perfect results (Figure 7b). In the case of the asymmetric distribution of Figure 7c the same remarks apply. The peak is again higher for RJ than for AS_2 at the cost of negative

40

parts in the distribution for the RJ method. For the bi-gaussian distribution (Figure 7d) the qualitative difference with the LINA method is again evident, both RJ and AS_2 show convincingly that there are two separate peaks.

The LOGA-method for discontinuous LIA

In the derivation of $f_{LOGA}(\log K)$ the parameter α was fixed at $\alpha = 0.5$. Loosening this restriction has the consequence that the local isotherm does intersect the true local isotherm at $\theta = 0.5$ discontinuously. When we use equation 29 with $\alpha \neq 0.5$ the resulting LOGA distribution is:
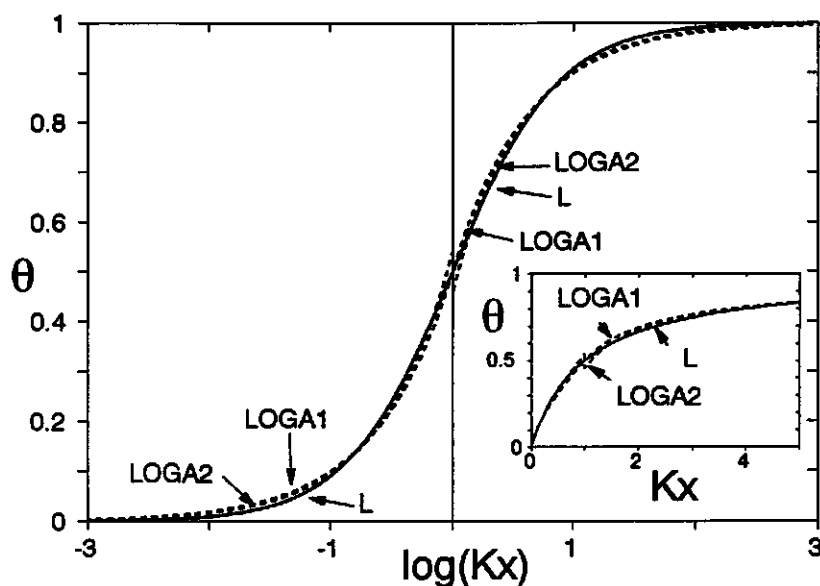

Figure 8: The $LOGA_1$ and $LOGA_2$ isotherm approximations and the Langmuir local isotherm as a function of $\log(Kx)$ and of Kx (inset).

$$f_{LOGA}(\log K) = \frac{\partial \Theta(x)}{\partial \log x} - \frac{0.189}{\beta^2} \frac{\partial^3 \Theta(x)}{\partial \log x^3} -$$

$$\frac{0.189(2\alpha - 1)}{\beta^2} \frac{\mathrm{d}^2 f_{LOGA}(\log K)}{\mathrm{d} \log K^2} \tag{40a}$$

$$\log K = -\log x \tag{40b}$$

So the approximation can only be given implicitly, in practice the distribution has to be determined iteratively starting with the distribution given by the first two parts of eq 40. The values of α en β (eq 29) can be optimized to get the best possible approximation of the Langmuir isotherm. For the LSS method the result is $\alpha = 0.54$ and $\beta = 0.75$, this will be denoted by LOGA2 (Figure 8).

Note that the isotherm jumps from $\theta = 0.54$ to $\theta = 0.46$, which is physically impossible. The aim of our optimization is, however, to obtain functions which approximate the Langmuir isotherm mathematically as close as possible.

The LD method results in $\alpha = 0.51$ and $\beta = 0.69$, which are left out in the further discussion because it is hardly an improvement with respect to the (explicit) LOGA1, which has coefficients $\alpha = 0.5$ and $\beta = 0.7$ (Figure 8).

Note that the CA method can be seen as a special case of LOGA.

Comparison of $f_{LOGA1}(\log K)$ and $f_{LOGA2}(\log K)$ with $f(\log K)$

To compare the best explicit LOGA (1; $\alpha = 0.5$ and $\beta = 0.7$) with the best implicit LOGA (2; $\alpha = 0.54$ and $\beta = 0.75$) some results are presented in Figures 9a-9d.

The LOGA1 method resembles the RJ distributions with the difference that in all distributions the peaks are slightly sharper and the negative parts are slightly larger. The LOGA2 method shows that the negative parts become less and that the peaks become still sharper. However the narrow peak of example A is still only moderately recovered (Figure 9a). The more heterogeneous example B (Figure 9b) gives perfect results. For the asymmetric example (C) the peak becomes somewhat sharper (Figure 9c) and the two peaks in Figure 9d are better resolved. The LOGA2 method is the best option within the LIA family presented, if exact data are available. The explicitly given LOGA1 method is the second best option, for which no iterations are needed.
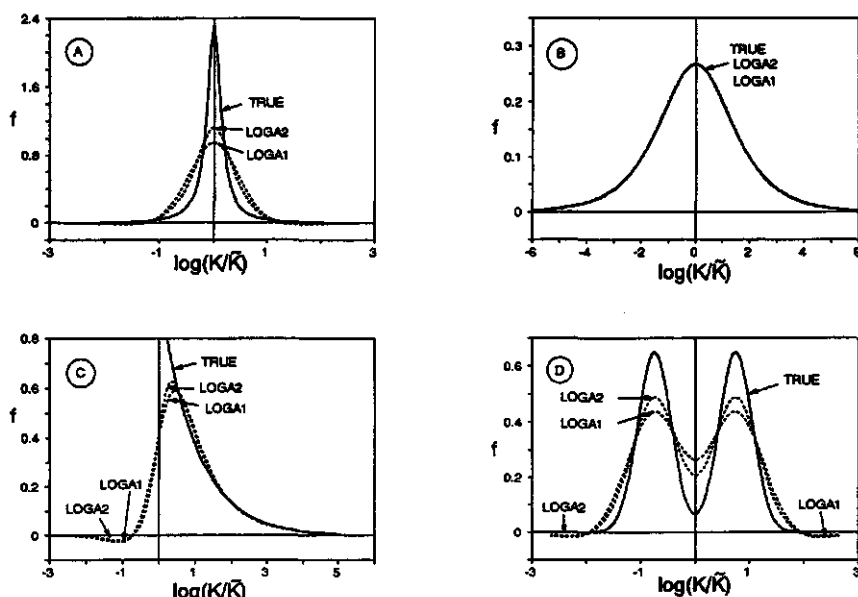
42

Figure 9: The LOGA$_1$ and LOGA$_2$ approximations and the true distributions of examples A, B, C and D (see fig. 1a).

Discussion

The presented LIA methods, compared with numerical methods which use the exact local isotherm, are relatively simple, the solution is stable, they don't cost much computation time and no iterations are needed, except for the last method (eq 40), in which $f(\log K)$ is given implicitly. When only a part of the isotherm, 'a window', is available the LIA method can still be applied, whereas in numerical methods this leads to severe instabilities. Another advantage of the LIA concept is that it provides a general framework which can be used to approximate different kinds of local isotherms. The method is worked out for Langmuir type equations.

The success of all LIA methods depends strongly on the quality of the data. In the present examples the error in the data was negligibly small. In practice this is of course an idealization and experimental errors will occur. The higher the derivative needed for an approximation the more is demanded from the data with respect to

43

both their number and quality. When large experimental errors are present the resulting distribution will reflect these errors as spurious peaks, which can also become negative. To suppress these effects pre-smoothing of the data is required (38). The possibilities and limitations of the presented methods for data with experimental errors will be discussed in a forthcoming paper.

It is clear from Figures 3, 5, 7 and 9 that the higher the order of the derivative of the overall isotherm used, the closer the true distribution function is approximated. However for heterogeneous systems that are characterised by a wide and smooth distribution function the higher order derivatives don't contribute much.
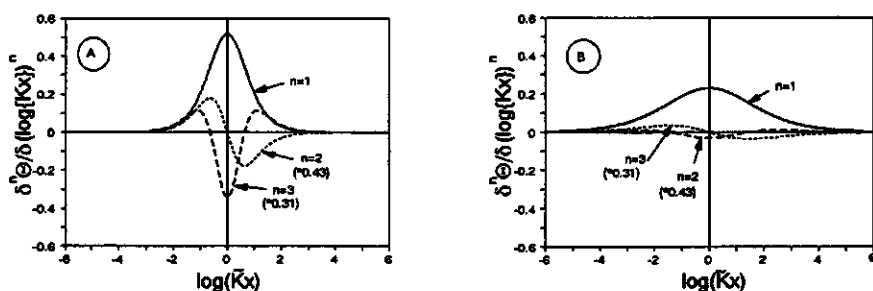

Figure 10: The first derivative of the Langmuir Freundlich overall isotherm with respect to $\log(\bar{K}x)$ (n=1), the second derivative multiplied with the constant used in the ACCA method (n=2) and the third derivative multiplied with the constant used in the RJ method. Fig. 10a corresponds with m=0.9 (eq 11) and Fig. 10b with m=0.4 (eq 11).

This is illustrated in Fig. 10, where the first, second and third derivatives of the overall isotherm are shown for a nearly homogeneous surface (eq 11, $m = 0.9$) and a rather heterogeneous surface (eq 11, $m = 0.4$). The second derivative is multiplied with a factor 0.43 as used in the ACCA method and the third derivative is multiplied by 0.31 as used in the RJ method. In general one can say that as soon as sudden changes in the distribution occur, as is the case in our asymmetric example and in the example with the two peaks, a closer approximation of the Langmuir local

44

isotherm is needed to describe the true distribution properly. This implies the use of higher derivatives of the overall isotherm for the construction of the distribution function.

```
                        ┌──────────┐
                        │   LIA    │
                        └──────────┘
             ┌──────────────┼──────────────┐
        ┌─────────┐   ┌──────────┐   ┌──────────┐
        │  STEP   │   │  LINA    │   │  LOGA    │
        └─────────┘   └──────────┘   └──────────┘
             │              │              │
        ┌─────────┐   ┌──────────┐   ┌──────────┐
        │   CA    │   │  ACCA    │   │  AS2     │
        │   AS1   │   │  LINA1   │   │  RJ      │
        └─────────┘   │  .......  │   │  LOGA1   │
                      └──────────┘   │  LOGA2   │
                                     │  .......  │
                                     └──────────┘
```
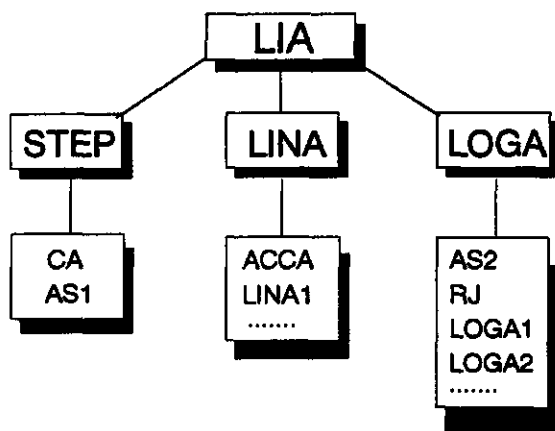
Figure 11: A schematic overview of the LIA family of methods used for the determination of affinity distributions.

The various specific local isotherm approximations (LIA) can be seen as members of one family, see Figure 11. The LIA family can be subdivided in three groups. The first uses a step function (STEP), the well-known CA method belongs to this group. The expression for $f_{CA}(\log K)$ uses the first derivative of the overall isotherm with respect to $\log x$. The second group uses a linear isotherm (LINA), of which the ACCA method is an example. This lead to a combination of the first and second derivative of the overall isotherm in the expression for $f_{LINA}(\log K)$. The ACCA method can be improved by taking another slope for the linear isotherm. The third group includes isotherm approximations that are symmetrical if the mole fraction scale is logarithmic (LOGA). A combination of a first and third derivative of the

45

overall isotherm is needed in the expression for $f_{LOGA}(\log K)$. The RJ method is equivalent to a member of this group. For exact data ($\log a \to 0$) the AS$_2$ method is equivalent to another member of this group. Optimization of the LOGA isotherm has resulted in two new expressions for the distribution function, eqs. 37 and 40.

Conclusions

- Well known methods to obtain an affinity distribution function from adsorption data, such as CA, AS, ACCA and RJ, fit in one general framework of methods that use an approximation of the local isotherm.
- An important advantage of the LIA methodology is that it is also applicable when only a 'window' of data is available.
- The LIA methodology can be applied to different types of local isotherms.
- The here derived LOGA2 method is a clear improvement over all previous known members of the LIA family (CA, ACCA, AS and RJ).
- The solutions given for the Langmuir local isotherm are shown to be directly applicable to cases where lateral interaction is important and the heterogeneity is of the random type.
- The more sharp details occur in a distribution function the closer the approximation of the local isotherm should be. This implies the use of higher derivatives of the overall isotherm with respect to $\log x$ (LOGA) in the expression for the distribution function.
- Pre-smoothing of the overall isotherm is required in case of the presence of experimental error.

Acknowledgment

References

1. House, W.A. Colloid Science **4**, 1 (1983), Specialist Periodical Report (Ed. D.H. Everett), Royal Soc. of Chem., London.
2. Jaroniec, M., Adv. Colloid Interface Sci. **18**, 149 (1983).
3. Jaroniec, M., Surface Sci. Rep. **6**, 65 (1986).
4. Sips, R., J. Chem. Phys. **16**, 490 (1948).
5. Sips, R., J. Chem. Phys. **18**, 1024 (1950).
6. Toth, J., Acta Chim. Acad. Sci. **30**, 1 (1962).
7. Van Riemsdijk, W.H., Bolt, G.H., Koopal, L.K. and Blaakmeer J., J. Colloid Interface Sci. **109**, 219 (1986).
8. Sircar, S. and Myers, A.L., Surface Sci. **205**, 353 (1988).
9. Noble, B. In "The State of the Art in Numerical Analysis" (D. Jacobs, Ed.) . Academic Press, p. 915 (1979).
10. Baker, The numerical treatment of differential equations. Oxford University Press, Oxford (1977).
11. Vos, C.H.W. and Koopal L.K., J. Colloid Interface Sci. **105**, 183 (1985).
12. Koopal, L.K. and Vos, C.H.W., Colloid Surf. **14**, 87 (1985).
13. Philips, D.L., J. Assoc. Comp. Mach. **9**, 84 (1962).
14. Tikhonov, A.N., Sov. Math. **4**, 1035, 1624 (1963).
15. Twomey, S., J. Assoc. Comp. Mach. **10**, 97 (1963).
16. House, W.A., J. Colloid Interface Sci. **67**, 166 (1978).
17. Merz, P.H., J. Comput. Phys. **38**, 64 (1980).
18. Ross, S. and Morrison, I.D., Surface Sci. **52**, 103 (1975).
19. Sacher, R.S. and Morrison, I.D., J. Colloid Interface Sci. **70**, 153 (1979).
20. Papenhuijzen, J. and Koopal, L.K., In "Adsorption from solution" (Ottewill, R.H., Rochester, C.H. and Smith, A.L. Eds.), Academic Press London, p. 211 (1983).
21. Roginsky, S.S., Adsorption and Catalysis on Heterogeneous Surfaces, Academy of Sciences of U.S.S.R., Moscow (1948) (in Russian).
22. Harris, L.B., Surface Sci. **10**, 129 (1968).
23. Cerofolini, G.F., Surface Sci. **24**, 391 (1971).
24. Cerofolini, G.F., Thin Solid Films **23**, 129 (1974).
25. Hsu, C.C., Wojciechowski, B.W., Rudzinski, W. and Narkiewicz, J., J. Colloid Interface Sci. **67**, 292 (1978).
26. Rudzinski, W. and J. Jagiello, J. Low. Temp. Phys. **45**, 1 (1981).
27. Rudzinski, W., Jagiello, J. and Grillet, Y., J. Colloid Interface Sci. **87**, 478 (1982).
28. Ninomiya, K. and Ferry, J.D., J. Colloid Interface Sci. **14**, 36 (1959).
29. Hunston, D.L., Anal. Biochem. **63**, 99 (1975).
30. Thakur, A.K., Munson, P.J., Hunston, D.L. and Rodbard, D., Anal. Biochem. **103**, 240 (1980).

31. Nederlof, M.M., Riemsdijk, W.H. and Koopal, L.K. In "Heavy metals in the hydrological cycle" (M. Astruc and J.N. Lester, Ed.) Selper Ltd., p. 361 (1988).

32. Frumkin, A., Z. Phys. Chem. 116, 466 (1925).

33. Frumkin, A., J. Electro. Anal. Chem. 7, 152 (1964).

34. Fowler, R.H. and Guggenheim, E.A., Statistical Thermodynamics, Cambridge University Press, Cambridge, p. 431 (1949).

35. De Wit, J.C.M., Van Riemsdijk, W.H. and Koopal, L.K. In "Heavy metals in the hydrological cycle" (M. Astruc and J.N. Lester, Ed.) Selper Ltd., p. 369 (1988).

36. De Boer, J.H., The Dynamical Character of Adsorption, The Clarendon Press, Oxford (1953).

37. Hill, T.L., J. Chem Phys. 14, 441 (1946).

38. Nederlof, M.M., Van Riemsdijk, W.H. and Koopal, L.K., Proceedings 7th international conference "Heavy Metals in the Environment", CEP Consultants Ltd, Edinburgh (UK) (1989)

CHAPTER 3

Comparison of Semianalytical Methods to Analyse Complexation with Heterogeneous Ligands

Abstract

The binding of ions to natural ligands is influenced by the chemical heterogeneity of these ligands. An estimate of the affinity distribution can be obtained on the basis of the overall binding function. Three methods to calculate the affinity distribution are compared: the Local Isotherm Approximation (LIA) method, the Affinity Spectrum (AS) method and the Differential Equilibrium Function (DEF) method. Starting point for the LIA and the AS method is the integral adsorption equation. Of the LIA methods the Condensation Approximation (CA), which replaces the local binding function by a step function and the 'LOGA' approximation, which follows the local binding function closely, are discussed. Some attention is paid to the Asymptotically Correct Approximation (ACA), which approximates the local isotherm by a linear function. The first and second order AS methods turn out to be in principle equivalent to the CA and LOGA method respectively, although their derivation is different. The DEF method starts with the mass action law and leads to a weighted average affinity parameter. It is shown that the DEF distribution can also be interpreted as resulting from a local isotherm approximation. The DEF local isotherm is however physically unrealistic, although it resembles for low concentrations the ACA local isotherm.

Comparison of the methods on the basis of accurate synthetic data on binding using known distribution functions confirm the theoretical analysis of the methods. Results obtained with the LOGA method are rather good, but in general the distribution is somewhat flattened. The CA method gives a too smooth impression of the distribution function. Affinity distributions obtained with the DEF method are asymmetrically distorted, but the position of a small peak with a high affinity at the outer end of a distribution is well recovered.

Introduction

The binding of metal ions and other chemical species to naturally occurring poly-functional ligands is of importance with respect to bioavailability and transport of these species in natural systems. The ligands may be present as small dissolved molecules or as reactive sites at the surface of colloids that may be mobile or immobile. Problems with the understanding of the binding of species to natural ligand systems arise because these systems are not well defined.

One of the complications is that natural colloids such as fulvic and humic acids possess different types of reactive groups, that is to say they are chemically heterogeneous. Another complication is that many natural binding agents exhibit variable charge characteristics. Often this aspect is not taken into account explicitly, which makes interpretation of results complicated. Only in favourable cases it is possible to consider the variable charge effects separately from the chemical heterogeneity effects (1,2).

In the study of the binding behaviour on natural ligands, heterogeneity analysis is a valuable tool and it may provide arguments for choosing a realistic model for the description of the binding. Early work on the heterogeneity of polyfunctional ligands goes back to, for instance, the work of Simms (3), Scatchard et al. (4), Tanford (5) and Klotz and Hunston (6) who treated the ligand system as a discrete series of site types and to Karush and Sonenberg (7), Posner (8) and Gamble (9) who considered a continuous distribution of the heterogeneity. Gamble (9) realized already two decades ago the importance and the problems of the chemical heterogeneity in relation to the binding of metal ions to natural ligands. Hunston (10) drew attention to the heterogeneity analysis by applying the work of Ninomiya and Ferry (11) to small molecule-macromolecule binding.

In the last decade there has been an increasing interest in the topic with contributions of various authors (12-35). In the field of physical chemistry the effect of heterogeneity of a surface on the adsorption of small molecules is also much studied, see the reviews by Jaroniec (36), House (37) and Jaroniec and Bräuer (38). Both purely numerical and semianalytical methods of heterogeneity analysis have been published.

In general the methods for heterogeneity analysis can be divided into (a) a group of methods that start with the assumption of a discrete distribution of heterogeneity and (b) a group that assumes the presence of a continuous distribution. In the environmental field, the Scatchard graphical analysis method (4) presents a classical example of the first group. In this method a limited number of affinity constants and their fractions can be determined when the binding function is known (6). Recently Brassard et al. (33) have developed a numerical method that is able to determine a large set of discrete affinity constants together with their fractions.

Apart from the physical arguments in favour of continuous distributions for natural polyfunctional ligands as given by Altmann and Buffle (27) and Buffle et al. (31, 32) a practical argument against a discrete distribution is that for the description of the binding often a large number of parameters is required, i.e. for each site type a binding constant and a fraction. A wide and smooth continuous distribution can be approximated with only a few parameters. In addition, on the basis of the heterogeneity analysis it can still be decided whether the heterogeneity has the characteristics of a discrete distribution (several sharp peaks) or that of a smooth continuous one.

The affinity spectrum (AS) method (10, 39) is a well known example of the group of methods based on a continuous distribution. Similar type of methods from the adsorption literature are the Condensation Approximation (CA) (40, 41), the Asymptotic Correct Approximation (ACA) (42, 43), the Rudzinsky-Jagiello (RJ) method (44, 45) and the LOGA method (30). The CA, ACA and LOGA method are based on various approximations of the local binding function, that is the binding function for a homogeneous subset of sites. Nederlof et al. (30) called these the Local Isotherm Approximation (LIA) methods. They also showed that the distribution obtained with the RJ method can be interpreted within the LIA concept. The differences in the quality of the results of the various methods can be seen as resulting from differences in the quality of the local isotherm approximation.

Gamble (9) and later Buffle (18) also developed a semi-analytical method for the heterogeneity analysis called the Differential Equilibrium Function (DEF) method. The DEF approach is based on applying the mass action law to a heterogeneous system, an idea originally proposed by Simms (3).

In the present paper a discussion will be given on the semianalytical methods for heterogeneity analysis based on continuous distributions. Because of the large number of this type of analysis methods a critical comparison of the various methods may help future users to select a method. As we recently discussed the different LIA methods (30), the emphasis in the present paper will be on the comparison of the LIA methods with the AS method and the DEF method.

In the first part of the paper the fundamentals of the three approaches will be discussed. It will be shown that all three methods can be interpreted within the LIA concept. This allows us to compare the methods on the basis of local isotherm approximations. In addition the methods will be discussed in terms of weighted true distribution functions or true affinities, this approach however is less suited to compare the methods with each other. In the second part of the paper a 'practical' comparison of the methods will be made on the basis of binding data obtained for known (synthetic) distributions. The distributions used have been taken from literature (26,30,31). At the end a brief discussion will be given on the applicability of methods to data exhibiting an experimental error. In a subsequent paper this aspect will be treated in detail.

Before turning to the heterogeneity analysis as such, some attention will be paid to the equations describing the binding of a species to a polyfunctional ligand system.

Binding Equations for Heterogeneous Systems

In order to avoid confusion first the entity to which the binding may take place will be discussed. In the most simple case the reactive entity is a small molecule with one reactive group or binding site only. One step more complicated is a homogeneous colloid such as a homo-polyelectrolyte characterized by a number of identical binding sites or a mineral particle with only one site type on the surface. In these cases the reactive entities are chemically homogeneous. The reactive entity may however also be heterogeneous, characterised by the presence of different site types. Schematically, in this situation the equivalent sites can either be grouped together in large patches (patchwise heterogeneity) or randomly mixed with the other groups (random heterogeneity).

53

The heterogeneity of a polyfunctional ligand system may be due to a mixture of different in itself homogeneous colloids (patchwise heterogeneity), or the heterogeneity may arise from heterogeneous entities (patchwise or random). In the worst case the heterogeneity of a natural sample may be caused by a combination of different homogeneous and heterogeneous polyfunctional ligands. For polyfunctional ligands such as polyelectrolytes and mineral surfaces the locations of the binding sites on the colloid are fixed and one speaks of localized binding. In this situation strong lateral electrostatic interactions between the sites may occur and influence the binding behaviour. For the moment we will neglect these lateral interactions, but at the end of this section a discussion will be given on the complications which arise if the sites do interact.

The binding of a species M to a site of type i, S_i can be written as:

$$S_i + M \; \underset{\longrightarrow}{\longleftarrow} \; S_i M \tag{1}$$

where S_i is the free and $S_i M$ the complexed site. By applying the law of mass action to this equilibrium under the assumption of ideality (both in the solution and at the ligand system) the affinity constant K_i may be defined as:

$$K_i = \frac{\{S_i M\}}{\{S_i\}[M]} \tag{2}$$

where $[M]$ is the concentration of the species M in solution and $\{S_i M\}$ and $\{S_i\}$ are the site concentrations of complexed and free sites respectively. When M is the only species reacting with $\{S_i\}$, the fraction of sites of type i occupied by M, θ_i, equals:

$$\theta_i = \frac{\{S_i M\}}{\{S_i\} + \{S_i M\}} \tag{3}$$

It follows from eq 2 and 3 that:

$$\theta_i = \frac{K_i[M]}{1 + K_i[M]} \qquad (4)$$

Equations 3 and 4 are equivalent to the well known Langmuir equation. From eq 4 it simply follows that the fraction of free sites equals:

$$1 - \theta_i = \frac{1}{1 + K_i[M]} \qquad (5)$$

Equations 4 and 5 apply to both a solution with a large number of equal single site ligands and to one with homogeneous polyfunctional ligands each containing a number of equal sites. This is a consequence of the assumed ideality.

For a heterogeneous system a series of different site types i is present and the binding equation (eq 4) now applies to each site type separately. For a heterogeneous system eq 4 is therefore called the *local* binding function. In the ideal case the *overall* binding function is simply obtained by a weighted summation of the local contributions, i.e. :

$$\theta_t = \sum_i f_i \theta_i \qquad (6)$$

where θ_t is the total fraction of sites occupied with M and f_i is the weighting factor. θ_t is experimentally accessible when the total number of sites is known and can be expressed as:

$$\theta_t = \frac{\sum_i \{S_i M\}}{\sum_i \{S_i M\} + \sum_i \{S_i\}} \qquad (7a)$$

or

55

$$\theta_t = \frac{\{LM\}}{\{LM\} + \{L\}} \tag{7b}$$

where $\{LM\} = \sum\{S_i M\}$ is the total concentration of metal bound to the ligand system and $\{L\} = \sum\{S_i\}$ the total concentration of free sites of the ligand system. The weighting factor f_i is the fraction of site type i with respect to the total concentration of sites of the system:

$$f_i = \frac{\{S_i M\} + \{S_i\}}{\{LM\} + \{L\}} \tag{8}$$

The fraction f_i also equals the metal binding capacity of sites i relative to the binding capacity of the entire system.

Equation 6 applies to a heterogeneous system with a discrete number of site types. When the differences between the K_i or rather the $\log K_i$ values become infinitesimal, eq 6 can be written as an integral equation:

$$\theta_t = \int_\Delta \theta(K,[M])f(\log K)d \log K \tag{9}$$

where $\theta(K,[M])$ is the local binding function, $f(\log K)$ is the distribution function and Δ indicates the range of $\log K$ values present. The distribution of $f(\log K)$ can be interpreted as a probability density function, that is $f(\log K)$ indicates the probability of finding sites with an affinity in the range $\log K + d \log K$. The product $f(\log K)d \log K$ is equivalent to the fraction f_i in the discrete case. Note that in eq 9 the sub i is left out because individual site types can no longer be considered separately. Equations 6 and 9 are equivalent expressions for the generally used *ideal* overall binding function of a heterogeneous ligand system and the starting point for a further analysis.

When the distribution of $\log K$ values is known, θ_t can be calculated using eq 4 as local isotherm. In practice however $f(\log K)$ is often unknown and eq 9 (or eq 6) provides a basis to obtain the distribution function if the binding function θ_t and

the relationship for a homogeneous subset of sites $\theta(K,[M])$ are known. In principle θ_t can be determined experimentally (see eq 7) and for $\theta(K,[M])$ a theoretical relation can be used, such as eq 4. Inversion of the integral will provide $f(\log K)$. Above it has been assumed that the total concentration of sites of the system $\{S_t\} = \sum\{S_tM\} + \sum\{S_t\}$ is known. In some cases it is however difficult to determine the total site concentration experimentally and eq 9 is preferably written as:

$$\{LM\} = \{S_t\} \int_\Delta \theta(K,[M])f(\log K)d\log K \tag{10}$$

It follows that $\{S_t\}$ is essentially a normalization constant. If $\{S_t\}$ is unknown the distribution of $f(\log K)$ can still be obtained, but it will not be normalized.

An alternative approach to the heterogeneity analysis which has received much attention in literature (3,9,12,18,24,26,27,28,31,32) starts with the application of the mass action law to the overall ligand system. The metal binding to the ligand system is in this case represented as:

$$L + M \quad \overset{\longleftarrow}{\longrightarrow} \quad LM \tag{11}$$

and for each value of $[M]$ the law of mass action is applied:

$$\overline{K} = \frac{\{LM\}}{\{L\}[M]} \tag{12}$$

$\overline{K}$ is called a weighted average equilibrium function (9,12,18). $\overline{K}$ is not a constant but a function of $[M]$ or the metal loading of the ligand system. A plot of $\overline{K}$ versus, for instance, $\{LM\}$ provides an indication of the course of this weighted average affinity as a function of the metal complexation. Gamble et al. (9,12,26) and later Buffle et al. (18,24,28,31,32) have elaborated this concept and analysed $\overline{K}$ or

quantities derived from it in great detail. For the interpretation of these quantities eqs 2 to 9 are used. Also in this approach the main goal is to get insight in the binding heterogeneity.

Because of the central role of eq 9 in the analysis, a brief discussion of the assumption of ideality made to derive eq 9, is appropriate. In the case of ion binding to a colloidal ligand system this assumption cannot be satisfied in general, because electrostatic effects will be present and these may lead to rather strong interactions. In the bulk solution the correction for the electrostatic interactions can easily be made by using the Debye-Hückel theory or one of its extensions such as the Davies equation (46). The non-ideality at the reactive colloid can be calculated in a similar way, but in this case the electrostatic potential may become much higher than for a simple ion (1,5). In general upon binding of a metal cation to a ligand site the charge of the ligand-metal complex will become more positive (or less negative) and this will result in a decrease in affinity (other things being equal) for the metal ions. The simplest way to account for this type of interactions is to consider the solution concentration of metal ions in the diffuse layer at the location of the binding site, $[M]_s$ instead of that in the bulk, $[M]$. $[M]$ and $[M]_s$ are related by a Boltzmann factor incorporating the coulombic interactions.

To calculate $[M]_s$ a model is required to describe the electrostatic interactions and the type of heterogeneity should be known (35, 47). In the case of patchwise heterogeneity the charge density and thus the electrical potential near the ligand will be different for different patches. Such a situation occurs for instance at different crystal planes of a metal (hydr)oxide particle. In the case of random heterogeneity the electrical potential is assumed to be the same for the entire particle. Also the shape and size of the colloid will affect the electrostatic interaction.

When little is known about the heterogeneity, as is often the case in studies of metal binding to natural ligands, the electrostatic potential is generally assumed to be the same near all sites present. One thus assumes a random heterogeneity and an average shape and size for the colloids. Here the word 'apparent' is used to differentiate between purely chemical or intrinsic heterogeneity and heterogeneity due to both electrostatic interactions and chemical heterogeneity. For chemically heterogeneous systems the overall 'heterogeneity' will be a function of both the intrinsic (chemical) heterogeneity and the heterogeneity induced by the electrostatics. In favourable cases (e.g. with proton binding) the electrostatic interactions

can be filtered out before the heterogeneity analysis, leading to an intrinsic affinity distribution (1,2). In most cases however, the electrostatics are included in the affinity function, leading to an apparent affinity distribution. In this case the heterogeneity analysis of even a chemically homogeneous colloid will reveal a substantial apparent heterogeneity (35).

Heterogeneity Analysis

In literature a series of methods mentioned in the introduction is proposed in which, for known values of θ_t and a given local binding function θ, $f(\log K)$ is obtained by solving eq 9. Equation 9 is a so called Fredholm integral equation of the first kind which is difficult to solve numerically for $f(\log K)$. Good results are obtained with regularization (48,49) and singular value decomposition (50,51) for very accurate data that cover the whole range of concentrations. So far none of these methods has been used for the analysis of ion binding.

By making some approximations it is also possible to solve eq 9 analytically for $f(\log K)$ without making a priori assumptions with respect to the distribution function. Here we concentrate on these analytical methods (10,30,39-45) and on the Differential Equilibrium Function (DEF) method of Gamble and Buffle (9,12,18,24,26,27,28,31,32).

Local Isotherm Approximation (LIA) methods.

In the LIA methods the kernel θ (the equation for the local binding function) of the integral equation 9 is replaced by another function which approximates the local isotherm in such a way that the integral equation can be solved analytically for the distribution function $f(\log K)$. Deviations of the "LIA function" from the true local binding function will in principle result in deviations of the calculated distribution function from the true distribution function. The better the LIA function approximates the local binding function, the closer will the distribution function resemble the true one. A review of the older LIA functions and some results obtained for a new LIA function can be found in (30). Here we will discuss the so called Condensation Approximation (CA) and the new LIA function named LOGA. Also the ACA method is briefly mentioned.

Condensation Approximation (CA)

A classical and very illustrative method to solve eq 9 for $f(\log K)$ is the Condensation Approximation (40,41). In this method the local isotherm function is replaced by a step function. This is equivalent with assuming that the heterogeneous binding sites are occupied sequentially, i.e. the sites with the highest affinity first, then those with the second highest affinity, etc. In order to achieve this the local isotherm should be a step function. In this case with each infinitesimal increase in concentration just one site type is transformed from entirely free to completely occupied. In reality such sequential filling of the different site types will only occur at zero Kelvin when entropy effects can be neglected. For temperatures considerably away from zero Kelvin both enthalpic and entropic factors are important. Consequently, at a given concentration all site types have some coverage, the highest affinity sites a relatively high coverage, the lowest affinity sites a low coverage. Nevertheless the CA is a useful simplification in the heterogeneity analysis, since it is a simple concept that leads to a simple expression for the distribution function. In addition the CA method can be used for different types of local isotherms.

The replacement of the local binding function by a step function is the main feature in the CA method. The position of the step is depending on the local binding function and determined by a best fit criterion. In the case of eq 4 as local isotherm the best fit is obtained when the step function intersects the Langmuir isotherm at $\theta = 0.5$. This can be clearly seen in Figure 1 where the Langmuir function is shown together with the CA local isotherm.

According to eq 4 at $\theta = 0.5$ it applies that $K[M] = 1$, so that in the CA the affinity, K_{CA} can be replaced by $1/[M]$ and the approximation of the local binding function becomes:

$$\theta_{CA} = 0 \qquad \text{for} \qquad [M] < 1/K_{CA} \qquad (13a)$$

$$\theta_{CA} = 1 \qquad \text{for} \qquad [M] \geq 1/K_{CA} \qquad (13b)$$

where θ_{CA} is used to indicate that eq 13 is the CA approximation of the true local binding function (eq 4). By substitution of eq 13 into the integral equation one obtains:
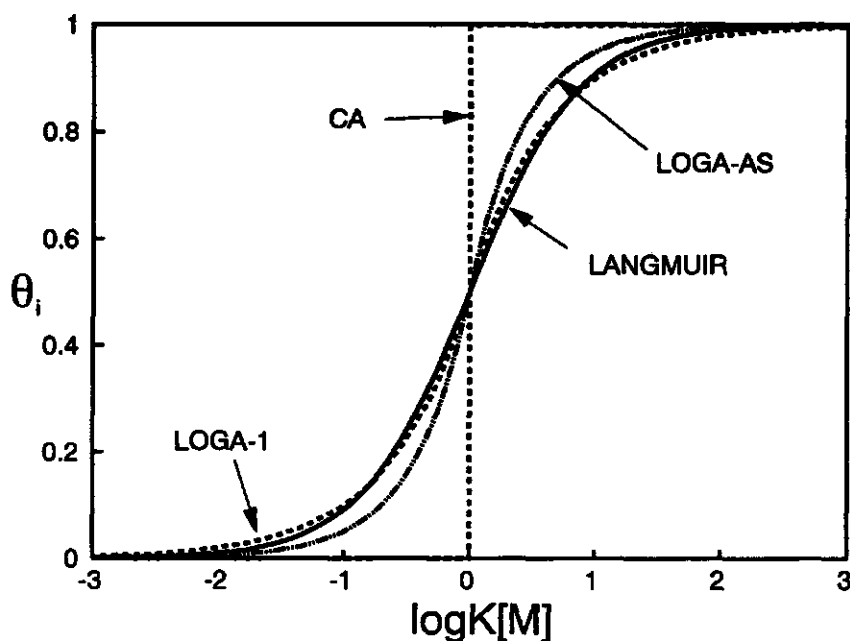
Figure 1: Local isotherm approximations (CA, LOGA-1 and LOGA-AS) in comparison with the Langmuir local binding function.

$$\theta_t(\log[M^\#]) = \int_{\log K^\#}^{\infty} 1.f(\log K)\, d\log K \qquad (14)$$

where $[M^\#](= 1/K_{CA}^\#)$ is any value of $[M]$. Note that in reality the high affinity sites are filled first, whereas the integration starts at the low affinities. Inversion of the integral is simply done by taking the first derivative of θ_t with respect to $\log[M]$:

$$f_{CA}(\log K_{CA}) = \frac{d\,\theta_t[M]}{d\log[M]} \qquad (15a)$$

$$\log K_{CA} = -\log[M] \qquad (15b)$$

61

According to Harris (41) the CA distribution can be seen as a weighted true distribution. At each point the weighting involves the first derivative of the local isotherm with respect to $\log M$. This derivative (or weighting function) is shown in Figure 2.
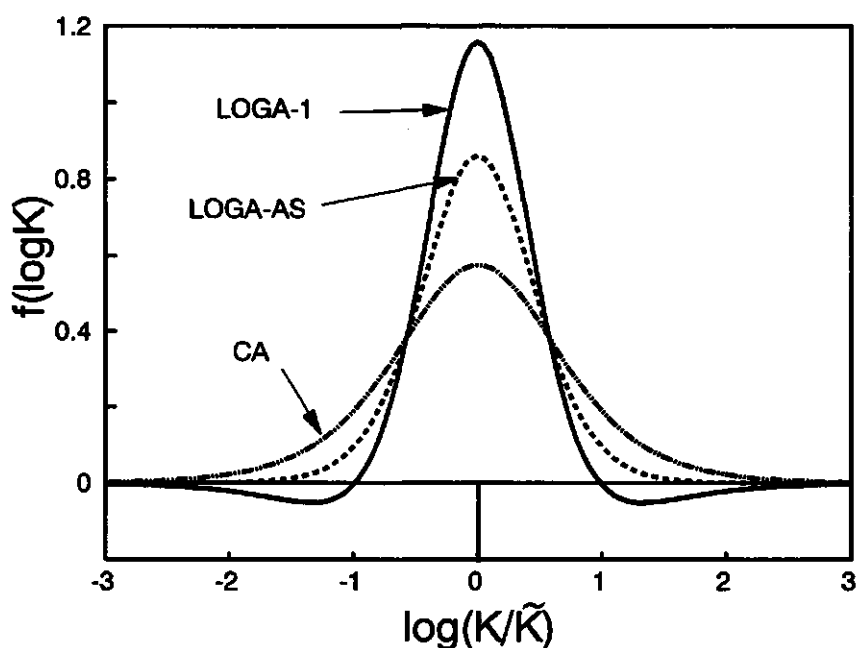

Figure 2: Weighting functions of the LIA methods (CA, LOGA-1, LOGA-AS) presented as the distribution functions for the homogeneous case.

As a consequence of the weighting the distribution function is widened. This can be simply illustrated for a homogeneous ligand system for which the true distribution is a Dirac Delta function, so that $f_{CA}(\log K_{CA})$ is equivalent to Figure 2.

62

Asymptotically Correct Approximation (ACA)

The ACA method, also called Asymptotically Correct *Condensation* Approximation (ACCA), was developed by Cerofolini (42,43) as a first improvement of the CA method. A discussion of the ACA method is presented in (30). Here we mention the method because of the similarity with the local isotherm derived for the DEF method (see DEF section). The ACA local isotherm can be written as:

$$\theta_{ACA} = K[M] \qquad \text{for} \qquad [M] \le 1/K_{ACA} \qquad (16a)$$

$$\theta_{ACA} = 1 \qquad \text{for} \qquad [M] > 1/K_{ACA} \qquad (16b)$$

The approximation of the distribution function is:

$$f_{ACA}(\log K) = \frac{d\,\theta_t([M])}{d\log[M]} - 0.43\frac{d^2\theta_t([M])}{d\log[M]^2} \qquad (17a)$$

$$\log K_{ACA} = -\log[M] \qquad (17b)$$

The ACA distribution results in an asymmetrical deformation of the true distribution function (30), which is a serious disadvantage of the method.

The LOgarithmic Symmetrical Approximation (LOGA)

The CA and ACA local isotherms are rather poor approximations of the Langmuir function. A much better approximation is obtained with the LOGA function (30). With LOGA the Langmuir eq 4 is replaced by:

$$\theta_{LOGA} = \alpha\,(K[M])^{\beta} \qquad \text{for} \qquad [M] \le 1/K_{LOGA} \qquad (18a)$$

$$\theta_{LOGA} = 1 - \alpha\,(K[M])^{-\beta} \qquad \text{for} \qquad [M] > 1/K_{LOGA} \qquad (18b)$$

63

where α and β have to be optimized to fit the chosen local isotherm. Equation 18 is point symmetrical in $\theta_{LOGA} = 0.5$ when θ_{LOGA} is plotted versus $\log[M]$. Similarly as for the CA, the LOGA function intersects the Langmuir isotherm at $\theta_{LOGA} = 0.5$ which leads to the relation $\log[M] = -\log K_{LOGA}$.

The approximated local binding function (eq 18) is only continuous at $\theta_{LOGA} = 0.5$ for $\alpha = 0.5$ and we will restrict ourselves to this situation. Insertion of eq 18 with $\alpha = 0.5$ in the integral equation, followed by inversion of the integral leads to the LOGA distribution function (30):

$$f_{LOGA}(\log K) = \frac{d\,\theta_t([M])}{d\log[M]} - \frac{0.189}{\beta^2}\frac{d^3\,\theta_t([M])}{d\log[M]^3} \tag{19a}$$

$$\log K_{LOGA} = -\log[M] \tag{19b}$$

The coefficient 0.189 ($=0.43^2$) occurs because of the use of $\log K$ instead of $\ln K$. By fitting eq 18 to the Langmuir function using a least sum of squares method the value of β can be optimized. The LOGA equation with $\alpha = 0.5$ approximates the Langmuir equation most closely for $\beta = 0.7$. In Figure 1 this approximation is indicated by LOGA-1. For $\beta = 1$ the approximation intersects the Langmuir function only in $\theta = 0.5$ which implicates that the resulting distribution will always be positive. In Figure 1 this approximation is indicated by LOGA-AS, because it is equivalent with the second order affinity spectrum as will be shown in the next section.

Similarly as $f_{CA}(\log K_{CA})$ also $f_{LOGA}(\log K_{LOGA})$ is an approximation of the true distribution function. The weighting function is however considerably sharper than that of $f_{CA}(\log K_{CA})$ (see Figure 2), indicating that the approximation is much better. It is clearly shown in Figure 2 that for $\beta = 0.7$ (LOGA-1) the sharpest weighting function is obtained, but two slightly negative parts appear and that for $\beta = 1$ (LOGA-AS) the weighting function is somewhat less sharp but it remains positive. In literature expressions for the distribution function have been reported that appear to be special cases of eq 19, but the derivations of these functions are different from that given by Nederlof et al. (30). Nevertheless, use of eq 19 may be interpreted as being the result of using an approximation of the local binding function. For $\beta = 0.79$

equation 19 corresponds with an expression found by Hsu et al. (44) and Rudzinski et al. (45) and for $\beta = 1$ the distribution corresponds with a limiting case of the affinity spectrum method (10,39), as will be discussed in the next section.

Although the LOGA-method leads in principle to better results than the CA-method a disadvantage is that not only the first but also the third derivative of the binding function is required.

Affinity Spectrum Methods (AS)

A second way to solve eq 9 analytically for $f(\log K)$ is presented in the Affinity Spectrum methods. These methods have become well-known as a tool to study ligand equilibria through the work of Hunston (10), Thakur et al. (39) and Shuman et al. (14).

The basis of the affinity spectrum methods goes back to the work of Nolle (52), Schwarzl and Staverman (53,54) and Ninomiya and Ferry (11), who studied the viscoelastic behaviour of materials. Nolle (52) found a similar integral equation for the viscoelastic relaxation function as our overall binding function (eq 9), but the kernel was different from eq 4 (our local binding function). By replacing his kernel by a step function, a first derivative of the relaxation function was obtained as an approximation of the relaxation spectrum. Schwarzl and Staverman (53) showed that when the kernel is an exponential function, the Laplace transform can be used to obtain an approximation of the relaxation spectrum. The result appeared to be a combination of the first and higher order derivatives of the relaxation function, the more derivatives the better the approximation became. In a later article Schwarzl and Staverman (54) extrapolated their results to other kernels. Ninomiya and Ferry (11) contributed by suggesting a specific calculation method, which in their opinion had the advantage that the calculation of derivatives of the relaxation function is avoided.

In the next sections the work of Nolle and Schwarzl and Staverman will be discussed and it will be shown that the original equations on which the AS methods are based are essentially identical to eq 15 and 19 of the LIA methods.

First Order Affinity Spectrum

The basic idea behind the generalization used by Schwarzl and Staverman (54) to find the distribution function is that the integral equation should be transformed in such a way that the kernel becomes a sharp bell shaped function. If this bell shaped function may be approximated by a Dirac-Delta function the integral equation can be solved directly for the distribution function. Hence, the sharper the kernel, the better the distribution function is approximated. Application of the first order approximation to the present problem leads to the first derivative of eq 9:

$$\frac{d\,\theta_t([M])}{d\log[M]} = \int_\Delta \frac{d\,\theta(K,[M])}{d\log[M]} f(\log K)\, d\log K \tag{20}$$

The kernel of eq 20, $d\theta/d\log[M]$, with θ given by eq 4 is the bell shaped function shown in Figure 3 indicated by AS1. Approximating this function by a Dirac-Delta function results in the approximation for the distribution function given by eq 15. This procedure is fully equivalent to replacing eq 4 by a step function as was done by Nolle (52) and in the CA method.

Ninomiya and Ferry (11) wanted to avoid the use of differentials and obtained a comparable result by using linear combinations of the kernel function, which leads to linear combinations of the overall function. For our situation the result can be written as:

$$f_{AS1}(\log K_{AS1} = -\log[M]) = \frac{\theta_t([M]a) - \theta_t([M]/a)}{2\log a} \tag{21}$$

where $\log a$ is the distance between two data points in a (hypothetical) series of equidistant data. Equation 21 can be seen as a numerical approximation of the first derivative of the binding function, for $\log a \to 0$ eq 21 is equivalent to eq 15. Thakur et al. (39) applied the approach of Ninomiya and Ferry to ligand binding and introduced the term (first order) *affinity spectrum*.
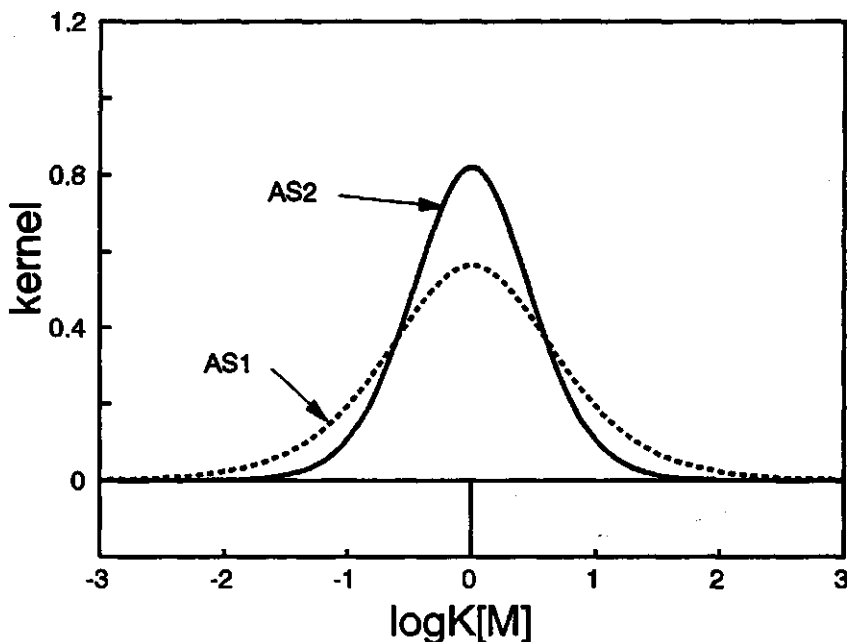
66

Figure 3: The kernels of the integral equation in the first order (AS1) and second order (AS2) Affinity Spectrum method.

Higher Order Affinity Spectra

To improve the result of the first order approximation the generalized method of Schwarzl and Staverman (54) can be used. For a third order approach the procedure starts with the assumption that the kernel of eq 9 can be transformed in a sharp peak by using a linear combination of the first, second and third derivative of the local binding function. As a consequence the overall function θ_t is transformed in a linear combination of the first, second and third derivative of the integral function. In general this may be written as:

$$\hat{\theta}_t = \int \hat{\theta} f(\log K) d \log K \tag{22}$$

67

where $\hat{\theta}_t$ and $\hat{\theta}$ are the transformations of θ_t and θ respectively. Note that the distribution function is not affected by this transformation. The third order approach leads to the following distribution function by approximating $\hat{\theta}$ by a Dirac-Delta function:

$$f_{SS3}(\ln K_{SS3}) = p \cdot \frac{d\theta_t}{d\ln[M]} + q \cdot \frac{d^2\theta_t}{d\ln[M]^2} + r \cdot \frac{d^3\theta_t}{d\ln[M]^3} \tag{23}$$

i.e. also the distribution function is a linear combination of derivatives of θ_t,. SS3 stands for the third order approximation according to Schwarzl and Staverman and p, q and r are multiplication factors which occur in all three linear combinations. The problem is now to find values for p, q and r. To achieve this, we follow Schwarzl and Staverman (54) and formulate a number of constraints for the kernel $\hat{\theta}$ of the transformed integral:

(1) The kernel should always be positive, since both the affinity distribution and the overall binding function are positive.
(2) The kernel should be normalized to 1.
(3) The kernel should have one and only one maximum at $\log K = -\log[M]$ and become zero at $\log K = \pm\infty$.
(4) The kernel should stay symmetrical in order to obtain the sharpest possible kernel.

From constraint (4) it follows that q must be zero because of the fact that the second derivative of eq 4 is an odd function (see Figure 4), which would make the kernel asymmetrical.
The first and the third derivative of eq 4 are symmetrical (see Figure 4). Since the integral of the third derivative from minus infinity to plus infinity is zero it follows that p should be equal to one in order to get a normalized kernel. Finally the value of r has to be determined using constraints (1) and (3). Working out the first and third derivative of the local binding function and demanding that the first minus r times the third derivative should be positive over the whole concentration
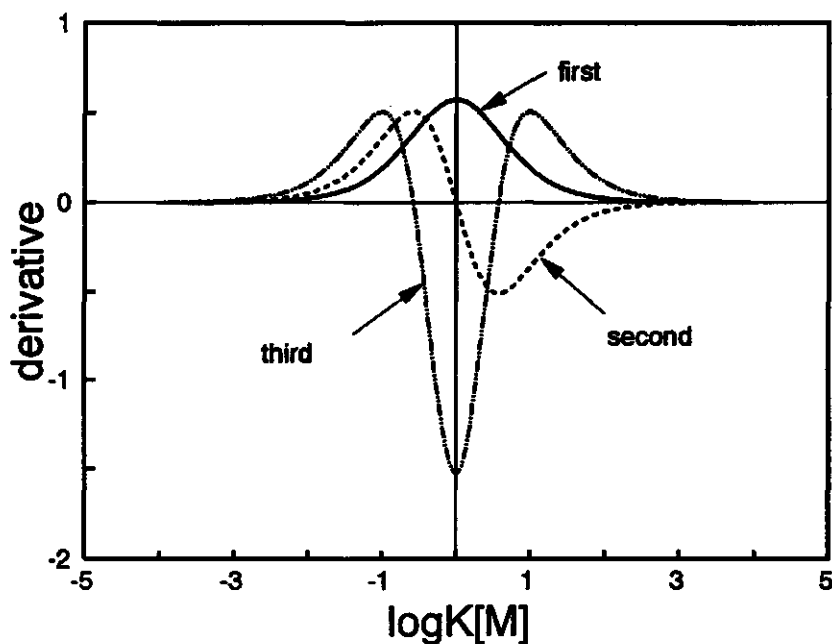
Figure 4: The first three derivatives of the local binding function eq 4 with respect to $\log[M]$.

range results in r=1. Figure 3 shows the kernel in this case (indicated by AS2). By substitution of the values for p, q, and r in eq 23 and replacing $\ln[M]$ by $\log[M]$ the following expression is obtained:

$$f_{SS3}(\log K_{SS3}) = \frac{d\,\theta_t([M])}{d\log[M]} - 0.189\frac{d^3\,\theta_t([M])}{d\log[M]^3} \tag{24a}$$

$$\log K_{SS3} = -\log[M] \tag{24b}$$

Comparison of eq 24 with eq 19 shows that both equations are identical for $\beta = 1$.

69

Ninomiya and Ferry (11) who intended to obtain their spectra without using derivatives of the integral function again used linear combinations of the binding functions to obtain higher order approximations. Hunston (10) applied this concept to the ion binding problem and found:

$$f_{AS2}(\log K = -\log[M]) = \frac{\theta_t([M]a) - \theta_t([M]/a)}{2\log a} -$$

$$\frac{a}{(a-1)^2} \frac{\{\theta_t([M]a^2) - \theta_t([M]/a^2)\} - 2\{\theta_t([M]a) - \theta_t([M]/a)\}}{2\log a} \tag{25}$$

Although less obvious than with the first order approximation this reduces to eq 19 when $\log a \to 0$. Ninomiya and Ferry (11) advise to use eq 25 with $\log a = \Delta \log[M]$ in the range 0.2 to 0.4.

For finite values $\log a$ acts as a primitive smoothing parameter to eliminate very small experimental errors (10,14,39). When the error problem is treated separately, a possible advantage of using eq 21 or 25 over eq 15 or 24 is lost and the affinity spectrum methods (for $\log a \to 0$) become identical to the CA and the LOGA method respectively.

Differential Equilibrium Function Method (DEF)

At first sight the differential equilibrium method is rather different from both the LIA methods and the AS methods in spite of the fact that the main goal is the same, namely to get insight in the binding heterogeneity of a ligand system. The DEF method is based on the mass action law approach (3,9,12,18,24, 26-28,31,32) and starts with eq 12 instead of the general binding equation (eq 9). However also in the derivation of the DEF functions the basic relations eqs 2 to 9 are applied.

After normalization of the concentration of bound and free sites by the total site number $\{S_t\}$, eq 12 can also be written as :

$$\overline{K} = \frac{\theta_t}{[M](1 - \theta_t)} \tag{26}$$

For a homogeneous ideal ligand system eq 26 equals eq 2 and the correct affinity constant is obtained. For a heterogeneous system $\overline{K}$ is a function of the concentration and the extent of binding θ_t and represents a special weighted average affinity.

According to Gamble et al. (9,12,26) disadvantages of $\log\overline{K}$ are that (1) for its calculation the total number of sites of the ligand system $\{S_t\}$ is needed and (2) that $\log\overline{K}$ as a function of θ_t gives a poor representation of the underlying heterogeneity. In order to meet these problems, Gamble introduced the 'differential equilibrium function', K_{DEF}, which is intended to be more closely related to K_i and defined as (9,12):

$$K_{DEF} = \frac{d\{\overline{K}(1 - \theta_t)\}}{d(1 - \theta_t)} \tag{27}$$

Substitution of eq 26 in 27 gives:

$$K_{DEF} = -\frac{d(\theta_t/[M])}{d\theta_t} \tag{28a}$$

or

$$K_{DEF} = -\frac{d(\{LM\}/[M])}{d\{LM\}} \tag{28b}$$

from which it follows that for the calculation of K_{DEF}, $\{S_t\}$ is not required. The reasoning of Gamble and co-workers, leading to the definition of K_{DEF} will be analysed below.

Buffle et al. (18,24,28,31,32) contributed to the DEF method by deriving the relation between K_{DEF} and the individual K_i values. This relation helps to interpret K_{DEF} and related functions. The interpretation of K_{DEF} in terms of K_i values according to Buffle and co-workers will be treated in a separate paragraph.

Gamble et al. (9,12,26) accept a plot of $\log K_{DEF}$ versus the concentration of complexed sites θ, as a sufficient characterization of the heterogeneity. Buffle et al. (27,30,31) extended the DEF method with a distribution function by stating that $\theta_i(\log K_{DEF})$ can be seen as a 'good estimate' or 'analogue' of the true cumulative distribution function of $\log K_{DEF}$. The distribution density becomes:

$$f(\log K_{DEF}) = -\frac{d\theta_t}{d\log K_{DEF}} \tag{29}$$

The last paragraph in the DEF section deals with the interpretation of the DEF distribution function within the LIA concept.

Gamble's Derivation of K_{DEF}

For the derivation of K_{DEF} Gamble et al. (9,12) start with the definition of $\overline{K}$ (eq 26) and introduce the relation between the overall binding and the contributions of the individual sites (eq 6), so that eq 26 can be written as:

$$\overline{K}(1 - \theta_t) = \frac{1}{[M]}\sum_i f_i\theta_i \tag{30}$$

Then θ_i in the RHS of eq 30 is replaced by:

$$\theta_i = K_i[M](1 - \theta_i) \tag{31}$$

which follows directly from the Langmuir equation (eq 4). The result is:

$$\overline{K}(1 - \theta_t) = \sum_i K_i f_i(1 - \theta_i) \tag{32}$$

Next Gamble et al. (9,12) assume that each small change in the overall binding, $\Delta\theta_t$, can be attributed to a change in the coverage of one site type only. This assumption is a simplification of reality and not in accordance with eq 31. Based on this assumption eq 32 is written as:

$$\overline{K}(1 - \theta_t) = \sum_j K_{DEF,j}\Delta(1 - \theta_t)_j \tag{33}$$

Because of the assumption involved K_i and f_i are replaced by their DEF approximations $K_{DEF,j}$ and $f_{DEF,j}$ respectively.

When it is assumed that a very large number of site types is present, the summation in eq 33 can be replaced by an integral (9,12):

$$\overline{K}(1 - \theta_t) = \int_0^{1-\theta_t^*} K_{DEF}\, d(1 - \theta_t) \tag{34}$$

where θ_t^* is the coverage at a certain concentration $[M] = [M]^*$. Finally the definition of K_{DEF} (eq 27) is obtained by differentiation of eq 34 with respect to $(1 - \theta_t)$.

In a later article Gamble and Langford (26) derived K_{DEF} in a slightly different way. They considered a small change in the overall binding, for which it follows from eq 33 that :

$$\Delta\{\overline{K}(1 - \theta_t)\} = K_{DEF,j}\Delta(1 - \theta_t)_j \tag{35}$$

Rewriting eq 35 gives again an expression for K_{DEF}:

$$K_{DEF} = \frac{\Delta\overline{K}(1 - \theta_t)}{\Delta(1 - \theta_t)} \tag{36}$$

In eq 36 $K_{DEF,j}$ is replaced by K_{DEF} because eq 36 can be applied at each value of θ_t (or [M]). For a continuous affinity distribution, eq 36 reduces to the definition of K_{DEF} (eq 27).

With eq 33 and 35 it was assumed that only one site type is involved at any change of θ_t, $\Delta\theta_t$. However in reality all sites contribute and the correct expression for a change in $\overline{K}(1 - \theta_t)$ is according to eq 32:

$$\Delta\{\overline{K}(1 - \theta_t)\} = \sum_i K_i f_i \Delta(1 - \theta_i) \tag{37}$$

By comparison of eq 37 with 35 it follows that both equations are equivalent only when the site type involved changes from completely empty to completely occupied at an infinitesimal increase in concentration corresponding to $\Delta\theta_t$. Thus $\Delta(\theta_j) = 1$ and $\Delta(1 - \theta_j) = -1$, this means that the sites are filled sequentially. Equation 35 may now be written as:

$$\Delta\{\overline{K}(1 - \theta_t)\} = -K_{DEF,j} f_{DEF,j} \tag{38}$$

It also follows that (compare eqs 38 and 35):

$$\Delta(1 - \theta_t)_j = -f_{DEF,j} \tag{39}$$

or that the fraction $f_{DEF,j}$ corresponding to $K_{DEF,j}$ is found as:

$$f_{DEF,j} = \Delta\theta_{t,j} \tag{40}$$

For a continuous distribution where $f_{DEF},j = f_{DEF}(\log K_{DEF})\Delta \log K_{DEF}$, the distribution function of $\log K_{DEF}$ (eq 29) follows directly from eq 40 for $\Delta \to 0$:

$$f_{DEF}(\log K_{DEF})_{\Delta \to 0} = -\frac{\Delta\theta_t}{\Delta \log K_{DEF}} \tag{41}$$

74

which is equivalent to eq 29.

Buffle's Interpretation of K_{DEF}

In order to obtain more insight in K_{DEF} and to derive the relation between K_{DEF} and the individual K_i values Altmann and Buffle (27) substituted equivalent expressions for $\overline{K}(1-\theta_t)$ and $(1-\theta_t)$ in terms of the contributions of the individual sites in eq 27. This results in:

$$K_{DEF} = \frac{\sum_i K_i f_i \, d\theta_i/d[M]}{\sum_i f_i \, d\theta_i/d[M]} \tag{42}$$

Equation 42 illustrates that K_{DEF} is a weighted average of all K_i values. The K_i values are weighted by the contribution of the individual site types to the change in θ_t at a given concentration M, since

$$\frac{d\theta_t}{d[M]} = \sum f_i \frac{d\theta_i}{d[M]} \tag{43}$$

By working out the differentials in eq. 42, Altmann and Buffle (27) obtained finally:

$$K_{DEF} = \frac{\sum_i K_i f_i \theta_i (1-\theta_i)}{\sum_i f_i \theta_i (1-\theta_i)} \tag{44}$$

According to eq 44 the K_i values are weighted on a linear K scale. It should be noted that when a weighted binding energy is wanted, weighting on a logarithmic scale is more appropriate since $\log K$ is proportional to the binding energy ΔG. By weighting K_i on a linear scale high affinities contribute more than low affinities. As a result the distribution of K_{DEF} is asymmetrically distorted with respect to the true distribution function.

75

Interpretation of the DEF Method in Terms of the LIA Concept

K_{DEF} can also be interpreted in terms of the LIA concept. When it is assumed that the DEF distribution $f_{DEF}(\log K_{DEF})$ gives an approximation of the true distribution, a DEF local isotherm, θ_{DEF} can be sought that is an approximation of the true local isotherm, under the condition that:

$$\theta_t = \int_\Delta \theta_{DEF} f_{DEF}(\log K_{DEF}) \, d\log K_{DEF} \tag{45}$$

To derive an expression for θ_{DEF} we go back to the analysis of Gamble and co-workers. The assumption that θ_i goes from zero to 1 instantaneously at an infinitesimal increase in coverage, means that sites are filled sequentially. Due to this simplification an approximation of K_i is found defined as K_{DEF}. One would expect that due to the sequential filling, the DEF distribution would resemble the CA distribution and that the DEF local isotherm would resemble the CA isotherm. However, this is not the case, because the sequential filling concept used in the derivation of Gamble is inconsistent with the use of eq 31. In eq 31. θ_i appears at both the LHS and the RHS. Gamble et al. (9,12) replace θ_i at the RHS by a step function and obtain a new expression for θ_i. So two types of local isotherms which are in conflict with each other are used in one and the same equation. The resulting θ_i at the LHS, which we will denote as θ_{DEF}, now becomes linearly dependent on [M]:

$$\theta_{DEF} = K_{DEF}[M] \qquad \text{for} \qquad [M] \le [M]^* \tag{46a}$$

$$\theta_{DEF} = 0 \qquad \text{for} \qquad [M] > [M]^* \tag{46b}$$

where $[M]^*$ is the concentration corresponding with K_{DEF} as obtained by eq 27. It follows from eq 46 that $K_{DEF}[M]^*$ is both the point where the isotherm θ_{DEF} is split in two parts (the breakpoint) and the maximum value that θ_{DEF} can have. Normally speaking θ_{DEF} should have a maximum value of 1, that is at $K_{DEF}[M] = 1$. However, this is only the case if $K_{DEF} = 1/[M]$, which is in general not the case (in fact only in one point of the isotherm). This means that for $K_{DEF} < 1/[M]$ θ_{DEF} does not reach the

value 1 (the site is not completely filled) and that for $K_{DEF} > 1/[M]$ θ_{DEF} becomes larger than 1 (the site becomes oversaturated). The breakpoint value of θ_{DEF} follows from eq 28a by first working out the differentiation and then multiplying the result with [M]:

$$(K_{DEF}[M])_{[M]^{*}} = \left(\frac{d \log[M]}{d \log \theta_{t}} \right)_{[M]^{*}} - 1 \tag{47}$$

Equation 47 shows that the 'breakpoint' value of θ_{DEF} is not a fixed value but depends on [M] and θ_{t}. In the previously discussed LIA approximations, the breakpoint value at any concentration $[M]^{*}$ occurs at $K_{LIA}[M]^{*} = 1$, independent of the overall isotherm.

Another strange phenomenon is the fact that after its maximum θ_{DEF} drops to zero, that is the site is emptied when the concentration becomes higher, which is physically unrealistic.

A graphical representation of the true and approximated local isotherm is shown in Figure 5. In Figure 5a the local isotherm is plotted as $\theta_{i}(K[M])$, which clearly shows the linear relationship for the initial part of the isotherm. Figure 5b shows the $\theta_{i}(\log K[M])$ plot which can be compared directly with the plots shown in Figure 1. At low [M] the DEF isotherm is equivalent to the ACA isotherm, however at the breakpoint θ_{ACA} reaches $\theta = 1$, whereas the DEF function reaches a maximum not equal to 1 and drops after the breakpoint to zero. As θ_{DEF} is not a logical approximation of eq 4 the obtained distribution function is hard to interpret in terms of a weighted true distribution as was done with the CA and LOGA method.

The formula for the distribution function was already suggested by Buffle, but can now be derived by introducing eq 46 in the overall adsorption equation (eq 45) for any fixed value of $[M]^{*}$:

$$\theta_{t} = \int_{0}^{\log K_{DEF}^{*}} K_{DEF}[M]^{*} f_{DEF}(\log K_{DEF}) \, d \log K_{DEF} \tag{48}$$
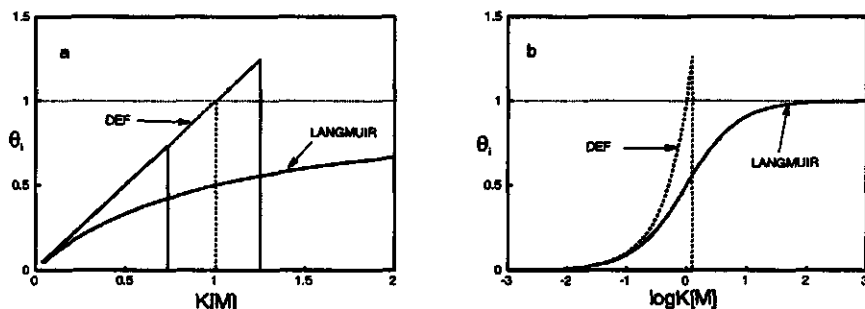
Figure 5: The LIA interpretation of the DEF method, θ_{DEF}, for details see text.

Dividing both sides of eq 48 by $[M]^{\#}$ gives:

$$\frac{\theta_t}{[M]^{\#}} = \int_0^{\log K_{DEF}^{\#}} K_{DEF} f_{DEF}(\log K_{DEF}) \, \mathrm{d} \log K_{DEF} \tag{49}$$

As eq 49 applies for each value of $[M]^{\#}$ the distribution of $\log K_{DEF}$ can be obtained by taking the first derivative of $\theta_t/[M]$ with respect to $\log K_{DEF}$:

$$\frac{\mathrm{d}(\theta_t/[M])}{\mathrm{d} \log K_{DEF}} = K_{DEF} f_{DEF}(\log K_{DEF}) \tag{50}$$

Substitution of eq 28a for K_{DEF} in eq 50 results finally in eq 29. The fact that this result is obtained shows that K_{DEF} and $f_{DEF}(\log K_{DEF})$ indeed can be interpreted within the LIA concept. Similarly as $f_{CA}(\log K_{CA})$ and $f_{LOGA}(\log K_{LOGA})$, $f_{DEF}(\log K_{DEF})$ is an approximation of the true distribution function $f(\log K)$.

Because of the strange behaviour of the DEF local isotherm it is hard to predict what the DEF distribution will look like for a given situation. A few major characteristics can be given. First, for high values of K_{DEF}, especially when $K_{DEF} > 1/[M]$ (that is at very low concentrations where the high affinity sites are filled) the method tends to blow up details due to the fact that the low maximum in θ_{DEF} must be compensated

78

by a larger density of the distribution. For intermediate values of K_{DEF} the density is somewhat higher than the true distribution due to the fact that sites with a higher affinity are already emptied and don't contribute to θ_t any more. In the low affinity part the densities are lowered because of the large maximum in θ_{DEF}. In addition the integral of the distribution function should be one, so when parts of the DEF distribution are higher than the true one, other parts should be lower than the true one.

Practical Comparison

Based upon the fundamentals of the methods it is easy to see that, in the absence of experimental error, the LOGA method will in general result in a better approximation of the true distribution than the CA method. From the derivation of the DEF method it follows that this method results in a perfect approximation for a homogeneous system, but in an asymmetrically deformed distribution function for heterogeneous systems. Apart from this crude general understanding a more detailed insight in the quality of the methods, if applied to highly accurate data, is required. To test this quality we will use overall binding functions that are calculated based upon known affinity distributions. Only in such a way it is possible to compare the outcome of a certain method with the true distribution function. As the selection of examples for this comparison is arbitrary we will include two examples which have been selected before by Gamble and Langford (26) and Buffle et al. (31) to illustrate the DEF method.

The first example, taken from Gamble and Langford (26), describes a system consisting of a discrete mixture of four monofunctional ligands, see Table 1. The $\Delta \log K$ between two successive ligand types ranges from 0.6 to 0.9 $\log K$ units which is a rather narrow interval.

In Figure 6 both $\log K_{DEF}$ and $\log K_{CA}$ are plotted as a function of θ_t, the way in which Gamble plots his results. A comparison of Table 1 and Figure 6 shows that the $\log K_{DEF}$ range is somewhat smaller than the range of the true affinity constants. For extremely low θ_t values $\log K_{DEF}$ corresponds with the highest affinity constant of the ligand system. In the rest of the curve K_{DEF} is a weighted function of the four affinity values as presented by eq 44. The curve does not reach the value of the smallest affinity since it is weighted by larger values. The CA method gives a dif-

i	compound	fraction	logK
1	malonate	0.32	5.55
2	carbohydrazide	0.22	4.92
3	glycine ethyl ester	0.16	4.14
4	tartrate	0.30	3.20

Table 1 : Discrete ligand mixture, example taken from (26).

ferent result. Both at low and high values of θ_t a range of $\log K_{CA}$ values is found which do not exist in reality. Consequently the whole range of $\log K_{CA}$ values found is much larger than in the case of the DEF method.

The "Gamble-plots" presented in Figure 6 are not intended to be distribution functions. They indicate the course of $\log K_{CA}$ and $\log K_{DEF}$ as a function of θ_t. For a comparison of the obtained results with the actual distribution function, $f(\log K)$ should be plotted. However, both the distribution function obtained with the DEF method and the CA (or LOGA) method are continuous distribution functions, whereas the chosen example is based on a discrete distribution. Since the ligand fractions, f_i, and the affinity density, $f(\log K)$, are different quantities it is impossible to compare the resulting distribution function with the true distribution in an unarbitrary way in one figure: there will always be an arbitrary scaling factor involved. This problem can be overcome by calculating the cumulative distribution function $F(\log K)$, for both the true (discrete) distribution, and the distributions functions resulting from a LIA or DEF method. The cumulative LIA and DEF distributions can be obtained from their distribution function by integration. The value of $F(\log K)$ for a certain value of $\log K$ corresponds with the area under the distribution function up to this $\log K$ value. In case of a normalized distribution function the maximum value of $F(\log K)$ is the surface area under the entire distribution function which equals one. For CA and DEF the cumulative distributions can directly be obtained by plotting θ_t versus $\log K_{CA}$ or $\log K_{DEF}$.
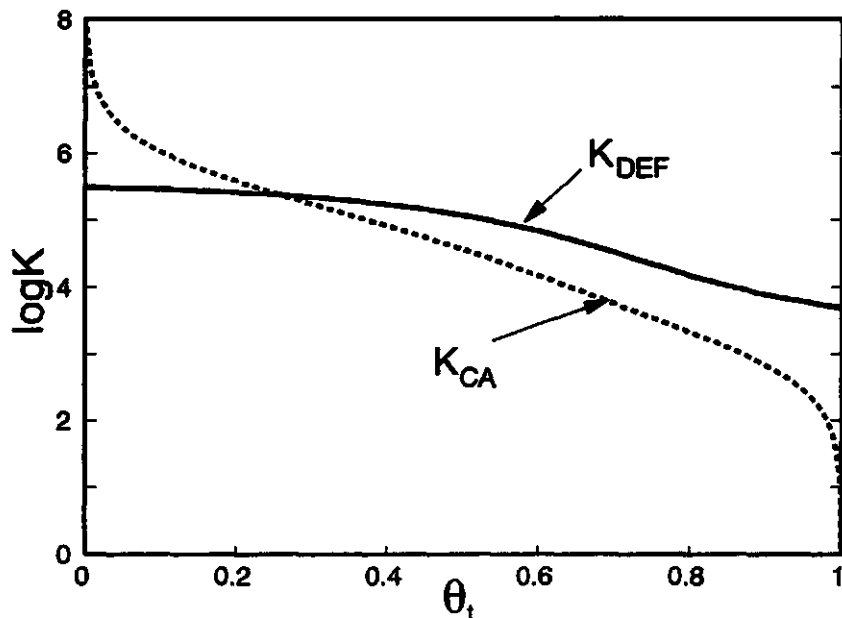
Figure 6: 'Gamble plots' of the DEF ($\log K_{DEF}(\theta_t)$) and CA ($\log K_{CA}(\theta_t)$) results for the first example. See Table 1 for the true K_i values and the corresponding fractions.

In Figures 7 a, b and c the true cumulative distribution is compared with the results obtained using the DEF, CA and LOGA method respectively. All these methods result in smooth curves, which is in contrast with the "staircase" like true cumulative distribution. The DEF method (Figure 7a) only approximates the true distribution closely for the highest $\log K$ value. Both the CA (7b) and the LOGA (7c) follow the true distribution pattern over the whole range of the distribution although the steps are smoothed to a continuous function. The LOGA method (Figure 7c) follows the true distribution most closely as is to be expected. It should be noted that the cumulative DEF and CA distributions are essentially the same as the result presented in Figure 6. The reason for this is that for both the DEF and CA $\theta_t(\log K)$ is equivalent to $F(\log K)$. For the LOGA method $\theta_t(\log K)$ is not equal to $F(\log K)$.
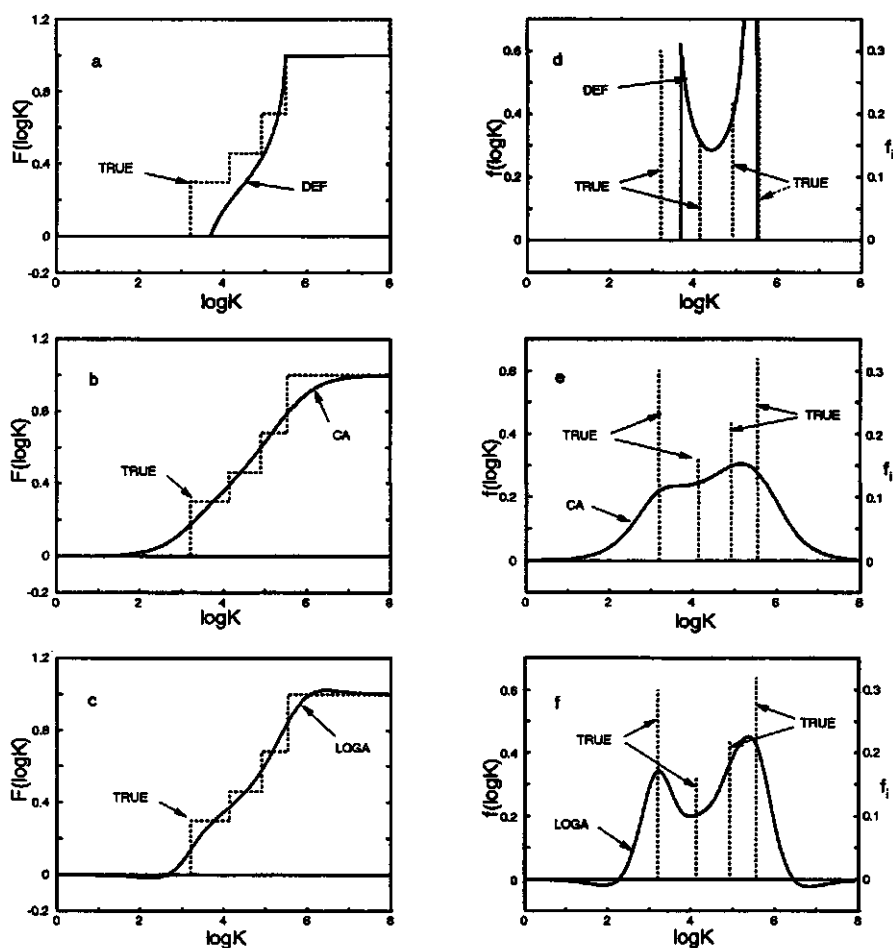
Figure 7: Cumulative and differential distributions obtained with the DEF, CA and the LOGA method for the first example, see for details of the true distribution Table 1. In Figures 7a, 7b and 7c the cumulative distributions are presented in combination with the true cumulative distribution. In Figures 7d, 7e and 7f the differential distributions are presented obtained with the DEF, CA and LOGA method respectively in combination with the true differential distribution.

Hence with the DEF and CA method the Gamble plots, although constructed slightly different are cumulative distribution functions. In the following we will therefore only present the cumulative distributions and no longer the Gamble plots. Although the cumulative distribution allows the best comparison of results for this example, in Figures 7d, e and f the differential distributions are shown together with the true distribution. As stated before the vertical scales belonging to both representations cannot be matched. Nevertheless the real $\log K$ values of the ligand mixture and their relative occurrence are directly evident from respectively the position and the length of the spikes. On the y-axis on the right hand site the values of the fractions can be read.

In Figure 7d the resulting DEF distribution is given. The distribution is rather featureless and is not capable to indicate the presence of the four individual ligands with the small $\log K$ interval. At $\log K_{DEF} = 5.5$ an unrealistic value (10.7) for the density is obtained, which is far out of the range of the $f(\log K)$ axis in Figure 7d. The CA distribution, given in Figure 7e, is a rather broad featureless distribution and is also not capable to indicate the presence of the four ligands. In Figure 7f the LOGA distribution is compared with the true distribution. The LOGA method results in two clearly separated peaks instead of four individual peaks.

In general it may be concluded that all three methods are incapable to resolve the affinity distribution if the peak positions of the individual ligands making up the system are closer than about one $\log K$ unit.

The second example is a combination of two gaussian distributions with a difference in peak position of 1.5 $\log K$ units (see figure caption of Figure 8 for details). The example is taken from Nederlof et al. (30). In Figures 8a, b and c the true cumulative distribution is given together with the results obtained with the DEF, the CA and the LOGA method respectively. For this case the result obtained with the DEF method deviates strongly from the true cumulative distribution over almost the entire $\log K$ interval. The CA cumulative distribution deviates strongly at the extremes of the distribution. The LOGA distribution follows the true distribution closely, but it is not as pronounced as the true distribution. In Figures 8d, e and f the results are replotted as differential distributions.
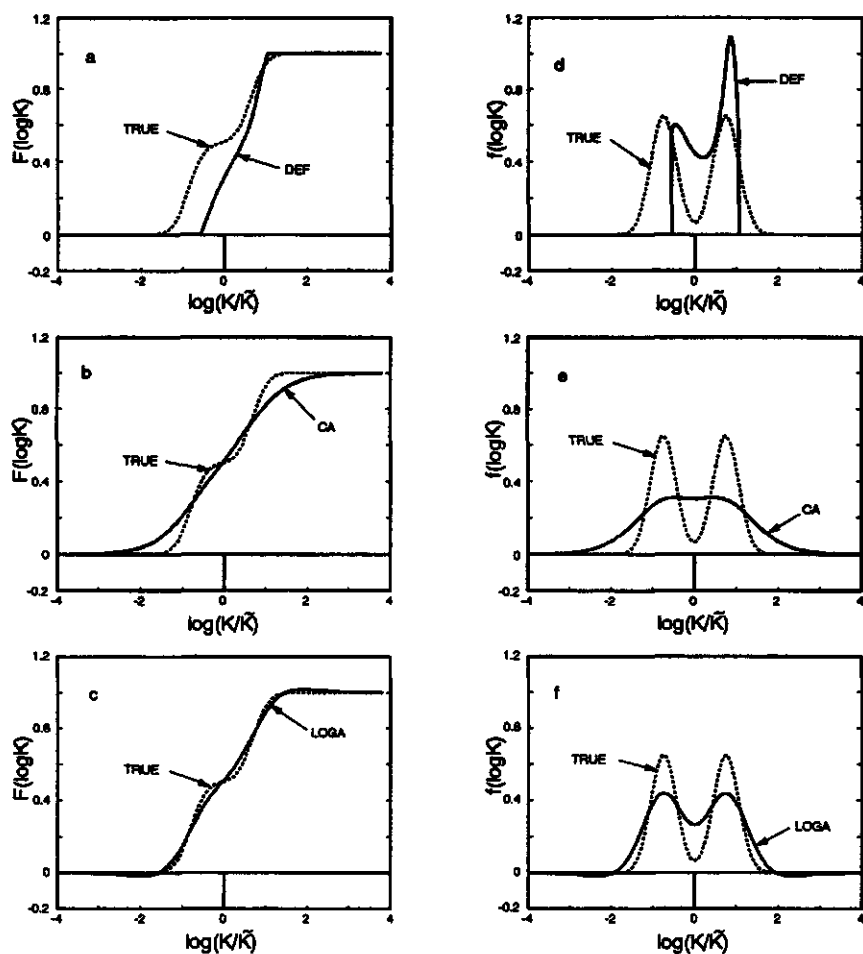
Figure 8: Cumulative and differential distributions obtained with the DEF, CA and the LOGA method for the second example. The true distribution is a bi-gaussian distribution with a difference of 1.5 $\log K$-unit in peak positions and a width of 1. The results are presented in the same order as in Figure 7.

84

It follows that the DEF method does not retain the symmetry (Figure 8d), the highest affinity peak dominates strongly over the lower affinity peak. Moreover, the positions of both peaks are shifted and the entire distribution has become too narrow. The shift of the high affinity peak is small, but the lower affinity peak is shifted to a considerably higher affinity. This result is due to the fact that each $\log K_{DEF}$ value is weighted by the distribution itself. The first peak area contributes substantially in the weighting of $\log K$ to obtain the second part of the distribution. The distribution obtained with the CA method (8e) results in one broad peak, whereas the LOGA method (8f) is capable to clearly distinguish the two separate peaks, although they are smooth and broader than the original ones. The positions of the two maxima and the minimum in the LOGA distribution correspond exactly with those of the true distribution and the symmetry of the distribution is retained. The last example is comparable to one of the examples used by Buffle et al. (31). The example is a continuous Sips distribution (semi - Gaussian) with m = 0.5 (55) with three discrete site types superposed on it. The discrete site types are in the high affinity range compared to the position of the continuous distribution (see figure caption of Figure 9 for details). According to Buffle et al. (31) such sites are important for the binding of heavy metal ions. Buffle calls them the dominant minor sites, the Sips distribution represents the major sites. In Figures 9a, b and c the resulting cumulative distributions of $\log K_{DEF}$, $\log K_{CA}$ and $\log K_{LOGA}$ are given together with the true distribution. In the high affinity range the $F(\log K_{DEF})$ and the true distribution are fairly similar. Around $\log K \approx 3$ (the position of the largest discrete peak) the true and the DEF distribution begin to deviate seriously. For the lower affinities the DEF result is systematically shifted towards too high affinities. The CA cumulative distribution (9b) is much closer to the true one than the DEF cumulative distribution (9a). The LOGA method (9c) follows the true cumulative distribution rather closely over the whole affinity range with a rather smooth step for the largest minor site. The two small minor sites can hardly be discovered in the cumulative distribution.

In Figures 9d, e and f the calculated differential distributions are compared with the true distribution. As in the first example it should be stressed that plotting a combination of a continuous and a discrete distribution in one graph is problematic due to the different types of the vertical scale. The height of the discrete spikes
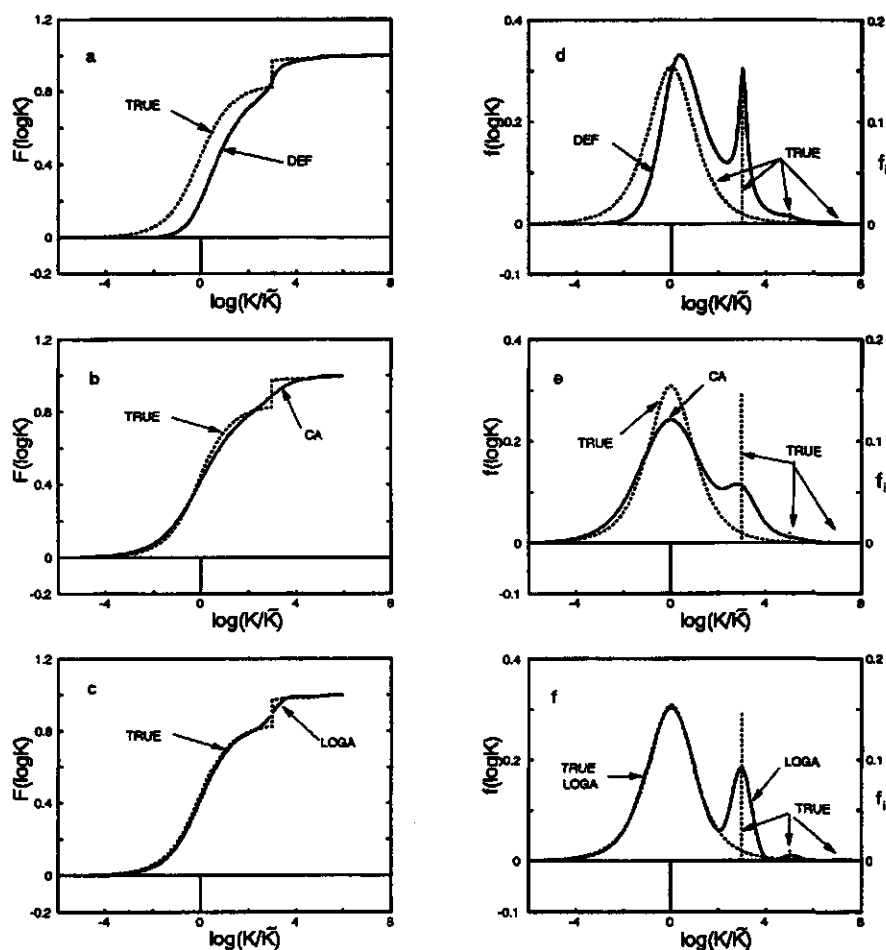
Figure 9: Cumulative and differential distributions obtained with the DEF, CA and the LOGA method for the third example. The true distribution is built up from a Sips distribution (m=0.5) (55) with three discrete site types superposed on it. The $\log K_i/\tilde{K}$ values of these sites are 3, 5 and 7 respectively, the corresponding discrete fractions are 0.144, .0101 and .002. The results are presented in the same order as in Figure 7.

86

cannot be compared directly with the height of a continuous peak at the same position of the affinity axis. The fractions can be read on the y-axis on the right hand side of Figure 9d-f. The DEF approximation (9d) shifts the broad peak towards higher affinities compared to the true distribution. The first discrete ligand (with the highest affinity) shows up very pronounced at about the correct position, whereas the other two discrete peaks appear as shoulders in the distribution. As expected the CA method (9e) results in broadened peaks. Nevertheless a clear indication of the largest minor site peak and its position is obtained. The small discrete peaks are not seen. The LOGA (9f) method follows the main broad peak almost perfectly and also the three discrete peaks are recovered.

To show the small peaks in the distribution clearly, Buffle usually plots the distribution on a log frequency scale. In addition he is mainly interested in the high affinity part (27). In that case the small peaks become indeed more prominent for both the LOGA and DEF method. The question is, however, whether the determination of the derivatives can be done accurately enough to allow this enlargement in practice. Even small errors in the data at low concentrations may be blown up in the distribution to unrealistic peaks.

Discussion

So far the comparison of the different methods was based on exact data. In each method at least the first derivative of a binding function is needed. Experimental errors may easily give rise to spurious peaks in the distribution function obtained (56,57), because of the difficulties in the determination of derivatives of experimental data. The higher the derivative needed the more difficulties are expected. In principle it is possible to deal with these problems by applying sophisticated smoothing spline techniques to the data (58-61), in which the extent of smoothing is related to the experimental error in the data, before applying a heterogeneity analysis technique. In general it is necessary to have such a smoothing technique available before the methods can be applied in practice. A smoothing spline technique adapted to the present problem will be presented in a forthcoming paper.

The CA method needs only a first derivative and is thus the least prone to errors. Although the LOGA-method leads in principle to better results than the CA-method, in practice this may not be the case because the third derivative of a

smoothed binding function is very small when the original data are smoothed strongly. Despite the fact that the Affinity spectrum method was designed with a smoothing parameter 'log(a)' it was shown that only for very small experimental errors (max. 0.1%) the smoothing was enough (39). For larger experimental errors spurious peaks result. This problem has brought some discredit to the affinity spectrum method (56,57). In our opinion the problem can be solved by the use of a sophisticated smoothing technique, which deals with the experimental errors, prior to the application of the affinity spectrum method for $\log a \rightarrow 0$. By using such a procedure the affinity spectrum methods become identical to either the CA or the LOGA method.

According to eq 27 $\log K_{DEF}$ is based on a (first) derivative and for the determination of the distribution function of $\log K_{DEF}$ a second differentiation is needed (eq 29). Since the CA method needs only one differentiation it follows that $f_{DEF}(\log K)$ is more prone to errors than $f_{CA}(\log K)$. The sensitivity to experimental errors of the DEF method is probably comparable to that of the AS_2 and LOGA method.

It has been stated (26) that the 'Gamble plot', $\log K_{DEF}(\theta_t)$, is sufficient to describe the heterogeneity of a ligand system and that therefore only such 'Gamble' plots need to be stored after an experiment. As the LOGA method gives at least as much information as the DEF method does we think that the original θ_t values as a function of log[M] should be stored in order to be able to apply different methods. In addition it is useful to store the original measured data for the application of a proper smoothing technique.

Conclusions

In each of the methods studied, approximations are made to derive analytical expressions for the distribution function, the results obtained will therefore deviate from the real distribution. All methods can be interpreted within the framework of the Local Isotherm Approximations (LIA). The Condensation Approximation (CA), in which the local isotherm is approximated by a step function, provides the most simple solution. A considerable improvement of the CA result can be achieved with the LOGA method. The LOGA ($\beta = 0.7$) approximates the Langmuir isotherm very well. The first and second order Affinity Spectrum (AS) methods turn out to be essentially equivalent to respectively the CA and the LOGA ($\beta = 1$) method. From

a fundamental point of view the Differential Equilibrium Function (DEF) is the least satisfactory. The local isotherm turns out to be approximated by a physically unrealistic 'saw tooth' type isotherm.

All methods result in a continuous distribution also when the true distribution is discrete, the different sites show up as peaks if the logK values of the site types are sufficiently different. The LOGA-method results in a series of peaks with peak positions corresponding with the positions of the actual peaks if the peaks are separated more then roughly one logK unit. Each peak area equals the fraction of the sites of the corresponding discrete ligand. The resolving power of the CA method is considerably less than that of the LOGA method and always a rather smooth distribution results. Peaks in the CA spectrum are only resolved when they are more than two logK units apart. Also with the DEF method peaks which are closely together cannot be discriminated. All peak positions will be shifted and peak areas will not result in a correct impression of the site fractions.

For smooth continuous distributions with one or more well separated peaks the LOGA method gives very good results. The DEF method will lead to distortions of the distributions. The CA method will result in too wide distribution functions, except if the distribution is very wide and smooth with a single peak.

In the case of discrete site fractions superposed on a smooth continuous distribution the LOGA method corresponds most closely with the true function. The DEF method works reasonably well for the high affinity minor sites, but results in a distorted distribution at the lower affinity end. The CA method smoothes the distribution strongly and small details are lost.

In general it may be concluded that for exact data, the LOGA method is the best of the methods studied, both from a fundamental point of view and from the point of view of the results obtained for the test functions.

Comparison of the LOGA distribution with the DEF distribution gives a clear indication of the limits of the logK range. The LOGA distribution is always somewhat too wide, the DEF distribution is always too narrow.

Experimental errors constitute a problem for all the methods discussed and, as indicated before, they should and can be treated separately.

References

(1)   De Wit, J.C.M.; Van Riemsdijk, W.H.; Nederlof, M.M.; Kinniburgh, D.G.; Koopal, L.K. *Anal. Chim. Acta* **1990**, *232*, 189-207.

(2)   De Wit, J.C.M.; Nederlof, M.M.; Van Riemsdijk W.H.; Koopal, L.K. *Water Air and Soil Pollution* **1991**, *57-58*, 339-349.

(3)   Simms, H.S. *J. Am. Chem. Soc.* **1926**, *48*, 1239-1250.

(4)   Scatchard, G.; Scheinberg, I.H.; Armstrong, S.H. Jr. *J. Am. Chem. Soc.* **1950**, *72*, 535-540.

(5)   Tanford, C. *Physical chemistry of macromolecules.* Wiley Interscience, New York, 1961.

(6)   Klotz, I.M.; Hunston, D.L. *Biochemistry* **1971**, *10*, 3065-3069.

(7)   Karush, F.; Sonenberg, M. *J. Am. Chem. Soc.* **1949**, *71*, 1369-1376.

(8)   Posner, A.M. *Trans. Int. Congr. Soil Sci.* **1967**, *8*, 161-174.

(9)   Gamble, D.S. *Canadian J. Chem.* **1970**, *48*, 2662-2669.

(10)   Hunston D.L. *Anal. Biochem.* **1975**, *63*, 99-109.

(11)   Ninomiya, K.; Ferry, J.D. *J. Colloid Interface Sci.* **1959**, *14*, 36-48.

(12)   Gamble, D.S.; Underdown, A.W.; Langford, C.H. *Anal. Chem.* **1980**, *52*, 1901-1908.

(13)   Benjamin, M.M.; Leckie, J.O. *J. Colloid Interface Sci.* **1981**, *83*, 410-419.

(14)   Shuman, M.S.; Collins, B.J.; Fitzgerald, P.J.; Olson, D.L. In *Aquatic and Terrestrial Humic Materials*; Christman, R.F.; Gjessing, E.T., Eds.; Ann Arbor Science: Ann Arbor, 1983; Chapter XVII.

(15)   Langford, C.H.; Gamble, D.S.; Underdown, A.W.; LEE, S. In *Aquatic and Terrestrial Humic Materials*; Christman, R.F.; Gjessing, E.T., Eds.; Ann Arbor Science: Ann Arbor, 1983; Chapter XI.

(16)   Perdue, E.M.; Lytle, C.R. In *Aquatic and Terrestrial Humic Materials*; Christman, R.F; Gjessing, E.T., Eds.; Ann Arbor Science: Ann Arbor, 1983; Chapter XIV.

(17)   Kinniburgh, D.G.; Barker, J.A.; Whitfield, M. *J. Colloid Interface Sci.* **1983**, *95*, 370-384.

(18)   Buffle, J. In *Circulation of Metals in the Environment*; Sigel, H., Ed.; Metal Ions in Biological Systems 18., M. Dekker: New York, 1984; pp 165-221.

(19) Cabaniss, S.E.; Shuman, M.S.; Collins, B.J. In *Complexation of Trace Metals in Natural Waters*; Kramer, C.J.M.; Duinker, J.C., Eds.; Martinus Nijhoff/ Dr.W. Junk Publishers: The Hague, 1984, pp 165-179.

(20) Sposito, G. *CRC Crit. Rev. Environ. Control* **1986**, *16*, 193-229.

(21) Van Riemsdijk, W.H.; Bolt, G.H.; Koopal, L.K.; Blaakmeer, J. *J. Colloid Interface Sci.* **1986**, *109*, 219-228.

(22) Van Riemsdijk, W.H.; De Wit, J.C.M.; Koopal, L.K.; Bolt, G.H. *J. Colloid Interface Sci.* **1987**, *116*, 511-522.

(23) Van Riemsdijk, W.H.; Koopal, L.K.; De Wit, J.C.M. *Neth. J. Agric. Sci.* **1987**, *35*, 241-257.

(24) Buffle, J.; Altmann, R.S. In *Aquatic Surface Chemistry: Chemical Processes at the Particle-Water Interface*; Stumm, W., Ed.; J. Wiley & Sons: New York, 1987; pp 351-383.

(25) Nederlof, M.M.; Van Riemsdijk, W.H.; Koopal, L.K. In *Heavy Metals in the hydrological cycle*; Astruc, M; Lester, J.N., Eds.; Selper Ltd.: London, 1988; pp 361-368.

(26) Gamble, D.S.; Langford, C.H. *Environ. Sci. Technol.* **1988**, *22*, 1325-1336.

(27) Altmann, R.S.; Buffle, J. *Geochim. Cosmochim. Acta* **1988**, *52*, 1505-1519.

(28) Buffle, J. *Complexation Reactions in Aquatic Systems: An Analytical Approach*. Ellis Horwood: Chichester, 1988.

(29) Nederlof, M.M.; Van Riemsdijk, W.H.; Koopal, L.K. In *Heavy Metals in the Environment*; Vernet, J.P., Ed.; CEP Consultants Ltd.: Edinburgh, 1989; vol.2, pp 400-403.

(30) Nederlof, M.M.; Van Riemsdijk, W.H.; Koopal, L.K. *J. Colloid Interface Sci.* **1990**, *135*, 410-426.

(31) Buffle, J.; Altmann, R.S.; Filella, M.; Tessier, A. *Geochim. Cosmochim. Acta* **1990**, *54*, 1535-1553.

(32) Buffle, J.; Altmann, R.S.; Filella, M. *Anal. Chim. Acta* **1990**, *232*, 225-237.

(33) Brassard, P.; Kramer, J.R.; Collins, P.M. *Environ. Sci. Technol.* **1990**, *24*, 195-201.

(34) Filella, M.; Buffle, J.; Van Leeuwen, H.P. *Anal. Chim. Acta.* **1990**, *232*, 209-223.

(35) Van Riemsdijk, W.H.; Bolt, G.H.; Koopal, L.K. In *Interactions at the Soil Colloid - Soil Solution Interface*; Bolt, G.H.; De Boodt, M.F.; Hayes, M.H.B.; McBride, M.B., Eds.; Kluwer Academic Publishers: Dordrecht, 1991; pp 81-114.

(36) Jaroniec, M. *Adv. Colloid Interface Sci.* **1983**, *18*, 149-225.

(37) House, W.A. In *Colloid Science* Specialist Periodical Report 4; Everett, D.H., Ed.; Royal Soc. Chem.: London, 1983; pp 1-58.

(38) Jaroniec, M.; Bräuer, P. *Surf. Sci. Rep.* **1986**, *6*, 65-117.

(39) Thakur, A.K.; Munson, P.J.; Hunston, D.L.; Rodbard, D. *Anal. Biochem.* **1980**, *103*, 240-254.

(40) Roginsky, S.S. *Adsorption catalysis on heterogeneous surfaces*. Academy of Sciences U.S.S.R.: Moscow, 1948; (in Russian).

(41) Harris, L.B. *Surface Sci.* **1968**, *10*, 129-145.

(42)   Cerofolini, G.F. *Surf. Sci.* 1971, 24, 391-403.

(43)   Cerofolini, G.F. *Thin Solid Films* 1974, 23, 129-152.

(44)   Hsu, C.C.; Wojciechowski, B.W.; Rudzinski, W.; Narkiewicz, J. *J. Colloid Interface Sci.* 1978, 67, 292-303.

(45)   Rudzinski, W.; Jagiello, J.; Grillet, Y. *J. Colloid Interface Sci.* 1982, 87, 478-491.

(46)   Davies, C.W. *Ion association*. Butterworth: London, 1962.

(47)   Koopal, L.K.; Van Riemsdijk, W.H. *J. Colloid Interface Sci.* 1989, 128, 188-200.

(48)   Merz P.H., *J. Comput. Phys.* 1980, 38, 64-85.

(49)   House, W.A. *J. Colloid Interface Sci.* 1978, 67, 166-180.

(50)   Koopal, L.K.; Vos, C.H. *Colloids Surf.* 1985, 14, 87-95.

(51)   Vos, C.H.; Koopal, L.K. *J. Colloid Interface Sci.* 1985, 105, 183-196.

(52)   Nolle, A.W. *J. Polym. Sci.* 1950, 5, 1-54.

(53)   Schwarzl, F.; Staverman, A.J. *Physica* 1952, 18, 791-798.

(54)   Schwarzl, F.; Staverman, A.J. *Appl. Sci. Res.* 1953, 4, 127-141.

(55)   Sips, R. *J. Chem. Phys.* 1950, 18, 1024-1026.

(56)   Turner, D.R.; Varney, M.S.; Whitfield, M.; Mantoura, R.F.C.; Riley, J.P. *Geochim. Cosmochim. Acta* 1986, 50, 289-297.

(57)   Fish, W.; Dzombak, D.A.; Morel, F.M.M. *Environ. Sci. Tech.* 1986, 20, 676-683.

(58)   Reinsch, C.H. *Numer. Math.* 1967, 10, 177-183.

(59)   Craven, P.; Wahba, G. *Numer. Math.* 1979, 31, 377-403.

(60)   Woltring, H.J. *Adv. Eng. Software* 1986, 8, 104-107.

(61)   Koopal, L.K.; Nederlof, M.M.; Van Riemsdijk, W.H. *Progress Colloid Polymer Sci.* 1990, 82, 19-27.

CHAPTER 4

Heterogeneity Analysis for Binding Data Using an Adapted Smoothing Spline Technique

Abstract

Heterogeneity analysis is a helpful tool to select a proper model for the description of ion binding to polyfunctional ligands. Two approaches of heterogeneity analysis are described, the Local Isotherm Approximation (LIA) method and the Differential Equilibrium Function (DEF) method. For the determination of an approximate distribution function for a given ligand system derivatives of an experimentally obtained binding function need to be determined. To obtain reliable derivatives an existing smoothing spline routine was adapted for the present problem. The smoothing parameter is determined by a Generalized Cross Validation criterion in combination with physical constraints related to the binding function. The distribution function is calculated on the basis of the spline function. Error bars for the obtained distribution function can be calculated using the variance in the spline function. The error bars indicate whether peaks in the distribution are significant. The methodology is firstly applied to a synthetic data set to illustrate its capabilities and limitations and secondly to an experimental data set to illustrate its use in practice. Finally it is shown how a binding model can be selected on the basis of the obtained distribution function.

Introduction

The binding of chemical species to natural polyfunctional ligands is a much studied subject (see e.g. refs. (1-5)), because it affects e.g. the mobility and bioavailability of the species present. In environmental sciences especially the role of organic macromolecules such as fulvo and humic acids are considered to be important with respect to ion binding. The chemical behaviour of this kind of materials is strongly influenced by their binding heterogeneity. Heterogeneous ligands possess different functional groups that have different affinities for the species that may bind to these ligands.

The different functional groups constitute an 'intrinsic heterogeneity'. Apart from the 'intrinsic' chemical binding heterogeneity, other factors may also affect the binding behaviour at a given concentration in solution, like electrostatic effects, competition with protons, stoichiometry, and particle conformation (2,4).

Modelling of binding to heterogeneous ligands is often done by a priori assuming a type of binding function followed by fitting the model parameters. Munson and Rodbard (6) developed a computer program that essentially fits the constants of a multiple discrete site binding model. The program was developed as a major improvement of the (graphical) Scatchard analysis (7) method. The latter is used to determine the number of site types in the model of Munson and Rodbard. Perdue (8) used a gaussian distribution to model metal ion binding to humic material. Since different models lead to equally good descriptions for a given set of binding data, this is not a very satisfactory approach. Analysing the binding in terms of a distribution function of affinity constants without a priori assumptions with respect to the type of distribution allows us to select an appropriate binding model.

Only in favourable cases it is possible to discriminate between the intrinsic chemical heterogeneity and 'secondary' effects. For proton adsorption to humic and fulvic acids it was shown that the electrostatic effects can be accounted for before analysing the intrinsic heterogeneity (9,10). In all other cases the determination of an 'apparent distribution' may be useful to study the binding behaviour, and it may form a basis for the selection of a proper binding model.

Several methods, both purely numerical and semianalytical, have been developed to study the heterogeneity of polyfunctional ligands on the basis of binding experiments. Main objective of these methods is the calculation of a distribution function of affinity constants. Several computer programs have been developed to

calculate the distribution function for natural systems numerically. Good results have been reported for gas adsorption studies with singular value decomposition (SVD) (11) and regularization (12,13) for relatively accurate data that cover a wide range of coverages. Recently Yuryev (14) developed a program based on the Tikhonov regularization (12) but results are not yet published. Mechanik and Peskin (15) used the Fourier transform technique to obtain the distribution function. Synthetic distributions were recovered very well, but it appeared difficult to discriminate between spurious peaks and true affinity peaks.

In this study we focus on the semianalytical methods that find an analytical expression for the distribution function. Nederlof et al. analysed methods of several authors (16-18) and found that all these methods can be interpreted as local isotherm approximations. With the semianalytical methods the distribution is obtained by taking the first and higher derivatives of the binding curve with respect to the concentration of the species that binds. The fact that always derivatives are required provides the basis of the present work. Taking derivatives of experimental data without preprocessing the data easily leads to spurious peaks (19-21), resulting from experimental errors. Thus, in order to apply semianalytical methods and to obtain reliable derivatives, a data processing procedure should be available which deals with the error in experimental data.

One of the classical methods that addresses the problem of spurious peaks due to experimental error is the Affinity Spectrum (AS) method (22-24). The AS method includes a parameter 'a' that should be able to suppress the effects of experimental errors. However several authors have shown (17,19-21) that in general the smoothing is not enough and that spurious peaks may still result that can easily be misinterpreted as (discrete) site types. In order to overcome this problem Fish et al. (20) have used a cubic smoothing spline to describe the data and applied the AS technique to the smoothed data. In principal spurious peaks could be smoothed away by increasing the smoothing parameter, but according to the authors there was no sound basis to decide which smoothing parameter was appropriate. Therefore, they concluded that the AS method was not reliable when experimental errors are present. Turner et al. came to a similar conclusion (21).

In this paper an adapted smoothing spline method is presented that, when applied to the experimental data, removes all inflections that lie within the range of experimental error. This does not mean that these inflections can not be realistic, but that within the range of experimental error no distinction can be made between inflections resulting from experimental errors and inflections caused by functional groups. The problem of finding a proper smoothing parameter is tackled by applying the Generalized Cross Validation (GCV) technique (25,26) in combination with physical constraints that should be fulfilled. Once a proper smoothing parameter is determined it is possible to represent the data with a spline, and to calculate the distribution function on the basis of that spline. In addition, from the variance in the spline, the uncertainty in the distribution function can be indicated by confidence intervals. The latter indicate whether peaks found are significant.

To test and illustrate the method the whole procedure is applied to both a synthetic and to an experimental data set. Experimental data were taken from Hansen et al. (27), who measured Copper binding to humic material. The data sets are described in the next section, which is followed by a brief overview of the semianalytical heterogeneity analysis methods. The smoothing spline technique and the determination of the smoothing parameter are discussed subsequently. The smoothing spline method and the heterogeneity analysis are applied to the synthetic data set with a known distribution function and to the experimental data set for which the true distribution function is not known. It will be shown how on the basis of the distribution function obtained for the experimental data an adsorption model can be selected. Finally a general discussion will be given of the presented methodology.

Data Sets

First a synthetic data set based on a known distribution function is used. This has the advantage that the results obtained can be compared with the true distribution. In addition a sensitivity analysis can be performed to study the capabilities and limitations of the procedure. The second data set consists of data measured by Hansen et al. (27) to illustrate the procedure in practice.

Synthetic Data Set

The synthetic data set strongly resembles the experimental data obtained by Hansen et al. (27). The binding function is given by a combination of three Langmuir-Freundlich equations. The Langmuir-Freundlich equation is given by:

$$\{M_b\} = \{S_t\}\frac{(\bar{K}[M])^m}{1+(\bar{K}[M])^m} \tag{1}$$

where $\bar{K}$ is the mean affinity of the distribution, m is a measure of the width of the distribution ($0<m<1$), [M] is the concentration of free M, $\{M_b\}$ is the amount of M bound and $\{S_t\}$ is the total concentration of sites (both bound and free). Sips (28) derived the analytical expression for the distribution function corresponding with eq 1. The result is a semi-gaussian distribution given by:

$$f(\log K) = \frac{\ln(10)\sin(\pi m)}{\pi\{2\cos(\pi m)+(K/\bar{K})^m+(K/\bar{K})^{-m}\}} \tag{2}$$

Figure 1a shows the bimodal distribution for the parameters given in Table 1. Using the analytical expression for the binding function, 100 data points ($\log[M]$, $\{M_b\}$) were generated equally spaced on the $\log[M]$ scale in the range from $\log[M] =-9$ to $\log[M]=-4$. This means that at the highest concentration no saturation of all the sites is reached. Thus only a part of the real distribution can be found with the

	fraction	$\log\bar{K}$	m
1	0.925	3.0	0.50
2	0.050	6.0	0.95
3	0.025	8.0	0.95

Table 1: Langmuir Freundlich parameters of the synthetic data set. The total site concentration is $\{S_t\}=2*10^4$ M.

heterogeneity analysis (indicated by the dashed line in Figure 1a). In practice it is quite common that only such a 'window' of the true distribution can be obtained. For sake of argument we will assume that the data set describes metal ion binding to a polyfunctional ligand. When [M] is measured by an ion selective electrode (ISE)
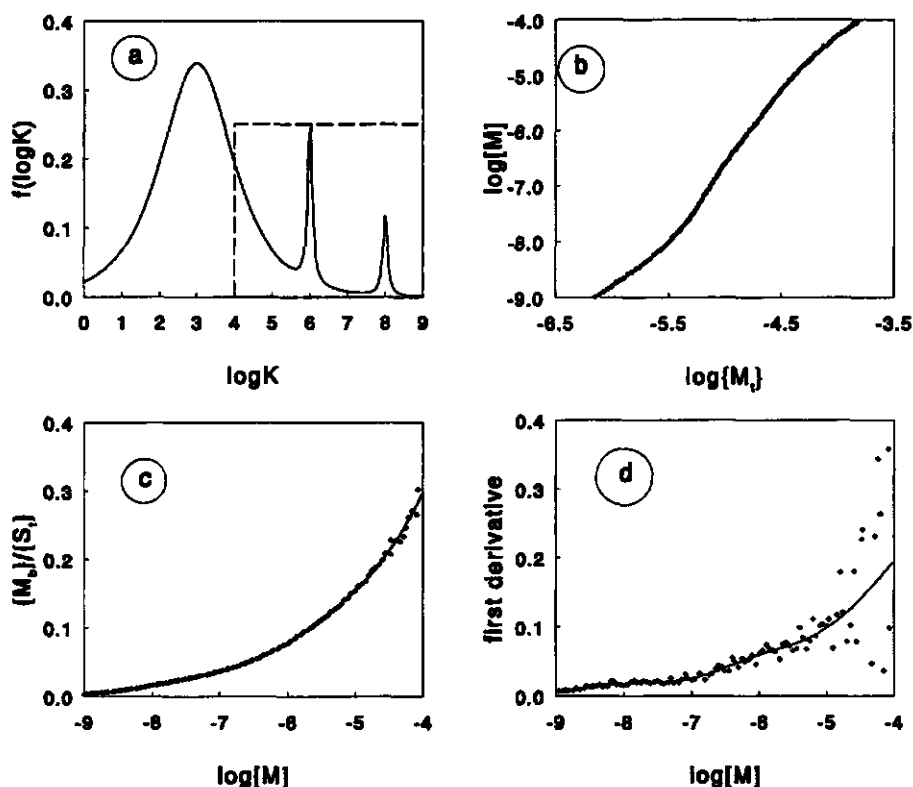

Figure 1: Synthetic data set. a) Normalized distribution function used to calculate the synthetic binding curve. The dashed line indicates the range of affinities that corresponds with the data presented in b). For the parameters of the distribution, see Table 1. b) The 'basic data' (log[M] as a function of $\{M_t\}$), on which an error is imposed with $\sigma = 0.01$, are indicated by the symbols, the solid line indicates the exact curve. c) The binding curve obtained on the basis of the basic data of figure b) (symbols), the solid line represents the exact curve. Both are normalized with respect to $\{S_t\}$. d) The first derivative of the binding curve with respect to log[M], the solid line indicates the exact curve.

the data obtained are potentials (mV) as a function of added volume. When the calibration curve of the electrode is linear on a log[M] scale, it follows that mV is direct proportional to log[M]. The added volume is directly proportional to $\{M_t\}$, the total concentration of metal ions in the system. In practice the experimental results will thus consist of log[M] data as a function of $\{M_t\}$. It is assumed that M can be added very accurately and thus the error in $\{M_t\}$ will be negligible. The absolute random error in log[M] is assumed to be constant with a standard deviation of $\sigma = 0.01$, which corresponds to a relative error of 2,5 % in [M]. With a random generator the random error in log[M] was imposed on the synthetic data set.

Figure 1b shows the obtained 'basic data' log[M] as a function of $\{M_t\}$. The error in log[M] is hardly visible on this scale. However, when the data are replotted as a binding curve, that is bound M, $(\{M_b\}=\{M_t\}-[M])$, as a function of log[M], it appears that for high concentrations irregularities occur (Figure 1c). The solid line represents the exact binding curve. Values of $\{M_b\}$ were normalized with respect to $\{S_t\}$. Thus, processing the data into a binding curve enlarges the error. This becomes more clear when the first derivative of the binding curve with respect to log[M] is calculated (numerically), see Figure 1d. Now also for lower concentrations deviations from the solid line become visible. The effects will become worse for higher derivatives, which are needed for the higher order heterogeneity analysis methods.
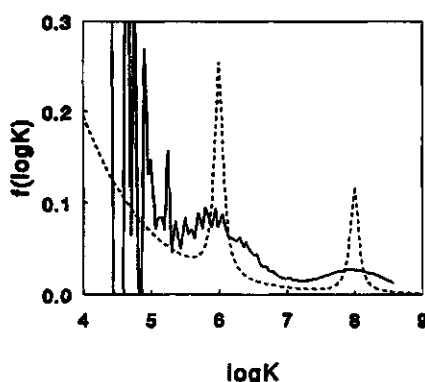

Figure 2: The Affinity Spectrum obtained from the synthetic data set when no preprocessing of the data is carried out. The dashed line indicates the true distribution function, corresponding to the window in Figure 1a.

100

This is illustrated in Figure 2, where the second order Affinity Spectrum (a=0.2) is shown: large spurious peaks occur for low affinities, corresponding with high concentrations, and for high affinities a rather smooth distribution is obtained. The AS method was applied directly after transformation of the basic data to a binding curve without further data processing. This was possible since the data were generated equidistantly on a log[M] scale. From these examples it becomes clear that a type of preprocessing of the data is needed before the heterogeneity analysis methods can be applied.

Experimental Data Set

The second data set consists of measured data taken from Hansen et al. (27) who studied copper binding to aquatic humic material. Filtrated water samples from three coastal lagoons in Mexico were titrated with a copper solution at pH=6 and 25°C. The cupric ion activity was measured with an ion selective electrode. In this way 36 data pairs log[M] as a function of total copper added, $\{M_t\}$, were obtained, see Figure 3a. Figure 3b shows the corresponding binding function which is normalized with respect to DOC (22.2 mg/l). When we assume that the variance of the random error in the measured electrode potential is constant and that the calibration curve of the electrode is linear over the whole measured range, then the variance in the error in log[M] is also constant as was the case with the synthetic data set. The solid curves and the error bars in Figures 3a and 3b are the result of the spline analysis to be discussed later.

Heterogeneity Analysis Methods

Basic Equations

The binding of a chemical species to a heterogeneous ligand is considered as the sum of the contributions of the binding to individual sites, each following the same type of binding reaction. The binding of a species M to an individual surface site S_i may be formulated as:

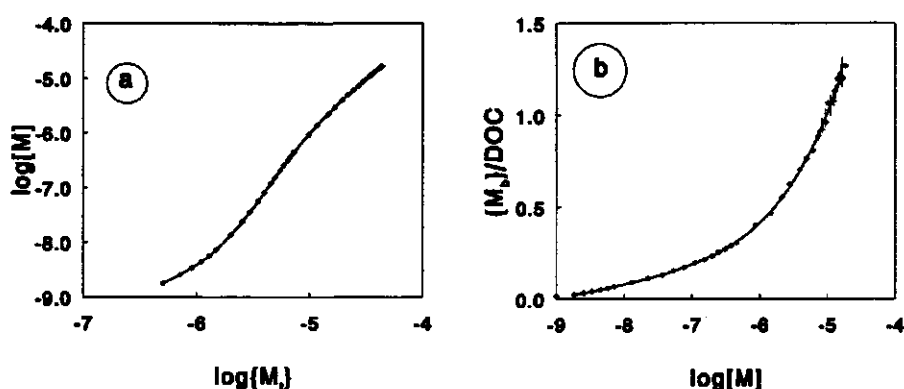$$S_i + M \rightarrow S_iM \tag{3}$$

Figure 3: Experimental data set of Hansen et al.(27). a) Basic data (symbols), the solid line indicates the spline calculated for these data, the uncertainty is indicated by the error bars. b) The binding curve calculated on the basis of the spline function and the points calculated directly from the basic data. The binding curve is normalized with respect to DOC (22.2 mg/1); the amount metal bound is expressed in mmol/g DOC.

where S_i is the empty site and S_iM the complexed site. The proportion of sites of type i that is occupied by M, indicated by θ_i , is usually described by a Langmuir isotherm, which is called the 'local isotherm':

$$\theta_i = \frac{K_i[M]}{1 + K_i[M]} \qquad (4)$$

where K_i is the affinity of a site i for the species M and [M] is the concentration of M. The proportion of the total number of sites occupied by M, θ_t, is given by the sum of the contributions of the individual sites weighted by their fractions f_i :

$$\theta_t = \sum_{i=1}^{n} f_i \theta_i \qquad (5)$$

It is often assumed that a very large number of different site types is present and then the summation can be written as an integral:

102

$$\theta_t = \int_{\Delta} \theta f(\log K) \, d \log K \qquad (6)$$

where θ is the local binding function, $f(\log K)$ is the distribution function and Δ is the range of possible $\log K$ values. Finding a distribution function implies the inversion of eq 6, which is a Fredholm integral equation of the first kind.

In the semianalytical methods two approaches can be distinguished to invert eq 6. The first is the group of Local Isotherm Approximation (LIA) methods (16,17) in which the local binding function is replaced by another function in order to solve eq 6 analytically for the distribution function. The Affinity Spectrum methods were shown to be equivalent with special cases of LIA (16,17). The second approach, the Differential Equilibrium Function (DEF) method (29-31), is based on the application of the Law of Mass Action to the whole ligand system. A discussion of the DEF method in relation to the LIA methods can be found elsewhere (18).

The Local Isotherm Approximation Methods

The simplest LIA method replaces the local isotherm by a step function, this leads to the following expression for the distribution function (32,33):

$$f_{CA} = \frac{d\theta_t}{d \log[M]} \qquad (7a)$$

$$\log K_{CA} = -\log[M] \qquad (7b)$$

The CA approximation of the Langmuir isotherm is poor and therefore the approximation of the distribution function is also poor. This is shown for the synthetic data set in Figure 4a. The main course of the distribution is reproduced, but the two high affinity peaks are very weakly reproduced. So the details of the distribution function are lost because of the approximate nature of the technique. Note that for the CA distribution only a first derivative of the binding function is required.

A first improvement of the CA method, proposed by Cerofolini (34) and extended by Nederlof et al. (16), replaces the local isotherm by a linear function, i.e. a LINear local isotherm Approximation (LINA). This results in the following expression for the distribution function:

$$f_{LINA} = \frac{\partial \theta_t}{\partial \log[M]} - 0.43 \frac{\partial^2 \theta_t}{\partial \log[M]^2} \tag{8a}$$

$$\log K_{LINA} = -\log[M] - \log \alpha \tag{8b}$$

where α is the slope of the linear isotherm. For $\alpha = 0.5$ the best correspondence with the Langmuir isotherm was found. Figure 4a shows the resulting distribution. The two high affinity peaks are somewhat more clearly reproduced than by using the CA method. In addition the main broad distribution is followed more closely. However, we are not in favour of the LINA method because it produces an asymmetric deformation of the true distribution function (see also (16)). Only in those cases where in addition to the first only a second derivative can be determined reliably, this method may reveal some more details than the CA method.

The third and best approximation of the local isotherm is called the LOGarithmic symmetrical Approximation (LOGA). The expression for the LOGA distribution is (16):

$$f_{LOGA} = \frac{\partial \theta_t}{\partial \log[M]} - \frac{0.189}{\beta^2} \frac{\partial^3 \theta_t}{\partial \log[M]^3} \tag{9a}$$

$$\log K_{LOGA} = -\log[M] \tag{9b}$$

In literature eq 9 has been reported with different values of β (16,35). The best approximation of the Langmuir equation is found for $\beta = 0.7$, we will indicate the resulting distributions as LOGA-1. The LOGA distribution with $\beta = 1$ is equivalent with the Affinity Spectrum method and is called therefore LOGA-AS. The LOGA-AS has the important advantage that the distribution remains always positive, whereas the LOGA-1 may give small negative parts for narrow distributions.
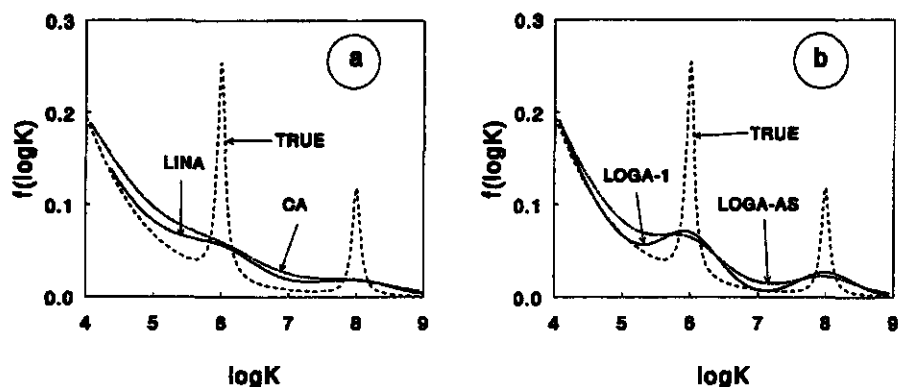
Figure 4: LIA distributions obtained for the exact synthetic data set compared with the true distribution (dashed line). a) The CA and LINA distribution; b) the LOGA-AS and LOGA-1 distribution.

Figure 4b shows the LOGA-1 and LOGA-AS distributions. The LOGA-1 follows the course of the main peak in the distribution very closely and the peaks at logK=6 and logK=8 are discerned more clearly than in the LOGA-AS case. Both the LOGA-1 and LOGA-AS distributions provide considerably better approximations of f(logK) than either the CA or the LINA distribution (see Figure 4a). The use of the LOGA method is restricted to cases where the third derivative can be determined accurately.

Differential Equilibrium Function

The DEF method starts by applying the Law of Mass Action to the whole ligand system which leads to the definition of an average equilibrium function (29,30):

$$\overline{K} = \frac{\theta_t}{[M](1 - \theta_t)} \tag{10}$$

Since the average parameter gives a poor representation of the underlying distribution function the Differential Equilibrium Function was derived which was intended to be closely related to the individual K_i values (29,30):

105

$$K_{DEF} = \frac{d\overline{K}(1-\theta_t)}{d(1-\theta_t)} = -\frac{d(\theta_t/[M])}{d\theta_t}$$ (11)

The expression for the distribution function reads (18,31):

$$f_{DEF}(\log K_{DEF}) = -\frac{d\theta_t}{d\log K_{DEF}}$$ (12a)

$$\log K_{DEF} = \log\left\{-\frac{d(\theta_t/[M])}{d\theta_t}\right\}$$ (12b)

The DEF distribution is shown in Figure 5a from which it follows that the distribution is shifted to higher affinities for the largest part of the distribution. The highest peak stays however on the right position and is remarkably well recovered. The second high affinity peak at logK=6 is less well reproduced.

An important difference between the CA or LOGA and the DEF method is that with the DEF method the logK axis is not simply obtained by transforming the log[M] scale into a logK scale by logK=-log[M], but that it is a weighted function of the logK values present. A comparison of K_{DEF} and K_{LOGA} for the present example is made in Figure 5b; it follows that at low concentration logK$_{DEF}$ decreases only slowly, whereas logK$_{LOGA}$ decreases linear with log[M]. After log[M]=-7 the logK$_{DEF}$ curve runs approximately parallel to logK$_{LOGA}$.

Sensitivity of Heterogeneity Analysis Methods

The quality of the distribution function obtained depends on the one hand on the capabilities of a given heterogeneity analysis method and on the other hand on the reliability with which the distribution can be obtained from experimental data. The quality of the distribution obtained for a given data set with a certain error depends strongly on the procedure to obtain a smooth curve through the data and the amount of smoothing applied. Whether the data have been smoothed enough in order to remove unwanted details can be tested by applying various physical constraints, that can be derived for a binding function, to the smoothed data.
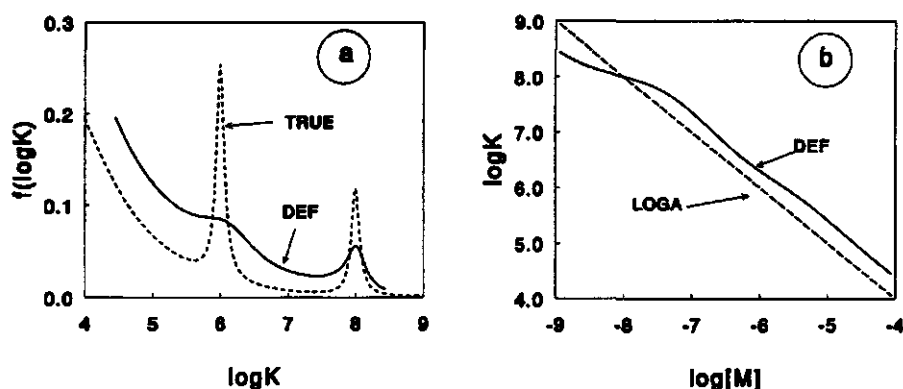
Figure 5: DEF distribution obtained for the exact synthetic data set. a) DEF distribution; b) comparison of K_{DEF} and K_{LOGA}.

Theoretical Accessibility of the Distribution Function

From calculations with exact synthetic data sets the sensitivity of methods can be studied in terms of their ability to reproduce a known underlying distribution function. The distribution obtained in this case represents the best possible result. In the presence of experimental error the result will always be worse. The capabilities of the LIA and DEF methods were studied extensively in Nederlof et al. (16-18). Some general conclusions may be drawn.

The LIA methods are capable of resolving wide and smooth distributions almost perfectly. Narrow peaks on a low and flat background are always broadened. If two peaks are separated less than approximately 1 logK unit the individual peaks will not be resolved. Peaks that are present on a steep background are difficult to resolve. The ability of identifying small peaks increases in the order CA, LINA, LOGA-AS, LOGA-1.

The DEF method is able to resolve the highest affinity peak in a distribution very distinctly. The lower affinity part of the distribution is flattened and shifted to higher affinities. The DEF method is less suitable to obtain an impression of the general shape of a distribution. Figures 4 and 5a illustrate these conclusions.

107

Experimental Accessibility of the Distribution Function

First of all eqs 6-12 suggest that for the determination of a distribution function the total number of sites $\{S_t\}$ should be known, since the functions are expressed in terms of the proportion of sites occupied by M. However when θ_t is replaced by $\{M_b\}/\{S_t\}$ it follows that a non normalized distribution function can be obtained as:

$$F(\log K) = f(\log K).\{S_t\} \tag{13}$$

where F(log K) is the non-normalized distribution function. The total number of sites is often unknown, but still a distribution function can be calculated. The shape of the distribution function obtained is not affected by the fact that the distribution is not normalized.

For the calculation of distribution functions the first and higher derivatives are needed. The higher the derivatives needed, the closer will the true distribution be approximated in principle, but the more will the result be prone to errors. For the LIA methods the sensitivity for experimental errors will be in the order CA, LINA, LOGA. It is difficult to place the DEF distribution in this sequence because it can't be written explicitly as a nth derivative of the binding function. Since there are two differentiation steps involved, one for the determination of K_{DEF} (eq 11) and one for the determination of the distribution function the net sensitivity will be probably in between LINA and LOGA. Note that for the determination of a so called "Gamble plot" (29,30), that is K_{DEF} as a function of $\{M_b\}$, only one derivative is needed.

Not only the density of the distribution is prone to errors, but also the values of logK. With the LIA methods the logK values are found by rescaling the log[M] axis by $logK=-log[M]- log\alpha$, where α is a constant (equal to zero for CA and LOGA). This means that for the LIA methods the uncertainty in the logK values due to experimental error is equal to that in log[M]. In the DEF method K_{DEF} is obtained from a differentiation. The uncertainty in $logK_{DEF}$ due to experimental error may be considerable, especially for values derived for the high concentration range, and should be accounted for.

The procedure of the data treatment should indicate whether it is justified to use higher derivatives. The unjustified application of higher order derivatives will lead to a very large uncertainty in (parts of) the distribution function. This can be checked

by calculating error bars for the distribution. Large error bars can be suppressed by increasing the amount of smoothing. Then, the spline procedure will flatten the binding curve and lower the values of the higher derivatives. This means that the LOGA distribution becomes approximately equal to the CA.

Physical Constraints
Some properties of the overall binding function can be used to decide whether peaks in a distribution are the result of an underlying heterogeneity or of an experimental error. These properties will be called 'physical constraints', because they are functions independent of the experimental conditions, the type of distribution and the magnitude of the experimental error.

Since, according to the local isotherm, the binding of a species to an individual site type increases with the concentration of the species, it follows that the sum of the binding to all individual site types also increases with the concentration. This means that the first derivative of the binding curve with respect to log[M] should always be positive. Thus also the CA distribution should always be positive. In terms of experimentally accessible quantities, [M] and $\{M_t\}$, the first constraint is:

$$\frac{d\{M_t\}}{d[M]} \geq 1 \tag{14}$$

This constraint is generally valid, the second and third constraint depend on the Langmuir function as local isotherm. Since the Langmuir isotherm is a convex function, when plotted on a linear [M] scale, the sum of the individual contributions is also a convex function. Thus the second derivative of the binding curve with respect to [M] should always be negative. In terms of $\{M_t\}$ and [M] the second constraint can be given as:

$$\frac{\partial^2\{M_t\}}{\partial[M]^2} \leq 0 \tag{15}$$

In most cases this is equivalent with demanding that the LINA distribution is positive. It follows also from the Langmuir functionality that the LOGA-AS distribution should always be positive (17). This leads to the third and most severe constraint:

$$\frac{\partial \theta_t}{\partial \log[M]} - 0.189 \frac{\partial^3 \theta_t}{\partial \log[M]^3} \geq 0 \qquad (16)$$

The third constraint has the disadvantage that it can not be applied directly to the basic data. In order to apply eq 16 the basic data should be converted to a binding curve for each adaptation step of the smoothing parameter, which is computationally not efficient.

It also follows from the Langmuir functionality that the Gamble plot, i.e. $K_{DEF}(\{M_b\})$, should always be a decreasing function as function of $\{M_b\}$ (or [M]). This means that the DEF distribution should always be positive. Since the DEF distribution is extremely sensitive for high affinity peaks the use of this property to find a smoothing parameter might lead to oversmoothing and will not be used as a constraint. It may help however in evaluating calculated results.

The use of a certain constraint can be coupled to the heterogeneity analysis method used. For the CA method at least the first constraint should be fulfilled, for the LINA the first and second and for DEF and LOGA all three constraints should be obeyed. The role of the constraint is that when the constraint is not fulfilled, there are apparently to many inflections left in the binding curve that should be smoothed away and thus the smoothing parameter should be increased.

Smoothing Spline Technique

Principle of Smoothing Spline

A well known method for describing noisy data is fitting a polynomial. The advantage of a polynomial is that the function is determined by a limited number of parameters and fitting can be done on the basis of a least sum of squares criterion. However, with a polynomial the type of function is fixed and therefore also a functionality of the distribution function is assumed beforehand. As the main goal

of heterogeneity analysis is to determine the distribution function and not assume one a priori, a polynomial fit to the data is not a useful way to go. The smoothing spline technique does not need a priori assumptions with respect to the functionality, therefore it is preferred over a polynomial fit.

The smoothing spline method is based on the assumption that the measured data can be represented as:

$$y_i(x_i) = g(x_i) + \varepsilon_i \tag{17}$$

where $g(x_i)$ is the sought value of the unknown function $g(x)$, $y_i(x_i)$ is the measured value as function of x_i and ε is assumed to be a normally distributed random error in y only. The spline procedure gives a non-parametric estimate of g and it was formulated by Schoenberg (36) and Reinsch (37). We use the software developed by Woltring (38) who combined a number of existing routines with his own experience. A good overview of the smoothing spline method is given by Silverman (25).

The basic principle of the smoothing spline technique is that a piecewise polynomial is constructed that connects 'knodal points'. The fitting of a polynomial is thus not carried out over the whole data range but only between two knots. Here the data points itself are taken as knodal points. The polynomials are connected at the knodal points in such a way that at these points the spline is continuous up to the $(2v - 2)^{th}$ derivative, where v is the order of the spline. A vth order spline means that $(2v - 1)$ order polynomials are used between each two successive knots. For the present purpose it is convenient to use a third order spline $(v = 3)$, because it is continuous up to the fourth derivative. Then all heterogeneity analysis methods can be applied on the basis of one and the same spline function.

An ordinary spline connects all the data points themselves, that is all the data points lie on the spline function. For noisy data this is not realistic, since there is a range of uncertainty around them. A smoothing spline takes this into account by fixing only the x_i-values of the measured data for the knodal points. It is assumed that these x_i-data represent the independent variable, in our case $\{M_i\}$. The amount of smoothing is determined by the smoothing parameter p, which regulates the trade off between the goodness of fit and the smoothness of the curve.

111

The goodness of fit is calculated as the weighted sum of squares of the differences between the smoothing spline, indicated by $s_p(x_i)$ and the measured values $y_i(x_i)$. The smoothness of a vth order spline is defined as the integral of the norm of the vth derivative of the spline over the whole x-range Δ ; it is a measure of the local variation. For a given smoothing parameter p the spline function is obtained by minimizing the function C_p:

$$C_p = \sum_{i=1}^{n} w_i \{y_i(x_i) - s_p(x_i)\}^2 + p \int_{\Delta} |s_p^{(v)}(x)|^2 \, dx \qquad (18)$$

where n is the number of data points, w_i is a weighting factor and $s_p^{(v)}(x)$ the vth derivative of the spline function. The weighting factors differ from $w_i=1$ when the variances of the individual points are not the same. It follows from eq 18 that the higher the smoothing parameter the more weight is given to the smoothness of the curve and the lower the smoothing parameter is the more weight is given to the goodness of fit. Thus, a small experimental error corresponds to a low smoothing parameter value and a large experimental error to a large one.

Ideally the smoothing should be large enough to assure that fluctuations due to experimental error are smoothed away, but small enough to conserve inflections that are due to existing functional groups. However, when the latter inflections are only as large as the deviations resulting from experimental errors, no method can discriminate between the two and the inflections will then be smoothed away.

This general understanding is however not enough to determine the value of the smoothing parameter. In the next paragraphs techniques to obtain the value of the smoothing parameter will be presented for the cases that the experimental error is known and unknown.

Determination of the Smoothing Parameter for Known Error

For known error the variance in the data can be used to find a proper smoothing parameter. In addition to the variance, two quantities are needed that can be calculated for a given smoothing parameter. The goodness of fit is expressed by the mean squared residual, R_p:

$$R_p = \frac{1}{n}\sum_{i=1}^{n} w_i \{y_i(x_i) - s_p(x_i)\}^2 \qquad (19)$$

This quantity is equal to the goodness of fit criterion in eq 18 divided by n. Figure 6a shows a plot of R_p as function of log(p) for the synthetic data set. For low values of the smoothing parameter R_p is very low because the spline follows the data closely. For values larger than log(p)=-5 the function sharply increases because the spline starts to deviate from the original data.

The smoothness of the function is controlled by the quantity Q_p. Q_p is an estimate of the relative number of degrees of freedom of the residual sum of squares, which means the relative number of degrees of freedom left in the residuals. It is defined by:

$$Q_p = 1 - \frac{1}{n}Trace(A_p) \qquad (20)$$

where A_p is the influence matrix which maps the original data y_i to the corresponding spline estimates g_i. This can be written as:

$$s_p(x_i) = \sum_{j=1}^{n} A_{p,ij} y_j \qquad (21)$$

The Trace of the matrix A_p is the sum of the diagonal elements of matrix A_p, these are equal to the factors $A_{p,ii}$ in eq 21. According to eq 21 each point $s_p(x_i)$ is a weighted average of the measured values y_i. The larger the value of $A_{p,ii}$ the more $s_p(x_i)$ resembles y_i. Thus the higher the sum of these diagonal elements the closer the spline will follow the data. Trace A_p can also be interpreted as the effective number of freely estimated parameters n_p. In eq 20 n_p is normalized by the number of data points n. Thus the closer n_p is to n the more accurate are the data. It follows that the higher the value of Q_p the smoother is the spline. Figure 6b shows Q_p as function of the smoothing parameter. For log(p) values larger than -13 the smoothness of the
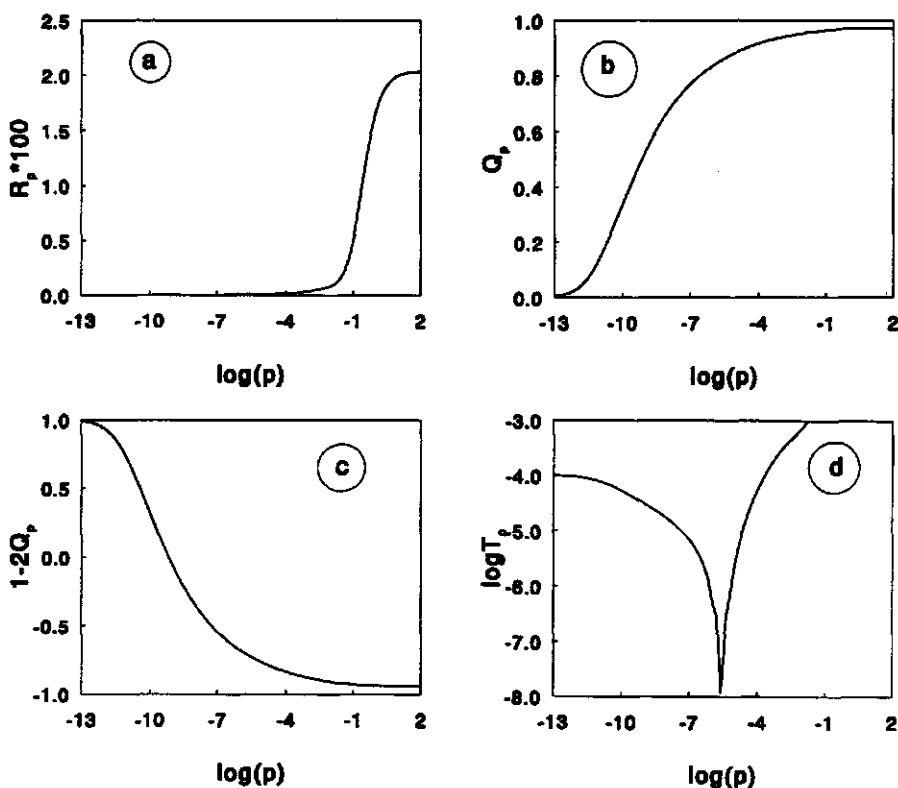
Figure 6: Quantities obtained from the spline function analysis, calculated for the synthetic data set with an error of σ = 0.01 as a function of the smoothing parameter. a) The mean squared residual R_p, values were multiplied by a factor 100 ; b) An estimate of the number of degrees of freedom of the residual sum of squares Q_p; c) Functionality of Q_p used for the minimizing function T_p; d) Minimizing function for known error, plotted as $\log T_p$.

spline function gradually increases. In other words the number of effectively estimated parameters n_p decreases. Comparison of Q_p with R_p shows that some smoothing of the spline occurs before R_p starts to increase.

R_p and Q_p are used together with the known variance in a criterion to determine the smoothing parameter. A proper smoothing parameter is found by minimizing the 'true predicted mean squared error', defined as (25):

114

$$T_p = R_p + \sigma^2(1 - 2Q_p) \tag{22}$$

Minimizing T_p means that R_p is kept as low as possible to assure a good fit and the number of effective estimated parameters, $\text{Trace}(A_p)$, is kept as low as possible to assure a smooth function. Figure 6c shows the $(1-2Q_p)$ function, which decreases gradually with increasing $\log(p)$. Figure 6d shows the $\log T_p$ function for the synthetic data set. A clear minimum in the function is found at $\log p = -5.6$.

Determination of the Smoothing Parameter for Unknown Error.

For unknown error Craven and Wahba (26) showed that a suitable criterion to determine a proper smoothing parameter is provided by the (Generalized) Cross Validation (GCV) function. The basic idea of the Cross Validation is to leave the data points out one at a time and then to select a smoothing parameter that predicts the missing data point the best. Thus the CV criterion that is to be minimized is given as:

$$CV_p = \frac{1}{n} \sum_{i=1}^{n} w_i \{y_i - s_p^{-i}(x_i)\}^2 \tag{23}$$

where $s_p^{-i}(x_i)$ is the spline value at x_i calculated on the basis of all data except (x_i, y_i). Craven and Wahba have shown that this function can be written in a computationally more convenient form (26):

$$CV_p = \frac{1}{n} \sum_{i=1}^{n} \left(\frac{w_i \{y_i - s_p(x_i)\}^2}{(1 - A_{p,ii})^2} \right) \tag{24}$$

The GCV is derived by replacing the diagonal elements $A_{p,ii}$ by their average value $\text{Trace}(A_p)/n$. Craven and Wahba showed that this computationally easier form gives asymptotically the best possible value of p. The GCV criterion can thus be written in terms of R_p and Q_p:
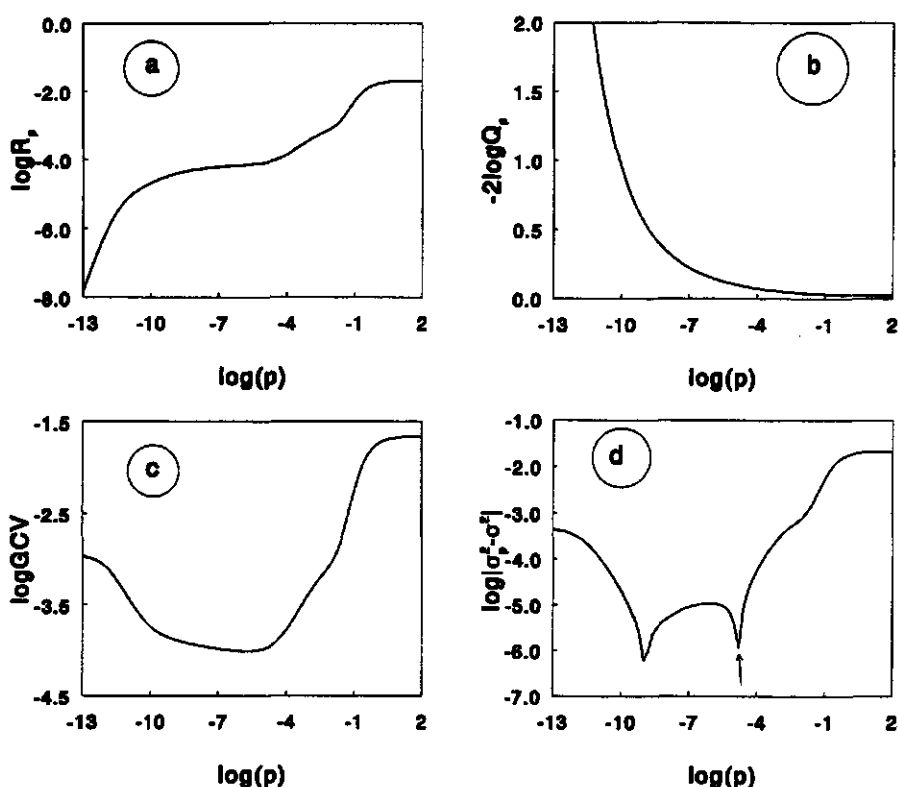
115

Figure 7: Quantities obtained from the spline function analysis for the synthetic data set with a random error of $\sigma = 0.01$. a) The logarithm of R_p; b) The logarithm of $1/Q_p{}^2$; c) The logGCV function; d) The logarithm of the absolute difference between σ_p^2 and σ^2.

$$GCV_p = \frac{R_p}{Q_p^2} \tag{25}$$

When plotted on a logarithmic scale the GCV function can be seen as a balance between $\log(R_p)$ and $-2\log(Q_p)$. These two quantities are plotted in figure 7a and 7b respectively for the synthetic data set. $\log(R_p)$ increases with $\log(p)$ and $-2\log(Q_p)$

decreases with log(p) as discussed in the previous section. The logGCV function itself is shown in Figure 7c. The minimum is found at log(p)=-5.8 , which is close to the value found using the known error (where a value of log(p)=-5.6 was found). Several authors report that the GCV estimate for the smoothing parameter some-times deviates from the proper value (see e.g. 39). In our case we found that GCV criterion results in either the correct or a too low value for the smoothing parameter. It is therefore sometimes necessary to add additional information to find the proper value of the smoothing parameter. We use the physical constraints for this purpose. In principle the constraints can be built in in the spline algorithm (40). However, no flexible algorithm is available yet for a combined use of the constraints and the GCV criterion.

When a proper estimate of the smoothing parameter is obtained, an estimate can be given of the variance σ_p^2 of the spline function (25):

$$\sigma_p^2 = \frac{1}{2} R_p (1 + Q_p)/Q_p^2 \tag{26}$$

σ_p^2 can be used in a variance analysis of the spline.

It should be remarked that the value of σ_p^2 can also be compared with an estimate of the experimental variance σ^2. Figure 7d shows the logarithm of the difference between the calculated variance, σ_p^2 , and the known experimental variance, σ^2 , as a function of log(p) for the synthetic data set. Two minima are found. The experience with the GCV function indicates that the second one at log(p)=-4.8 is the most realistic.

Variance of the Distribution Function

When the variance in y is either known or estimated by eq 26 it is also possible to calculate the covariance matrix of the spline coefficients. For linear functionals of the spline $s_p(x)$ the variance of the function can be calculated directly from the variance in the spline function. Since we assume here a non-linear relationship between the spline and the desired quantity, the variances have to be calculated by

117

Monte-Carlo simulation. For this purpose we used 100 realizations of the spline. In order to understand the basic idea it should be realised that the spline can be given in terms of n basis functions, β_i, and n spline coefficients γ_i (41):

$$s_p(x) = \sum_{i=1}^{n} \gamma_i \beta_i(x) \tag{27}$$

It is assumed that γ is multivariate normal with mean $\hat{\gamma}$ and covariance matrix S. Each realization of the spline is obtained by a realization of the set of spline coefficients γ. For each realization of the spline, the desired functionality can be calculated. In this way confidence intervals can be computed for the distribution functions. We used the Bayesian approach to obtain S (25,26,38). Although, according to Craven and Wahba (26), this procedure cannot be fully correct in a spline smoothing context it is often used, and since our purpose is not to quantify exactly the variances in the distribution, but 'only' to get an idea of the reliability, we consider the approach as a helpful tool for a further analysis.

Determination of the Distribution Function

In this section the heterogeneity analysis will be applied to both the synthetic data with the imposed artificial error and the experimental binding data. In the analysis the smoothing parameter is determined using the GCV smoothing spline technique in combination with the physical constraints. From the resulting spline 250 data points are generated equidistantially spaced on the log[M] axis. The CA, LINA, LOGA-AS, LOGA-1 and DEF method are applied to these calculated spline data to obtain the distribution functions by numerical differentiation. Finally confidence intervals are calculated using the Monte Carlo simulations to judge whether details in the distributions are significant.

Synthetic Data set
From the spline procedure for known error a smoothing parameter of log(p)=-5.6 was obtained. The GCV estimate was shown to be log(p)=-5.8. The splines based on these two values of the smoothing parameter obey the first and second physical constraint. In order to fulfil the third constraint the smoothing parameter has to be

118

raised to log(p)=-5.0. Thus it follows that for the synthetic example the procedures for known and unknown error in combination with the physical constraints, lead to the same smoothing parameter.

The resulting distributions for log(p)=-5.0 are shown in Figures 8a-8d and 9a. Each distribution is presented by a solid curve. The error bars indicate the uncertainty in the distribution and range from plus the standard deviation to minus the standard deviation respectively.
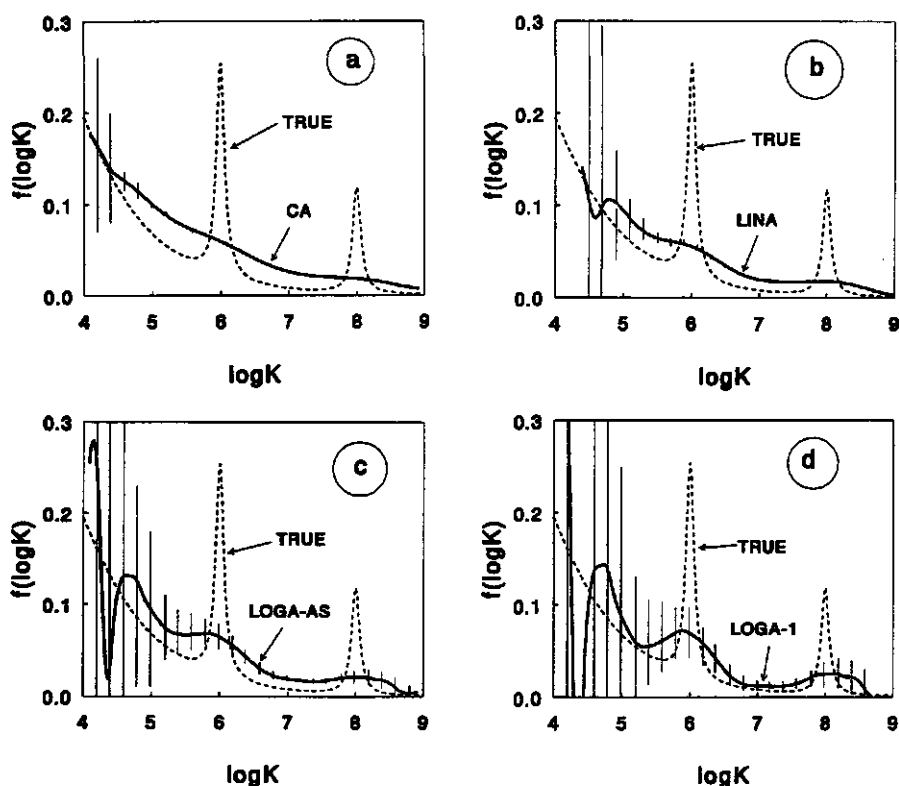

Figure 8: Distribution functions obtained on the basis of the spline function calculated for the synthetic data set with a random error of $\sigma = 0.01$. The dashed line represents the true distribution function. The confidence interval is indicated by bars. a) CA distribution; b) LINA distribution; c) LOGA-AS distribution; d) LOGA-1 distribution.
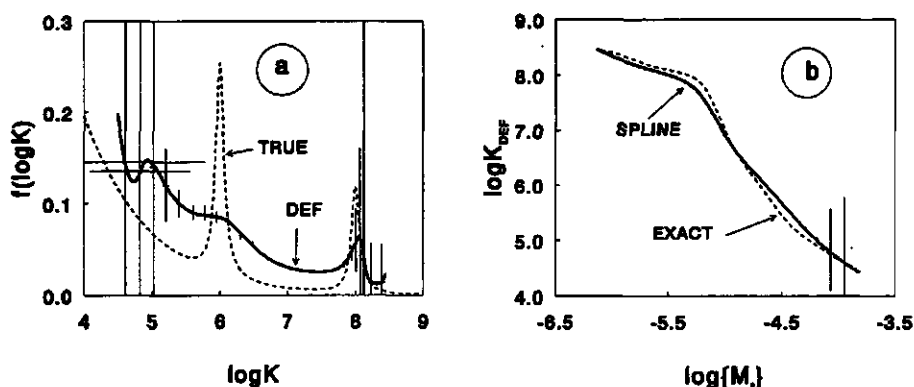
119

Figure 9: Distribution functions obtained on the basis of the spline function calculated for the synthetic data set with a random error of $\sigma = 0.01$. The dashed line represents the true distribution function. The confidence interval is indicated by bars. a) DEF distribution; b) $logK_{DEF}$ as a function of total metal added $\{M_t\}$. The dashed line was calculated with the exact data.

Note that these confidence intervals do not mean that the true distribution lies within this interval, but that for other realizations of the random experimental error, a result is found that lies within the indicated range with a probability of 66%.

The CA distribution (Figure 8a) is rather smooth and featureless. The result is nearly the same as the distribution obtained for the exact data (Figure 4a). The two high affinity peaks are reproduced very weakly. The variance in the result is rather low, only for affinity values lower than logK=5 is the variance distinct. Here the result slightly deviates from the result found in Figure 4a. The LINA distribution (Figure 8b) is slightly better than the CA distribution. Both high affinity peaks are weakly resolved. The variance has increased with respect to the CA result, especially for low affinities. This has the consequence that the variance at the position of the high affinity peak at logK=6 is not negligible any more.

The LOGA-AS and LOGA-1 (Figures 8c and 8d) clearly resolve both high affinity peaks. However, the variances have strongly increased as compared to CA and LINA, this is due to the third derivative involved. For affinity values below logK=5 the LOGA-AS result is not reliable any more. For the LOGA-1 result the situation

120

is slightly worse. The LOGA-1 distribution gives the best impression of the true distribution function but the variances are also the largest. The high affinity peak at logK=8 is shifted slightly to higher values.

The DEF distribution (Figure 9a) reproduces the peak around logK=8 very well, but the height of the peak is poorly defined, since the variance in the result is very large. Between logK=5 and logK=8 the variances are reasonably low, slightly worse than the LINA result. Except for the high affinity peak the shape of the DEF distribution is similar to the LINA result, but shifted to higher affinities. Note that for low affinities the variance in $\log K_{DEF}$ is considerable (horizontal error bars). Figure 9b shows the K_{DEF} calculated on the basis of the spline compared to those calculated from exact data. It follows that the spline result is somewhat flattened and that only for high $\{M_t\}$ values the error in $\log K_{DEF}$ is considerable.

Experimental Data

We start by applying the smoothing spline procedure ($v = 3$) to the data set of Hansen et al. (27). This is done to the basic data, i.e. $\log[M]$ versus $\{M_t\}$. In this way the error is the same in all the data points and the weighting factors may be set to 1. For $\{M_b\}$ data versus $\log[M]$ different weighting factors have to be used which leads to a far more complicated situation. From the GCV plot (Figure 10) it follows that a distinct GCV minimum is found at $\log(p)=-4.6$. Next, the spline obtained for $\log p=-4.6$ is checked with respect to the physical constraints. Only the first constraint is obeyed yet. Both other constraints are obeyed after increasing the smoothing parameter to $\log(p)=-4.3$. This value of $\log(p)$ is used for a further analysis. The resulting spline and the binding curve calculated from this spline are shown in Figures 3a and 3b respectively (solid lines). From the spline statistics for $\log p=-4.3$ an estimate of the error variance is obtained of $\sigma^2 = 2.2 \, 10^{-4}$. This means a relative error in $[M]$ of approximately 3.5%, which seems reasonable for an ISE experiment. The variances are indicated with error bars.

The resulting CA distribution (Figure 11a) is a smooth exponentially shaped curve with low densities for high affinities and an increasing density for low affinities. This indicates that the experimental window only allows the calculation of the high
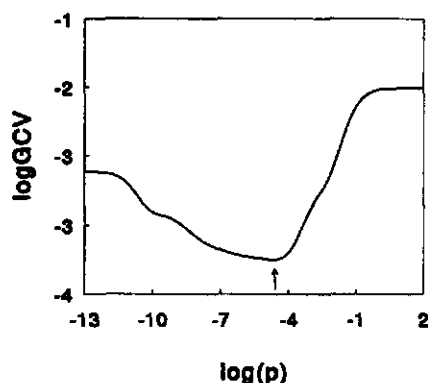
121

Figure 10: GCV plot for the experimental data set. A minimum was found at log(p)=-4.6.

affinity part of the distribution. The experiment reveals no information about affinities smaller than logK=5. The error bars indicate that the result is significant over almost the whole logK range.

The LINA distribution (Figure 11b) shows more or less the same picture despite the second derivative involved. The densities for low affinities are somewhat lower and at the end of the distribution at logK=9 the density drops clearly to zero. For affinity values lower than logK=6 the result is not reliable any more.

The LOGA-AS distribution (Figure 11c) exhibits on top of the main exponentially shaped distribution a high affinity peak at logK=8.5 and a very weak shoulder at logK=5.5. The shoulder is not significant because the variance is very large in that region. With the LOGA-1 (Figure 11d) the high affinity peak at logK=8.5 becomes more distinct, however the variance is also larger. Below logK=6 the distribution is not reliable any more.

The DEF distribution (Figure 12a) is shifted somewhat to higher affinities as was to be expected. Similarly as for the LOGA method the DEF distribution is not reliable for affinities lower than logK=6. Note that in that region also the variance in $logK_{DEF}$ is considerable. In addition a strange phenomenon occurs: at the high affinity end of the distribution negative values of the distribution were found at logK values in the range $7.2<logK_{DEF}<8.1$. To investigate this effect the $logK_{DEF}$ is plotted as a function of $\{M_j\}$ in Figure 12b. It follows that for low concentrations K_{DEF} increases with increasing concentration, which is physically impossible.
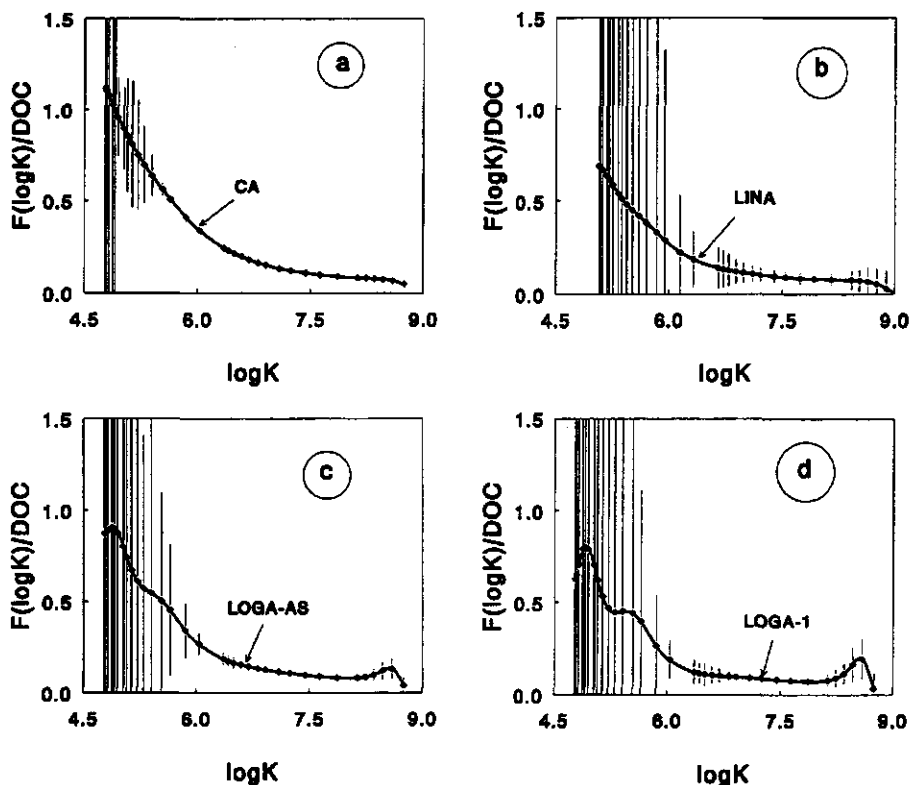
122

Figure 11: Distribution functions for the experimental data set based on the spline function $(\log(p)=-4.3)$. The symbols indicate the position of the original data on the logK axis. The confidence interval is indicated by the bars. Results are normalized with respect to DOC. a) CA distribution; b) LINA distribution; c) LOGA-AS distribution; d) LOGA-1 distribution.

After a maximum at about $\log K_{DEF}=8.1$ the values of $\log K_{DEF}$ decrease in the usual way. The values at the LHS of the maximum are responsible for the strange irregularity in the distribution function in the $\log K_{DEF}$ interval between 7 and 8. The strange behaviour is probably caused by a slightly non linear behaviour of the calibration curve of the copper electrode for low concentrations. Note also that the variance in $\log K_{DEF}$ is considerable for low values of $\{M_j\}$.
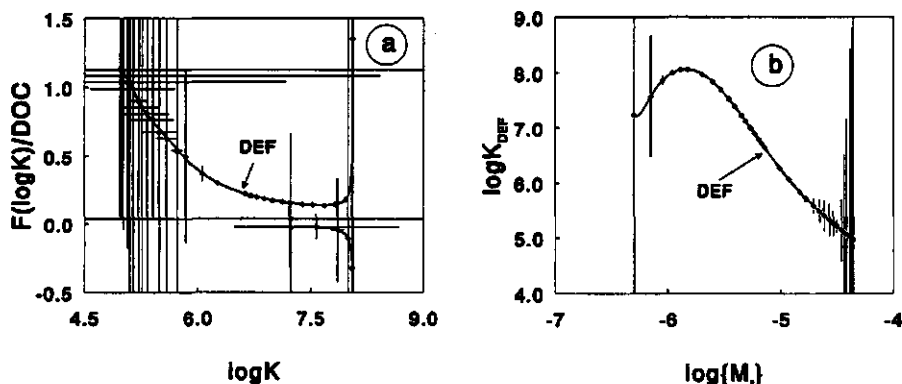
Figure 12: Distribution functions for the experimental data set based on the spline function (log(p)=-4.3). The symbols indicate the position of the original data on the logK axis. The confidence interval is indicated by the bars. Results are normalized with respect to DOC. a) DEF distribution; b) $logK_{DEF}$ as a function of total metal added $\{M_t\}$.

Selection of a Binding Model

The distribution that is obtained by the CA method shows a relatively wide and smooth distribution. If this would be the only information available, one might select for instance a Langmuir-Freundlich type distribution to describe the binding data, which is equivalent with using eq 1. In Figure 13a the best possible result of applying this equation is shown. Although the result is satisfactory for higher concentrations, the data systematically deviate from the calculated curve in the range $-8 < log[M] < -6$. The deviation is also much larger than the experimental uncertainty in the data in this region. This means that the model used cannot be a correct model. The fact that one broad distribution is not appropriate to describe this data set accurately follows also directly from the affinity distributions that are obtained with the LOGA and the DEF method. These methods show that in the high affinity range the site density can never be described properly by assuming only one simple continuous distribution.

In order to describe the binding behaviour over the whole range one may use a combination of two Langmuir-Freundlich type distributions. Another possibility is the introduction of a discrete high affinity site. Since the high affinity peak is rather narrow, and since less model parameters are involved, the use of a discrete site is
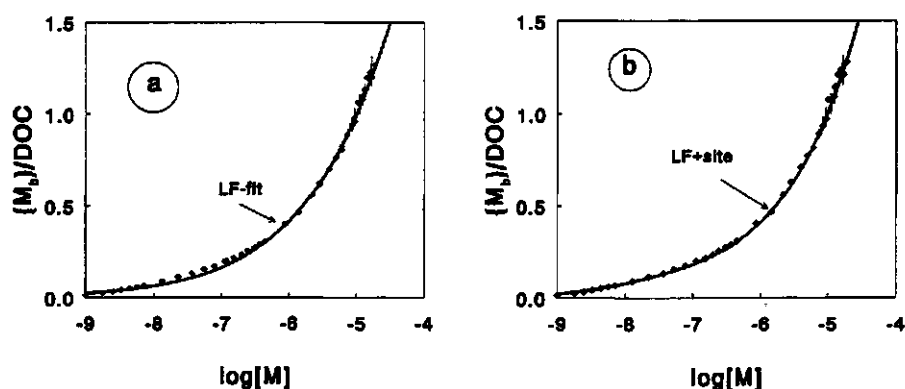
124

Figure 13: Model fit for the experimental data set compared with the binding curve calculated from the basic data. a) Langmuir-Freundlich isotherm (m=0.42, log$\tilde{K}$=3.04 and {S_t}=1.7*10^{-4} mol/l); b) Langmuir-Freundlich isotherm (m=0.48, log$\tilde{K}$=3.04 and {S_t}=2.0*10^{-4} mol/l) combined with a homogeneous high affinity site (logK=8.1, {S_t}=1.5*10^{-6} mol/l).

to be preferred in this case. According to the LOGA distribution it is expected that the affinity of the additional discrete site should be around logK=8.5, whereas the DEF method indicates a value of about logK=8.0.

When a Langmuir-Freundlich type distribution is combined with a discrete site type, the best results are obtained for a site at logK=8.1 with a density of 1.5 10^{-6} mol/l. This result is thus in very good agreement with the heterogeneity analysis. The parameters for the main peak are found as m=0.48, logK=3.04 and {S_t}=2.1 10^{-4} mol/l. Using this approach the binding data can be described correctly over the whole range within the experimental error as can be seen in Figure 13b. Although the site density of the high affinity site is small compared to the site density of the broad distribution it has a considerable effect on the binding curve especially for low concentrations.

Figure 14a and 14b show respectively the LOGA and DEF distribution based on the fitted Langmuir-Freundlich equation over the measured concentration range. In both cases it follows that the distribution calculated on the basis of the binding function with the extra high affinity site corresponds very well with the distribution
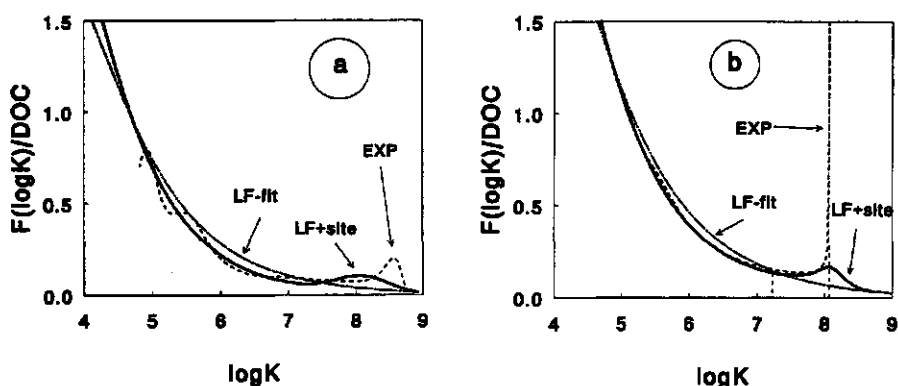
125

Figure 14: Distribution functions obtained from the experimental data compared with the distributions obtained on basis of the isotherm description of Figures 13 a) and b). a) LOGA distributions; b) DEF distributions.

obtained from the experimental data. For comparison the LOGA and DEF distributions are shown based on the Langmuir-Freundlich model without an extra high affinity site.

Note that the position of the high affinity peak in the experimental LOGA distribution is shifted to higher logK values with respect to the model result. This may the result of a slight deviation of the calibration curve from a straight line as was suggested in the discussion of the obtained K_{DEF} plot (Figure 12b).

Discussion

Evaluation of Methods

In a previous paper we compared the LIA (CA, LINA and LOGA) with the DEF method on the basis of their derivation and the results obtained for accurate synthetic data (18). In the present paper we analysed the extra problems involved when dealing with experimental data. From the LIA methods the CA method is the simplest and most stable method with experimental data. Generally the CA method results in too wide and too flattened distribution functions, except in those cases where the true distribution is already rather smooth and wide. The advantage of the CA method is that only a first derivative of the binding function is needed, which

126

makes it the least sensitive for error problems. Especially at high metal ion con-
centrations, where the absolute error is large in a typical ISE experiment and higher
derivatives can not be obtained reliably, the CA can still give the main characteristics
of the distribution.

The LINA method gives slightly better results than the CA, but the variance in the
result is also larger. Especially in cases where the third derivative cannot be
determined reliably the LINA method may give additional information. For high
quality data the method is less suitable because it results in an asymmetric defor-
mation of the true distribution.

The LOGA method gives in principle the best results, but is restricted to high quality
data. The general shape of a distribution function is well recovered in the region
where the third derivative can be determined reliably. For poor data, details within
the range of experimental error are smoothed away and the LOGA distribution will
resemble the CA distribution. For the low affinity part of a distribution the variance
in the LOGA density is often large and a more reliable impression of the distribution
is obtained with the CA method. All the physical constraints are needed in addition
to the GCV criterion to determine the smoothing parameter, to assure that the LOGA
distribution does not become negative and to prevent spurious peaks.

The DEF method was shown to be especially suitable for discriminating a single,
'minor sites affinity peak' at the high affinity end of a distribution. Other peaks at
lower affinities are considerably less well reproduced. Apart from the highest
affinity peak a rather smooth distribution results that is similar to the LINA result,
but shifted to higher affinities and less accurate. The DEF method is the least suitable
to determine the shape and position of a wide background distribution. Also for
the DEF method the physical constraints are needed to determine the smoothing
parameter and to prevent large oscillations in the high affinity range.

Concluding, the methods presented each have a right of existence. The CA is useful
because it is simple and even for poor data a global impression is obtained of the
distribution in the entire window. The LINA gives additional information when
the third derivative can not be determined. The LOGA gives a good picture of the
heterogeneity for accurate data sets and the DEF method tends to discern the
position of a high affinity peak most distinctly.

Resolving Power

The example from Hansen et al. discussed in the previous section shows the importance of the resolving power of the heterogeneity analysis methods. With the LOGA and DEF method a high affinity peak was found. Although the peak represents only a small fraction of the total (estimated) sites, these sites may play a major role at low concentrations, since they are occupied preferentially. This has special significance for practical problems in the environment where heavy metals are often present in trace amounts. Under these conditions only the "strongest" sites will be occupied by metal ions.

The high affinity sites are occupied at low concentrations. Since $\{M_b\}$ is found as $\{M_t\}$-[M] the absolute error in $\{M_b\}$ is equal to that in [M], assuming that $\{M_t\}$ is error free. Since the relative error in [M] is constant, the absolute error in [M] at low concentrations and thus in $\{M_b\}$ is very small. This has the consequence that in principle a (small) high affinity peak can be discerned better than a low affinity peak. This is especially the case when a relatively large concentration of sites is present.

Low affinities correspond with high concentrations of [M], in this case the difference $\{M_b\}=\{M_t\}$-[M] is relatively small and the absolute error in [M] is relatively large so that the value of $\{M_b\}$ is rather inaccurate. Hence, for a given accuracy in $\log[M]$, the resolution of the distribution function decreases with increasing $\log[M]$, or the lower the logK value of a peak, the harder it is to resolve this peak.

Besides the effect of the experimental error there is a clear effect of the background distribution. This was already shown in figure 4 for the synthetic data set without experimental error: in the calculated distributions the peak at logK=6 is smeared out over the exponential course of the distribution, whereas the peak at logK=8 is clearly discovered. So when the peak is situated at the tail of a distribution, as was the case in the Hansen example, the situation is favourable, a sharp peak placed on a steep part of a background distribution, however, reduces to a 'shoulder' in the calculated spectrum. The position of the high affinity peak on a broad distribution is thus critical for the resolution of that peak.

Remarks with Respect to an Experimental Data Set

In this paper 'basic data' were smoothed that is $\log[M]$ as a function of $\log\{M_b\}$. Often data are presented in literature as $\{M_b\}$ as a function of $\log[M]$. This means that if only these data are available smoothing has to be performed on this transformed data set. As mentioned above the variance in the error in $\{M_b\}$ may vary strongly with $[M]$, this indicates that the relative accuracy of the data should be individually accounted for by weighting factors, so that the larger the variance the less weight is given to the data point. Often the problem occurs that these variances are difficult to quantify, Silverman describes an approach (25) in which the weighting factors are determined iteratively. Model calculations on our synthetic data set show that for a relatively good data set, that is with sufficient data points (about 100) and a not too large error (<2.5%), the weighting factors have not much influence. For poor data serious problems occur with the determination of the smoothing parameter. In practice it is more easy to neglect the weighting factors and to rely on the physical constraints which for poor data lead to a large smoothing parameter and hence a flat distribution.

In general, three quantities characterise the quality of a data set: the number of points per $\log[M]$ unit, the variance of the experimental error and finally the range of $\log[M]$ measured (the experimental window). The number of data and the magnitude of the experimental error turn out to have a (partly) complementary effect. A larger error can be partly compensated by increasing the number of data points. Since for a given experimental method the accuracy of the measurement is generally hard to improve, it is advisable to create relatively large data sets (at least 10 data points per decade in the concentration, the total number of data should be at least about 40).

Enlarging the experimental window under the same conditions gives for low concentrations more information on the high affinity sites and for high concentrations on the low affinity sites. Within the LIA methods for each extra unit in $\log[M]$ another unit in $\log K$ can be obtained if also the isotherm still increases. Provided that low concentrations can be measured accurately, the high affinity sites can be determined reliably. At the other end of the distribution problems will occur when $[M]$ comes in the same order of magnitude as $\{M_t\}$, the error becomes large and the determination of a derivative is not possible any more.

129

When the experimental error can be estimated, it may be compared with the GCV estimate of the variance. In order to apply the GCV technique on basic data such as mV as function of added volume, the added volume should be known exactly so that mV may be considered the dependent variable. For the GCV analysis the assumption that the experimental error is random is crucial; it means that the error in any two measurements should be independent. When this is not the case and an irregularity in the experiment takes up a few data points, the resulting inflection in the binding curve will be interpreted as heterogeneity. This type of error may be a problem in situations were the measurement signal is recorded continuously.

Conclusions

- The present work shows that distribution functions can be obtained from experimental data, provided that the error problem is properly accounted for.
- Various semianalytical methods for the determination of f(logK) are available, the choice of a method depends on the quality of the data available.
- Determination of an affinity distribution from binding data is a very powerful tool for the selection of an appropriate binding model.
- A main problem in the heterogeneity analysis is the determination of derivatives of a binding curve on the basis of experimental sorption data, which are prone to experimental error. To obtain this curve a smoothing spline technique is most appropriate.
- To establish the smoothing parameter in an unarbitrary way the GCV technique in combination with physical constraints is recommended.
- For an optimal application of the GCV criterion it is essential to perform the smoothing procedure on the signal that is measured and not on an already 'transformed' data set, unless the propagation of experimental error is properly accounted for by weighting factors.
- Data with a relatively large experimental error will always lead to rather smooth distributions due to the necessary smoothing.
- Small peaks in a distribution function are hard to recover with the available methods when the peaks are present on a 'background' of a continuous distribution. A small, high affinity peak at the tail of a distribution can be discovered rather well with either the DEF or the LOGA method.

- Since there are several methods that have there own merits we strongly recommend archiving the originally measured basic data as much as possible.

References
(1)   Shuman, M.S.; Collins, B.J.; Fitzgerald, P.J.; Olson, D.L. In "Aquatic and terrestrial humic materials"; Christman, R.F.; Gjessing, E.T., Eds.; Ann Arbor Press: Ann Arbor, 1983, pp 349-370.

(2)   Perdue, E.M. In "Humic substances in soil, sediment and water: chemistry, isolation and characterization"; Aiken, G.R.; Mcknight, D.M.; Wershaw, R.L.; Maccarthy, P., Eds.; Wiley Interscience: New York, 1985, pp 493-526.

(3)   Dzombak, D.A.; Fish, W.; Morel, F.M.M. *Environ. Sci. Technol.* 1986, *20*, 669-675.

(4)   Buffle, J. "Complexation in aquatic systems: an analytical approach"; Ellis Horwood: Chichester, 1988.

(5)   Van Riemsdijk, W.H.; Bolt, G.H.; Koopal, L.K. In *Interactions at the Soil Colloid- Soil Solution Interface;* Bolt, G.H. De Boodt, M.F., Hayes, M.H.B., McBride, M.B., Eds.; Kluwer Academic Publishers: Dordrecht, The Netherlands, 1991; pp 81-114.

(6)   Munson, P.J.; Rodbard, D. *Anal. Biochem* 1980, *107*, 220-239.

(7)   Scatchard, G. *Ann. N.Y. Acad. Sci.* 1949, *51*, 660-672.

(8)   Perdue, E.M.; Lytle, C.R. *Environ. Sci. Technol.* 1983, *17*, 654-660.

(9)   De Wit, J.C.M.; Van Riemsdijk, W.H.; Nederlof, M.M.; Kinniburgh, D.G.; Koopal, L.K. *Anal. Chim. Acta,* 1990, *232*, 189-207.

(10)   De Wit, J.C.M.; Nederlof, M.M.; Van Riemsdijk, W.H.; Koopal, L.K. *Water Air and Soil Pollution,* 1991, *57-58*, 339-349.

(11)   Vos, C.H.W.; Koopal, L.K. *J. Colloid Interface Sci.* 1985 , *105*, 183-196.

(12)   Tikhonov, A.N. *Sov. Math.* 1963, *4*, , 1624-1627; 1035-1038.

(13)   House, W.A. *J. Colloid Interface Sci.* 1978, *67*, 166-180.

(14)   Yuryev, D.K. *J. Immunological methods* 1991, *139*, 297.

(15)   Mechanick, J.I.; Peskin, C.S. *Anal. Biochem* 1986, *157*, 221-235.

(16)   Nederlof, M.M.; Van Riemsdijk, W.H.; Koopal, L.K. *J. Colloid Interface Sci.* 1990, *135*, 410-426

131

(17)   Nederlof, M.M.; Van Riemsdijk, W.H.; Koopal, L.K. In " Heavy metals in the environment, trace metals in the environment 1"; Vernet, J.-P., Ed.; Elsevier, Amsterdam, 1991, pp 365-396.

(18)   Nederlof, M.M.; Van Riemsdijk, W.H.; Koopal, L.K. *Environ. Sci. Technol.*, **1992**, *26*, 763-771.

(19)   Fish, W.; Morel, F.M.M. *Can. J. Chem.* **1985**, *63*, 1185-1193.

(20)   Fish, W.; Dzombak, D.A.; Morel, F.M.M. *Environ. Sci. Technol.* **1986**, *20*, 676-683.

(21)   Turner, D.R.; Varney, M.S.; Whitfield, M.; Mantoura, R.F.C.; Riley, J.D. *Geochim. Cosmochim. Acta*, **1986**, *50*, 289-297.

(22)   Ninomiya, K. and Ferry, J.D. *J. Colloid Interface Sci* **1959**, *14*, 36-48.

(23)   Hunston, D.L.; *Anal. Biochem.* **1975**, *63*, 99-109.

(24)   Thakur, A.K.; Munson, P.J.; Hunston, D.L.; Rodbard, D. *Anal. Biochem.* **1980** , *103*, 240-254.

(25)   Silverman, B.W. *J.R. Statist. Soc. B.* **1985**, *47*, 1-52.

(26)   Craven, P.; Wahba, G. *Numer. Math* **1979**, *31*, 377-403.

(27)   Hansen, A.M.; Leckie, J.O.; Mandelli, E.F.; Altmann, R.S. *Environ. Sci. Technol.* **1990**, *24*, 683-688.

(28)   Sips, R. *J. Chem. Phys.* **1950**, *18*, 1024-1026.

(29)   Gamble, D.S.; Underdown, A.W.; Langford, C.H. *Anal. Chem.* **1980**, *52*, 1901-1908.

(30)   Gamble, D.S.; Langford, C.H. *Environ. Sci. Technol.* **1988**, *22*, 1325-1336.

(31)   Buffle, J.; Altmann, M.; Filella, M; Tessier, A. *Geochim. Cosmochim. Acta* **1990**, *54*, 1535-1553.

(32)   Roginsky, S.S. "Adsorption catalysis on heterogeneous surfaces", Academy of Sciences U.S.S.R., Moscow, 1948.

(33)   Harris, L.B. *Surf. Sci.* **1968** , *10*, 129-145.

(34)   Cerofolini, G.F. *Surf. Sci* **1971** , *24*, 391-403.

(35)   Rudzinski, W.; Jagiello, J.; Grillet, Y. *J. Colloid Interface Sci.* **1982** , *87*, 478-491.

(36)   Schoenberg, I.J. *Proc. Nat. Acad. Sci. U.S.A.* **1964** , *52*, 947-950.

(37)   Reinsch, C. *Numer. Math.* **1967** , *10*, 177-183.

(38)   Woltring, H.J. *Adv. Eng. Software* **1986**, *8*, 104-107.

(39)   Merz, P.H. *J. Comp. Phys.* **1980**, *38*, 64-85.

(40)   Elfving, T.; Andersson, L. *Numer. Math.* **1988**, *52*, 583-595.

(41)   De Boor, C. "A practical guide to splines", Springer Verlag, New York, 1978.

CHAPTER 5

Determination of Proton Affinity Distributions for Humic Substances

Abstract

Binding heterogeneity analysis is applied to charge-pH curves measured by Dempsey and O'Melia on fulvic acid samples. To calculate the affinity distribution function, derivatives of the overall proton adsorption isotherm are required. These derivatives are obtained by processing the basic data (pH as a function of added volume) by a smoothing spline algorithm. The smoothing parameter is obtained by the Generalized Cross Validation technique in combination with physical constraints. The spline function is used to calculate the adsorption isotherm and its derivatives. Confidence intervals of the calculated distribution functions are obtained on the basis of the variance in the spline.

Apparent affinity distributions are calculated on the basis of charge-pH curves for two values of the ionic strength. The distributions depend on the ionic strength, due to the electrostatic effects.

For the calculation of the intrinsic affinity distributions the "master curve" procedure developed by De Wit et al. is applied. To account for the electrostatic effects an electrostatic double layer model for rigid spheres is used. A master curve results for r=0.75 nm, using 1 g/cm^3 as density for the fulvic acids. The intrinsic affinity distribution obtained on the basis of the master curve can be described by a combination of two semi-gaussian peaks. Combination of the intrinsic affinity distribution with the electrostatic double layer model leads to a perfect prediction of the charge-pH curve for a third intermediate ionic strength.

Introduction

Humic substances are important in natural environments for their role in regulating ion concentrations in solution. Especially metal ions bind strongly to these materials (1-5). The binding is influenced by the variable charge properties and the chemical heterogeneity of humic material (6,7). As a consequence ion binding to these materials depends not only on the ion concentration itself, but also on environmental conditions such as pH and ionic strength. For a given set of experimental conditions ion binding may be described empirically by fitting a chosen binding function (2). Although data can be described reasonably well in this case, little insight is gained in the processes underlying the binding behaviour. In order to gain understanding in the binding mechanism and to develop a model for ion binding under different conditions, the charging behaviour of humic materials should be known (8-11).

The charging behaviour can be studied by performing acid/base titrations on the humic substances in absence of specifically adsorbing ions. Charge-pH curves for different salt levels can be obtained in this way. Applying heterogeneity analysis methods to such curves lead to affinity distributions (12,13). However, the obtained distributions depend on ionic strength and are called "apparent" affinity distributions. In order to obtain "intrinsic" affinity distributions De Wit et al. (6,7,14,15) have developed the "master curve procedure" for the analysis of the charge-pH curves. The approach consists of two steps. First the ionic strength dependency is filtered out by applying an electrostatic double layer model. With the double layer model the pH is transformed to pH_s, the local pH near the charged sites. When a proper electrostatic model is used, the charge-pH_s curves at different ionic strength values merge into one "master curve". The obtained master curve depends on the chemical heterogeneity of the material only and an intrinsic affinity distribution can be determined using heterogeneity analysis techniques (6). In this way the chemical heterogeneity can be analysed separately from the electrostatic effects.

In this paper the methodology to calculate proton affinity distributions is illustrated with experimental data measured by Dempsey and O'Melia (16,17). First the titration curves themselves are presented and the transformation to charge-pH curves is discussed. On the basis of the charge-pH curves apparent affinity distributions are calculated, which include both the chemical and the electrostatic interactions. The derivatives of the charge-pH curves, needed for calculation of the distribution function, are obtained by applying a smoothing spline procedure. The

smoothing spline procedure is applied to the basic pH(ml) data to be able to perform a proper error analysis of the calculated distribution functions. In addition it enables us to judge whether the use of higher derivatives in the calculation of distribution functions is allowed. The smoothing parameter is obtained objectively by the GCV method in combination with physical constraints (18-24).

For the determination of intrinsic affinity distributions an electrostatic model is evaluated using the master curve procedure. A rigid sphere model is applied for this purpose. The resulting master curve is used to calculate the intrinsic affinity distribution. On the basis of the obtained distribution an analytical isotherm equation is selected which is fitted to the master curve. Finally the charge-pH curve for a ionic strength different from those used for the analysis is predicted using the spherical double layer model with the value of the radius r that results from the master curve procedure in combination with the intrinsic affinity distribution which is derived from the master curve.

Theory

Charge (pH) Curves and the Overall Degree of Protonation

From experimental titration data the change in charge as a function of pH can be determined. Results are usually expressed as ΔQ in meq negative charge per gram total organic carbon (TOC) or per gram fulvic acid (FA). For absolute values of the charge, Q, the charge at the beginning of a titration experiment should be known. This quantity is in general difficult to obtain experimentally and often only an estimate of this initial charge can be given (6,25). The $Q(pH)$ curves can be used to determine affinity distributions

In order to determine a normalised affinity distribution the fraction of sites, θ_t, that is occupied by the protons, should be known. For a fulvic acid the relation between the degree of protonation θ_t and the charge Q is:

$$\theta_t = 1 - Q/Q_{max} \tag{1}$$

136

where Q_{max} is the maximum charge of the fulvic acid, that is when the sample is fully dissociated. Although the sign of the absolute charge is negative, for convenience we define Q to have positive values.

The degree of protonation of a heterogeneous sample is the weighted sum of the the degrees of protonation of individual site types, θ_i, weighted by their fractions f_i:

$$\theta_t = \sum_i f_i \theta_i \tag{2}$$

For humic materials often a continuous distribution of site types is assumed, eq 2 then becomes an integral equation:

$$\theta_t = \int_\Delta \theta f(\log K) d \log K \tag{3}$$

where f(log K) is the affinity distribution, Δ the range of possible log K values and θ is the local isotherm. Equation 3 is the general overall binding equation. For θ the Langmuir isotherm is often used (26). To calculate f(logK) semianalytical methods have been developed on the basis of eq 3 (23, 27).

Apparent Affinity Distributions

For the heterogeneity analysis derivatives of the charge-pH curves are needed. These derivatives are obtained on the basis of a smoothing spline function through the data. An existing smoothing spline procedure of Woltring (22) was extended for this purpose. A quintic spline is used, so that derivatives required for the analysis, are continuous. The advantage of a smoothing spline above a polynomial is that no type of functionality for the experimental curves is assumed (21).

A spline is a piecewise polynomial function which connects so called knodal points. We assume here that the added volume titrant (ml) is the independent variable and the pH (or rather mV) is the dependent variable. Therefore the titrant volume data are used as x-coordinates of the knodal points. When the mV(pH) calibration curve is linear and the error in mV is constant also the error in pH is constant. The

137

smoothing spline procedure is applied to the basic data in order to assure that the weighting factors in the spline algorithm can be put equal to one. In addition, the propagation of the error in the pH can be studied on the basis of the variance in pH, for which an estimate can be obtained from the spline calculation.

The amount of smoothing applied depends on the value of the smoothing parameter, which determines the trade-off between the goodness of fit of the spline and the smoothness of the curve. At too low values of the smoothing parameter the spline would follow the data points too closely so that random errors may be interpreted in terms of pH changes. On the other hand a too large value of the smoothing parameter might smooth details in the data away that are realistic. The optimal value of the smoothing parameter removes details that lie within the range of experimental error and retains details outside this range.

To determine a proper smoothing parameter the Generalized Cross Validation (GCV) method (20) was used in combination with physical constraints (24). The initial value of the smoothing parameter is found by minimizing the GCV criterion as a function of the smoothing parameter. Physical constraints are often needed (23,24) because the GCV method tends to result in slightly too low values of the smoothing parameter for the present type of data. In addition the GCV method applies strictly speaking to large data sets with a normally distributed error only.

The first constraint states that the charge-pH curve should be a monotonically increasing function since the charge increases with increasing pH. The second constraint is based on the fact that the local isotherm is a convex function, so that also the overall binding curve plotted as a function of [H] should be convex. The third constraint demands that the second order Affinity Spectrum is always positive (24). This is the case when a Langmuir functionality as local isotherm is assumed.

Once the charge-pH curve is established with the help of the spline through the basic data, the corresponding apparent distribution function can be calculated on the basis eq 3 using a Langmuir type equation as local isotherm:

$$\theta_i = \frac{K_{app}[H]}{1 + K_{app}[H]} \tag{4}$$

138

In eq 4 [H] is the concentration of protons and K_{app} is the apparent affinity, which incorporates both the non-coulombic (intrinsic) and coulombic interactions. The subscript "app" is used to indicate that the results will depend on electrostatic interactions too. Using this subscript the overall isotherm θ_t, eq 3, can be rewritten as:

$$\theta_t([H]) = \int_\Delta \theta(K_{app},[H])f(\log K_{app})\,d\log K_{app} \tag{5}$$

where $f(\log K_{app})$ is the apparent affinity distribution function, which can be obtained by inversion of the integral equation. However, eq 5 is difficult to solve for $f(\log K_{app})$. Nederlof et al. (27) compared a number of semi-analytical methods that use an approximation of the local isotherm in order to solve eq 5 for the distribution function. As a consequence of the approximation of the local isotherm, also an approximation of the apparent distribution is obtained.

The simplest method for the calculation of $f(\log K_{app})$ replaces the local isotherm by a step function and is called the Condensation Approximation (CA). The approximation of the distribution function is:

$$f_{CA}(\log K_{app}) = -\frac{\partial\theta_t(pH)}{\partial pH} \tag{6a}$$

$$\log K_{app} = pH \tag{6b}$$

Although the step approximation of the local isotherm (eq 4) is crude, the advantage of the method is that it is not very sensitive to experimental error, because only a first derivative is required. For narrow distributions a much too flat and widened result is obtained with the CA method, but when the distribution is wide and smooth the CA result is quite good (27).

An alternative is provided by the LOGA method which uses a close approximation of the local isotherm (27). The LOGA method can pick up details in a distribution. A major disadvantage is that it needs a third derivative of the adsorption isotherm, which can only be obtained reliably for very accurate data. The apparent distribution function is obtained as:

139

$$f_{LOGA}(\log K_{app}) = -\frac{\partial \theta_t(pH)}{\partial pH} + 0.386 \frac{\partial^3 \theta_t(pH)}{\partial pH^3} \qquad (7a)$$

$$\log K_{app} = pH \qquad (7b)$$

It follows from eqs 1, 6 and 7 that $f(\log K_{app})$ can also be obtained directly from the charge-pH curves:

$$f_{CA}(\log K_{app}) = \frac{1}{Q_{max}} \frac{\partial Q}{\partial pH} \qquad (8a)$$

$$\log K_{app} = pH \qquad (8b)$$

and

$$f_{LOGA}(\log K_{app}) = \frac{1}{Q_{max}} \left\{ \frac{\partial Q}{\partial pH} - 0.386 \frac{\partial^3 Q}{\partial pH^3} \right\} \qquad (9a)$$

$$\log K_{app} = pH \qquad (9b)$$

When Q_{max} is not known a non-normalised distribution $F(\log K_{app})$ can be obtained by applying the CA and LOGA method to the charge-pH curves directly. The relation between $F(\log K_{app})$ and the normalised $f(\log K_{app})$ is:

$$F(\log K_{app}) = Q_{max} f(\log K_{app}) \qquad (10)$$

Since the value of Q_{max} is difficult to determine it is preferable to determine a non-normalised distribution, before further interpretation (6). Note that for the determination of an apparent distribution also the absolute charge values are not needed:

$$\frac{\partial Q}{\partial pH} = \frac{\partial (Q_{ini} + \Delta Q)}{\partial pH} = \frac{\partial \Delta Q}{\partial pH} \qquad (11)$$

where Q_{ini} is the initial charge and ΔQ the change in charge measured poten-tiometrically. It follows that the apparent heterogeneity can be obtained with a minimum number of assumptions. A disadvantage is that the result depends on experimental conditions.

Intrinsic Affinity Distributions

In order to obtain intrinsic distributions, the electrostatic effects that cause the ionic strength dependency of the titration curves, should be accounted for. For the calculation of the electrostatic potential at the surface the absolute values of the charges and thus also the initial charge is needed. The local isotherm is now written as:

$$\theta_i = \frac{K_{int}[H_s]}{1 + K_{int}[H_s]} \tag{12}$$

where K_{int} is the intrinsic affinity constant depending on non-coulombic intercations only and $[H_s]$ is given by:

$$[H_s] = [H]\exp(-F\psi_s/RT) \tag{13}$$

where ψ_s is the electric potential at the surface and F,R and T have their usual meanings. The electrostatic potential can not be measured directly and must be estimated from an electrostatic model that gives the relation between the charge of the surface and its potential. De Wit et al. (6,7,14,15) have developed a procedure to determine a proper electrostatic model. The fulvic acid molecules are assumed to be rigid particles with a uniform surface potential and a simple geometry: either spherical or cylindrical. The use of such simple models for humic materials is dis-cussed by Bartschat et al. (28). For large values of the radius of curvature of the particles (typically > 10nm) the electrical double layer properties resemble those of a flat plate (29). For small values of the radius a lower value of the potential is found than for a flat plate at a given charge. This is due to the radial shape of the electric field. By adapting the radius of the particles in the model the potential - charge

141

relation can be adjusted to fit the data. If a certain value of the particle density is assumed, the only adjustable parameter in the spherical double layer model is the radius (the site density follows from these parameters). De Wit et al. reasoned on the basis of literature data that the density of fulvic acids should be in the range 0.7-1.7 g/cm^3 FA (7) and concluded that a density of 1 g/cm^3 is a convenient choice. The charge data are usually expressed as meq per gram fulvic acid. To apply an electrostatic double layer model the data must be converted to C/m^2. To be able to do this the specific surface area A_{sp} of the fulvic acids is needed. Assuming a spherical particle with radius r [nm] and density ρ [g/cm^3], A_{sp} [m^2/g] is given by:

$$A_{sp} = \frac{3000}{\rho r} \tag{14}$$

The surface charge density σ [C/m^2] can now be obtained from:

$$\sigma = \frac{FQ}{A_{sp}} \tag{15}$$

where Q is expressed in meq/g FA.

For a given value of σ the potential is obtained by solving the Poisson-Boltzmann equation numerically for the assumed geometry (30). With the electric potential pH_s can be calculated using eq 13. When the Q(pH) data points are replotted as $Q(pH_s)$ points the latter should merge into one master curve when the chosen electrostatic model is appropriate (6).

For spherical particles also an estimate can be given of the 'electrostatically' weighted molecular weight once r is determined:

$$M = \frac{4}{3}\pi r^3 N_A \rho \tag{16}$$

where N_A is Avogadro's number. The thus obtained value of M can be compared with M obtained by other techniques.

Approximations of the intrinsic affinity distribution can be obtained from the $Q(pH_s)$ curves:

$$f_{CA}(\log K_{int}) = \frac{1}{Q_{max}} \frac{\partial Q}{\partial pH_s} \tag{17a}$$

$$\log K_{int} = pH_s \tag{17b}$$

using the Condensation Approximation and

$$f_{LOGA}(\log K_{int}) = \frac{1}{Q_{max}} \left\{ \frac{\partial Q}{\partial pH_s} - 0.386 \frac{\partial^3 Q}{\partial pH_s^3} \right\} \tag{18a}$$

$$\log K_{int} = pH_s \tag{18b}$$

using the LOGA method. Note that also here non-normalised distributions can be obtained when Q_{max} is not known:

$$F(\log K_{int}) = Q_{max} f(\log K_{int}) \tag{19}$$

Although some modeling is required an advantage of the method is that no a priori assumptions have to be made with respect to the chemical heterogeneity other than the assumption that the ensemble of heterogeneous molecules can be represented by a mixture of chemically heterogeneous particles of the same size, shape and surface potential.

Experimental data

Titration Curves
Experimental data were taken from the thesis of Dempsey (16), see also (17). Dempsey used fulvic acid (FA) samples from Lake Drummond (Virginia, U.S.A.). The site was selected for its high TOC content (45 mg TOC/l), which predominantly consists of fulvic acids. The FA material was separated into four fractions based on

desorption from a nonionic resin (XAD-7) at pH values 4, 7 and 10. The fraction obtained at pH=4 was split into two fractions, because it was the largest fraction. The fractions appeared to be similar in molecular weight and no differences were found when analysed with IR and UV spectroscopy. The fractions were titrated with acid and base at three different salt levels to study the charging behaviour of the FA material. Results were expressed in meq negative charge per gram TOC. Also here differences between samples were small.

For the fulvic acid sample indicated by #2 the raw titration data, that is pH as a function of added acid or base, are plotted by Dempsey (16). These data are read from the graph and used in the present paper. In the experiment 25 ml sample #2 with TOC= 501 mg/l was titrated with 0.1 M HCl or NaOH at three salt levels (I=0.01, I=0.1 and I=1 M KCl). The temperature was kept at 24 ± 1 °C and the pH was measured with a glass electrode, with a claimed accuracy of 0.001 pH unit, which is very accurate. Additional errors may result from electrode drift and junction potentials, these errors can easily exceed 0.001 pH unit.

In Figures 1a and 1b the titration curves of sample #2 are replotted for I=0.01M and I=1.0M respectively. The curves are combinations of a base titration, indicated by positive values of the added volume, and an acid titration indicated by negative values.
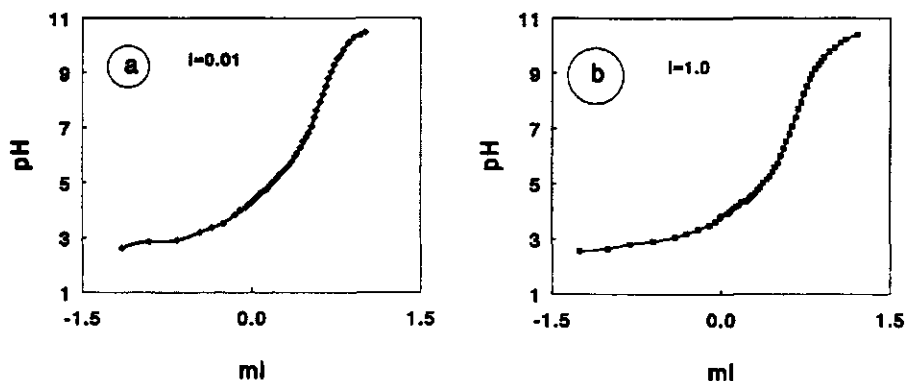

Figure 1: Titration curves of fulvic acid obtained for a) I=0.01M and b) for I=1.0M. Data were taken from the thesis of Dempsey (16). The solid lines indicate the spline representations.

144

Charge-pH Curves

Since we want to perform an error analysis on the distribution functions, the basic data must be analysed in order to be able to follow the propagation of error. Therefore we cannot take the charge-pH data from Dempsey directly, we have to recalculate these from the basic pH(ml) data.

In order to transform titration data to charge-pH curves the charge of the fulvic acid at the beginning of the experiment should be known, because from the titration curves only changes in charge can be calculated. In addition a blank should be determined experimentally or calculated theoretically. The initial charges of the samples at I=1.0M and I=0.01M were estimated by Dempsey and O'Melia from the charge balance in solution at the beginning of the experiment. The obtained values are Q_{ini}=6.91 meq/gTOC for the I=0.01M sample and Q_{ini}=7.13 for the I=1.0M sample (16). As no blank titrations are reported, we have to rely for the present calcultions on a theoretical blank. For the calculations we used the extended Debye-Hückel equation to obtain activity coefficients for I=0.01M (31), which leads to γ_H = 0.914 and γ_{OH} = 0.899 and the mean salt method for I=1.0M (32,33), which leads to γ_H = 1.084 and γ_{OH} = 0.946. In order to reproduce the charge-pH curves of Dempsey and O'Melia we had to adjust the titer of both the acid and base to 0.095 M. Although this may seem close to 0.1M it has large consequences for the absolute values of the charge. The origin of the discrepancy is unclear to us.

The recalculated charge-pH curves are shown in Figure 2a and 2b. It follows from Figure 2 that the fulvic acid is more negatively charged at a certain pH for high ionic strength. The dissociation is thus enhanced with increasing salt level. This can be explained by the fact that the charge is better screened by the electrolyte ions and therefore dissociation is less hindered by electrostatic effects.

The negative charge at the lowest pH measured (pH=3) is already considerable and is roughly one third of the maximum negative charge that is measured at pH=11. Dempsey and O'Melia concluded from this that very acidic groups must be present. For I=1.0 a small but sharp increase is found at about pH=4.5, which does not occur for I=0.01M.
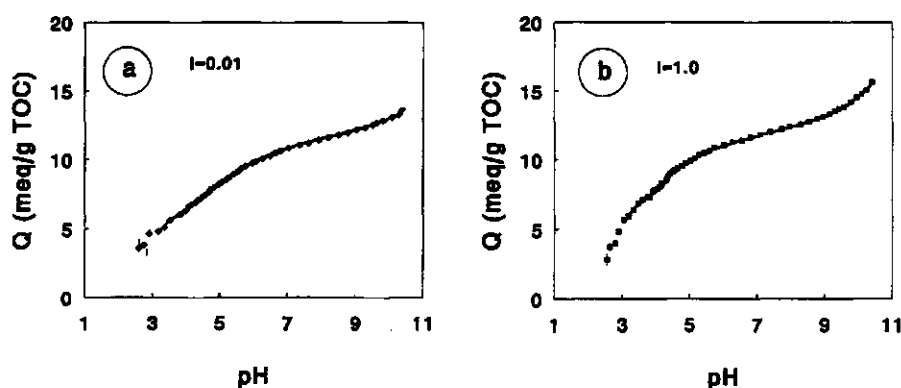
145

Figure 2: Charge-pH curves of fulvic acid obtained from the titration curves of Figure 1 for a) I=0.01M and b) I=1.0M. The solid lines are calculated on the basis of the spline representation of the titration curve.

Distributions Functions

Apparent Distribution Functions

In order to be able to calculate apparent distribution functions the smoothing spline procedure is applied to the pH(ml) data. In this way a continuous representation of the titration curve is obtained. First the GCV technique is applied to the titration curves of Figures 1a and 1b. According to the GCV method the optimal value of the smoothing parameter $\log(p)$ corresponds to the minimum in the GCV function. Minima were found at $\log(p)=-8.4$ (I=0.01M) and $\log(p)=-7.4$ (I=1.0M). In each case the spline function obtained with the smoothing parameters did not obey the physical constraints. By increasing the smoothing parameter no value of the smoothing parameter could be found corresponding to a spline that fulfilled the constraints. By omitting the data points that show irregular behaviour in the charge-pH curves, i.e. typically values below pH=3.5, smoothing parameters could be found that satisfied the constraints. The GCV functions for the titration curves of Figures 1a and 1b are shown in Figures 3a and 3b respectively. Final values of

the smoothing parameter are log(p)=-7.1 for I=0.01M and log(p)=-6.1 for I=1.0M. For the latter the third constraint was still not obeyed, this is probably caused by the sharp increase in Q at pH=4.5.
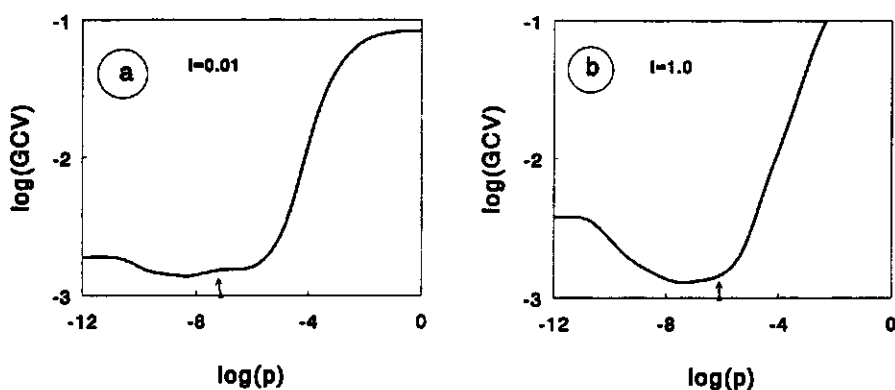

Figure 3: GCV plots obtained for the titration curves of Figure 1. Minima were obtained for log(p)=-8.4 (I=0.01M) and log(p)=-7.4 (I=1.0M). Application of the physical constraints lead to log(p)=-7.1 and log(p)=-6.1 respectively (indicated by the arrows).

Variances in pH values calculated by the spline algorithm are in both cases estimated to be $var = 1.2 \, 10^{-3}$. This variance is considerably larger than the variance obtained from the electrode accuracy: $var = 1.0 \, 10^{-6}$. The discrepancy is probably caused by the fact that pH(ml) data were read manually from the graphs in the thesis of Dempsey (16), which results in an extra error in the data. In addition, the error estimate of Demspey and O'Melia (0.001 pH unit) might also be too optimistic.
The spline representations of the titration curves are shown in Figures 1a and 1b together with the original points. From the spline function 250 points were generated to calculate 250 corresponding points of the charge-pH curves (solid lines in Figures 2a and 2b).
Error bars were calculated using Monte Carlo simulations with 100 realisations of the pH(ml) spline. Since the error in pH is relatively small the error bars (0.06 pH units long) in Figures 1a and 1b lie within the thickness of the symbols. In Figures 2a and 2b in principle error bars should be drawn in both vertical and horizontal

direction. However, the error in pH is so small that the error bars are not visible in Figure 2. Vertical error bars, corresponding to an error in Q are also hardly visible. Note that the low Q(pH) values were omitted in the final spline analysis, since the error for these points is strongly dependent on the blank titration.

Although the errors in Q(pH) are small, they still have consequences for the calculated CA distributions because a first derivative is needed. Derivatives were calculated numerically from the 250 data points of the charge-pH curve. The resulting non-normalised apparent proton affinity distribution using the CA method is shown in Figure 4. The error bars were calculated using derivatives obtained from the 100 Monte Carlo realisations of the charge pH curve. For low and high values of $\log K_{app}$ a relatively large uncertainty in $F_{CA}(\log K_{app})$ is obtained. Also here the error bars in $\log K_{app}$ are not visible because the error in $\log K_{app}$ corresponds to that in the pH.

Roughly speaking, the shape of the two distributions presented in Figures 4a and 4b is very similar. A large "valley" is obtained in the middle of the logK range and at the outer ends the density increases. Functional groups at the low end and at the high end of the logK range are therefore relatively important. In the distribution function obtained for I=0.01 three peaks are found around logK=5.
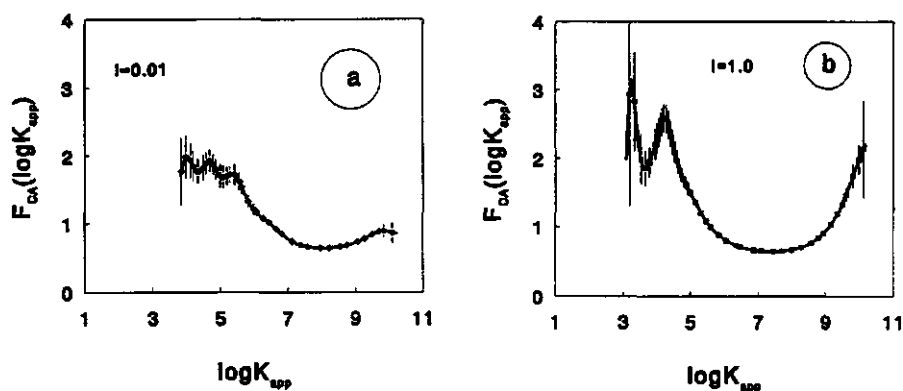

Figure 4: Apparent CA affinity distributions of fulvic acid obtained from the charge-pH curves for a) I=0.01M and b) I=1.0M. Error bars indicate 66% confidence intervals.

However, these peaks can not be interpreted as the result of separate functional groups, because the error bars indicate a large uncertainty. At the other end of the distribution a slight indication of the presence of a peak at about logK=9.5 is obtained. The distribution function obtained for I=1.0M is far more pronounced and the position of the "valley" is shifted about 1 log K unit to lower affinities, which illustrates the suppression of the electrostatic effects by the high ionic strength. In addition a sharp peak is found at logK=4.5, which seems to be significant when looking to the error bars. The peak corresponds with a small step in the titration curve around pH=4.5 (Figure 2b). However such a sharp peak is not expected when the CA method is used since the method tends to flatten and widen (narrow) peaks (27). The peak may also be caused by other effects, such as conformational changes. The fact that for this case the third constraint was not fulfilled is also an indication of a strange behaviour. Repeating the experiment for the same and other values of the ionic strength may give an idea of the significance of this peak.

Intrinsic Distribution Functions

In order to apply the master curve method the charge values expressed per gram material have to be converted into charge per unit surface area, σ [C/m^2], using eqs 14 and 15. However Q is expressed here per gram TOC, whereas A_{sp} is expressed per gram FA. When it is assumed that 1 gram TOC corresponds with approximately 2 grams of FA, as follows approximately from element analysis (1,4,34), the results obtained via eq 15 have to be divided by 2.

Merging charge-pH curves were obtained by using the spherical double layer model with a radius of 0.75 nm and a fixed density of 1 g/cm^3 FA, see Figure 5a. The parameters correspond with a molecular weight of 1060 g/mol, and a specific surface area of A_{sp} = 4000 m^2/g FA. The parameters are close to the ones found by De Wit et al. for sample #3 (7) (r=0.7 nm and M=900 g/mol). The value of the molecular weight is somewhat lower than that found with X-ray scattering, which resulted in 1500-2500 g/mol (16).

To determine the intrinsic affinity distribution the derivatives of the mastercurve were first obtained by applying the smoothing procedure directly to the master curve data of Figure 5a. Nine points at the lower end and two points at about pH$_s$=8.2 were omitted to avoid artifacts in the distribution, these are the points corresponding

149

to those omitted in the analysis of the titration curves. **Figure 5b** shows the GCV plot for the master curve. A minimum is found at $\log(p)=-2.2$. With this value of $\log(p)$ all constraints are fulfilled. The solid line in **Figure 5a** shows the obtained spline function.
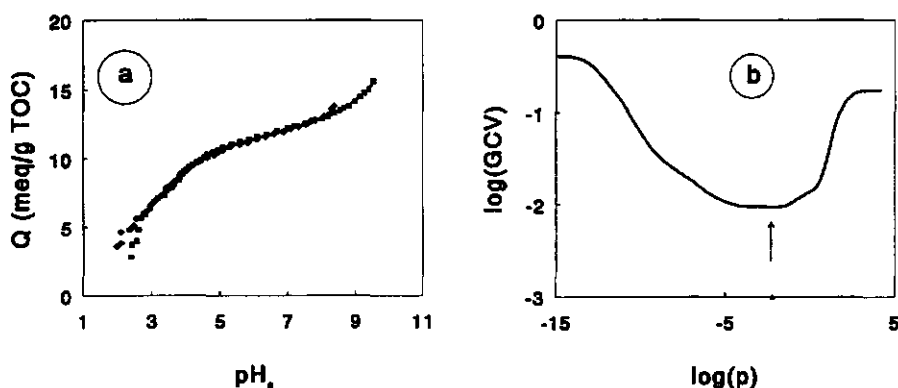

Figure 5: a) Master curve obtained when a spherical double layer model is applied with $r=0.75$ nm. The solid line represents the spline function obtained for $\log(p)=-2.2$. b) GCV plot obtained for the master curve. A minimum is found at $\log(p)=-2.2$.

The CA and LOGA distributions based on the spline function shown in Figure 5a are shown in Figures 6a and 6b respectively. The basic shape is similar to that found for the apparent affinity distributions, a valley with increasing densities for $\log K_{int}$ values <5 and for values >8. With respect to $\log K_{app}$ the entire distribution is shifted to lower $\log K_{int}$ values because of the use of $\log K_{int}=pH_s$ instead of $\log K_{app}=pH$. The LOGA distribution, although in principle capable to show more detail, does not give additional information due to the large error bars. The error indicate that it is not meaningful to use higher order approximations in this case.

However, the error that is present in the original pH(ml) data is not properly accounted for when the distribution is directly derived from the master curve. By applying the smoothing spline method to the master curve it is assumed that the error in Q is the same over the whole pH range and that the error in pH is negligible.
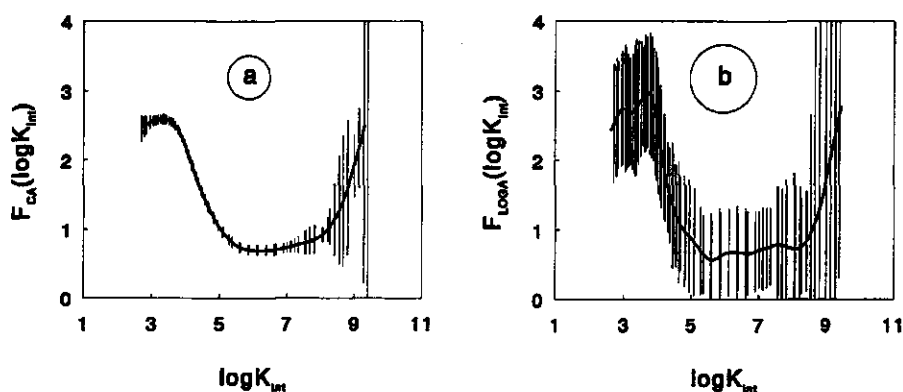
150

Figure 6: Intrinsic affinity distribution functions calculated on the basis of the spline representation of the master curve. a) CA distribution; b) LOGA distribution. Error bars indicate how close the original charge-pH$_s$ curves coincide.

This is of course not true. An additional source of error is the fact that the curves merge not equally well over the full pH range. This is reflected by the error bars in Figures 6a and 6b. In the region were large error bars are found (e.g. $\log K_{int} > 8$) the curves of 0.01M and 1.0M merge less well than in the region where error bars are small. When the individual curves consituting the master curve deviate from each other details in the distribution can not be interpreted even when the original data for the separate curves are very accurate.

Interpretation of the propagation of the error in the original data is possible when the charge-pH$_s$ curves are treated separately and the error propagation is taken into account properly. In order to carry out this analysis, the charge-pH curves have to be plotted separately for I=0.01M and I=1.0M as a function of pH$_s$ starting with the basic titration data and using the parameters of the electrostatic model. The distributions are calculated from the individual Q(pH$_s$) curves. Error bars are calculated using Monte Carlo simulations. Figures 7a and 7b show the resulting CA distributions. Although the basic features of the CA distributions are the same as found in Figure 6a, the error bars give an entirely different picture. The uncertainty in the measured millivolts does not lead to visible error bars in horizontal direction, corresponding to an uncertainty in $\log K_{int}$. The vertical bars are large for low and high $\log K_{int}$ values. The three peaks around $\log K_{int}=4$ for I=0.01M, also encountered

151

in the apparent distribution function, are again covered by large error bars and should not be considered as significant. The sharp peak at $\log K_{int}=4$ for $I=1.0$ M was also already encountered in the apparent distribution function.

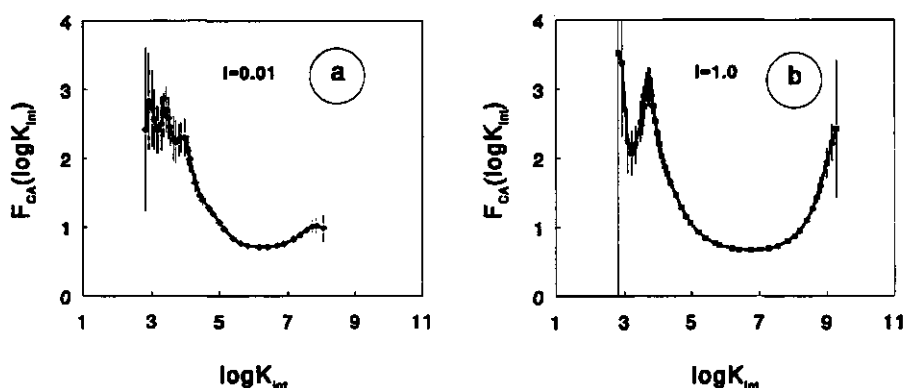Figure 7: Intrinsic affinity distribution functions obtained on the basis of the individual curves for a) $I=0.01$M and b) $I=1.0$M derived from the spline functions through the basic data (Figure 1). Error bars indicate 66% confidence intervals.
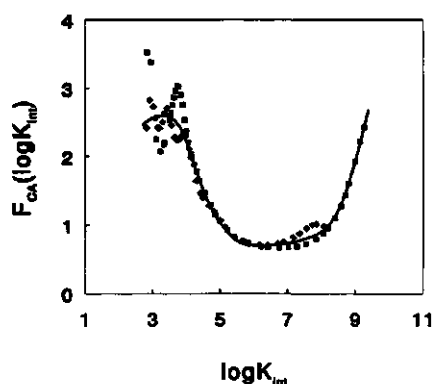

Figure 8: Intrinsic CA distribution based on the master curve (solid line) compared with the CA distributions based on the separate charge-pH_s curves (symbols).

In Figure 8 the CA distributions of Figures 6a, 7a and 7b are replotted in one figure. For low values of $logK_{int}$ the result of Figure 6a lies within the error bars of Figure 7a and the sharp peak obtained in Figure 7b is smoothed away. The distributions at the left hand side of the "valley" correspond very well. For $logK_{int} > 7$ the distributions obtained for I=0.01M and I=1.0M deviate somewhat and the distribution based on the master curve takes an average position. It may be concluded that the distribution obtained on the basis of the master curve itself is a reasonable average of the distributions obtained on the basis of the analysis of the separate charge-pH$_s$ curves. To obtain a good impression of the error propagation from basic data to the intrinsic affinity distributions, the curves should be treated separately and the smoothing spline through the basic data should be the starting point. The closeness of the merging of the different data sets to a master curve is shown by the bars in Figure 6.

The obtained intrinsic affinity distribution corresponds reasonably well with those calculated by De Wit et al. (7) for other FA samples. For most FA samples a peak is found at logK=3-4, corresponding to carboxylic type of groups. Since the experimental pH range is often limited also the range of obtained affinities is often limited and only one broad peak around logK=3-4 is found in most cases. For the charge-pH curve of sample #3 of Dempsey and O'Melia a second peak was found at about logK=8.5, which is somewhat lower than the second peak position obtained in the present case. The higher affinity sites may correspond with phenolic type of groups.

Modelling of Charge-pH Curves

When the master curve can be described by an analytical function and when a proper electrostatic model is chosen, the charge-pH curves for the measured ionic strength values can be described and curves for other values of the ionic strength can be predicted. Because two peaks are present in the intrinsic affinity distribution it is logical to describe the mastercurve with a combination of two Langmuir-Freundlich equations (5,35,36). Each Langmuir-Freundlich equation corresponds with a semi-gaussian peak in the distribution function. By using such a combination the charge-pH$_s$ function can be described as:

$$Q = Q_{max} - Q_{max}\left\{f_1 \frac{(\tilde{K}_1[H_s])^{m_1}}{1 + (\tilde{K}_1[H_s])^{m_1}} + f_2 \frac{(\tilde{K}_2[H_s])^{m_2}}{1 + (\tilde{K}_2[H_s])^{m_2}}\right\} \tag{20}$$

where $\tilde{K}_1$ and $\tilde{K}_2$ correspond with the peak positions of the first and second peak respectively. Initial estimates for $\tilde{K}_1$, $\tilde{K}_2$, f_1 and f_2 were obtained from the distribution presented in Figure 8. Final parameters are given in Table 1. Figure 9a shows the description of the master curve using eq 20. Figure 9b shows the corresponding intrinsic affinity distribution. The dotted lines indicate the $\log K_{int}$ interval for which information can be derived from the experiments. Such a range is sometimes called the "experimental window". The decrease in the density for very low and very high affinity that follows from the double Langmuir-freundlich distribution is almost fully outside the experimental window. The shape of the distribution between the peaks correspond very well with the calculated intrinsic affinity distribution functions.
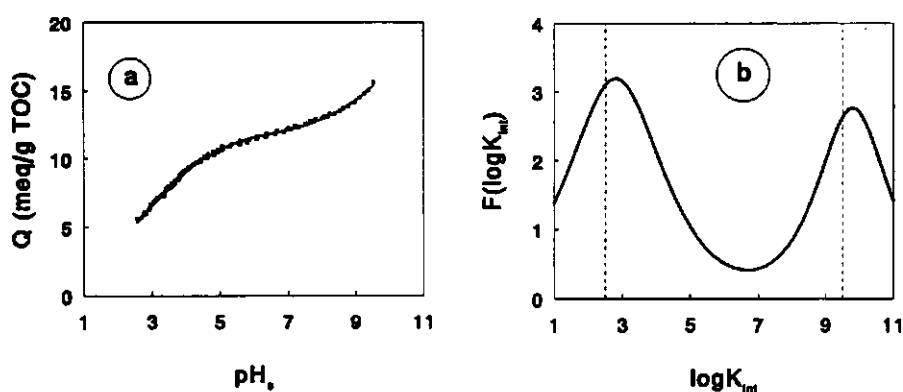

Figure 9: a) Model description of the master curve using a double Langmuir-Freundlich equation (eq 20) using the parameters shown in Table 1.; b) The distribution function corresponding to eq 20 for the given set of parameters. The dotted lines indicate the width of the experimental window.

	i=1	i=2
$\log \bar{K}_i$	2.8	9.8
m_i	0.4	0.48
f_i	0.6	0.4

Table 1: Parameters of the double LF model (eq 20), Q_{max} was estimated to be 20 meq/g TOC.

By combining the electrostatic model with the Langmuir-Freundlich model for the description of the master curve we are now able to describe the charge-pH curves for I=1. M and I=0.01 M and to predict independently the charge-pH curves for other ionic strength values. Figure 10a shows the description of the two charge pH curves that were used to obtain the master curve and the intrinsic affinity distribution. The solid lines represent the (transformed) data very well. Figure 10b shows the predicted result for I=0.1M. The data points are obtained from the thesis of Dempsey (16) and were only presented in this form. The agreement is excellent.
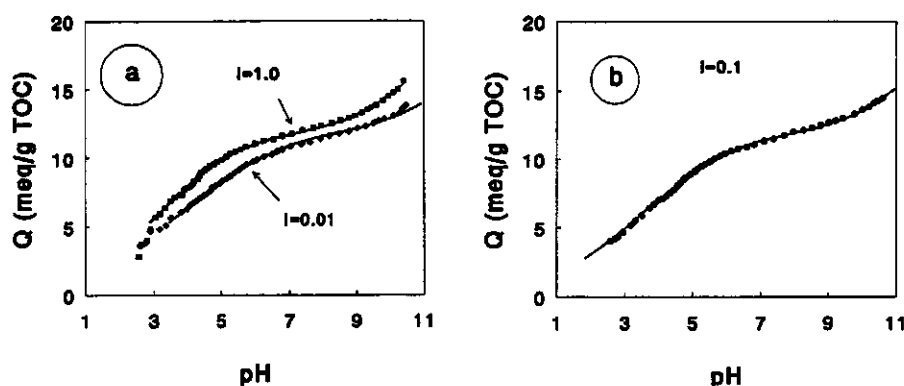

Figure 10: Model results when the analytical description of the master curve is combined with the electrostatic double layer model. a) Charge-pH curves for I=0.01M and I=1.0M respectively, solid lines indicate the model description; b) Model prediction for I=0.1M (solid line) compared with the results measured by Dempsey (16) (symbols).

155

Conclusions

- The charging behaviour of fulvic acids is strongly influenced by chemical heterogeneity, but also electrostatic effects influence the charge-pH curves.
- To determine affinity distributions accurate titration data are required. Especially in the ranges pH<3 and pH>10 large uncertainties may occur in the charge-pH curves due to the necessary subtraction of the blank from the titration.
- Apparent affinity distributions are ionic strength dependent and only of limited help for the derivation of a mechanistic model.
- The master curve procedure can be succesfully applied to the FA charge-pH curves. Merging charge-pH curves for the samples studied can be obtained assuming a spherical double layer model with particle radius r=0.75nm and a fixed density of 1 gram per cm^3 FA. These numbers correspond to an electrochemical molecular weight of the sample of 1060 g/cm^3.
- The intrinsic affinity distribution can be derived from a smoothing spline representation of the master curve. However, for a proper estimate of the uncertainty in the intrinsic distribution due to experimental error, the intrinsic distributions for different salt levels should be calculated separately based upon the smoothing splines obtained from the experimental pH(ml) data. For the present data it is only relevant to calculate $f(logK_{int})$ with the CA method.
- The intrinsic proton affinity distribution function for the present FA sample can be described with a combination of two semi-gaussian peaks positioned at logK=2.8 and logK=9.8. Results are in fair agreement with results obtained for other FA samples. The obtained distribution matches with a double Langmuir-Freundlich equation, which fits the master curve.
- The binding model including both chemical heterogeneity and electrostatic effects is able to give a very good prediction of the charge-pH curve as a function of the ionic strength without introduction of extra parameters.

References

(1) Stevenson, F.J. *Humus Chemistry. Genesis, Composition, Reactions* Wiley-Interscience, New York, 1982.

(2) Sposito, G. *CRC Crit. Rev. Environ. Control* **1986**, *16*, 193-229.

(3) Buffle, J. In *Circulation of Metal Ions in the Systems*; Sigel, H., Ed.; Metal Ions in Biological Systems 18; M. Dekker: New York, 1984, pp 165-221.

(4) Aiken, G.R.; McKnight, D.M.; Wershaw, R.L.; MacCarthy, P. *Humic Substances in Soil, Sediment and Water. Geochemistry, Isolation and Characterisation.* Wiley, New York, 1985, 692 p.

(5) Buffle, J. *Complexation Reactions in Aquatic Systems: An Analytical Approach*, Ellis Horwood Limited, Chichester, 1988.

(6) De Wit, J.C.M.; Van Riemsdijk, W.H.; Nederlof, M.M.; Kinniburgh, D.G.; Koopal, L.K. *Anal. Chim. Acta* **1990**, *232*, 189-207.

(7) De Wit, J.C.M.; Van Riemsdijk, W.H.; Koopal, L.K. *Water, Air and Soil Pollution* **1991**, *57-58*, 339-349.

(8) Tipping, E.; Backes, C.A.; Hurley, M.A. *Wat. Res.* **1988**, *22*, 597.

(9) Tipping, E.; Reddy, M.M.; Hurley, M.A. *Environ. Sci. Technol.* **1990**, *24*, 1700-1705.

(10) Ephraim, J.; Alegnet, S.; Mathuthu, A.; Bicking, M.; Malcolm, R.L.; Marinsky, J.A. *Environ. Sci. Technol.* **1986**, *20*, 354.

(11) Marinsky, J.A.; Wolf, A.; Bunzl, K. *Talanta* **1980**, *27*, 461.

(12) Van Riemsdijk, W.H.; Koopal, L.K.; De Wit, J.C.M. *Neth. J. Agr. Sci.* **1987**, *35*, 241.

(13) Van Riemsdijk, W.H.; Bolt, G.; Koopal, L.K. in *Interactions at the Soil Colloid - Soil Solution Interface*, Bolt, G.H.; De Boodt, M.F.; Hayes, M.H.B.; McBride, M.B., Eds., Kluwer Academic Publishers, Dordrecht, 1991, pp 81-114.

(14) De Wit, J.C.M.; Van Riemsdijk, W.H.; Koopal, L.K. submitted to Environ. Sci. Technol.

(15) De Wit, J.C.M.; Van Riemsdijk, W.H.; Koopal, L.K. submitted to Environ. Sci. Technol.

(16) Dempsey, B.A. *The Protonation, Calcium Complexation, and Adsorption of a Fractionated Aquatic Fulvic Acid* Ph.D. thesis, The Johns Hopkins University, Chapel Hill, 1981, pp. 201.

(17) Dempsey, B.A.; O'Melia, C.R. In *Aquatic and Terrestrial Humic Materials*; Christman, R.F., Gjessing, E.T., Eds.; Ann Arbor Science: Ann Arbor, MI, 1983; Chapter XII, pp 239-273.

(18) Schoenberg, I.J. *Proc. Nat. Acad. Sci. U.S.A.* **1964**, *52*, 947-950.

(19) Reinsch, C. *Numer. Math.* **1967**, *10*, 177-183.

(20) Craven, P.; Wahba, G. *Numer. Math.* **1979**, *31*, 377-403.

(21) Silverman, B.W. *J.R. Statist. Soc. B.* **1985**, *47*, 1-52.

(22) Woltring, H.J. *Adv. Eng. Software* **1986**, *8*, 104-107.

157

(23)   Nederlof, M.M.; Van Riemsdijk, W.H.; Koopal, L.K. In *Heavy Metals in the Environment 1*; Vernet, J.-P., Ed.; Elsevier, Amsterdam, 1991, pp 365-396.

(24)   Nederlof, M.M.; Van Riemsdijk, W.H.; Koopal, L.K., 1992, submitted to *Anal. Chem.*

(25)   Turner, D.R.; Varney, M.S.; Whitfield, M; Mantoura, R.F.C.; Riley, J.P. *Geochim. Cosmochim. Acta* 1986, *50*, 289.

(26)   Dzombak, D.A.; Fish, W.; Morel, F.M.M. *Environ. Sci. Technol.* 1986, *20*, 669-675.

(27)   Nederlof, M.M.; Van Riemsdijk, W.H.; Koopal, L.K. *J. Colloid Interface Sci.* 1990, *135*, 410-426.

(28)   Bartschat, B.M.; Cabaniss, S.E.; Morel, F.M.M. *Environ. Sci. Technol.* 1992, *26*, 284-294.

(29)   De Wit, J.C.M.; Van Riemsdijk, W.H.; Koopal, L.K. In *Metals Speciation, Separation, and Recovery*, Proc. of the Second International symposium on Metals Speciation, Separation and Recovery, Rome, 1989, 329-357.

(30)   Loeb, A.L.; Overbeek, J.Th.G.; Wiersema, P.H. *The Electrical Double Layer around a Spherical Particle*, M.I.T. Press Cambridge, USA.

(31)   Kielland, J. *J. Am. Chem. Soc.* 1937, *59*, 1675-1678.

(32)   Garrels, R.M.; Christ, C.L. *Solutions, Minerals, and Equilibria*, Freeman, Cooper & Company, San Francisco, 1965.

(33)   Weast, R.C. *Handbook of Chemistry and Physics*, CRC Press, 1974.

(34)   Schnitzer, M. in *Soil Organic Matter*, Schnitzer, M.; Khan, S.U., Eds., Developments In Soil Science 8 , Elsevier, Amsterdam, 1978, Chapter 1.

(35)   Van Riemsdijk, W.H.; Bolt, G.H.; Koopal, L.K.; Blaakmeer, J. *J. Colloid Interface Sci.* 1986, *109*, 219-228.

(36)   Sips, R. *J. Chem. Phys.* 1950, *18*, 1024-1026.

CHAPTER 6

Determination of First Order Rate Constant Distributions

Abstract

Three methods are discussed for the determination of first order rate constant distributions. All three methods lead to an analytical expression of the distribution function. The Laplace transform technique leads to a series of approximations of the distribution function expressed in terms of derivatives of the overall decay function, the higher the order of the approximation, the more derivatives are required. The second method is based on the work of Schwarzl and Staverman, and is analogous to the Affinity Spectrum method for binding equilibria. The quality of the approximation can be visualised by the sharpness of the kernel of the integral equation. The method turns out to be equivalent with the Laplace transform method, except for the third order approximation for which a slightly better result could be obtained. The third method is newly developed, it uses an approximation of the local decay function. The local decay approximation or LODA method is completely analogous to the LIA method for equilibrium studies. The LODA method also calculates the distribution function on the basis of derivatives of the overall decay function. The three methods are compared on the basis of two synthetic data sets, one composed of exact data and one of non-exact data. It is shown that the newly developed LODA-G2 method, which needs the first and second derivative of the overall decay function, combines a good resolution with a relatively low sensitivity to experimental error.

Introduction

Knowledge of the rate of a reaction is important for many processes, both in industrial practice and in natural environments. In many cases a first order or pseudo first order reaction is assumed. For complicated systems the overall reaction rate is not determined by just one reaction rate constant, but by a series of rate constants. Methods to determine the distribution of the rate constants are discussed in the present paper. The methods are generally valid, i.e. for any kind of first order reaction. For sake of simplifying the reasoning the treatment of the methods will be focussed on the dissociation of metal-ligand complexes.

In natural systems often poorly characterised heterodisperse macromolecular ligands are present. Such molecules possess different reactive groups which can bind small molecules or ions with different affinity and rate constants, i.e. they are chemically heterogeneous. Little is known about the dynamics of such systems. Kinetic features of these systems are often expressed in terms of residence times or half life times. The latter expresses the time after which half of the initial amount of a complex is dissociated. From a half life time value an average reaction rate constant can be calculated assuming a first order reaction. This average constant characterizes the kinetic properties of heterogeneous ligands only poorly. This problem is also encountered in equilibrium studies, where it has been shown that an average affinity gives a poor indication of the binding heterogeneity (1).

Heterogeneity analysis methods can be used to characterise binding both under equilibrium conditions (2-5) and non-equilibrium conditions (6-7). Even when the reaction is not purely first order, a kinetic heterogeneity analysis method may be used to get an impression of the kinetic heterogeneity. In addition the analysis provides a tool to study the influence of the reaction conditions, for instance, in the case of metal binding distributions may be compared that have been obtained for different pH values.

For complicated materials, such as humic acids, methods are needed that estimate the rate constant (or a distribution of rate constants) without any a priori assumptions with respect to the number of constants or the functionality of a decay function. A few approaches have been developed on the basis of a (pseudo) first order assumption. In analogy with the Scatchard graphical method (8) to find equilibrium constants, Mark and Rechnitz (9) developed a graphical method to obtain a (limited) number of rate constants with their fractions.

161

Connors (10) developed a method to obtain continuous rate constant distribution functions based on the first derivative of the decay function. In his later work (11) he abandoned this approach and worked out a method based on product distribution curves that pass through a maximum. This latter method is only capable to analyse the kinetics of mixtures with a small number of reactants. Olson et al. developed a technique to obtain continuous distributions based on the Laplace transform technique and applied the method to Copper dissociation from estuarine humic material (7,12,13).

Lavigne and Langford (14) have used the spectrum obtained with the method of Olson et al. (7) to estimate the parameters of a limited number of functional groups. A nonlinear regression routine was applied to improve the obtained estimates of the parameters. The large standard deviation of the final estimate indicated that the parameters obtained could be the mean of distributed quantities. Lavigne and Langford (14) also came to the conclusion that a proper treatment of the data with respect to experimental error is crucial to obtain a reliable kinetic spectrum. In addition, their regression routine appeared to be sensitive to artifacts in the input parameters, obtained from the spectrum.

In this paper we will evaluate existing methods for kinetic heterogeneity analysis on the basis of decay functions and compare the results with newly derived methods. The derivation of the new methods is based upon techniques that were developed for the determination of affinity distributions. Before the results of the various methods are compared, the basic assumptions and equations on which the methods are based are discussed.

The first group of methods to determine rate constant distributions is based on the Laplace transform technique (15,16), which was further developed and applied by Olson et al.(7,12,13). The second group of methods has been developed by Schwarzl and Staverman (17,18) to study the viscoelastic behaviour of materials. Recently Nederlof et al. analysed the application of their concept to determine affinity distributions on the basis of equilibrium binding data (3-5). Here it will be shown how the same approach can be used for the determination of rate constant distributions. The third group of methods approximates the local decay function by another mathematical function which enables the derivation of analytical expressions for the rate constant distribution. The latter methods are directly related to the LIA methods derived for the equilibrium case (3).

Since all the methods under consideration use derivatives of the decay function, special attention has to be paid to the data treatment. The data should be treated by a smoothing procedure that takes into account the experimental error before any analysis method is applied. We will use an adapted smoothing spline method similar to the one developed for the evaluation of equilibrium affinity distributions (19-21). A synthetic example will be used to show the possibilities and limitations of the various methods.

Basic Assumptions and Equations

The kinetics of the dissociation of ligand-metal complexes in solution can be studied by monitoring the amount of metal ions that is released as a function of time according to the dissociation reaction:

$$ML_i \rightarrow L_i + M \tag{1}$$

The amount of released metal can be followed by adding a sink S that instantaneously takes away the ion M that is released:

$$M + S \rightarrow MS \tag{2}$$

The process described by eq 1 can be followed indirectly by measuring the amount of MS formed, when the dissociation reaction is the rate limiting step. The amount of MS can often be measured accurately by a photometric technique (13,14).

When it is assumed that the dissociation of the complex ML_i, into M and L_i, is a first order reaction, the amount $C_i(t)$ of complex ML_i, left at time t can be written as:

$$C_i(t) = C_i(0) e^{-k_i t} \tag{3}$$

where k_i is the rate constant of the dissociation reaction and $C_i(0)$ is the amount of ML_i at t=0. For a heterogeneous ligand mixture $C_i(t)$ is called the *local decay function*

because each ligand type i has its own rate constant k_i. The overall dissociation of a mixture of ligands is given by the summation of the decay contributions of all the individual site types, resulting in an *overall decay function*:

$$C(t) = \sum_{i=1}^{n} C_i(0) e^{-k_i t} \tag{4}$$

For a continuous range of dissociation constants eq 4 is written as an integral equation:

$$C(t) = C_t(0) \int_0^{+\infty} g(k) e^{-kt} dk \tag{5}$$

where $C_t(0) = \sum C_i(0)$ is the total amount of ML at t=0 and g(k) is the normalized rate constant distribution function. Since the value of the rate constant may vary several orders of magnitude, the rate constant distribution function is often expressed as a function of $\log(k)$, in this case eq 5 becomes:

$$C(t) = C_t(0) \int_{-\infty}^{+\infty} f(\log k) e^{-kt} d\log k \tag{6}$$

where f(log k) is the normalized distribution function when plotted on a log k scale. The relation between g(k) and f(log k) can be derived by realizing that the integrals of both distributions over respectively k and logk should be equal to one:

$$\int_\Delta g(k) dk = \int_\Delta f(\log k) d\log k = 1 \tag{7}$$

Since $d\ln k = dk/k$ and $\log k = 0.43 \ln k$ it follows that:

$$f(\log k) = 2.3k\, g(k) \tag{8}$$

164

The rate constant distribution can in principle be obtained by inversion of eq 5 or 6, when $C(t)$ is known either from an experiment or from a model function and when first order reactions are assumed. However, eqs 5 and 6 are Fredholm equations of the first kind, which are difficult to solve for the distribution function, both analytically and numerically. In literature either a finite set of rate constants of individual ligands is assumed (e.g. (14)) or an approximation is used to obtain an analytical expression for the rate constant distribution. In this paper these semianalytical methods will be discussed.

Note that when $\sum C_i(0)$ is not known, as is often the case in practical situations, a non-normalized distribution can be defined as:

$$G(k) = C_t(0)g(k) \tag{9a}$$

or

$$F(\log k) = C_t(0)f(\log k) \tag{9b}$$

Since we are dealing with synthetic examples in this paper $C_t(0)$ is known and eq 9 is used to obtain normalized distributions.

Synthetic Data Set

The methods to be studied in this paper will be illustrated by a synthetic example based on a multi-gaussian distribution:

$$f(\log k) = \frac{1}{\sqrt{\pi}} \sum_{i=1}^{n} (a_i \sqrt{(b_i)}) \exp\{-b_i[2.3 \log(k/\bar{k}_i)]^2\} \tag{10}$$

where $\log \bar{k}_i$, b_i and a_i are the mean, the reciprocal width and the fraction of the individual peak i respectively, and n is the number of gaussian peaks in the distribution. The use of a synthetic example has the advantage that the true distribution

165

can be compared with the result of an (approximate) analysis method. We constructed a distribution with four peaks as shown in Figure 1a. The parameters are given in table 1.

peak	1	2	3	4
mean, $\bar{K}_i$	-2.	-1.25	-0.5	1.
width, b_i	20.	20.	20.	0.25
fraction, a_i	0.1	0.1	0.1	0.7

Table 1: Synthetic data set, parameters of the distribution function.

Note that a large value of the reciprokal width, b_i, corresponds with a narrow peak and that a small value corresponds with a wide peak. The synthetic decay function was obtained by performing the integration of eq 6 numerically using eq 10 as distribution function.
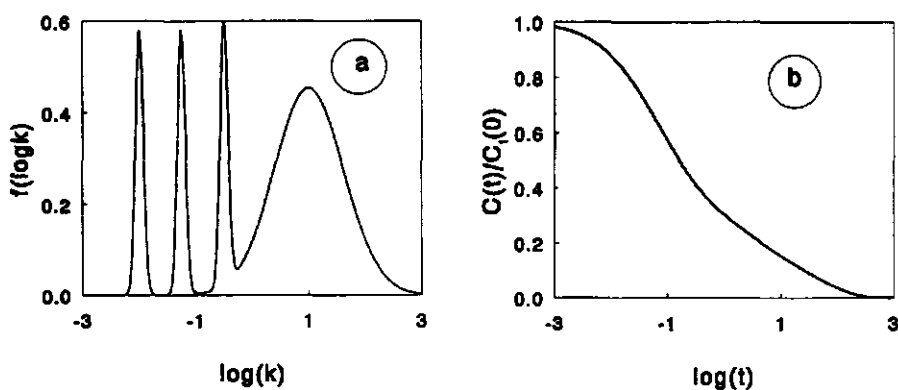

Figure 1: The rate constant distribution function (a) and the corresponding overall decay function (b) used to illustrate the methods. See table 1 for the parameters.

166

The result, expressed as $C(t)/C_t(0)$, is shown in Figure 1b; A smooth monotonically decreasing function is obtained without distinct steps, whereas in the distribution sharp peaks are present.

To illustrate the effect of a random error in the data a second data set is generated which is identical to the first one except for the presence of a small error of $\sigma \approx 1.10^{-3}$ in the overall decay function.

Methods to Determine Rate Constant Distributions

Laplace Transform Technique

In fact eq 5 is the definition of the Laplace transform (15,16), where $g(k)$ is the original function and $C(t)/C_t(0)$ is the image function. Note that usually the original function is given as a function of time. The distribution of rate constants $g(k)$ can be obtained by inverting eq 5 using the inverse Laplace transform. In tables of the Laplace transform (e.g. 15,16,22) expressions for $g(k)$ can be found for a limited number of given decay functions or vice versa. However, in general the decay function can not be described with a simple analytical function and the general inversion formula of the Laplace transform has to be used (15,16) to obtain an expression for the distribution function. The result is an infinite derivative of the decay function with respect to t:

$$G_{LT}(k) = \lim_{m \to \infty} \left(\frac{(-1)^m}{m!} \right) \left(\frac{m}{k} \right)^{m+1} \frac{\partial^m C(m/k)}{\partial t^m} \tag{11}$$

where $G_{LT}(k)$ indicates the Laplace Transform approximation of $G(k)$ and $C(m/k)$ indicates that t corresponds with m/k for any computed value of $G_{LT}(k)$. In practice the infinite derivative cannot be determined from experimental data. Approximations can be obtained by taking a finite value of m. The first order approximation is obtained for m=1:

$$G_{LT1}(k) = -1 \left(\frac{1}{k} \right)^2 \left(\frac{\partial C(t)}{\partial t} \right)_{t=1/k} \tag{12}$$

167

In practice it is convenient to express the distribution function as a function of log k and the decay function as a function of log t. First, the derivative with respect to t can be transformed to a derivative with respect to log t by $\partial t = 2.3 t \partial \log t$. Introducing this in eq 12 gives with t=1/k :

$$G_{LTl}(k) = -\frac{0.43}{k}\left(\frac{\partial C(t)}{\partial \log t}\right)_{t=1/k} \tag{13}$$

With eqs 8 and 9 it follows that:

$$F_{LTl}(\log k) = -\left(\frac{\partial C(t)}{\partial \log t}\right)_{t=1/k} \tag{14a}$$

$$\log k = -\log t \tag{14b}$$

The result of the first order method applied to the synthetic example is shown in Figure 2a. The obtained distribution is too wide and flattened compared to the true distribution. The three sharp peaks are reduced to very weak shoulders. The shape of the broad peak is reasonably well reproduced, but its position has been shifted slightly to higher values of log k. The peak positions of the sharp peaks can only be poorly estimated from the position of the shoulders in the obtained distribution.
The second order approximation of F(log k) results for m=2, it has been used by Olson et al. (7,12,13) to study the dissociation kinetics of Cu-ligand complexes. For m=2 eq 11 becomes, after analogous manipulations as done for the first order approximation:

$$F_{LT2}(\log k) = -\frac{\partial C(t)}{\partial \log t} + 0.43\frac{\partial^2 C(t)}{\partial \log t^2} \tag{15a}$$

$$\log k = \log 2 - \log t \tag{15b}$$

where 0.43 is needed for the transformation from ln t to log t. In addition to the first derivative of the decay function now also the second derivative with respect to log t is needed.
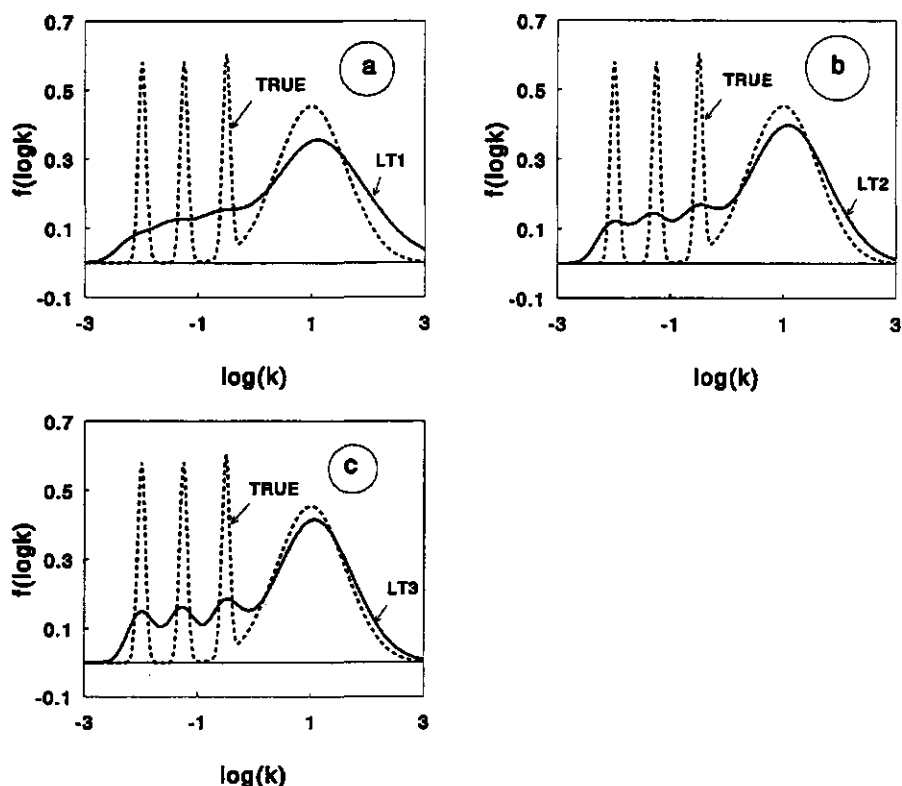
168

Figure 2: Comparison of the distribution functions obtained with the Laplace transform technique with the true distribution function. a) First order method; b) second order method; c) third order method.

The resulting distribution obtained for the synthetic example is shown in Figure 2b. The three sharp peaks are now clearly resolved. However they are not as sharp as the true ones. The broad peak is reproduced slightly better than with the first order method. The peak positions of the sharp peaks are approximately correct, whereas the peak position of the broad peak is shifted to slightly higher rate constants. Thus, as a result of the use of a second derivative more details of the distribution are discerned.

Although not used before, it is also possible to derive the third order approximation for m=3:

$$F_{LT3}(\log k) = -\frac{\partial C(t)}{\partial \log t} + 0.65\frac{\partial^2 C(t)}{\partial \log t^2} - 0.094\frac{\partial^3 C(t)}{\partial \log t^3} \qquad (16a)$$

$$\log k = \log 3 - \log t \qquad (16b)$$

It follows that, for the calculation of the third order approach, also a third derivative of the overall decay function is needed. Figure 2c shows that with the third order method the small peaks are better separated and the broad peak is slightly better reproduced than with the first and second order approach.

In general eq 11 implies for an m order approach the use of a series of derivatives with respect to log t up to the mth derivative. Since derivatives are hard to obtain from experimental data we consider differentials of order higher than three experimentally inaccessible. However, if an analytical expression for the decay function C(t) is available, higher order derivatives may be used to derive the corresponding distribution function.

Schwarzl and Staverman Approach

Schwarzl and Staverman (17,18) generalized eq 11 for any type of kernel by stating that an mth order approximation can be obtained by a combination of the first m derivatives. Distributions determined with the Schwarzl and Staverman approach will be indicated as SS_m:

$$F_{SSm}(\log k) = \sum_{v=1}^{m} a_v (0.43)^{v-1} \frac{\partial^v C(t)}{\partial \log t^v} \qquad (17a)$$

$$\log k = \log \gamma - \log t \qquad (17b)$$

where the factors $0.43^{(v-1)}$ are again needed for the conversion of ln t to log t. Substituting eq 6 for C(t) in eq 16 gives:

$$F_{SSm}(\log k) = C_t(0) \int_0^\infty \left\{ \sum_v^m a_v (0.43)^{v-1} \frac{\partial^v e^{-kt}}{\partial \log t^v} \right\} f(\log k) d \log k \qquad (18a)$$

$$\log k = \log \gamma - \log t \qquad (18b)$$

Compared to eq 6 the local decay function is replaced by a combination of its derivatives with respect to log t. The combination of derivatives is the kernel of the integral equation. The factor γ determines the transformation from a log t axis to a log k axis. The approximation of the distribution function is obtained by assuming that the kernel, the term between brackets in eq 18, can be approximated by a Dirac-Delta function, then $F_{SSm}(\log k) \approx F(\log k)$. So the better the kernel resembles a Dirac-Delta function the closer will $F_{SSm}(\log k)$ approximate $F(\log k)$. The higher m the sharper the kernel can be made by adjusting the coefficients a_v and γ.

The coefficients a_v and γ are determined by demanding the kernel to be as sharp as possible. This demand was translated in a few simple constraints by Schwarzl and Staverman (18):

1) The kernel should always be positive since both the distribution function and the overall C(t) function are positive.

2) The kernel should be normalized to 1.

3) The kernel should have one and only one maximum at $\log k = \log \gamma - \log t$, which is as high as possible.

4) The kernel should become zero at $\log kt = \pm\infty$

The transformation from log t to log k is determined by the position of maximum of the kernel.

For the first order approximation only the coefficient in front of the first derivative need to be determined. It follows from constraint 2) that $a_1 = -1$. The position of the maximum is found at $kt = \gamma = 1$. This corresponds to the first order approximation of the Laplace approach. The corresponding kernel is shown in Figure 3a. The kernel is a skewed and rather broad function, which poorly resembles a Dirac-Delta function. Note that the kernel can be seen as a weighting function which maps the true distribution into the first order approximation. It follows that a broad kernel results in a too flat distribution function and that details in the distribution are lost.
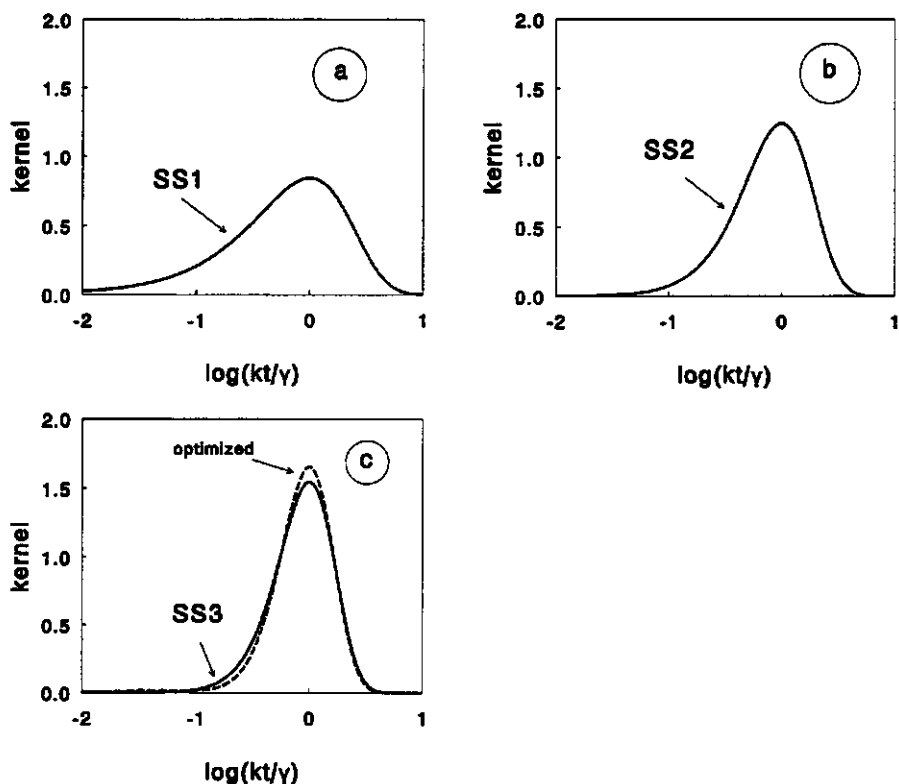
171

Figure 3: Kernels of the integral equation (eq 18a) after applying the Schwarzl and Staverman approach. a) First order method; b) second order method; c) third order method. In Figure c the solid line corresponds with the third order Laplace transform expression, the dashed line corresponds with the SS method for which the coefficients were obtained by numerical optimization.

Sharper kernels can be obtained by introducing higher derivatives. Since the second and higher derivatives add nothing to the integral of the kernel the coefficient a_1 remains -1 for all further approximations in order to keep the kernel normalized. With the second order approximation the kernel is sharpened by the second derivative, under the condition that the kernel remains positive. This leads to $a_2=1$.

172

The maximum of the kernel is found at $kt = \gamma = 2$. The corresponding kernel is shown in Figure 3b. Thus, also the second order SS approximation corresponds to the Laplace approach.

For the third order SS approach several possibilities exist. When the position of the maximum of the kernel is fixed at $kt = 3$ as was found for the third order Laplace method, constraints 1 and 3 lead to $a_2=3/2$ and $a_3=-1/2$, which corresponds to the third order Laplace transform. The corresponding kernel is shown in Figure 3c (solid line). A slightly sharper kernel can be obtained by optimizing the parameters a_2, a_3 and γ. A sharper kernel could be obtained by enlarging a_2 and lowering a_3. For too large values of a_2 and too low values of a_3 the kernel tends to get a second peak in the region $\log kt = -1.5$. This situation is not desirable, because then 'false peaks' will be created in the distribution function. The sharpest kernel under constraint 3), which forbids a second maximum, is obtained for $a_2=1.56$ and $a_3=-0.66$. The position of the maximum is then found at $kt = 3.3$. The result is only slightly better than that obtained with $a_2=1.5$ and $a_3=-0.5$, as is shown in Figure 3c (dashed line). For this reason the result will be neglected in the further analysis.

It can be concluded that the first three Laplace approximations can be interpreted in terms of the Schwarzl and Staverman concept. From Figure 3 it becomes clear that the sharpness of the kernel increases in the order SS_1, SS_2, SS_3, thus the SS_3 approximation should give the best approximation of the true distribution. This conclusion corresponds to the results shown in Figure 2.

LOcal Decay Function Approximation (LODA).

A new approach is to approximate the local decay function by another mathematical function so that eq 6 can be solved analytically for f(log k). This type of approach was applied successfully for the analysis of equilibrium binding data and it was called in that case Local Isotherm Approximation, LIA (3). A general and flexible approximation of the local decay function, which we will abbreviate as LODA, is:

173

$$\xi_{1,LODA} = 1 - \alpha_1 \left(\frac{kt}{\gamma} \right)^{\beta_1} \qquad for \qquad kt \leq \gamma \qquad\qquad (19a)$$

$$\xi_{2,LODA} = \alpha_2 \left(\frac{kt}{\gamma} \right)^{-\beta_2} \qquad for \qquad kt > \gamma \qquad\qquad (19b)$$

where $\xi_{1,LODA}$ and $\xi_{2,LODA}$ indicate that the true local decay function is replaced by the LODA approximation, γ is the 'breakpoint' which divides the approximation in its two parts and α_i and β_i are constants. To obtain explicit expressions for the distribution function in general two constraints should be obeyed ($a_1 \neq 1$) :

$$1 - \alpha_1 - \alpha_2 = 0 \qquad\qquad (20a)$$

$$\alpha_1 \beta_1 - \alpha_2 \beta_2 = 0 \qquad\qquad (20b)$$

Thus for a given set of α_1 and β_1, α_2 and β_2 are fixed.

Analogous to the Condensation Approximation (CA) (23,24) in the LIA approach, the simplest approximation is to replace the exponential function by a step function. This will be denoted by LODA-S. The approximation is obtained by taking $\alpha_1 = \alpha_2 = 0$ in eq 19:

$$\xi_{1,LODA - S} = 1 \qquad for \qquad kt \leq \gamma \qquad\qquad (21a)$$

$$\xi_{2,LODA - S} = 0 \qquad for \qquad kt > \gamma \qquad\qquad (21b)$$

This means that at time $t = \gamma/k$ the complex of type i dissociates instantly (see Figure 4). The position of the step is determined by a best fit criterion. We applied the least sum of squares method on a log(kt) scale and obtained the best fit for $\gamma = 0.7$ (see Figure 4, solid line).
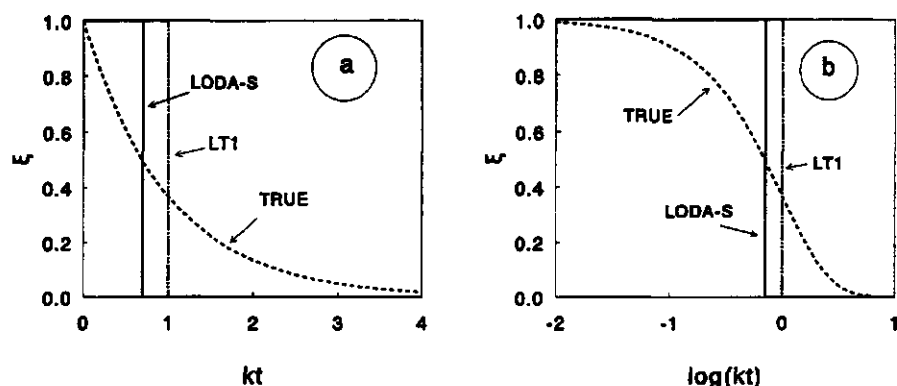
Figure 4: Approximations of the local decay function for the LODA-S method and the true local decay function, plotted a) on a linear kt scale and b) on a logarithmic kt scale.

The expression for the distribution function becomes:

$$F_{LODA-S}(\log k) = -\frac{\partial C(t)}{\partial \log t} \tag{22a}$$

$$\log k = \log \gamma - \log t \tag{22b}$$

Note that for $\gamma = 1$ the expression for the first order Laplace method is obtained. This corresponds with the step at kt=1 (see Figure 4, dash-dotted line). In Figure 5 the distribution function is shown for the synthetic example with $\gamma = 0.7$. With respect to Figure 2a the distribution is shifted only 0.15 log k units to lower rate constants. This means that the position of the broad peak is now at the right place, but that the shoulders of the three small peaks are found at slightly too low values of the rate constant. Thus the $\gamma = 0.7$ result is not really an improvement with respect to the first order Laplace method. Note that when the fit was done on a linear kt scale probably a higher value of γ would have been obtained.
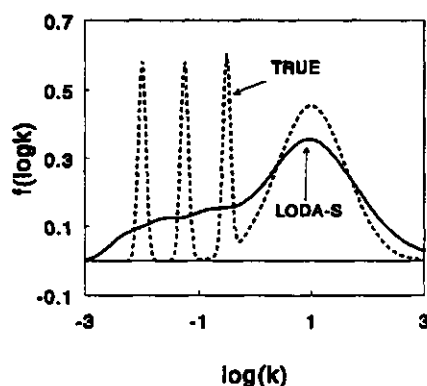
175

Figure 5: Distribution function obtained for the best fit of the LODA-S method compared with the true distribution function.

A second simple approximation of the exponential function is a linear function with slope $1/\gamma$, this approximation will be indicated by LODA-L. The method is analogous to the LINA approximation of the Langmuir isotherm in the equilibrium situation. With LODA-L $\alpha_1 = \beta_1 = 1$ is taken in eq 19:

$$\xi_{1,LODA-L} = 1 - \frac{kt}{\gamma} \qquad for \qquad kt \le \gamma \qquad (23a)$$

$$\xi_{2,LODA-L} = 0 \qquad for \qquad kt > \gamma \qquad (23b)$$

This means that the linear function goes from $\xi = 1$ at kt=0 to $\xi = 0$ at $kt = \gamma$. The expression for the distribution function resembles the second order Laplace approach:

$$F_{LODA-L}(\log k) = -\frac{\partial C(t)}{\partial \log t} + 0.43\frac{\partial^2 C(t)}{\partial \log t^2} \qquad (24a)$$

$$\log k = \log \gamma - \log t \qquad (24b)$$

176

The optimal slope is determined by the least sum of squares method applied on a log(kt) scale. The best fit of the local decay function was found for $\gamma = 1.6$, see Figure 6 (solid line). Again, when the fit had been done on a linear kt scale a higher value would have been obtained.
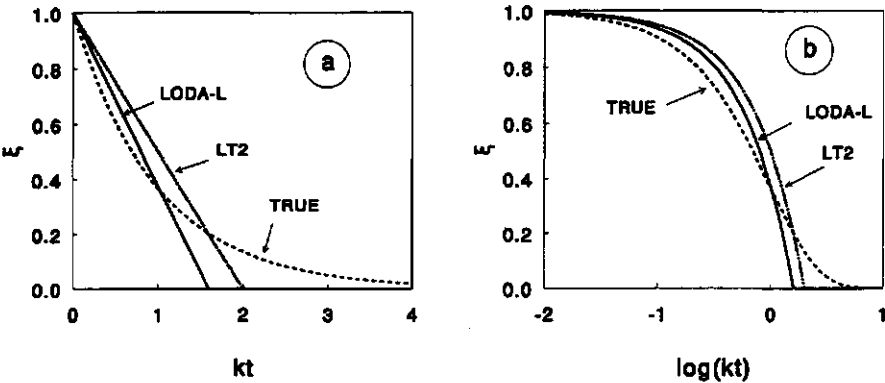

Figure 6: Approximations of the local decay function for the LODA-L method and the true local decay function when plotted on a) a linear kt scale and b) a logarithmic kt scale.
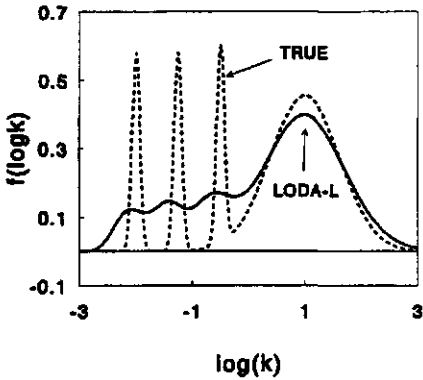

Figure 7: Distribution function obtained for the best fit of the LODA-L method compared with the true distribution function.

177

The distribution for $\gamma = 1.6$ is shown in Figure 7. The distribution is shifted 0.1 log k unit to lower values of log k with respect to the second order Laplace method, which is obtained for $\gamma = 2$ (see Figure 6, dash-dotted line). This again results in the right position of the broad peak and slightly too low values for the small peaks. However, the differences in peak positions are small. For other values of γ the shape of the resulting distributions remain the same, but the peak positions shift according to eq 24b. For $\gamma = 1$ the initial slope of the approximation is correct, which is analogous to the ACA (25) method in the equilibrium case.

The general expression for the LODA approximation, eq 19, is analogous with the LOGA approximation for the equilibrium situation (3) and will be indicated by LODA-G. The corresponding expression for the distribution function is:

$$F_{LODA-G}(\log k) = a_1 \frac{\partial C(t)}{\partial \log t} + 0.43 a_2 \frac{\partial^2 C(t)}{\partial \log t^2} + 0.19 a_3 \frac{\partial^3 C(t)}{\partial \log t^3} \tag{25a}$$

$$\log k = \log \gamma - \log t \tag{25b}$$

where

$$a_1 = -1$$

$$a_2 = \frac{\beta_2 - \beta_1}{(\alpha_1 \beta_1^2 + \alpha_2 \beta_2^2)}$$

$$a_3 = \frac{1}{(\alpha_1 \beta_1^2 + \alpha_2 \beta_2^2)} \tag{25c}$$

The best approximation of the local decay function is obtained for $\gamma = 1.1$, $\alpha_1 = 0.68$ and $\beta_1 = 0.77$, see Figures 8a,b.
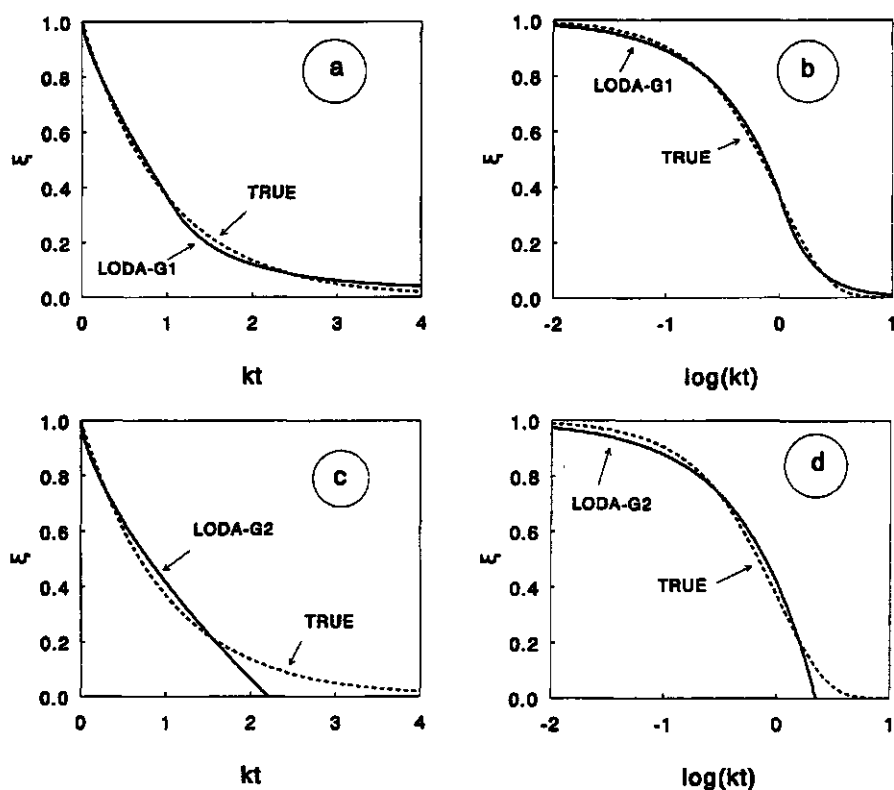
Figure 8: Approximations of the local decay function for the LODA-G1 method (a,b) and the LODA-G2 method (c,d) and the true local decay function when plotted on a linear kt scale (a,c) and a logarithmic kt scale (b,d).

The corresponding distribution function is indicated by LODA-G1 and is obtained from eq 25 by taking $a_1=-1$, $a_2=0.69$ and $a_3=0.79$:

$$F_{LODA-G1}(\log k) = -\frac{\partial C(t)}{\partial \log t} + 0.30\frac{\partial^2 C(t)}{\partial \log t^2} + 0.15\frac{\partial^3 C(t)}{\partial \log t^3} \qquad (26a)$$

$$\log k = \log(1.1) - \log t \qquad (26b)$$

179
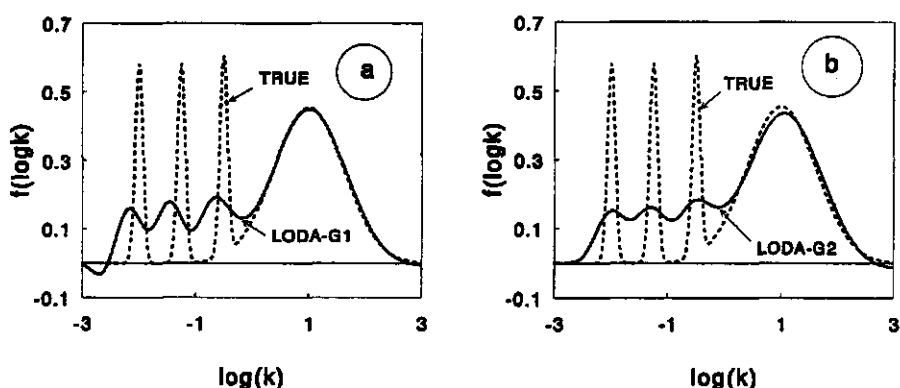
Figure 9: Distribution functions obtained with the LODA-G method in comparison with the true distribution function; a) result obtained with the LODA-G1 method; b) result obtained with the LODA-G2 method.

The resulting distribution for the synthetic data set is shown in Figure 9a. The broad peak is reproduced almost perfectly. The three small peaks are well discerned but shifted to lower values of the rate constant. At very low values of the rate constant the distribution becomes negative, which is physically unrealistic. The coefficient a_3 in front of the third derivative is now 0.15 which means that the method relies more on the third derivative than the third order Laplace method, which uses a coefficient of 0.094.

For cases that the third derivative can not be determined reliably a fit was found which resulted in a zero coefficient for a_3, by fixing the α_1 parameter to 1. Note that the distribution function does not follow from the general formula (eq 25) since an exception was made for $\alpha_1 = 1$ in eq 20. For the special case of $\alpha_1 = 1$ the second constraint is not necessary and the distribution function is derived separately. The method will be indicated by LODA-G2:

$$F_{LODA-G2}(\log k) = -\frac{\partial C(t)}{\partial \log t} + 0.64 \frac{\partial^2 C(t)}{\partial \log t^2} \qquad (27a)$$

$$\log k = \log(2.2) - \log t \qquad (27b)$$

180

Thus only the two first derivatives are needed. The fit was obtained for $\alpha_1 = 1$, $\beta_1 = 0.68$ and $\gamma = 2.2$, see Figures 8c,d. The coefficient a_2 in front of the second derivative becomes 1.47, so that this approximation relies more strongly on the second derivative than both the LODA-G1 and the second order Laplace methods. Compared to the third order Laplace Transform method the term with the third derivative of the decay function is neglected. The resulting distribution is shown in Figure 9b. The broad peak is resolved rather good and the small peaks are in the right place and clearly resolved.

It appears that no combination of parameters can be found that correspond to the third order Laplace method. However eq 16 can be seen as an average of two distributions:

$$F_{LT3}(\log k) = \frac{3}{2} F_{LODA-L}(\log k) - \frac{1}{2} F_{LODA-G}(\log k) \qquad (28a)$$

$$\log k = \log(3) - \log t \qquad (28b)$$

F_{LODA-L} corresponds to a linear approximation with $\gamma = 3$ and F_{LODA-G} corresponds to an approximation according to eq 19 with $\alpha_1 = \alpha_2 = 0.5$, $\beta_1 = \beta_2 = 1$ and $\gamma = 3$.

Evaluation of methods

From the Laplace transform method it becomes clear that the higher the order of the approximation the better the results obtained. Since each method is determined by an arbitrarily chosen cut-off of an infinite series, the quality of a specific method is hard to discuss in general terms. Only with an arbitrarily chosen synthetic example some features can be shown. In order to discern narrow peaks that are closely together on the log k-axis at least a second order approach is needed. It appeared that the peak position of a broad peak is shifted to slightly higher log k values.

This may be explained by the asymmetrical kernels of the Schwarzl and Staverman (SS) approach. This is in contrast with the equilibrium case (3,4) where symmetric kernels were found for the analogous Affinity Spectrum methods. The first and second order SS approach are equivalent with the Laplace technique. When the position of the maximum of the kernel is fixed at kt=3, this is also the case for the

181

third order method. Thus the kernels of Figure 3 can be used to discuss the quality of both the Laplace and the SS methods. Note that the kernel can be seen as a weighting function which maps the true distribution function into its approximation. It is also the distribution function obtained for the kinetically homogeneous case. It is obvious that the kernels poorly resemble a Dirac-Delta function, which would result in the exact distribution function. The third order method could be improved a little by adjusting the coefficients in front of the second and third derivative under the condition that the constraints are still fulfilled. However, the improvement is only minor. Thus, with the SS approach no significantly different expressions for the distribution function are obtained compared with the LT method, but the SS approach provides an elegant way to visualise the quality of the approximation in terms of the sharpness of the kernel.

The LODA methods are conceptually the simplest, the quality of a method can be seen directly from the agreement of the LODA function with the true local decay function. We fitted the approximations on a log(kt) scale which resulted for the LODA-S and LODA-L methods in a shift of the distribution to lower rate constants, compared to the LT distributions. This means that the position of a broad peak shifts to the right place but that the position of narrow peaks are shifted to too low rate constants. For the LODA-G approximations the situation is different. With the best LODA-G approximation, LODA-G1, it strikes that the coefficient in front of the third derivative becomes higher than with the third order Laplace. In general the three narrow peaks are discerned more clearly, but they are shifted to lower log k values. The broad peak is resolved perfectly. The LODA-G2 method that does not need a third derivative is the most promising. Although the peaks are somewhat less distinctly resolved than with the LODA-G1 method, the narrow peaks are in the right position and slightly better resolved than with the second order Laplace method. In addition the broad peak is considerably better resolved than with the LT2 method. The LODA-G2 result is comparable to the LT3 result, that is the broad peak is resolved slightly better and the narrow peaks are resolved slightly worse. Important difference, however, is that the LODA-G2 method will be less sensitive for experimental error, since it does not need a third derivative.

Data Treatment

From the previous section it follows that in order to obtain a reasonable distribution at least the first and second derivative of the overall decay function are needed. Derivatives of experimental data, which are prone to errors, are hard to obtain. To deal with this problem a smoothing spline procedure, derived to study the affinity constant distribution (19-21), can be adapted for the present problem.

The first step of the procedure is to find a proper smoothing parameter. This quantity determines the trade off between the goodness of fit and the smoothness of the spline function (19). This is done by minimizing the GCV criterion (26). In our previous work it was found that the GCV estimate of log p is often too low. Therefore in addition to the GCV statistics a number of physical constraints have to be formulated, that should be obeyed. Especially in cases where the error is not purely random the constraints may help to find an appropriate smoothing parameter. Also when only few data points are available, the GCV might not lead to a proper smoothing parameter.

Since the first derivative of the local decay function with respect to t is negative and the distribution function is always positive, it follows that the first derivative of the overall decay function with respect to t should always be negative or equal to zero. From the same reasoning it follows that the second derivative should always be positive or equal to zero and that the third derivative should be negative or zero. In general:

$$\frac{\partial^v C(t)}{\partial t^v} \leq 0 \qquad (29a)$$

for odd derivatives and

$$\frac{\partial^v C(t)}{\partial t^v} \geq 0 \qquad (29b)$$

for even derivatives. Moreover, it should be remarked that the SS distribution should be positive since both kernel and true distribution are positive in eq 18. This

can also be used as an additional constraint. The constraints can be adjusted to the heterogeneity analysis method to be used. A practical way is to take the highest derivative needed for a certain method as a constraint according to eq 29.

The procedure in practice is as follows. First the GCV minimum is calculated, subsequently the spline corresponding to the GCV smoothing parameter is tested for the constraints. When one or more constraints are not obeyed the smoothing parameter is enlarged until all the constraints are fulfilled.

We calculated confidence intervals of the distribution functions on the basis of the variance in the spline result using Monte Carlo simulations. With the Monte Carlo method the variance of the distribution is calculated on the basis of 100 realisations of the spline .

To illustrate the procedure for experimental kinetic data we have imposed a random absolute error on the synthetic data set of Figure 1. Since the formed complex is assumed to be measured accurately we used a variance of the random error of only $\sigma = 1.10^{-3}$. As a consequence, the relative error varies from 0.5% for high values of the decay function to 20% for low values of $C(t)$.
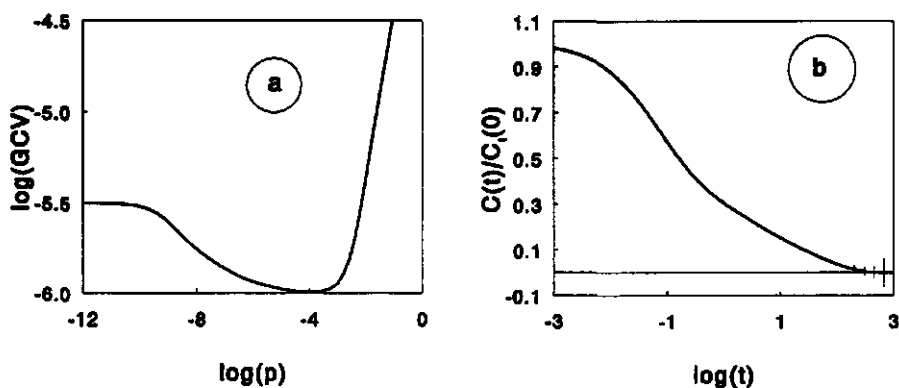

Figure 10: a) The log(GCV) function for the synthetic data set on which a random absolute error of $\sigma = 1.10^{-3}$ on $C(t)$ is imposed. Log(GCV) is plotted as a function of the smoothing parameter, log p. The minimum occurs at log(p)=-4.2. b) The smoothing spline representation of the overall decay function.

184

First the GCV minimum is calculated. The GCV function is shown in Figure 10a for a range of values of the smoothing parameter p. A minimum is found at $\log(p)=-4.2$. In the present case the value of $\log(p)=-4.2$ obeys all the constraints.

Calculated Distributions

The smoothing spline function for $\log p=-4.2$ representing the overall decay function corresponding with the synthetic data set with an error of $\sigma = 1.10^{-3}$ in $C(t)$ is shown in Figure 10b. The bars denote the confidence interval. It follows that only for high values of $\log t$, where the relative error is the largest, the uncertainty is significant. The distribution functions calculated using the various approximations are shown in Figure 11a-11e. The uncertainty in the decay function for high values of $\log t$ is reflected in a large uncertainty in the distribution for low values of $\log k$. For the first order Laplace approach (LT1, Figure 11a) a reliable result is obtained over almost the entire $\log k$ range, since only the first derivative is needed.

For the second order Laplace method (LT2, Figure 11b) the range where the resulting distribution is quite uncertain shifts to higher values of $\log k$. The lowest of the three small peaks is not resolved. The other two small peaks appear as a "foot" of the broad peak, which is recovered very well. Despite the fact that the third order Laplace approach (LT3, Figure 11c) has in principle the best resolving power the distribution function obtained in practice is not better than that shown in Figure 11b: details in the distribution function can not be interpreted due to the large error bars.

The situation is even worse for the LODA-G1 method (Figure 11e) since this method relies more strongly on the third derivative. Taking the large error bars into account the small peaks can not be found reliably. The LODA-G2 method (Figure 11f), that does not need a third derivative, results in much smaller error bars and a slightly better result than the second order Laplace method. Also here, the peak with the smallest rate constant is lost.
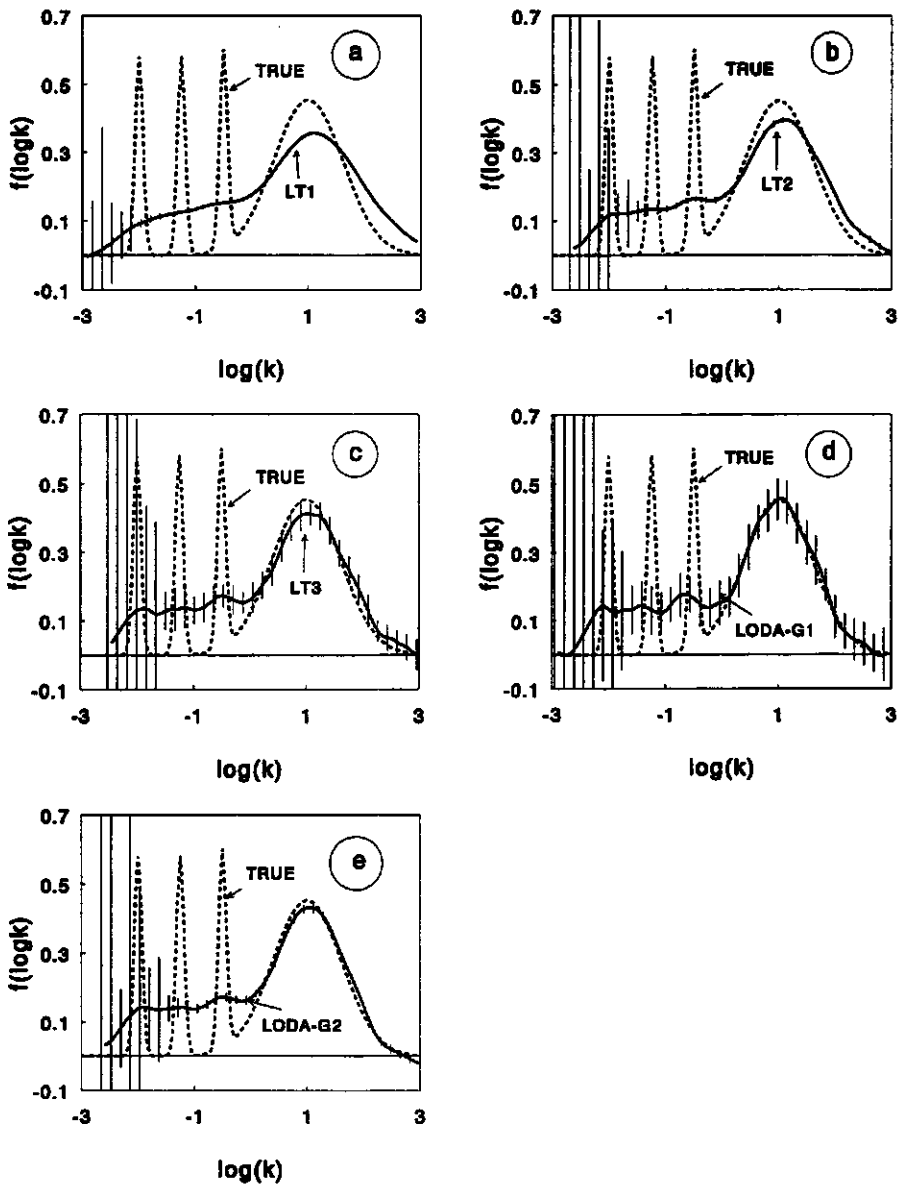
185

Figure 11: The distribution functions calculated for the synthetic data set containing a small error. The distributions are calculated on the basis of the spline function shown in Figure 10b. The error bars indicate 66% confidence intervals. a) First order Laplace method; b) Second order Laplace method; c) Third order Laplace method; d) LODA-G1 method; e) LODA-G2 method.

186

Discussion

We are now able to compare the results obtained for exact synthetic data with those obtained for data on which a random error was imposed. It follows that even for small experimental errors the first order methods are not capable to resolve narrow peaks in a distribution. Only for exact data narrow peaks are resolved as very weak shoulders. On the other hand for the third order methods it applies that the error bars are too large to allow the interpretation of small peaks, even for a small experimental error. Thus, only for highly accurate data higher order methods can be used. For the second order methods the peak with the smallest rate constant is "covered" by large error bars. Comparing the LT2 method with the newly developed LODA-G2 method it is found that the resolving power of the latter method is, also in the presence of a small error, slightly better than that of the LT2 method. The error bars over the whole range of the distribution are slightly larger for the LODA-G2 method than for the second order Laplace. In principle the third order Laplace method is capable to resolve the narrow peaks more distinctly, but the large error bars do not allow them to be interpreted as separate peaks. The broad peak is very well reproduced with the LODA-G2 method and is of much better quality than the approximation of the second order Laplace. Compared to the third order Laplace the broad peak is recovered only slightly worse, but the error bars are much smaller. In conclusion we might say that the LODA-G2 method is the most promising in practice.

The results of the whole procedure, that is a spline representation of the overall decay function and the rate constant distribution function calculated from the spline, can be used as input for the routine developed by Lavigne and Langford (14). The equidistant $C(t)$ data, needed for the routine, can be obtained directly from the spline function and estimates of peak positions and fractions can be obtained from the calculated spectrum.

However, modeling in terms of a continuous rate constant distribution might be more useful. The results with equilibrium data indicate that with a continuous distribution model, the data can be modelled with less parameters using analytical expressions for the decay function that correspond with a certain distribution function. For the equilibrium case the Sips formulas are suitable for this purpose (27,28). For the kinetic case no such convenient formulas are available yet, but may be derived using the Laplace transform technique, using eq 5 or 6.

187

Conclusions

- The overall decay function of a set of first order reactions can be analyzed to obtain the rate constant distribution. The traditional method to do this is the Laplace transform technique. Two alternative methods of analysis are presented in this paper. These methods are analogous to the Affinity Spectrum method and the LIA method for the analysis of equilibrium data and called respectively the Schwarzl and Staverman approach (SS) and the local decay function approximation (LODA) method.

- Expressions of the distribution functions obtained with the Laplace transform method can be interpreted both in terms of the SS approach and the LODA approach. Both the SS and LODA methods provide a means to visualise the quality of the approximations.

- In order to apply any of the three methods for kinetic heterogeneity analysis to experimental data, a treatment of the data is necessary with an adapted smoothing spline technique. The smoothing parameter is determined by applying the Generalized Cross Validation technique in combination with a number of physical constraints.

- In order to be able to obtain details in the distribution functions very accurate data are needed.

- Wide distributions of rate constants can be reproduced relatively well with all methods. Narrow distributions, or narrow peaks superposed on a distribution, are difficult to assess. The first order methods flatten and widen the distribution function and no details in a distribution can be recovered. The second order methods, although in principle less good than the third order methods, are most suited to reveal narrow peaks as they are less sensitive to experimental error than the third order methods.

- The newly developed LODA-G2 method is the most promising both with respect to its resolving power and with respect to the sensitivity to experimental error.

References

1   Gamble, D.S.; Underdown, A.W.; Langford, C.H. *Anal. Chem.* **1980**, *52*, 1901-1908.
2   Jaroniec, M.; Bräuer, P. *Surf. Sci. Rep.* **1986**, *6*, 65-117.
3   Nederlof, M.M.; Van Riemsdijk, W.H.; Koopal, L.K. *J. Colloid Interface Sci.* **1990**, *135*, 410-426.
4   Nederlof, M.M.; Van Riemsdijk, W.H.; Koopal, L.K. *Environ. Sci. Technol.* **1992**, *26*, 763-771.
5   Nederlof, M.M.; Van Riemsdijk, W.H.; Koopal, L.K.; In *Heavy Metals in the Environment*; Vernet, J.-P.; Elsevier, Amsterdam, 1991, pp 365-396.
6   Buffle, J. *Complexation Reactions in Aquatic Systems: An Analytical Approach*; Ellis Horwood: Chichester, 1988.
7   Olson, D.L.; Shuman, M.S. *Anal. Chem.* **1983**, *55* , 1103-1107.
8   Scatchard, G.; Scheinberg, I.H.; Armstrong, S.H. Jr. *J. Am. Chem. Soc.* **1950**, *72*, 535-540.
9   Mark, H.B., Jr.; Rechnitz, G.A. "Kinetics in Analytical Chemistry", Interscience, New York, 1968; Chapter 7.
10   Connors, K.A. *Anal. Chem.* **1975**, *47*, 2066-2067.
11   Connors, K.A. *Anal. Chem.* **1979**, *51*, 1155-1160.
12   Olson, D.L. *The kinetic spectrum method for analysis of smultaneous, first order reactions and its application to copper(II) dissociation form estuarine humic materials*; PhD thesis, Chapel Hill, 1983.
13   Olson, D.L.; Shuman, M.S. *Geochim. Cosmochim. Acta*, **1985**, *49*, 1371.
14   Lavigne, J.A.; Langford, C.H.; Mak, M.K.S. *Anal. Chem.* **1987**, *59*, 2616-2620.
15   Doetsch, G. *Theorie und Anwendung der Laplace Transformation*; Springer: Berlin, 1937.
16   Widder, D.V. *The Laplace Transform*; Princeton University Press: Princeton, 1946, p 406.
17   Schwarzl, F.; Staverman A.J. *Physica*, **1952**, *18*, 791-798.
18   Schwarzl, F.; Staverman A.J. *Apl Sci. Res. A.*, **1953**, *4*, 127-141.
19   Silverman, B.W. *J.R. Statist. Soc. B.*, **1985**, *47*, 1-52.
20   Woltring, H.J. *Adv. Eng. Software*, **1986**, *8*, 104-107.
21   Nederlof, M.M.; Van Riemsdijk, W.H.; Koopal, L.K. *Anal. Chem.*, **1992**, submitted for publication to Anal. Chem..
22   Abramowitz, M.; Stegun, I.A. *Handbook of Mathematical Functions*, Dover Publications, New York, 1970, pp 1019-1030.

23   Roginsky, S.S. *Adsorption catalysis on heterogeneous surfaces*, Academy of Sciences U.S.S.R., Moscow, 1948 (in Russian).

24   Harris, L.B. *Surf. Sci.* 1968, *10*, 129-145.

25   Cerofolini, G.F. *Thin Solid Films*, 1974, *23*, 129-152.

26   Craven, P.; Wahba, G. *Numer. Math.*, 1979, *31*, 377-403.

27   Sips, R. *J. Chem. Phys.* 1950, *18*, 1024-1026.

28   Van Riemsdijk, W.H.; Bolt, G.H.; Koopal, L.K.; Blaakmeer, J. *J. Colloid Interface Sci.* 1986, *109*, 219-228.

CHAPTER 7

Analysis of the Rate of Dissociation of Ligand Complexes

Abstract

Cu-humate dissociation data using humic material from different sampling points in the Ogeechee river (Georgia, U.S.A.) as measured by Olson et al. are analysed with the newly developed LODA-G2 method for the determination of rate constant distribution functions. The LODA-G2 method is based on an approximation of the local decay function. An adapted smoothing spline procedure is applied to the data in order to account for the experimental error in the data. The appropriate smoothing parameter is obtained on the basis of the Generalized Cross Validation technique in combination with physical constraints. Without data treatment spurious peaks occur in the distribution functions due to the experimental error. On the basis of the presented methodology a thorough interpretation of the distribution functions is possible .

.

Introduction

The speciation of trace metals in natural systems is controlled by the interaction of the metal ions with inorganic anions, organic ligands, reactive surfaces, such as clay minerals, and organisms. Bioavailability or toxicity is thought to depend on the concentration of free metal ions in solution (1,2). According to Shuman et al. (3) especially organic matter is important with respect to the regulation of the free metal ion concentration.

An important aspect with respect to bioavailability is the difference in reaction rate between the uptake by an organism and the dissociation from an adsorption complex (for instance humic material). When the dissociation from the adsorption complex is faster than the uptake by an organism the distribution between the free metal ion and the metal organic complex may be calculated based upon equilibrium constants. Alternatively, when the rate of uptake is faster than the dissociation rate, the uptake is dominated by the abiotic chemical kinetics (2,4). Hoffman (4) discussed the chemical dynamics of a lake system and he concluded that equilibrium calculations may be used as the kinetics are fast with respect to the residence time in the lake, whereas for slow kinetics reaction rates become important.

Only a few papers appeared in literature that deal with the determination of the rate of dissociation of metal ions bound to humic material. Shuman et al. (3) used the rotating disk electrode (RDE) in combination with anodic stripping voltammetry (ASV) to estimate such rate constants. With both methods a limited number of different functional groups can be discriminated.

Differences in kinetics for different metal ions may be explained from their difference in lability. With ASV it is possible to operationally define lability classes ranging from 'very labile' to 'inert', corresponding with high and low dissociation rate constants respectively (5). Another advantage of the ASV method is that trace concentrations of metal ions can be measured. The RDE method, however, is hindered by a narrow experimental time range.

Hering and Morel (6) studied the rates of ligand exchange reactions from CuNTA complexes and Cu-humate complexes to the fluorescent ligand calcein. The dissociation reaction could be followed by monitoring the amount of calcein-Cu complexes. The authors distinguish a disjunctive pathway from an adjunctive pathway. In the disjunctive pathway the initial complex first dissociates before the released metal ion is complexed with the calcein. With the adjunctive pathway the

193

initial complex is attacked by the incoming strong ligand. Both pathways were followed, but for high loadings the disjunctive pathway was found to predominate. They found that the rate constants were pH dependent. Hence, an apparent (conditional) rate constant is found that not only depends on the properties of the humic material, but also on the experimental conditions. Such dependencies complicate the interpretation of the results considerable.

Olson et al. (7-9) studied the dissociation of Cu from estuarine humic material. They used PAR (4-(2-pyridylazo)resorcinol) as a strong ligand to complex any released metal ion and monitored the reaction by measuring the PAR-M complex photometrically. Olson et al. assumed that the disjunctive pathway was followed and thus the rate of PAR-M complex formation is set equal to the rate of the (first order) dissociation of the Cu-humate complex. Lavigne and Langford (10) also used PAR in their study of the dissociation of Ni complexes with humic material.

Recently Nederlof et al. (11) have discussed the kinetic heterogeneity analysis method of Olson et al. (7). Their approximation was obtained with the Laplace transform technique (12,13). It was shown that the method could be interpreted with the concept of Schwarzl and Staverman (14), with which it was possible to evaluate the quality of the approximation in terms of the sharpness of the kernel of a transformed integral equation. In addition Nederlof et al. (11) developed a new technique based on an approximation of the local decay function (LODA). Moreover, in order to smooth the experimental data before an heterogeneity analysis method is applied, an existing smoothing spline routine was adapted (15-18) for the present purpose.

It is the aim of this paper to test and apply the methodology developed by Nederlof et al. (11) to experimental data. For this purpose three data sets measured by Olson et al. (9) were selected. In this paper, the basic assumptions of the kinetic heterogeneity analysis will be briefly summarised. Some information on the three data sets will be provided as this information is needed to interpret the calculated distribution functions. Smoothing of the decay functions, using the GCV smoothing spline technique, will be discussed. On the basis of the spline functions the distribution functions are calculated with the LODA method . Finally a brief discussion will be given on the applicability of the distribution functions in terms of the combined modeling of equilibrium and kinetic phenomena in natural environments.

Determination of Rate Constant Distributions

The rate of dissociation of a ligand-metal complex in solution can be studied by monitoring the amount of metal ions that is released as a function of time according to the dissociation reaction:

$$ML_i \rightarrow L_i + M \tag{1}$$

The amount of M released can, for instance, be determined by adding a sink S that instantaneously takes away the released M :

$$M + S \rightarrow MS \tag{2}$$

and measuring the amount MS formed. In the present case MS can be measured accurately by a photometric technique (8).

When it is assumed that the dissociation of the complex ML_i , into M and L_i is a first order reaction, characterised by the rate constant k_i ,the amount, $C_i(t)$, of complex ML_i , left at time t, can be written as:

$$C_i(t) = C_i(0) e^{-k_i t} \tag{3}$$

where k_i is the rate constant of the dissociation of ML_i and $C_i(0)$ is the amount of ML_i at $t = 0$. $C_i(t)$ is called the *local decay function*.

The *overall decay function* of the dissociation of a mixture of ligands is given by :

$$C(t) = \sum_{i=1}^{n} C_i(0) e^{-k_i t} \tag{4}$$

where n is the number of different ligand types. For a continuous range of dissociation constants eq 4 becomes an integral equation:

$$C(t) = C_t(0) \int_{-\infty}^{+\infty} f(\log k) e^{-kt} \, d\log k \qquad (5)$$

where $C_t(0)$ is the total amount of complex ML at $t = 0$ and $f(\log k)$ is a normalised distribution function. When $C_t(0)$ is not known a non-normalised distribution can be defined as:

$$F(\log k) = C_t(0)f(\log k) \qquad (6)$$

When $C(t)$ is measured and a first order reaction is assumed, the rate constant distribution can be obtained, in principle, by inversion of eq 5. Exact analytical or numerical solutions of eq 5 for the distribution function are not available. Olson et al. (7,11) used the Laplace transform technique to derive a second order approximation of the distribution function indicated by $F_{LT2}(\log k)$:

$$F_{L2}(\log k) = -\frac{\partial C(t)}{\partial \log t} + 0.43 \frac{\partial^2 C(t)}{\partial \log t^2} \qquad (7a)$$

$$\log k = \log 2 - \log t \qquad (7b)$$

Nederlof et al. (11) developed the LODA method which uses an approximation of the local decay function in order to be able to solve eq. 5 analytically for $F(\log k)$. The LODA-G2 approximation of the local decay function is (Figure 1):

$$\xi_{1,LODA-G2} = 1 - \left(\frac{kt}{\gamma}\right)^{\beta} \qquad \text{for} \qquad kt \le \gamma \qquad (8a)$$

$$\xi_{2,LODA-G2} = 0 \qquad \text{for} \qquad kt > \gamma \qquad (8b)$$

where γ is the 'breakpoint' which divides the approximation it its two parts and β is a constant. The parameters β and γ have been determined by fitting eq 8 to eq 3

196

on a log(kt) scale. The best fit was found for $\gamma = 2.2$ and $\beta = 0.68$. Solution of eq 5 after substitution of eq 8 with above coefficients provides the expression for the distribution function (11):

$$F_{LODA-G2}(\log k) = -\frac{\partial C(t)}{\partial \log t} + 0.64\frac{\partial^2 C(t)}{\partial \log t^2} \qquad (9a)$$

$$\log k = \log(2.2) - \log t \qquad (9b)$$

Note that, besides a slight difference in the transformation from a log(t) scale to a log(k) scale, $F_{L2}(\log k)$ merely differs from $F_{LODA-G2}(\log k)$ in the coefficient in front of the second derivative.
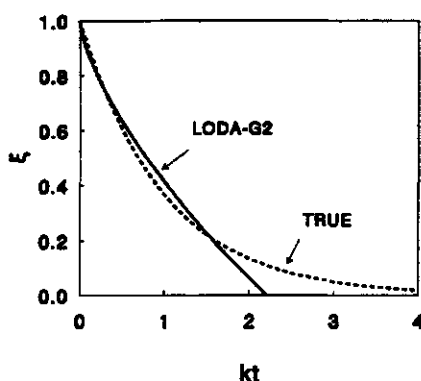
Figure 1: The LODA approximation of the local decay function compared with the true local decay function.

Data Sets

Data were taken from Olson et al. (9) who studied the dissociation of Cu from estuarine humic material. Samples were taken from the Ogeechee estuary (Georgia, USA). Three locations along the salinity gradient were selected. Samples were ultrafiltrated in three fractions using filters with different pore sizes: 1-1.3 nm, 1.3-3.1

197

nm and 3.1-450 nm. For our analysis we have chosen the data of the fraction that was obtained using the 1-1.3 nm filter. Details of sampling and analysis are described by Fitzgerald (19) and summarised in Table 1.

	salinity o/oo	pH	DOC mg/l
upstream	1.98	6.82	11.34
midstream	7.7	7.20	9.95
downstream	19.2	7.35	6.10

Table 1: Characteristics of the three chosen samples, data obtained from the original samples.

Olson carried out kinetic experiments to examine how the dissociation rate constants are distributed along the log k axis. In these experiments Cu(II) was added in proportion to the DOC content to the ultrafiltrated samples and equilibrated for 12 hours. Subsequently PAR, 4-(2-pyridylazo)resorcinol, was added to complex free Cu that is released during dissociation, according to the reaction:

$$CuL + 2PAR \rightarrow Cu(PAR)_2 + L \tag{10}$$

The Cu-PAR complex is highly coloured and can be measured photometrically. The dissociation of the CuL complex was assumed to be the rate limiting step. In addition it was assumed that the disjunctive pathway was followed. Under these conditions the rate of Cu-PAR formation equals the rate of dissociation of Cu-humate complexes:

$$-\frac{d\{ML\}}{dt} = \frac{d\{MS\}}{dt} \tag{11}$$

198

The amount of Cu-humate complexes left, indicated by $C(t)$, was determined as the amount of Cu-PAR complex present at $t = \infty$ minus the amount at $t = t$. According to Beer's Law $C(t)$ is obtained as:

$$C(t) = \frac{A_\infty - A_t}{\varepsilon b} \qquad (12)$$

where $A_\infty - A_t$ is the difference in absorbance, ε is the molar absorptivity (57.5 $dm^3 mol^{-1} cm^{-1}$) and b is the path length in the cuvette (1cm). Absorbance was measured at 508 nm. A mixture of humic material and PAR was used as a blank to make relatively small corrections in ΔA for PAR and humic material absorbance. The experimental conditions were kept constant at pH=7.5, T=25°C and I=0.1 M. Kinetic experiments were carried from 20ms to 6035s for the upstream and mid-stream samples and to 1835s for the downstream sample. From 20ms to 50s a stopped-flow system was used. After 50s the mixing was done manually and absorbance was measured in a stoppered cuvette (8).

To apply our analysis method we have selected the data obtained for the fraction with particles in the range 1-1.3 nm for each of the three locations. The three locations and the resulting data sets will be indicated by upstream, midstream and down-stream respectively. The measured decay functions are presented in Figure 2. Since the amount of Copper added was in proportion with DOC content, the scaled results can be compared directly with each other.

The recovery was expressed in the completeness of the overall reaction eq 10, that is the percentage of initial added Copper that was dissociated during the experiment. Values were found in the range from 76.9% to 87.6%. Pseudo-first order reaction kinetics was checked by doubling both total Cu(II) and L. The shape of the distribution function did not change and the area under the curve was doubled, indicating (pseudo-) first order kinetics. Experimental conditions are summarised in Table 2.
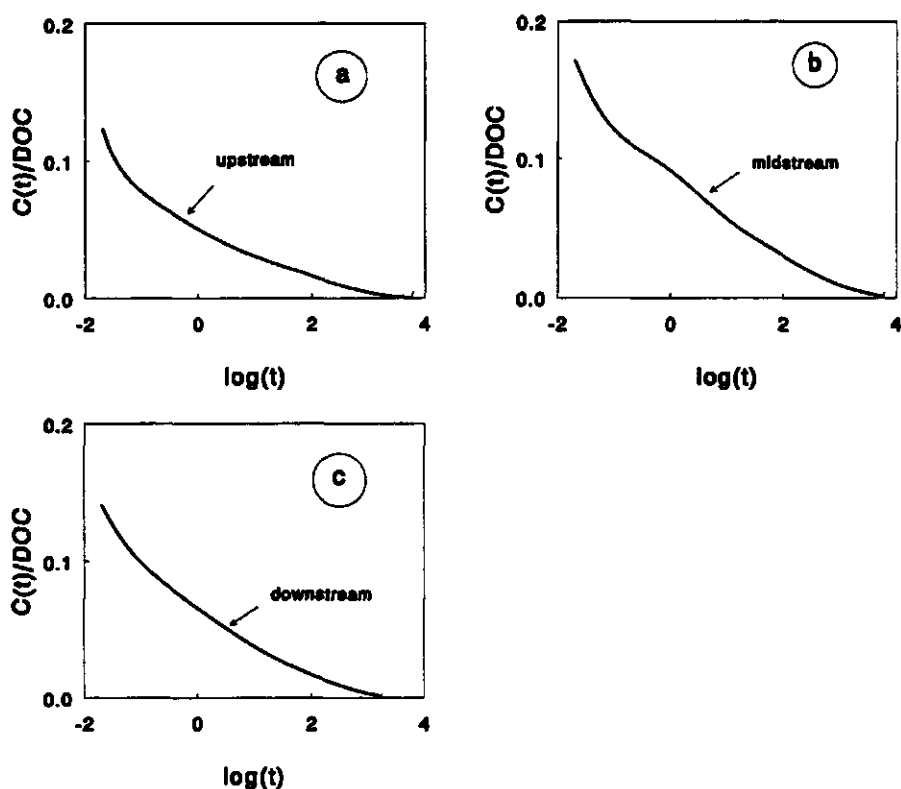
Figure 2: Spline representation of the decay functions of a) the upstream, b) the midstream and c) the downstream sample. Time is given in seconds and C(t) values are expressed mmol/g DOC.

Sampling point	DOC mg/l	Cu(II)$_t$	t$_{max}$ (s)	Number of data points	Recovery
upstream	15.33	5.15	6035	213	87.6
midstream	21.13	7.10	6035	213	76.9
downstream	42.25	14.2	1835	176	81.0

Table 2: Experimental conditions for generation of the kinetic spectra for the three chosen samples.

200

Data Treatment

In order to remove the effects of experimental errors in the data the developed smoothing spline technique was applied to the data (18). To determine the smoothing parameter the Generalized Cross Validation (GCV) was used in combination with physical constraints (11,15-18). First the GCV method was applied to the complete data sets assuming an absolute random error with a constant variance in $C(t)$. That is, the weighting factors in the spline program (17) are set to 1. For none of the three cases a clear minimum in the GCV function was found.
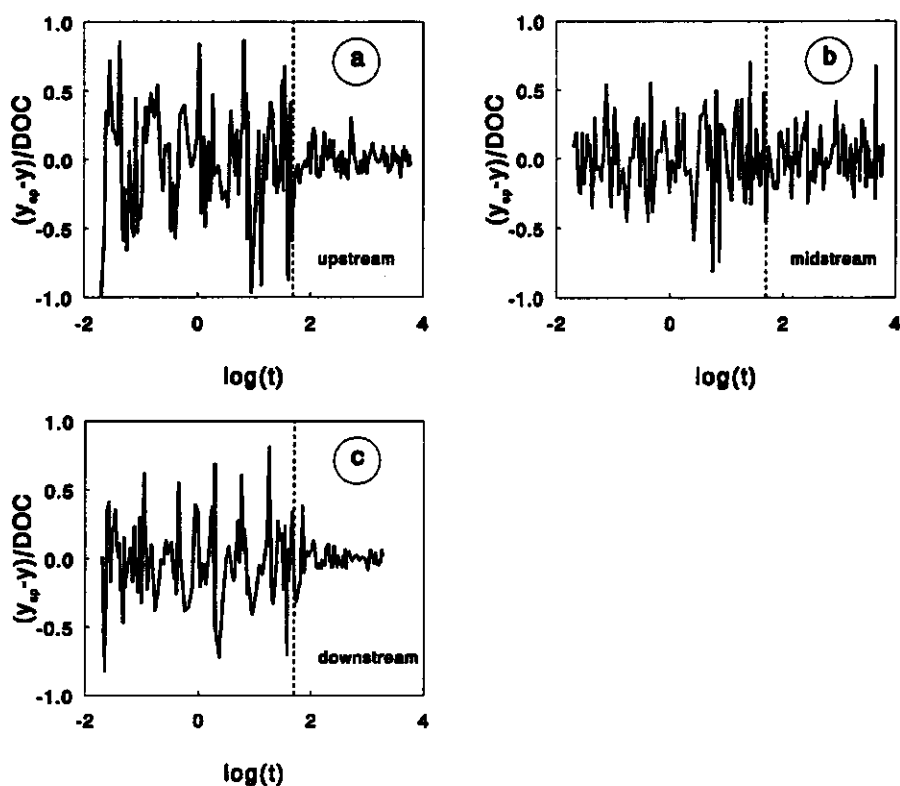

Figure 3: Residuals obtained from a preliminary spline analysis on the basis of the complete decay functions for a) the upstream sample, b) the midstream sample and c) the downstream sample. Results are expressed in μmol/g DOC.

201

From a preliminary spline fit obtained for log(p)=-4 it followed that the variance of the error was not constant over the whole $C(t)$ range, whereas the spline program implicitly assumes that the variance is the same over the whole time range. The fact that the variance of $C(t)$ is not constant is shown in Figure 3 where the residuals, that is the difference between spline estimates and measured data, are plotted for the three decay functions. It follows that differences occur in the residuals both within samples and between samples. The difference within a sample is probably caused by the different experimental set up for the first (t<50 s) and the second part of the curve (t>50s), indicated by the dashed lines in Figure 3. Evidently, the data resulting from the two ways of measurement should be treated separately.

Within each of the two parts no clear variation of the residuals occurred with time. Therefore, in the separate treatment of the two parts of the decay function the weighting factors were again set to 1. Still no clear minima in the GCV function could be obtained. A reason for this behaviour might be that the error is not purely random. This will be the case when the time scale of the fluctuations is larger than the data interval, so that pairs of data will be dependent. Whether or not this is the case can be analysed by reducing the data set through increasing the time interval between successive data. Doing this results in clear minima in the GCV functions, see Figure 4.

The spline function for the first part of the decay function for the upstream sample using log(p)=-5.2, found with the GCV function (Figure 4a), did not obey the constraints. Raising the smoothing parameter till all constraints were fulfilled resulted in log(p)=-4.0. This value is still somewhat smaller than the GCV smoothing parameter values found for both other samples, log(p)=-3.6 and log(p)=-3.4 respectively. For the second parts of the decay function multiple minima were found in the GCV function. Using the constraints resulted in the log(p) values corresponding to the minima in the GCV function with the highest smoothing parameter. The final values of the smoothing parameter and the resulting variances in $C(t)$, together with the number of data points on which the analysis is based, are summarized in Table 3.
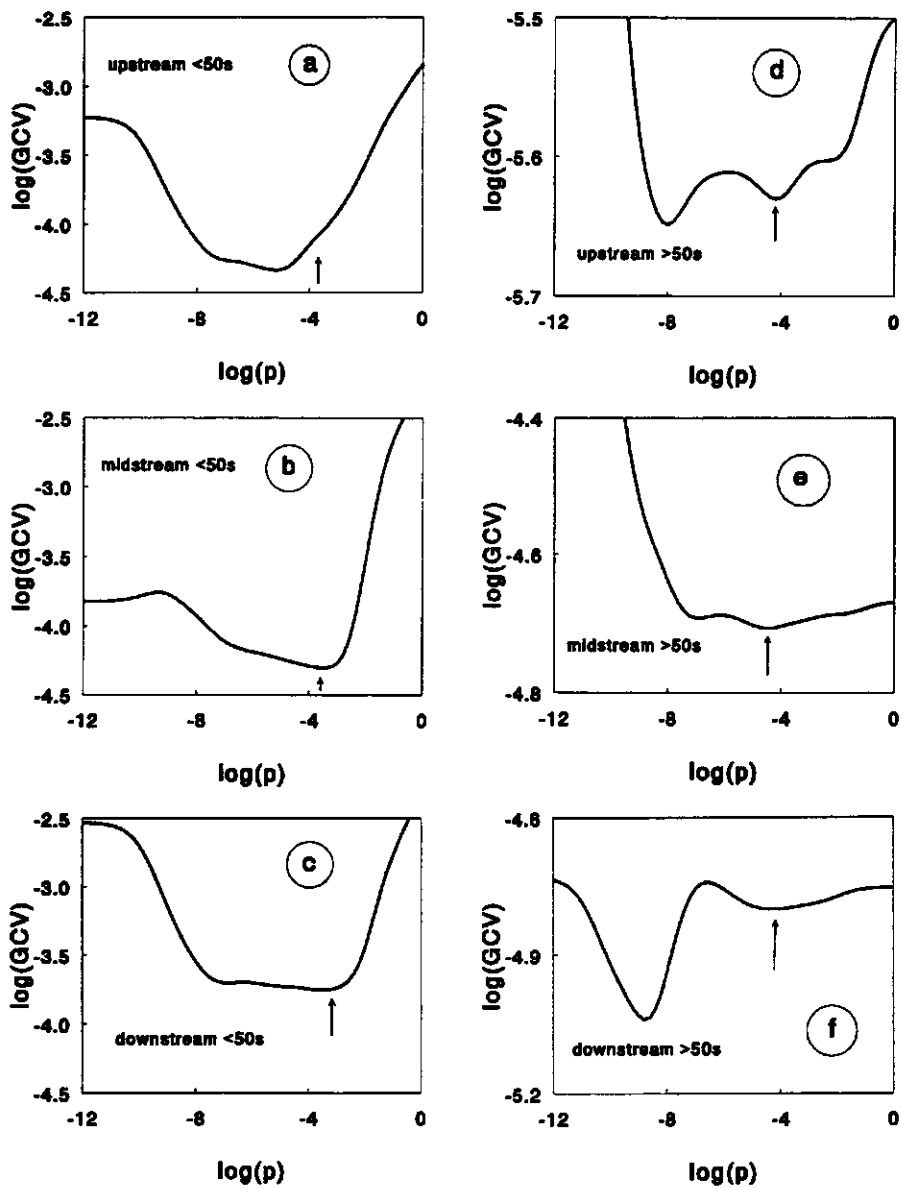
Figure 4: Log(GCV) functions obtained for the decay functions when the first part (t<50s) was treated separately from the second part (t>50s).

station	t<50s			t>50s		
	n_1	log(p)	variance	n_2	log(p)	variance
upstream	52	-4.0	$6.4 \, 10^{-5}$	55	-4.2	$0.2 \, 10^{-5}$
midstream	52	-3.6	$4.6 \, 10^{-5}$	55	-4.4	$1.8 \, 10^{-5}$
downstream	51	-3.4	$16. \, 10^{-5}$	38	-4.2	$1.4 \, 10^{-5}$

Table 3: Final characteristics of the spline function for the first (t<50s) and second parts (t>50s) of the decay functions of the upstream, midstream and downstream samples. The spline functions are based on n_1 and n_2 data points respectively.

Striking is the difference in variance in the different parts of the decay functions. This difference is, however, in correspondence with the residuals obtained in Figure 3. The different variances may be due to the difference in the absolute values of the decay function. The splines describing the data are shown in Figure 2. Note that in Figure 2 the differences between spline values and measured data are not visible.

Distribution Functions

The rate constant distributions calculated with the LODA-G2 method (eq 9) are shown in Figure 5. We used the LODA-G2 method because this method combines a relatively high resolution with a low sensitivity to experimental errors (11).

In general for values of log k < 0.5 a series of small peaks is found superimposed on a rather low background distribution. For values of log(k) > 0.5 a sharp increase in density is found. Hence, there is a large amount of fast dissociating sites and a tail of relatively slow dissociating sites.

For the upstream sample (Figure 5a) a distribution is obtained with four distinct small peaks in the range log k=-2 to log k=0.5 . The small peaks may be caused by individual site types. Note that there is some uncertainty in the value of the smoothing parameter in this case. When the smoothing parameter is raised to log(p)=-3.6 (as was found for the other samples) the peaks are somewhat flattened but still present.

204
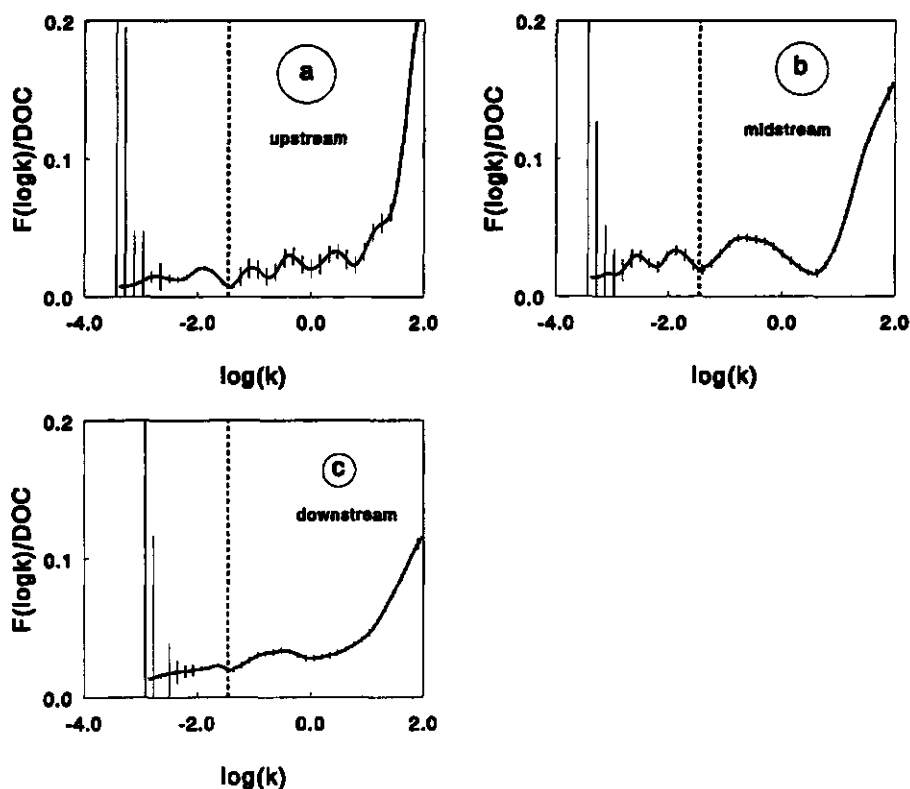
Figure 5: LODA-G2 distribution functions for a) the upstream, b) the midstream and c) the downstream sample. Error bars indicate 66% confidence intervals. Results are expressed in mmol/g DOC.

The peak at log k =-2.0 is a very distinct peak with very small error bars. The peaks at log k=-1, log k=-0.5 and log k=0.5 are distinct but also covered by relatively large error bars, which makes the interpretation as separate peaks instead of a continuous distribution less obvious. The small peak at log k=-2.7 can not be interpreted as such because of the large error bars.

However, when we look at the result for the midstream sample (Figure 5b), distinct peaks can be seen at log k=-2.5 and log k=-2. The combined information of up and midstream suggests that these peaks may be meaningful. The peaks at log k=-1, log k=-0.5 and log k=0.5 observed in the distribution for the upstream sample are

205

reduced to one broader peak at log k =-0.5. The downstream sample shows the least detail (Figure 5c). However still two peaks can be observed, one at log k= -1.8 and one at log k=-0.5. The peak at log k =-0.5 corresponds with that found for the midstream sample and the peak at log k =-1.8 may correspond to the peak at log k=-2 obtained for the mid- and upstream samples.

For comparison the distribution functions obtained by Olson et al. who used the second order Laplace method (eq 7) are shown in Figure 6. Olson et al. (7-9) used a less sophisticated, more conventional, smoothing spline technique where a subjective value of the smoothing parameter is used and no distinction is made between the different time domains. Compared to their distributions, we find in general more distinct peaks in the distribution. For the upstream sample (Figure 6a) the peaks in the distribution obtained by Olson are less pronounced than in our result. However, the large error bars in our result indicate a large uncertainty. As mentioned, raising the smoothing parameter reduces the height of the peaks. In that case more or less the same result is obtained. Furthermore, in Figure 6a a peak is found at log k=1.5, whereas in Figure 5a a sharp increase is obtained. For the midstream sample (Figure 6b) Olson obtained a rather smooth distribution function which corresponds reasonably well with our result. Small inflections found by Olson in the distribution function for the downstream sample (Figure 6c), that can not be caused by functional groups, have been smoothed away in Figure 5c.

The main difference between the treatment of Olson and ours is that here the smoothing parameter is obtained on a statistical basis in combination with some physical constraints, whereas Olson determined the smoothing parameter by hand. The procedures do not differ much in terms of the fitted decay function, but a slightly different value of the smoothing parameter may have (large) consequences for the obtained number and sharpness of peaks in the distribution functions as was shown in the examples. In addition our method has the advantage that error bars can be calculated indicating the reliability of the result and that the method is objective and automatic. That is, using the same principles each user finds the same results. On the basis of fitting by hand the results may differ considerably depending on the person who analyses the data.
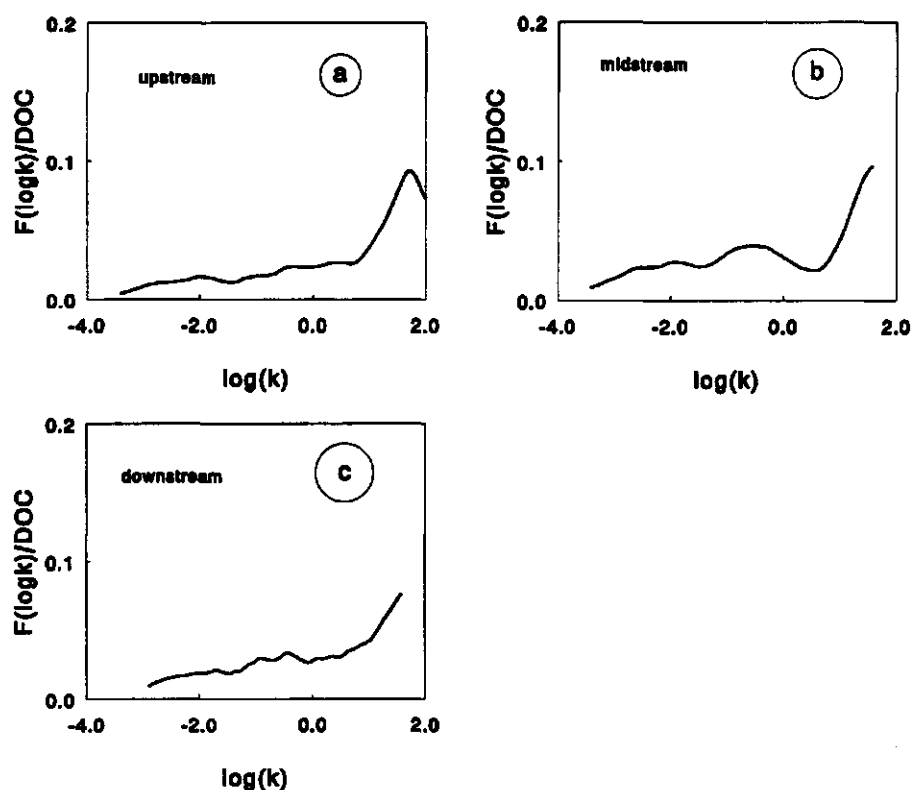
Figure 6: The second order Laplace distributions obtained by Olson et al. (8) for a) the upstream, b) the midstream and c) the downstream sample. Results are expressed in mmol/g DOC.

Discussion

It was found that the interval between the data points had to be increased to find a clear GCV minimum. This may be due to the fact that the error in the original data was not purely random. At short reaction times this might be reasonable since the mixing takes 5ms and the formation of Cu-PAR complexes about 20 ms. So, reaction time is larger than the time step in the beginning of the experiment. For larger times (t >50s) fluctuations in the spectrophotometer readings might play a role. The observed residuals indicate that the error is not purely random. It would be

worthwhile to investigate error propagation more thoroughly since it appears that a different data treatment may change the resulting distribution function considerably in some cases, as was shown in the examples.

Binding capacity of the estuarine humic material was estimated to be 2.5 μmol Cu(II)/mg DOC (19). The amount of Copper added was 0.33 μmol Cu(II)/mg DOC. This means that with the experiments only 13% of the total binding capacity was occupied. Percentage recovery was always lower than 90%. This means that approximately 10% of the initially bound Copper does not dissociate during the experiment. This means that 10% of 13% (is 1.3%) of the total binding capacity are sites that dissociate very slowly. This probably corresponds with sites that have a high affinity for Copper binding. A percentage of 1% high affinity sites was estimated by Nederlof et al. (18) for Copper binding to humic material in the equilibrium case.

The upper limit in log k, corresponding with the lower limit in time, is determined by the formation of the Cu-PAR complex, which takes about 20 ms. It appears that 28-54% of total added Copper dissociates in less than 50ms. This means that a large fraction is readily available. In practice this may not be the case either due to lower loadings or effects of longer incubation times. Other techniques (fluorescence) may be tried to measure shorter time ranges. Although for practical purposes it may be sufficient to know that a certain fraction is readily available.

The kinetic heterogeneity analysis shows that the dissociation behaviour in the range between log k =0.5 and log k=-3.5 may be the result of between two and five discrete site types. However the description of the experiment can probably be done equally well using either five discrete peaks or one smooth continuous distribution function for that range of dissociation constants. If one chooses to use discrete sites the various log k values can be estimated from the data analysis and also the various site concentrations can be estimated from the obtained distribution functions. Thus, to choose a model description based upon a heterogeneity analysis is much less arbitrary than making a priori a model choice and obtain model parameters by a curve fitting procedure.

With respect to practical situations a major problem in the interpretation of the distribution functions is that the samples were equilibrated with a Copper solution for only 12 hours, whereas total dissociation times were recorded during about half an hour for the downstream sample and during two hours for the mid- and upstream

208

samples. This might be too short, in practice much larger contact times exist and it would be useful to study the effect of longer equilibration and dissociation times. In soil systems, for instance, diffusion in micropores may also lead to slow release kinetics. Though this may not be a strictly first order reaction, the obtained apparent distribution function might indicate a fraction of slowly reacting functional groups. In soil systems such diffusion processes may play an important role, when the heavy metal ions have had years of time to react with the solid phase. This is for instance the case with old land fills. For practical relevant processes as heavy metal removal from polluted soil or bioavailability of the metal ions a non-negligible part of a total metal content may appear inert.

It would also be interesting to study the effect of pH and other environmental conditions to reveal some more insight in the mechanisms involved in metal ion binding to humic materials. For metal binding in the equilibrium case (see e.g. (20)) a large pH dependency is observed, with relatively high affinities for high pH values. Lavigne and Langford (10) found lower dissociation rates for higher pH values. This corresponds to the observed higher (apparent) affinity constants found in the equilibrium case. Also the pathway of dissociation which is followed might be investigated further. For instance the adjunctive pathway, as was found by Hering and Morel (6), might also play a role under certain conditions.

At first sight there seems to be some similarity between the affinity distribution and the rate constant distributions obtained from experimental data. Nederlof et al. (18) found for Cu binding to humic material that a large amount of groups had a low (apparent) affinity in the range of $\log K=3$ and a small amount of groups with a high affinity of about $\log K=8$. Olson (8) concluded for Cu binding to estuarine humic material, that the majority of groups had a dissociation rate constant of $\log k > 1$ and a relatively small amount of groups had a low dissociation constant. These results are confirmed in this study. Thus the large group of low affinity constants may correspond to high dissociation rate constants and the small group of high affinity constants may correspond to low dissociation rate constants. The coupled study of affinity distributions and rate constant distributions may reveal insight in the behaviour of ions in natural systems both under equilibrium and non-equilibrium conditions. Shuman et al (3) applied both equilibrium and kinetic methods to humic material from the Ogeechee river and observed three, possibly

209

corresponding, groups in both types of distributions. It would be interesting to recalculate and reinterpret their results with the newly developed methods for data treatment and heterogeneity analysis (11,18)

For the idealized case in which the stoichiometric coefficients in a chemical reaction correspond to the kinetic reaction orders, the law of microscopic reversibility is obtained (4). This law states that the equilibrium constant is equal to the quotient of the rate constants of the forward and backward reaction. With non-chelating 'simple ligands' the rate of formation of a ligand complex is determined by the rate of dehydration of the metal ion and a simple relation exist between the equilibrium affinity constant and the dissociation constant. For more complicated complexants this is only approximately correct and indicates a maximum value of the dissociation rate constant (21). Factors that may complicate this simplified picture of complex formation are the diffusion of a metal species to the ligand and conformational changes needed to form the complex.

Conclusions

- The newly developed LODA-G2 method for kinetic heterogeneity analysis in combination with the GCV smoothing spline method, provides a powerful tool to analyse first order dissociation behaviour of heterogeneous ligands.
- A proper data treatment is crucial in order to be able to calculate reliable rate constant distribution functions.
- For estuarine humic material it was found that the majority of functional groups have a rate constant larger than log k=0.5, that a considerable amount of groups have rate constants in the range -3.0 < log k < 0.5, and that a small fraction of functional groups have very low dissociation constants.

Acknowledgment

References

1   Sunda, W.G.; Guillard, R.R. *J. Mar. Res.* 1976, *34*, 511-529.

2   Anderson, M.A.; Morel, F.M.M. *Limnol. Oceanogr.* 1983, *27*, 789-813.

3   Shuman, M.S.; Collins, B.J.; Fitzgerald, P.J.; Olson., D.J. In *Aquatic and Terrestrial Humic Material;* Ann Arbor Press: Ann Arbor, 1983, Chapter 17, pp 349-370.

4   Hoffman, M.R. *Environ. Sci. Technol.* 1981, *15*, 345-353.

5   Figura, P.; McDuffie, B. *Anal. Chem.,* 1980, *52*, 1433-1439.

6   Hering, J.G.; Morel, M.M. *Environ. Sci. Technol.,* 1990, *24*, 242-252.

7   Olson, D.L.; Shuman, M.S. *Anal. Chem.* 1983, *55* , 1103-1107.

8   Olson, D.L.; Shuman, M.S. *Geochim. Cosmochim. Acta,* 1985, *49*, 1371.

9   Olson, D.L. *The kinetic spectrum method for analysis of simultaneous, first order reactions and its application to copper(II) dissociation form estuarine humic materials;* PhD thesis, Chapel Hill, 1983.

10   Lavigne, J.A.; Langford, C.H.; Mak, M.K.S. *Anal. Chem.* 1987, *59*, 2616-2620.

11   Nederlof, M.M.; Van Riemsdijk, W.H.; Koopal, L.K. submitted for publication to 'Analytical Chemistry'.

12   Doetsch, G. *Theorie und Anwendung der Laplace Transformation;* Springer: Berlin, 1937.

13   Widder, D.V. *The Laplace Transform;* Princeton University Press: Princeton, 1946, p 406.

14   Schwarzl, F.; Staverman A.J. *Apl. Sci. Res. A.,* 1953, *4*, 127-141.

15   Silverman, B.W. *J.R. Statist. Soc. B.,* 1985, *47*, 1-52.

16   Craven, P.; Wahba, G. *Numer. Math.,* 1979, *31*, 377-403.

17   Woltring, H.J. *Adv. Eng. Software,* 1986, *8*, 104-107.

18   Nederlof, M.M.; Van Riemsdijk, W.H.; Koopal, L.K. submitted for publication to 'Analytical Chemistry'.

19   Fitzgerald, P.J. *Dissociation rate constants of copper-estuarine organic complexes estimated with a rotating disk electrode technique,* M.S.P.H. Technical report, University of North Carolina at Chapel Hill, 1982.

20   Saar, R.A.; Weber, J.H. *Can. J. Chem.* 1979, *57*, 1263-1268.

21   Buffle, J. *Complexation Reactions in Aquatic Systems: An Analytical Approach;* Ellis Horwood: Chichester, 1988.

211

CHAPTER 8

Future Challenges

Several times the conclusion had to be drawn in the previous chapters that the LOGA method for the determination of equilibrium affinity distributions or the LODA method for the determination of first order rate constant distributions, could not be applied because available data were not accurate enough. With new measurement techniques and methods for digital data recording it is possible to create larger and more accurate data sets. Such data sets become available, for instance, in the framework of an EC project in which Kinniburgh performs measurements on proton and metal ion binding to humic acids. Data sets may be as large as 200 points, which seems to be a paradise compared to the data sets found in literature. In the near future such data sets will be analysed and then probably advantage can be taken of the possibilities of the newly developed methods for heterogeneity analysis. Preliminary calculations were already carried out but could not be included in this thesis any more. It may also be interesting to try to apply numerical techniques (1-5), that need no approximations of the local isotherm, on these high quality data.

Heterogeneity analysis may be a tool to get further insight in the binding behaviour of natural organic material and may aid the further development of model(s) for metal ion binding to these substances. Several models have already been proposed that take the chemical heterogeneity into account (6-9). A proper model should take both electrostatic effects and chemical heterogeneity into account (10-13) as was done for the proton binding in this thesis. In addition, the pH dependency should be accounted for by using multicomponent adsorption equations (14,15).

Also the further development of binding models for other soil components deserves attention. For clay minerals often cation exchange equations are used to describe metal ion binding (16-20). However, there are indications that (heavy metal) ions bind specifically to the edges of clay minerals. Binding seems to be enhanced by the negative electric field of the plate side of those clay minerals. To quantify this effect sophisticated numerical models are needed to solve the Poisson Boltzmann equation numerically (21-23).

The binding properties of metal(hydr)oxides are also much studied (24-27). Recently the multi site complexation (MUSIC) model was developed to predict the charging behaviour of metal(hydr)oxides (28,29). A number of papers have been published on metal ion binding by metal(hydr)oxides (30-32). The MUSIC model does not include metal ion binding yet.

215

In soils different components coexist. However, only few papers have been published that consider the interactions between soil components and the implications for the binding behaviour (33-35).

A big challenge is to relate models that were developed for the individual soil components under more or less idealized conditions, to the binding of ions to real soil samples. Do the same processes occur to the same extent and can the behaviour of the soil sample as a whole be considered as the sum of the behaviours of the individual components? Or are there so many complications and interactions that the behaviour observed for individual components is completely changed ?.

The main challenge for the future is thus the compilation of different submodels into one model that is able to describe and predict the ion binding behaviour of different soils under different conditions. When these are combined with a chemical equilibrium computer program (36,37), the speciation of a given chemical in the soil environment can be calculated. One step further is the combination of such a speciation program with programs that describe transport processes in soil or biological processes.

When the bioavailability of metal ions in the environment is to be quantified a new dimension, namely that of biota, is introduced. Many papers have been published that deal with the interactions of metal ions and organisms. Examples of biota that have been studied are plants (38-41), earthworms (42), nematodes (43), arthropodes (44), fish (45) and microorganisms (46,47). Most of these studies relate the interactions with biota to the free metal concentration in solution, since it is often assumed that interactions occurs via the free metal ion concentration in solution (48,49). However, uptake by and adsorption on biota (50,51) may strongly influence the speciation in solution. Therefore biota should be included as an extra component in chemical equilibrium programs.

Since biota are per definition dynamic systems, also kinetic considerations have to be taken into account. It was shown in this thesis that not only an equilibrium heterogeneity for humic material is present but also a kinetic heterogeneity exists (see also (52)). In order to study the dynamics of real systems with respect to uptake by biota the equilibrium binding heterogeneity may be coupled to the kinetic heterogeneity to estimate which fraction of bound metal is readily available in a certain time span for a certain organism. When the metal released from the solid phase is taken up directly by the organism the organism acts as a sink and the situation is

comparable to the experiment with PAR described in chapter 7. Alternatively desorption may be hindered when the organism removes the released ions only slowly. So the kinetics of dissociation should be viewed in proportion to the rate of uptake by biota.

Kinetic aspects of dissociation of strongly bound metal ions are also important when the cleaning of soil materials is considered. Several strong complexants have been proposed such as EDTA or chloric acid to "wash" the metal ions out of the soil (53-56). Comparing the affinity constants of EDTA for pollutants with those of organic material may provide a basis to estimate the feasibility of a cleaning technique, when organic matter plays a dominant role in the binding behaviour of the metal ions in soil. Especially a small fraction of about 1% of the organic matter may bind metal ions so strongly that the metal ions can not be removed economically to an acceptable level. This may result in problems to reach soil quality standards. On the other hand it may be questioned whether that amount can have any effect on leaching or on bioavailability. Soil quality standards may in this case demand too much from a cleaning technique. Since the bioavailability may be limited the ecotoxicological risk may be limited and therefore soil quality standards may have to be adjusted.

References

(1)   House, W.A. *J. Colloid Interface Sci.* 1978, *67*, 166-180.
(2)   Vos, C.H.W.; Koopal, L.K. *J. Colloid Interface Sci.* 1985 , *105*, 183-196.
(3)   Mechanick, J.I.; Peskin, C.S. *Anal. Biochem* 1986, *157*, 221-235.
(4)   Jaroniec, M.; Bräuer, P. *Surf. Sci. Rep.* 1986, *6*, 65-117.
(5)   Yuryev, D.K. *J. Immunological methods* 1991, *139*, 297.
(6)   Sposito, G. *CRC Crit. Rev. Environ. Control*, 1986, *16*, 193-229.
(7)   Fish, W.; Dzombak, D.A.; Morel, F.M.M. *Environ. Sci. Technol.* 1986, *20*, 676-683.
(8)   Buffle, J. *Complexation Reactions in Aquatic Systems, An Analytical Appraoch*, Ellis Horwood Chichester, 1988.
(9)   MacCarthy, P.; Perdue, E.M. in *Interactions at the Soil Colloid - Soil Solution Interface*, Bolt, G.H.; De Boodt, M.F.; Hayes, M.H.B.; McBride, M.B., Kluwer Academic Publishers, Dordrecht, 1991, Chapter 13, 469-489.
(10)   Tipping, E.; Backes, C.A.; Hurley, M.A. *Water Res.* 1988, *22*, 597-611.
(11)   Tipping, E.; Hurley, M.A. *J. Soil Sci.* 1988, *39*, 505-519.

(12)   De Wit, J.C.M.; Van Riemsdijk, W.H.; Nederlof, M.M.; Kinniburgh, D.G.; Koopal, L.K. *Anal. Chim. Acta* **1990**, 232, 189-207.

(13)   De Wit, J.C.M.; Nederlof, M.M.; Van Riemsdijk W.H.; Koopal, L.K. *Water Air and Soil Pollution* **1991**,(in press).

(14)   Van Riemsdijk, W.H.; De Wit, J.C.M.; Koopal, L.K.; Bolt, G.H. *J. Colloid Interface Sci.* **1987**, 116, 511-522.

(15)   Van Riemsdijk, W.H.; Bolt, G.H. in *Interactions at the Soil Colloid - Soil Solution Interface*, Bolt, G.H.; De Boodt, M.F.; Hayes, M.H.B.; McBride, M.B., Kluwer Academic Publishers, Dordrecht, 1991, Chapter 3, 81- 113

(16)   Gaines, G.L.; Thomas, H.C. *J. Chem. Physics.* **1952**, 21, 714-718.

(17)   Bolt, G.H. *Neth. J. Agric. Sci.* **1967**, 15, 81-103.

(18)   Ziper, C.; Komarneni, S.; Baker, D.E. *Soil Sci. Soc. Am. J.* **1988**, 52, 49-53.

(19)   Gaston, L.A.; Selim, H.M. *Soil Sci. Soc. Am. J.* **1990**, 54, 1525-1530

(20)   McBride, M.B. in *Interactions at the Soil Colloid - Soil Solution Interface*, Bolt, G.H.; De Boodt, M.F.; Hayes, M.H.B.; McBride, M.B., Kluwer Academic Publishers, Dordrecht, 1991, Chapter 5, 149-176

(21)   Secor, R.B.; Radke, J. *J. Colloid Interface Sci.* **1985**, 103, 237-244.

(22)   Nederlof, M.M.; Venema, P.; Van Riemsdijk, W.H.; Koopal, L.K. In *Proc. 7th Euroclay Conference Dresden*, Störr, M.; Henning,K.-H.; Adolphi, P., (Eds.), Greifswald, 1991, 795-800.

(23)   Beene, G.M.; Bryant, R.; Williams, D.J.A. *J. Colloid Interface Sci.* **1991**, 147, 358-369.

(24)   Kinniburgh, D.G.; Barker, J.A.; Whitfield, M. *J. Colloid Interface Sci.* **1983**, 95, 370-384.

(25)   Huang, C.P.; Hsiesh, Y.S.; Park, S.W.; Ozden Corapcioglu, M.; Bowers, A.R.; Elliot, H.A. in *Metals, Speciation, Separation and Recovery*, Patterson, J.W; Passino, R., Eds. Lewis Publishers, Michigan, 1987.

(26)   Dzombak, D.A.; Morel, F.M.M. *Surface Complexation Modeling. Hydrous Ferric Oxide*, Wiley, New York, 1990, pp 393.

(27)   Schindler, P.W.; Sposito, G. in *Interactions at the Soil Colloid - Soil Solution Interface*, Bolt, G.H.; De Boodt, M.F.; Hayes, M.H.B.; McBride, M.B., Kluwer Academic Publishers, Dordrecht, 1991, Chapter 4, 115-145.

(28)   Hiemstra, T.; Van Riemsdijk, De Wit, J.C.M. *J. Colloid Interface Sci.* **1989**, 133, 105-117.

(29)   Hiemstra, T.; Van Riemsdijk, W.H.; Bolt, G. *J. Colloid Interface Sci.* **1989**, 133, 91-104.

(30)   Benjamin, M.M.; Leckie, J.O. *J. Colloid Interface Sci.* **1981**, 79, 209-221.

(31)   Schenck, C.V.; Dillard, J.G. *J. Colloid Interface Sci.* **1983**, 95, 389-409.

(32)   Cowan, C.E.; Zachara, J.M.; Resch, C.T. *Environ. Sci. Technol.* **1991**, 25, 437-446.

(33)   Lockhart, N.C. *Clays and Clay Minerals*, **1981**, 29, 413-422.

(34)   Hendershot, W.H.; Lavkulich, L.M. *Soil Sci. Soc. Am. J.* **1983**, 47, 1252-1260.

218

(35)   Keizer, P.; Bruggenwert, M.G.M. in *Interactions at the Soil Colloid - Soil Solution Interface*, Bolt, G.H.; De Boodt, M.F.; Hayes, M.H.B.; McBride, M.B., Kluwer Academic Publishers, Dordrecht, 1991, Chapter 6, 177-203.

(36)   Westall, J.; Zachary, J.L.; Morel, F.M.M. *MINEQL- A computer program for the calculation of chemical equilibrium composition of aqueous systems*. Technical Note No. 18 Ralph M. Parsons Laboratory, M.I.T., Cambridge, Massachusetts, 1976.

(37)   Lindsay, W.L. *Chemical equilibria in Soils*. John Wiley & Sons, New York, 1979.

(38)   Lexmond, Th. M. *Neth. J. Agric. Sci.* 1980, *13*, 241-248.

(39)   McBride, M.B.; Tyler, L.D.; Hovde, D.A. *Soil Sci. Soc. Am. J.* 1981, *45*, 739-744.

(40)   Bjerre, G.K.; Schierup, H.H. *Plant and Soil* 1985, *88*, 57-69.

(41)   Sanders, J.R.; McGrath, S.P.; Adams, T.M. *Environ. Pollut.* 1987, *44*, 193-210.

(42)   Ma, Wei Chun; *Arch. Environ. Contam. Toxicol.* 1987, *39*, 933-938.

(43)   Bongers, T. *Oecologia*, 1990, *83*, 14-19.

(44)   Janssen, M.P.M.; Joosse, E.N.G.; Van Straalen, N.M. *Pedobiologia* 1990, *34*, 257-267.

(45)   Pagenkopf, G.K. *Environ. Sci. Technol.* 1983, *17*, 342-347.

(46)   Brookes, P.C.; McGrath, S.P. *J. Soil Sci.* 1984, *35*, 341-346.

(47)   Doelman, P.; Haanstra, L. *Plant and Soil* 1984, *79*, 317-327.

(48)   Sunda, W.G.; Guillard, R.R. *J. Mar. Res.* 1976, *34*, 511-529.

(49)   Anderson, M.A.; Morel, F.M.M. *Limnol. Oceanogr.* 1983, *27*, 789-813.

(50)   Grist, R.H.; Oberholser, K.; Shank, N.; Nguyen, M. *Environ. Sci. Technol.* 1981, *15*, 1912-1916.

(51)   Goncalves, M.L.S.; Sigg, L.; Reutlinger, M.; Stumm, W. *Sci. Tot. Environ.* 1987, *60*, 105.

(52)   Shuman, M.S.; Collins, B.J.; Fitzgerald, P.J.; Olson, D.L. In *Aquatic and Terrestrial Humic Materials*; Christman, R.F.; Gjessing, E.T., Eds.; Ann Arbor Science: Ann Arbor, 1983; Chapter XVII.

(53)   Versluijs, C.W.; Aalbers, Th.G.; Adema, D.M.M.; Assink, J.W.; Van Gestel, C.A.M.; Anthonissen, I.H. in *Contaminated Soil '88*, Wolf, K; Van den Brink, W.J.; Colon, F.J., Eds., Kluwer Academic Publishers, 1988, vol II,pp. 11-21.

(54)   Urlings, L.G.C.M.; Ackermann, V.P.; Van Woudenberg, J.C.; Van der Pijl, P.P.; Gaast, J.J. in *Contaminated Soil '88*, Wolf, K; Van den Brink, W.J.; Colon, F.J., Eds., Kluwer Academic Publishers, 1988, vol II,pp. 911-921.

(55)   Müller, G. in *Metals Speciation, Separation and Recovery*, Patterson, J.W.; Passino, R., Eds., Lewis Publishers, 1989.

(56)   Förstner, U. in *Interactions at the Soil Colloid - Soil Solution Interface*, Bolt, G.H.; De Boodt, M.F.; Hayes, M.H.B.; McBride, M.B., Kluwer Academic Publishers, Dordrecht, 1991, Chapter 16, 517-542.

Summary

Binding heterogeneity, due to different functional groups at a reactive surface, plays an important role in the binding of small molecules or ions to many adsorbents, both in industrial processes and natural environments. In Chapter 1 the role of binding heterogeneity with respect to ion binding in soil environments is discussed. Subsequently an overview is given of the existing heterogeneity analysis methods, which were developed in different fields of science. Binding heterogeneity is described by a distribution of affinity constants since the different functional groups have different affinities for the adsorbing ions.

In principle the affinity distribution function can be determined on the basis of a measured adsorption isotherm. The adsorption can be described with an integral equation based on a local isotherm and an affinity distribution. For the local isotherm often a Langmuir type behaviour is assumed. The determination of a distribution function boils down to the inversion of the overall adsorption equation. The integral equation is, however, difficult to solve for the distribution function, both numerically and analytically.

The heterogeneity methods are applied to ion binding to organic matter from solution. For organic materials a large range of different functional groups is present and thus also a large range of affinities for ion binding will exist. This range of affinity constants with their relative occurrence are considered to constitute a continuous distribution.

In Chapter 2 the Local Isotherm Approximation (LIA) methods are discussed. These methods use an approximation of the (Langmuir) local isotherm to solve the integral equation analytically. The well known Condensation Approximation (CA) replaces the local isotherm by a step function, it is the oldest and simplest method, but it does not always give a good representation of the binding heterogeneity. As a first improvement the Asymptotically Correct Approximation (ACA) was developed by Cerofolini and it is based on a linear approximation of the local isotherm. However, the ACA method results in an asymmetric deformation of the true distribution. In this thesis variants of the ACA were derived by generalizing the linear approximation (LINA). A close approximation of the Langmuir local isotherm is obtained with the LOGarithmic symmetrical Approximation (LOGA). The newly developed LOGA method gives promising results.

To calculate the approximations of the distribution function derivatives of the overall adsorption isotherm are needed: the first derivative for the CA method, the first two derivatives for the LINA methods, and the first three derivatives for the LOGA methods. The best results are obtained with the LOGA method, provided that accurate data are available. The Affinity Spectrum methods (AS), although derived in a different way, appear to be equivalent with members of the LIA methods. The difference is that derivatives are determined differently. The first order AS is equivalent with the CA method. The second order Affinity Spectrum method, which is often used in literature, appears to result in an expression, equivalent with a specific LOGA approximation.

The Differential Equilibrium Function (DEF) method introduced by Gamble and coworkers and worked out by Buffle and coworkers is based on a different approach and originally developed for the description of metal ion binding to organic material. It starts with the application of the mass action law to the whole ligand mixture to obtain the average equilibrium function, $\overline{K}$. Since this quantity gives a poor indication of the underlying heterogeneity the DEF function, related to $\overline{K}$, was derived, which was intended to be closely related to the individual K_i values. The distribution function is found as the first derivative of the overall adsorption isotherm with respect to this DEF function. In Chapter 3 the derivation of the DEF method is analysed extensively and it was found less elegant than the LIA approach. However, the method is powerful in detecting the group of highest affinity sites in a distribution function; especially the position of these sites on the affinity axis is well recovered. In general the distribution function is shifted to higher values of affinity with respect to the true distribution function.

In Chapter 3 also the derivation of the Affinity Spectrum methods is further analysed. By using the concept of Schwarzl and Staverman, the quality of the approximation can be visualised as the sharpness of the kernel of the transformed integral equation.

Each of the analysis methods discussed in Chapters 2 and 3 results in an expression of the affinity distribution function, which is a combination of one or more derivatives of the overall adsorption isotherm. The determination of these derivatives is dealt with in Chapter 4. Without preprocessing the data spurious peaks occur that cannot be the result of heterogeneity. A smoothing spline technique is applied that removes all inflections that lie within the range of experimental error.

224

A proper value of the smoothing parameter, which determines the amount of smoothing applied, is crucial to avoid unrealistic peaks and to retain at the same time details that result from heterogeneity as much as possible. We have used the Generalized Cross Validation (GCV) technique in combination with a series of physical constraints to obtain an objective estimate of the smoothing parameter. The physical constraints were derived using properties of the local and the overall adsorption isotherm.

In order to study the propagation of error in the calculations properly, the smoothing spline method should be applied to primary data. When ion adsorption is measured potentiometrically the primary data are the activity of the ion (or mV) as a function of total added volume of solution containing the ion. On the basis of the variance in the spline, confidence intervals can be calculated in the distribution function. It turns out that the CA method is the least sensitive to experimental error, since it needs only the first derivative of the adsorption isotherm. The LOGA methods, which have in principle a better resolving power, are the most sensitive, since they need a third derivative of the adsorption isotherm too. In practice very accurate data are needed to take advantage of the resolving power of LOGA. The DEF method is less predictable in terms of its sensitivity for experimental error, besides the distribution also the value of the affinity itself is sensitive to experimental error, because for the determination of log K_{DEF} already a differentiation is needed. This results in error bars in two directions. The error in log K_{LIA} is very small since it is directly related to the concentration measured.

To illustrate the methodology a set of Copper binding data on humic material, measured by Hansen et al. is analysed at the end of Chapter 4. It follows that the majority of functional groups have an (apparent) affinity around logK=3 and a small amount, about 1% of the total estimated sites, have a high affinity of about logK=8. In natural environments Copper is often present in trace amounts and in these cases these high affinity sites may play a major role in the binding. It turns out that error bars for low affinities, corresponding to high concentrations, are large, due to the small difference between total Cu in solution and free Copper. Copper was measured by an ion selective electrode using a linear calibration curve. Indications are obtained, however, that for low concentrations the calibration curve is not linear, resulting in artifacts in the distribution functions. A model description of the Cu binding is offered, based on the calculated distribution functions.

In the analysis of the Copper binding data, electrostatic effects and the pH dependency of metal ion binding were neglected. A first step on the way to tackle these problems is the study of the charging behaviour of the organic material as a function of pH. In Chapter 5 charge-pH curves obtained for fulvic acid by Dempsey and O'Melia are analysed using the "master curve" procedure, developed by De Wit et al. In this procedure first the electrostatic effects are filtered out by using a electrostatic double layer model. With this double layer model the pH can be recalculated in a pH value adjacent to the surface: pH_s. When a proper electrostatic model is applied the charge-pH_s curves merge into one "master curve". In the double layer model applied here the molecules have been considered as rigid spheres with a uniform charge and a uniform potential at the surface. When the density of the FA material was fixed to 1 g/cm^{-3} good merging curves were obtained for r=0.75 nm. This means that the resulting master curve is independent of ionic strength and only a function of the chemical heterogeneity. The CA method is applied to the master curve which resulted in a large "valley" in the distribution function with strongly increasing densities for low values of the intrinsic affinity and for high values of the intrinsic affinity. This indicates that at least two different groups of site types are present. On the basis of this result a double Langmuir-Freundlich (LF) equation was selected to describe the master curve. The corresponding distribution function corresponds well with the CA distribution function. Since the two semi-gaussian peaks are rather wide, the CA method suffices. With the combination of the LF description of the master curve and the electrostatic model, the charge-pH curves on which the analysis is based, can be described perfectly. In addition, the charge pH curve for a third ionic strength, not included in the analysis, was predicted very well. The advantage of the procedure is that the electrostatic effects can be treated separately from the intrinsic heterogeneity.

For the application of the master curve procedure assumptions had to be made concerning the initial charge of the material and an electrostatic double layer had to be assumed. When such information is not available, apparent affinity distributions can be obtained with a minimum number of assumptions. However, the disadvantage of such an approach is that the apparent distribution functions strongly depend on ionic strength. As a consequence the results are less suitable to predict the behaviour under different conditions.

So far, the ion binding at equilibrium conditions was considered. However, many processes in natural environments take place at non-equilibrium conditions. An example of such conditions is uptake of ions by organisms, which may cause a mass flux from the solid phase, where ions are adsorbed, via the solution, to the organism. Important aspect is whether the rate of dissociation of the solid phase complexes can keep up with the rate of uptake by the organism. Since the affinity constants of organic materials are distributed over a large logK range, it would be not surprising that also the dissociation rate constants are distributed. In addition, it might be the case that high affinity constants correspond with low dissociation rate constants and that low affinity constants correspond with high dissociation rate constants.

In Chapter 6 methods are discussed to calculate first order rate constant distributions. When the reactions are not first order, an "apparent" rate constant distribution may be defined, which at least gives an impression of the range of dissociation rate constants. In analogy with the equilibrium heterogeneity analysis a number of methods is evaluated and further developed to approximate the true rate constant distribution function on the basis of the overall decay function.

The overall decay function of an amount of complex is assumed to be the sum of decay functions for all the individual site types, weighted by their fractions. For a continuous range of rate constants, the overall decay function becomes an integral equation that must be solved for the distribution function. The behaviour of one individual site type is described by the local decay function, for which a first order expression is used. In principle the distribution function can be obtained by inverting the integral equation. However, as was the case for the equilibrium situation, the solution is difficult both analytically and numerically. In order to obtain analytical expressions for the distribution function, approximations have to be made.

A group of methods to calculate the distribution function used in literature is the inverse Laplace Transform (LT) technique. Application of the general inverse Laplace Transform formula to the integral equation results in an infinite derivative of the overall decay function. Specific approximations can be obtained by choosing a finite order of the derivative. For the first order LT method, the approximation of the distribution function is given by the first derivative of the overall decay function with respect to the logarithm of time, t. Higher order methods use higher order

227

derivatives up to the order of the approximation. The second order method that needs a first and a second derivative was used by Olson et al. to analyse Cu-humate dissociation data.

To study the quality of the different approximations we applied the LT methods to a synthetic data set. The chosen true distribution is a wide gaussian peak with three narrow peaks super posed on it. The quality of the calculated distributions increased with the use of higher derivatives, as was to be expected. Disadvantage of the LT technique is that the quality of the methods can only be illustrated with numerical examples.

The Schwarzl and Staverman (SS) approach also solves the integral equation for the rate constant distribution function. It uses the concept of sharpening the kernel of the integral equation by choosing a certain transformation of the overall decay function. The quality of the approximation can be directly visualised by the sharpness of the kernel. Three methods are derived that lead to the same expressions as found for the LT technique.

In analogy with the LIA methods the local decay function approximation (LODA) method is developed, which uses an approximation of the local decay function to solve the integral equation analytically for the distribution function. The LODA-S method replaces the local decay function by a step function and is analogous with the CA method. The position of the step has been optimized with a least sum of squares criterion. Also a step function is found that corresponds with the first order LT and SS approach. The second order method, named LODA-L, uses a linear approximation of the local decay function. The optimal slope was determined by a least sum of squares criterion. The method is analogous to the LINA methods for the equilibrium situation and results in a similar solution as the LT2 and the SS2 methods. The best approximation of the local decay function was obtained with a functionality inspired by the LOGA local isotherm and named LODA-G. The method corresponding to the closest fit of the local decay function, LODA-G1, gives a good approximation of the distribution function, but relies more strongly on the third derivative of the overall decay function than the third order LT and SS methods. A special LODA function is found, named LODA-G2, that results in an expression for the distribution function that needs only the first and second derivative of the overall decay function.

Since for the calculation of the kinetic spectrum derivatives are needed from experimental data, the same smoothing spline procedure is used as developed for the equilibrium heterogeneity analysis. The physical constraints are adapted to the present situation. When a small error is imposed on the synthetic data set, large error bars are obtained for the LODA-G1 method. The LODA-G2 method is considered the most promising, because it gives better results than the second order LT and SS method.

In Chapter 7 the LODA-G2 method in combination with the smoothing spline procedure is used to recalculate and evaluate the distribution functions obtained by Olson et al. for Cu-humate dissociation. From a preliminary error analysis it follows that the data sets have to be treated in two parts, since a different experimental set up was used for t<50s and for t>50s. The large majority of sites were found to have rate constants in the range log k>0.5, indicating that these sites dissociate relatively fast. A few peaks were found in the distribution that correspond with more slowly dissociating sites. Results are compared with those obtained by Olson et al. It follows that a more thorough interpretation of the spectra is possible, especially because the confidence intervals indicate whether peaks are significant or not.

An amount of 10% of total added Copper in the experiment was not dissociated and probably complexed with high affinity sites. The amount was estimated to be about 1% of the total amount of sites present, such an amount of sites roughly corresponds with the amount of high affinity sites found with the analysis of Copper binding data in Chapter 4. A problem with the interpretation with respect to environmental conditions is that relatively short reaction times were used (12 hours), which easily may be exceeded in nature. In reality reaction times of months or years exist and in soil systems, for instance, diffusion into the soil matrix may play an important role.

From the present work it may be concluded that when organic matter is considered to be an important factor in ion binding, the study of the combination of kinetic heterogeneity and equilibrium heterogeneity is a useful way to get insight in behaviour of ions in natural systems. In the case of cleaning polluted soil material, for instance, the fact that a certain amount of metal ions is bound very strongly, may have the consequence that the soil material can not be cleaned as far as a soil

quality standard demands. In addition, when a certain amount of bound metal ions, possibly corresponding with the strongly bound metal ions, is slowly desorbed, it means that for commercial soil cleaning plants, the cleaning takes too long to be economic.

Another implication concerns the bioavailability of metal ions. The fraction of a total metal content in a system that is able to affect biota, strongly depends on which part is bound relatively weakly. Also here kinetics may play a major role, especially the rate of uptake by the organism relative to the rate of release by the solid phase strongly determines what is going to happen. It is clear that the balance between the two strongly depends on the type of adsorbents and the organisms involved. The time scale at which a process is studied determines also whether it may be considered under equilibrium conditions or that the dynamics of the process should be taken into account.

Samenvatting

Sinds de affaire Lekkerkerk staat de bodemverontreiniging in Nederland volop in de belangstelling. Miljoenen guldens worden besteed aan de reiniging van vervuilde grond. Eén van de voorkomende vormen van verontreiniging is die met zware metalen, bijvoorbeeld Cadmium, Koper en Zink afkomstig van havenslib, meststoffen of zinksmelterijen.

Het Nationaal Speerpuntprogramma Bodemonderzoek is mede opgezet om informatie aan te dragen aangaande de risico's van verontreinigen in de bodem en de noodzaak tot sanering ervan. De intussen ingeburgerde ABC-normen worden gebruikt om te beoordelen of een bodem verontreinigd is of niet. De A-waarde is de referentiewaarde, overeenkomend met een gehalte zoals dat in natuurterreinen voorkomt, de B-waarde geeft aan dat nader onderzoek nodig is en de C-waarde geeft aan dat de bodem gesaneerd moet worden.

Deze normen staan de laatste tijd ter discussie, omdat a) sommige gronden in natuurterreinen gehaltes 'verontreinigingen' bevatten die veel hoger zijn dan de A-waarde en omdat b) het zeer moeilijk is om via reiniging de grond aan de A-waarde te laten voldoen. De normen zouden een beeld moeten geven van het risico van een bepaald gehalte van een verontreiniging. Een grond met een gehalte boven de C-waarde levert volgens deze redenering risico op voor het milieu ofwel de mens.

De normen zijn gebaseerd op totaalgehaltes in een bodem, welke bepaald worden met tamelijk agressieve extractiemiddelen. Het totaalgehalte geeft echter een slecht beeld van welk deel kan uitspoelen naar het grondwater en welk deel beschikbaar is voor opname door organismen. Dit laatste wordt aangeduid met de term biologische beschikbaarheid. Of een verontreiniging 'biologisch beschikbaar' is zal sterk afhangen van het gedrag van deze stof en de verdeling van de stof over de vaste fase van de bodem en de bodemoplossing. Wanneer een verontreiniging sterk gebonden is aan de vaste fase van de bodem, zoals het geval kan zijn bij klei- en veengronden, zal er relatief weinig beschikbaar zijn voor uitspoeling en voor organismen en dan is het risico voor het milieu dus relatief gering. Wanneer echter weinig wordt vastgelegd in de bodem, zoals het geval kan zijn bij zandgronden met een laag gehalte organische stof, is het risico bij eenzelfde totaalgehalte veel groter dan in eerder genoemd geval. Bovendien spelen omgevingsfactoren zoals de

233

zuurgraad van de bodem een grote rol in de mate van binding aan de vaste fase van de bodem. Normen zouden dus gedifferentieerd moeten worden naar bodemeigenschappen en omstandigheden.

Om tot verdere differentiatie van normen te komen moet het gedrag van verontreinigingen in de bodem grondig bestudeerd worden. Hierbij wordt vaak gebruik gemaakt van kolomstudies ('kokers' met grond) in het laboratorium om het transport van verontreinigingen te bestuderen en van zogenaamde schudproeven om de verdeling vast te stellen van een verontreiniging over vaste en vloeibare fase. Bij zo'n schudproef wordt een bekende hoeveelheid verontreiniging toegevoegd aan grond waaraan een zoutoplossing is toegevoegd en wordt gemeten welk deel vastgelegd wordt. Door dit bij verschillende hoeveelheden te doen, ontstaat een verband tussen vastgelegde hoeveelheid en de concentratie van de verontreiniging in oplossing.

De 'adsorptie-isothermen' of 'bindingscurven' die zo verkregen worden, worden veelal beschreven met empirische vergelijkingen. De parameters van zulke vergelijkingen worden vervolgens gerelateerd aan bodemeigenschappen. Echter, de gevonden relaties hebben een beperkte geldigheid en kunnen maar in beperkte mate worden gebruikt voor andere gronden en onder andere omstandigheden. In het ideale geval wil men voorspellen wat het bindingsgedrag van een verontreiniging is, gegeven een bepaalde samenstelling van de grond en gegeven de omstandigheden. Dan hoeft men niet overal monsters te nemen en heeft men een beter beeld van de risico's voor het milieu. Om dit te kunnen doen wordt het bindingsgedrag van bijvoorbeeld zware metalen in het laboratorium bestudeerd aan de hand van de afzonderlijke componenten van de bodem, zoals de organische stof (of 'humus'), de kleimineralen en de hydr(oxiden). Afhankelijk van bodemfactoren en omstandigheden, zoals de pH, zal het belang van een bepaalde bodemcomponent in de binding van zware metalen variëren.

In het kader van dit proefschrift is vooral aandacht besteed aan de binding van zware metalen aan de organische stof van de bodem. Hiervoor is gekozen, omdat relatief nog maar weinig bekend is over het bindingsgedrag van zware metalen aan de organische fractie van de bodem. Organische stof in de bodem wordt gekenmerkt door het feit dat het een mengsel is van ingewikkelde macromoleculen, die slecht gedefinieerd zijn. Onderzoek aan 'zuiver materiaal', zoals dat kan bij metaal(hydr)oxiden en klei, is dus slechts in beperkte mate mogelijk. Bovendien is het

234

moeilijk om organische stof uit de bodem te extraheren en vervolgens te gebruiken voor onderzoek. Fracties worden gedefinieerd overeenkomstig de manier van extraheren, zo worden er bijvoorbeeld humus- en fulvozuren onderscheiden. Binding van zware metalen vindt plaats aan zogenaamde functionele groepen, die gekenmerkt worden door een 'affiniteit' voor het zware metaal. Omdat de organische fractie een mengsel is van allerlei ingewikkelde molekulen zijn er verschillende functionele groepen die verschillen in affiniteit en die in verschillende mate kunnen voorkomen. Wanneer men het gedrag van zware metalen wil beschrijven heeft men dus niet genoeg aan één bindingsconstante. Dit verschijnsel wordt (chemische) heterogeniteit genoemd. Bovendien wordt de binding sterk beïnvloed door de zuurgraad en de zoutsterkte van de bodem, zodat de 'schijnbare affiniteit' af kan wijken van de 'intrinsieke affiniteit', die bepaald wordt door de eigenschappen van de functionele groepen zelf.

Onderwerp van dit proefschrift is de bepaling van de verdeling van bindingsconstanten op basis van een gemeten adsorptie-isothermen. Het basisconcept is dat de binding aan een mengsel van functionele groepen beschreven kan worden als de optelsom van de binding aan de afzonderlijke typen functionele groepen, gewogen naar hun relatieve voorkomen. Voor elk type functionele groep wordt een eenvoudig bindingsgedrag verondersteld, meestal wordt hiervoor de zogenaamde Langmuir isotherm gebruikt. Deze wordt de 'lokale isotherm' genoemd. In deze isotherm komt de affiniteit van de functionele groep voor de adsorberende stof, bijvoorbeeld een zwaar metaal, als parameter voor. De lokale isotherm en de fracties van de verschillende groepen bepalen dus het bindingsgedrag van het mengsel.

Voor organische stof wordt een continue verdeling (distributie) van affiniteitsconstanten aangenomen, waardoor de optelsom overgaat in een integraalvergelijking. Met de integraalvergelijking is de verdeling impliciet gegeven. Met bestaande technieken is het echter moeilijk om deze integraalvergelijking op te lossen met als doel de distributie te berekenen. Wel blijkt het mogelijk om een analytische uitdrukking voor de distributiefunctie te verkrijgen wanneer de lokale isotherm benaderd wordt door een andere wiskundige vergelijking. In hoofdstuk 2 worden methoden beschreven die op dit concept zijn gebaseerd. De methoden zijn in het algemeen aangeduid als LIA (Local Isotherm Approximation), dat wil zeggen gebaseerd op een benadering van de lokale isotherm. De eenvoudigste benadering is de CA (Condensation Approximation) methode, die de lokale isotherm vervangt

235

door een stapfunctie. De benadering van de distributie wordt gevonden als de eerste afgeleide van de adsorptie-isotherm naar de logaritme van de concentratie. De ACA (Asymptotically Correct Approximation) is ontwikkeld als een eerste verbetering van de CA-methode en maakt gebruik van een lineaire benadering van de lokale isotherm. Door de helling van de lineaire benadering te variëren ontstaan verschillende varianten (LINA). Bij de gevonden uitdrukking voor de distributie is nu ook een tweede afgeleide nodig. De beste benadering is verkregen met de nieuw ontwikkelde LOGA funktie, die symmetrisch is op een logaritmische concentratieschaal. Voor de distributie is nu ook een derde afgeleide nodig. De in de literatuur veel gebruikte tweede orde Affiniteits-Spectrum (AS) methode en de zogenaamde RJ-methode komen overeen met speciale gevallen van LOGA. De kwaliteit van de benaderingen is bestudeerd aan de hand van synthetische voorbeelden zodat bekend is wat de 'echte distributie' is. Het blijkt dat het oplossend vermogen van de verschillende methoden toeneemt gaande van CA via LINA naar LOGA.

In hoofdstuk 3 wordt de DEF (Differential Equilibrium Function) methode behandeld, die in de literatuur onder andere gebruikt wordt voor de analyse van metaalbinding aan organische liganden. Met name de afleiding van deze methode wordt uitvoerig besproken. Deze begint met de definitie van een 'gemiddelde affiniteit', die echter een slecht beeld geeft van de chemische heterogeniteit. Daarom is een differentiële grootheid afgeleid (de DEF-functie) die beter overeen zou moeten komen met de werkelijke affiniteiten van de verschillende functionele groepen voor de adsorberende stof. De distributie wordt verkregen als de eerste afgeleide van de adsorptie-isotherm naar deze DEF-functie. Naast de DEF-methode wordt de afleiding van de AS-methode nader onder de loep genomen.

In hoofdstuk 4 wordt ingegaan op het probleem van het bepalen van afgeleiden van experimentele gegevens. Wanneer er geen rekening gehouden wordt met de experimentele fout, ontstaan willekeurige pieken in de distributie die het gevolg zijn van meetfouten en niet van functionele groepen. Daarom worden, alvorens een heterogeniteits-analyse toe te passen, eerst alle onregelmatigheden in de gegevens die binnen de meetfout vallen 'gladgestreken'. Dit gebeurt met de zogenaamde 'smoothing spline'-techniek. Om naderhand een goede foutenanalyse mogelijk te maken moet de procedure toegepast worden op de directe metingen, meestal is dat een concentratie als functie van een toegevoegde hoeveelheid. De mate van gladstrijken wordt bepaald door de smoothing parameter, die objectief wordt vast-

gesteld door middel van de Generalized Cross Validation (GCV) techniek, in combinatie met randvoorwaarden die volgen uit algemene kenmerken van het bindingsgedrag.

De gehele analyse-methode is toegepast op koperadsorptie-gegevens voor humeus materiaal welke gemeten zijn door Hansen et al. Het blijkt dat het merendeel van de groepen een affiniteit rond de logK=3 hebben. Een kleine hoeveelheid, ongeveer 1% van het totaal, heeft een veel hogere affiniteit. Deze sterk bindende groepen kunnen belangrijk zijn bij lage concentraties, zoals die in het milieu voorkomen. Op basis van de gevonden verdeling kan een keuze worden gemaakt voor een adsorptiemodel met als doel het bindingsgedrag te beschrijven. Op deze manier kan een redelijk objectieve modelkeuze worden gemaakt. Het gekozen model blijkt een vrijwel perfecte beschrijving van de data te geven met een relatief beperkt aantal modelparameters. Bovendien is de grootte van de modelconstanten reeds vooraf redelijk in te schatten op basis van de bepaalde affiniteitsverdeling. De heterogeniteitsanalyse is dus een krachtig hulpmiddel bij het ontwikkelen van een verantwoorde en bruikbare modelvoorstelling.

Bij de analyse van de koperbinding zijn de pH-afhankelijkheid en elektrostatische effecten buiten beschouwing gelaten. Wanneer echter het bindingsgedrag onder andere omstandigheden voorspeld moet worden, is een ingewikkelder model, dat rekening houdt met deze effecten, nodig.

In hoofdstuk 5 wordt als eerste stap om tot een meer geavanceerd model te komen het ladingsgedrag van fulvozuur bestudeerd als functie van de zuurgraad (pH). Hiervoor wordt de 'mastercurve'-procedure, ontwikkeld door De Wit, toegepast. Allereerst wordt de afhankelijkheid van de zoutsterkte weggefilterd door een elektrostatisch dubbellaagmodel aan te nemen, dat de relatie geeft tussen de potentiaal en de lading van het oppervlak. Door deze potentiaal is de concentratie protonen aan het oppervlak groter dan die in de bulk. Wanneer een geschikt dubbellaagmodel is gebruikt en de lading wordt uitgezet als functie van de pH aan het oppervlak, ontstaat een curve die alleen nog maar afhangt van de chemische heterogeniteit. Op de gevonden 'mastercurve' is vervolgens de CA als heterogeniteitsanalyse toegepast. De verkregen distributie toont dat er relatief veel groepen voorkomen met een zeer grote affiniteitsconstante voor protonen met een logK rond de 10. Dit zouden phenolische-OH groepen kunnen zijn. Bij een veel lagere affiniteit,

237

rond logK=3, komen ook veel groepen voor. Deze groepen komen vermoedelijk overeen met carboxylgroepen (-COOH). In het gebied tussen beide grote groepen komen relatief weinig groepen voor.

Op basis van deze analyse is een model gekozen bestaande uit twee semi-gaussische ('klokvormige') pieken in de distributie. Parameters zijn verder door middel van optimalisatie aangepast om de analytische vergelijking voor de adsorptie-isotherm zo goed mogelijk overeen te laten komen met de mastercurve. Combinatie van dit bindingsmodel met het elektrostatisch dubbellaagmodel leidt tot een goede beschrijving van de resultaten waarop de analyse gebaseerd is. Bovendien kan het model een curve die niet in de analyse betrokken is en welke bij een andere zoutsterkte gemeten is, perfect voorspellen.

Tot zover is de binding van metalen en protonen onder evenwichtsomstandigheden beschouwd. In werkelijkheid zal er niet altijd sprake van evenwicht zijn. Bijvoorbeeld wanneer zware metalen opgenomen worden door organismen ontstaat er een massastroming van de vaste fase, waar de metalen aan geadsorbeerd zijn, via de oplossing, naar het organisme toe. Wanneer de biologische beschikbaarheid van zware metalen onderwerp van studie is, kunnen kinetische aspecten heel belangrijk zijn. De snelheid waarmee metaalionen vrijkomen van het bodemoppervlak wordt bepaald door de dissociatiesnelheids-constante. Omdat bij evenwicht een verdeling van bindingsconstanten gevonden werd, is het aannemelijk dat de verschillende functionele groepen ook een verschillende dissociatiesnelheidsconstante hebben. Dus ook hier kan een verdeling van constanten gedefinieerd worden.

In hoofdstuk 6 worden benaderende methoden beschreven om de distributie van snelheidsconstanten voor dissociatie te berekenen. De methoden zijn veelal analoog aan de methoden die ontwikkeld zijn voor de berekening van affiniteitsverdelingen voor de evenwichtssituatie. De afname van de gebonden hoeveelheid of van een complex in zijn algemeenheid wordt beschouwd als de som van de afnamen voor ieder type functionele groep, gewogen naar hun relatieve voorkomen. Wanneer een continu verloop van snelheidsconstanten wordt aangenomen, ontstaat weer een integraalvergelijking met het gedrag voor één type groep als 'lokale afname functie'. Ook deze integraalvergelijking is niet analytisch op te lossen en daarom worden weer benaderende methoden gebruikt.

238

Een groep van methoden die wordt gebruikt in de literatuur maakt gebruik van de inverse Laplace Transformatie (LT). Dit leidt tot een oneindige afgeleide van de afname functie naar de tijd, die uiteraard niet te bepalen is op basis van experimentele gegevens. Benaderingen worden gevonden door een reeks eindige afgeleiden te gebruiken. De reeks is hier beperkt tot drie, omdat voor hogere orde benaderingen ook hogere afgeleiden nodig zijn. Voor de eerste orde benadering (LT1) is de eerste afgeleide nodig, voor de tweede orde (LT2) de eerste en de tweede afgeleide, en voor de derde orde (LT3) komt daar de derde afgeleide bij. De tweede-orde-methode is gebruikt door Olson voor de analyse van de snelheid van dissociatie van een koper-humus-complex.

Alternatief voor de LT-methode is de benadering van Schwarzl en Staverman. De methode is analoog aan de AS-methode. De kwaliteit van de benadering kan zichtbaar gemaakt worden door middel van de kernel van de getransformeerde integraalvergelijking. Hoe scherper deze kernel, des te beter de benadering. Drie methoden zijn afgeleid gebaseerd op de eerste (SS1), de eerste en tweede (SS2) en de eerste, tweede en derde (SS3) afgeleide. De methoden komen overeen met de eerste drie LT methoden.

Analoog aan de LIA methode is de LODA (Local Decay Function Approximation) methode ontwikkeld. Bij de LODA-methode wordt de lokale afname functie benaderd door een eenvoudiger functie om de integraalvergelijking analytisch op te kunnen lossen. De simpelste methode (LODA-S) benadert de lokale afname functie door een stapfunctie, analoog aan de CA-benadering. Ook voor LINA en LOGA is een analogon afgeleid, respektievelijk de LODA-L en de LODA-G. Met behulp van de LODA-methoden kunnen de eerste twee ordes LT ook geïnterpreteerd worden als een benadering van de lokale afname functie.

De methoden zijn met elkaar vergeleken op basis van een synthetisch voorbeeld. Er worden meer details in een distributie gereproduceerd naarmate hogere afgeleiden gebruikt worden. De beste benadering wordt gevonden met de LODA-G1 die een derde afgeleide nodig heeft. Tevens is een variant van de LODA-G afgeleid die alleen een eerste en een tweede afgeleide nodig heeft, de LODA-G2. Qua oplossend vermogen doet de LODA-G2 nauwelijks onder voor de LODA-G1.

239

Omdat voor de berekening van de verdelingen van eerste orde reactiesnelheids-constanten weer afgeleiden van een gemeten functie nodig zijn, wordt ook hier de 'smoothing spline'-methode toegepast. De mate van gladstrijken wordt weer bepaald door het GCV-criterium, alleen nu worden andere randvoorwaarden toegepast. Het blijkt dat een kleine fout in de gegevens leidt tot grote onzeker-heidsmarges in de de LODA-G1 en de derde-orde-LT oplossing. De onzeker-heidsmarges geven aan dat details door de grote onzekerheid niet geïnterpreteerd mogen worden. De LODA-G2 blijkt een goed oplossend vermogen te combineren met een relatief geringe gevoeligheid voor experimentele fouten en geniet daarom de voorkeur.

In hoofdstuk 7 wordt de LODA-G2 methode toegepast op dissociatiegegevens van koper-humus complexen zoals gemeten door Olson et al. De verkregen verdelingen worden vergeleken met de door Olson berekende resultaten. Bij de analyse blijkt dat de afname functies in twee gedeelten moeten worden beschouwd, omdat voor t<50s en voor t>50s een andere meetopstelling gebruikt is, resulterend in een ander gedrag van de experimentele fout. De meeste groepen blijken een dissociatiesnel-heidsconstante te hebben die groter is dan log k=0.5, wat overeen komt met snel dissociërende groepen. In de distributie worden een aantal pieken gevonden die overeenkomen met groepen die veel langzamer dissociëren.

Een hoeveelheid van 10% van het toegevoegde koper bleek niet te dissociëren tijdens het experiment. Deze 10% is blijkbaar gebonden aan groepen met een zeer lage dissociatiesnelheid. De hoeveelheid groepen die dit betreft wordt geschat op 1.3% van het totaal aanwezige reactieve groepen wat ongeveer overeenkomt met het percentage hoge affiniteitsgroepen, gevonden in hoofdstuk 4.

Een probleem bij de interpretatie van deze distributies en de vertaling naar 'na-tuurlijke omstandigheden' is dat relatief korte reactietijden werden gebruikt (12 uur), terwijl in de natuur veel langere reactietijden kunnen voorkomen. In bodems bijvoorbeeld kan diffusie in de bodemmatrix een grote (vertragende) rol spelen.

Wanneer organische stof de belangrijkste fractie is in de metaalbinding voor een bepaalde bodem dan is het zinvol om zowel de kinetische als de evenwichtshe-terogeniteit in beschouwing te nemen. Wanneer zo'n bodem met een complex-vormer (bijvoorbeld EDTA) gereinigd moet worden, kan het feit dat een bepaald deel sterk gebonden is, de consequentie hebben dat de bodem niet zover schoongemaakt kan worden dat voldaan wordt aan de A-waarde. Bovendien,

wanneer een deel, mogelijk overeenkomend met het deel dat sterk gebonden is, slechts langzaam dissocieert, kan het betekenen dat reiniging economisch niet haalbaar is, omdat het proces te lang duurt en dus erk kostbaar wordt.

Een andere consequentie kan zijn dat een deel van het gebonden metaal niet biologisch beschikbaar is en dus ook een beperkt risico vormt voor het milieu. Het deel van een totaalgehalte dat in staat is effekt te resorteren op biota zal sterk afhangen van de aard van de vaste fase en de aard van het organisme. Ook hier spelen kinetische aspekten een rol, met name de opnamesnelheid door het organisme in verhouding tot de dissociatiesnelheid vanaf de vaste fase. De tijdschaal waarop processen bestudeerd worden bepaalt of evenwicht verondersteld mag worden of dat ook kinetische aspecten meegenomen moeten worden.

Inzicht in zowel de heterogeniteit van de binding onder evenwichtsomstandigheden als in de heterogeniteit van de dissociatiesnelheid is van groot praktisch belang. Dit geldt ten aanzien van ecotoxicologische interpretaties, ten aanzien van bodemreinigingstechnieken en ten aanzien van de concentraties in het bodemvocht dat door de bodem percoleert en dat de voeding vormt voor bijvoorbeeld drinkwater (via het grondwater).

In dit proefschrift zijn technieken ontwikkeld waarmee het mogelijk is, wanneer goede meetgegevens voorhanden zijn, om deze vormen van heterogeniteit te bestuderen. Bij het bepalen van de verdelingen en bij de interpretatie van de verdelingen is het noodzakelijk om op een goede en objectieve manier met de experimentele fout in de gegevens om te gaan. De ontwikkelde methoden maken het mogelijk om een goede schatting te geven van de onzekerheid in de berekende verdelingen. Dit laatste is van groot belang bij de interpretatie van de verdeling. Hoewel de methoden nog maar beperkt zijn toegepast, zijn de resultaten veelbelovend.

241

Levensloop

Maarten Nederlof werd geboren op 28 november 1962 in Veldhoven. In 1981 behaalde hij het diploma gymnasium-β aan het Eindhovens Protestants Lyceum. In 1981 begon hij met de studie Milieuhygiëne aan de Landbouwhogeschool te Wageningen (nu Landbouwuniversiteit geheten). Na het behalen van het kandidaatsdiploma in 1985 bracht hij van april tot september 1985 een deel van zijn praktijkijd door bij het Rijksinstituut voor de Volksgezondheid en Milieuhygiëne (RIVM) te Leidschendam. De rest van zijn praktijktijd bracht hij in de periode februari tot oktober 1987 door bij de Dienst Grondwaterverkenning (TNO) in combinatie met een afstudeervak bodemnatuurkunde. In 1987 slaagde hij voor zijn doctoraal examen met als hoofdvakken Bodemverontreiniging en Agrohydrologie en met als bijvakken Bodemnatuurkunde en Wiskunde (extra vak).

In de periode januari 1988 tot maart 1992 werd het in dit proefschrift beschreven promotie-onderzoek uitgevoerd bij de vakgroep Bodemkunde en Plantevoeding van de Landbouwuniversiteit. Sinds 1 maart 1992 is hij voor één jaar aangesteld in het kader van een 'topping-up' projekt van het Speerpuntprogramma Bodemonderzoek. Ook gedurende dit projekt verblijft hij bij de vakgroep Bodemkunde en Plantevoeding.

Iucundi acti labores